Liquid/liquid separation governed by kinetics

Sayed Ali Moussaoui

THÈSE POUR OBTENIR LE GRADE DE DOCTEUR DE L'UNIVERSITÉ DE MONTPELLIER

En Chimie Séparative, Matériaux et Procédés

École doctorale Sciences Chimiques Balard (ED 459)

Unité de recherche Institut de Chimie Séparative de Marcoule UMR 5257 - ICSM

Séparation liquide/liquide pilotée par la cinétique

Présentée par Sayed Ali MOUSSAOUI
Le 15 décembre 2021

Sous la direction de Damien BOURGEOIS

Devant le jury composé de

Bénédicte PRÉLOT, Directrice de recherche, Institut Charles Gerhardt Montpellier	Président du jury
Alexandre CHAGNES, Professeur des universités, Université de Lorraine	Rapporteur
Clarisse MARIET, Ingénieure, Framatome	Rapporteur
Colin BOXALL, Professeur des universités, Lancaster University	Examinateur
Anne LÉLIAS, Ingénieure, CEA Marcoule	Encadrante
Damien BOURGEOIS, Directeur de recherche, Institut de Chimie Séparative de Marcoule	Directeur de thèse

UNIVERSITÉ DE MONTPELLIER

Acknowledgements

First, I would like to thank all the members of the jury: Dr. Clarisse Mariet, Prof. Alexandre Chagnes, Prof. Bénédicte Prélot and Prof. Colin Boxall, for their insightful readings, their constructive comments and the very fruitful discussions they provided.

My heartfelt thanks go to my supervisors Dr. Damien Bourgeois and Dr. Anne Lélias, for their invaluable support in this project. Many thanks for your encouraging and always enlightening comments. Your keen eyes, insightful suggestions and rich experience pushed me to sharpen my thinking and bring my work to a higher level. The discussions we had were always rewarding, inspiring and motivating, and I have fond memories of them. I would also like to offer my special thanks to Dr. Daniel Meyer, who welcomed me to the Laboratory of HYbrid Systems for the separation (LHYS). Thank you for the encouragement and all the valuable discussions we had.

I would like to warmly thank Dr. Jérôme Maynadié, Dr. Michael Carboni, Dr. Olivier Diat, Dr. Pierre Bauduin, Dr. Nicolas Dacheux, Dr. Tony Chave, Dr. Stéphanie Szenknect, Dr. Xavier Deschanels, and Dr. Rachel Pflieger for the scientific discussions and for sharing their knowledge.

Throughout this thesis, I was pleased to supervise the internships of Yoan Bietry and Manon Brun, whom I thank for having contributed to some parts of my thesis through their assiduous laboratory work.

I would like to thank my friends and colleagues for the very pleasant time we spent together whether at work or outside for activities. Thus, I would like to thank Valentin, Halima, Régis, Fabrice, Maximilian, Jingxian, Élisa, Marine, Aline, Boushra, Abdel razzak, Sabrine, Raphaël, Tennesse, Éléonore, Émilie, Nathalie, Sébastien, Jérémie, David, Tania, Zijie, Mohan, Asmae, Max, Élise, Thibault, Sofiane, Lara, Alison, Pierre-François, Armand, Leila, Georges, Hamza, Kassem.

I would also like to express my appreciation to the secretaries of the ICSM, Véronique, Élizabeth, Alice and Aurélie, who took care of all the administrative procedures throughout my thesis. Special thanks go to Vainina for all the extraordinary moments, the support, the priceless discussions and the wonderful dinners in Avignon.

In addition, I would like to express my dearest thanks and gratitude to my Photoshop artist ‘Julie’, my hiking partner ‘Michael’, my disk jockey ‘Ioanna’, my travel buddy ‘Plamen’, my cook ‘Elizabeth’, my food carrier ‘Camille’ and my good listener ‘Mira’, for the precious moments we spent together and the support they provided me.

Finally, I would like to thank my family who supported me along with my thesis, my father and my mother, who always believed and put their trust in me until the end of this project, my brother and my sister for their unconditional love, their support, their tremendous understanding and their encouragement.

Résumé

L'optimisation des procédés d'extraction nécessite une analyse approfondie des caractéristiques thermodynamiques et cinétiques du système. Alors qu'il existe des données considérables sur les aspects thermodynamiques de l'extraction liquide/liquide des métaux, il y a beaucoup moins d'information disponible sur la cinétique d'extraction. Dans cette thèse, nous nous sommes intéressés à la caractérisation de la cinétique d'extraction de Pd(II), Nd(III) et Fe(III) avec deux malonamides de formule brute identique, mais de topologies différentes: *N,N,N',N'*- tetrahexylmalonamide (THMA) et *N,N,N',N'*- dimethyldibutyltetradecylmalonamide (DBMA). Tout d'abord, la caractérisation thermodynamique des systèmes d'extraction a été réalisée. Ensuite, la caractérisation de la cinétique d'extraction a été effectuée en utilisant la technique de la goutte unique, où les constantes globales de transfert de Pd(II), Nd(III) and Fe(III) dans l'extraction avec THMA et DBMA ont été déterminées. L'étude a ensuite été développée pour déterminer les lois de vitesse d'extraction des systèmes. Pour ce faire, une méthodologie expérimentale basée sur la méthode de la vitesse initiale, en réacteur classique sur petite échelle, a été mise en œuvre pour un dépistage rapide et fiable de la cinétique d'extraction. En procédant avec cette méthodologie, nous avons pu mettre en évidence les différences de cinétique d'extraction de Pd(II) avec THMA et DBMA. Les mécanismes d'extraction correspondants ont été proposés. Enfin, le criblage de la cinétique d'extraction dans des expériences en batch a permis de démontrer l'avantage d'un excès de dihexylamine (DHA) employée lors de la préparation du THMA par un gain en performance cinétique. Ainsi, un système moléculaire performant pour l'extraction de Pd(II) avec le THMA a été établi. En conclusion, ce travail a mis en évidence l'intérêt de maîtriser la cinétique de l'extraction liquide/liquide pour le développement de procédés sélectifs de séparation.

Abstract

The optimization of the extraction processes requires a thorough analysis of the thermodynamic and kinetic features of the system. While there is considerable literature on the equilibrium aspects of solvent extraction of metals, there is much less information available on the extraction kinetics. In this thesis, we characterized the extraction kinetics of Pd(II), Nd(III) and Fe(III) with two malonamides of the same molecular formula but different topologies: *N,N,N',N'*- tetrahexylmalonamide (THMA) and *N,N,N',N'*- dimethyldibutyltetradecylmalonamide (DBMA). Thermodynamic characterization of the extraction systems was first carried out, and THMA proved to be very selective for Pd(II) extraction compared to DBMA. Then, the characterization of the extraction kinetics was performed using the single drop technique, where the global transfer constants of Pd(II), Nd(III) and Fe(III) in the extraction with THMA and DBMA were determined. The study was further developed to determine the extraction rate laws of

the systems. For this purpose, an experimental methodology based on the initial rate method was implemented in small scale batch experiments for a fast and reliable screening of the extraction kinetics. Proceeding with this methodology, we could highlight the differences in Pd(II) extraction kinetics with THMA and DBM. The corresponding extraction mechanisms were proposed. Finally, screening extraction kinetics in batch experiments demonstrated the benefit of excess dihexylamine (DHA) employed during THMA preparation through a gain in kinetics performance. Thus, a performing molecular system for the extraction of Pd(II) with THMA was established. Altogether, this work has highlighted the interest in mastering the kinetics of solvent extraction for the development of selective processes of separation.

Glossary

List of symbols:

E_a: Activation energy ($J.mol^{-1}$)

γ: Activity coefficient

a: Activity of a solute

a_i: Area available per molecule ($m^2.molecule^{-1}$)

τ: Average diffusion time (s)

N_A: Avogadro number

μ: Chemical potential ($J.mol^{-1}$)

C: Concentration ($mol.m^{-3}$)

$[M_i]_{aq}$: Concentration of metal in the aqueous phase ($mol.m^{-3}$)

$[M_i]_{org}$: Concentration of metal in the organic phase ($mol.m^{-3}$)

ρ: Density ($kg.m^{-3}$)

d: Diameter of the drop (m)

Δ: Diffusional parameter ($cm^{-1}.s$)

$\mathcal{D}$: Diffusion coefficient ($cm^{-2}.s^{-1}$)

J: Diffusion flux ($mass.cm^{-2}.s^{-1}$)

δ: Diffusion layer thickness (m)

D_M: Distribution ratio

η: Dynamic viscosity ($kg.m^{-1}.s^{-1}$)

F: Energy ($m^2.kg.s^{-2}$)

K_{ads}: Equilibrium constant for Langmuir isotherm

k_f: Forward kinetic rate constant

R_f: Forward extraction rate ($mol.m^{-2}.s^{-1}$)

K_g: Global transfer constant

K_{aq}^{g}: Global transfer constant with respect to the aqueous phase

K_{org}^{g}: Global transfer constant with respect to the organic phase

g: Gravitational acceleration ($m^3.kg^{-1}.s^{-2}$)

A: Interfacial area (m^2)

σ : Interfacial tension ($mN.m^{-1}$)

ν : Kinematic viscosity ($m^2.s^{-1}$)

τ_{H_2O}: lifetime of water molecule in the first coordination sphere (s)

ϕ: Membrane porosity

L: Membrane thickness

P: Partition constant

r: Radius of the drop (m)

k_r: Reverse kinetic rate constant

Re: Reynolds number

SF: Separation factor

k_{aq}: Single transfer coefficient in the aqueous phase

k_{org}: Single transfer coefficient in the organic phase

Γ: Surface excess (mol/m^2)

S: Solute

Γ^{∞}: Surface excess at saturated interface (mol/m^2)

C^0: Standard concentration (mol.m^{-3})

A_{sz}: Szyszkowski parameter

B_{sz}: Szyszkowski parameter

θ: Tortuosity

E: Transfer efficiency

V: Volume (m^3)

E_0: Eötvös number

List of abbreviations:

ACP: Anglo American Platinum's converter plant

Alamine 336: *N,N*-dioctyl-1-octanamine

Aliquat 336: Tricaprylmethylammonium chloride

AMADEUS cell: Atalante Modified Armollex Design for Extraction USes

ARMOLLEX cell: Argonne MOdified Lewis Cell for Liquid-liquid Extraction

Brij S10: Polyethylene glycol octadecyl ether

CAP: Continuous aqueous phase

COP: Continuous organic phase

Cyanex-923: Commercial name of the mixture of dicotyl-hexylphosphine oxide, dihexyl-octylphosphine oxide, trihexylphosphine oxide and trioctylphosphine oxide

$CyMe_4$-BTP: 6,6'-*bis*(5,5,8,8-tetramethyl-5,6,7,8-tetrahydro-1,2,4-benzotriazin-3-yl)-2,2'- bipyridine

$CyMe_4$-BTPhen: 2,9-*bis*(5,5,8,8-tetramethyl-5,6,7,8-tetrahydro-1,2,4-benzotriazin-3-yl)-1,10-phenanthroline

D2EHP: Di-(2-ethylhexyl)-2-ethylhexyl phosphonate

DBMA: *N,N'*-dimethyl-*N,N'*-dibutyltetradecylmalonamide

DBSO: Dibutylsulfoxide

1,2-DCE: 1,2-Dichloroethane

DEHDMBA: *N,N*-di(ethyl-2 hexyl) dimethyl-2,2- butanamide

DEHiBA: Di-2-ethylhexylisobutyramide

DEM: Diethyl malonate

DHA: Dihexylamine

DHS: Dihexyl sulfide

DMDCHMA: *N,N'*-dimethyl-*N,N'*-dicyclohexylmalonamide

DMDOHEMA: *N,N'*-dimethyl-*N,N'*-dioctylhexylethoxymalonamide

DMDPHTDMA: *N,N'*-dimethyl-*N,N'*-diphenyltetraecylmalonamide

DOS: Dioctyl sulfide

FD: Dilution factor

HDEHP: Di-(2-ethylhexyl)phosphoric acid

ICP-AES: Inductively coupled plasma atomic emission spectroscopy

IFTs: Interfacial tension measurements

LIX 63: 5,8-diethyl-7-hydroxydodecan-6-oxime

LIX 64N: Commercial name of the mixture of LIX 63 with LIX 65N

LIX 65N: 2-hydroxy-5-nonylbenzophenone oxime

LIX84 I: 2-hydroxy-5-nonylacetophenone oxime

LOC: Limiting organic concentration

LoQ: Limit of quantification

MIBK: Methyl isobutyl etone

NTH: Nonylthiourea

P50: 5-nonyl-2-hydroxybenzaldoximes

PGMs: Platinum Group Metals

SAXS: Small-angle X-ray scattering

t-BHTE: 1,2-bis(tert-hexylthio)ethane

TBP: Tributyl phosphate

TDMA: *N,N,N',N'*-tetramethyltetradecylmalonamide

THF: Tetrahydrofuran

THDMMA: *N,N,N',N'*-tetrahexyl-2,2-dimethylmalonamide

THMA: *N,N,N',N'*-tetrahexylmalonamide

THEMMA: *N,N,N',N'*-tetrahexyl-2-methylmalonamide

TIBPS: Triisobutylphosphine

TODGA: *N,N,N',N'*-tetraoctyl diglycolamide

TOPO: Trioctylphosphine

TPH: Hydrogenated propylene tetramer

TTA: Thenoyltrifluoroacetone

Versatic 10 acid: Neodecanoic acid

WEEE: Waste from electrical and electronic equipment

Table of contents

List of figures

List of Tables

Introduction

Liquid/liquid extraction is a widely used process in nuclear fuel recycling, purification of metals from ores, petrochemical, pharmaceutical, food as fuel industries. Thus, considerable efforts have been devoted frequently developing new molecules and optimizing the extraction conditions.

The optimization of the extraction processes requires a thorough analysis of the thermodynamic and kinetic features of the system. However, the extraction performance is often studied by a complete system characterization when equilibrium is reached. This leads to a lack of insight into the extraction kinetics, which can limit the extraction performance due to slow mass transfer.

Classically, mass transfer in liquid/liquid extraction has been considered as a diffusion process between the two phases that depends on convection and diffusion of the solute in both feeds and by diffusion across the interface. Thus, the kinetic control of a process has been linked to the mechanical agitation of the phases. However, this approach quickly leads to an underestimation of the involvement of the chemical reaction rate in determining the overall reaction rate. An extraction reaction may involve several steps of different rates, one of which may be slow enough to limit the extraction transfer.

Although knowledge of the extraction kinetics is essential in developing an industrial-scale process, it can be quickly complicated. This is due to the many parameters that must be considered and the accuracy required to best evaluate them to describe the kinetic pathway of an extraction reaction. On the one hand, the mass transfer rate in liquid/liquid extraction is a function of the chemical reaction and the diffusion of components through the phases. On the other hand, the extraction reaction can occur in the two bulk phases or in the so-called interface region. In this regard, localization of the reaction and identification of the nature of the mass transfer limitations are critical elements for further investigations. Thus, adapted devices, allowing studying the extraction kinetics and detailed physicochemical characterization of the systems, are necessary. Several macrsoscopic tools have been designed for this purpose namely single drop technique, stirred cells with constant interfacial area, *i.e.* Lewis cell, Nitsch cell, ARMOLLEX cell or the highly stirred cells.

The most relevant studies on extraction kinetics have been conducted in hydrometallurgy. In addition to locating the extraction reaction, the nature of the limiting step has been identified. However, it should be mentioned that despite the abundant literature on the subject of extraction kinetics, there is still disagreement on the interpretation of most of the kinetic data and the suitability of the various experimental setups used. In particular, the characteristic hydrodynamics of each experimental technique leading to a total elimination or not of the diffusional limitations.

Besides the determination of mass transfer constants, some authors have proposed a description of the extraction mechanism based on the determined partial orders of the reactants in the extraction rate law. Nevertheless, the determination of the partial orders of reagents was carried out using the above mentioned macroscopic tools. In fact, screening the contribution of each reagent with these devices to determine the limiting step has several drawbacks: Besides being time-consuming, these devices consume a large amount of reagents that can be costly and generate a large volume of waste. Thus, developing a fast and reliable methodology for kinetic data acquisition is an ongoing challenge.

Between the need to investigate the extraction kinetics and the search for a straightforward methodology, this thesis work has led to the implementation of an experimental approach allowing easy access to the extraction kinetics, and in the best cases, to make it fast. This study was conducted by investigating the extraction of palladium Pd(II), iron Fe(III) and neodymium Nd(III) with malonamide extractants. These extractants, developed in the actinide/lanthanide partition framework, have recently attracted attention to recycling platinum group metals (PGMs).

Chapter 1: Bibliographic studies

Solvent extraction refers to the distribution of a solute between two immiscible liquid phases in contact with each other. This technique is widely used in many different sectors, where the solutes can be either inorganic or organic. The difference in the behavior of immiscible liquids arises from their different physicochemical properties. Various solutes differ in their affinities to water and organic solvents, leading to their distribution between the two phases. In addition to the properties of the solutes, chemical properties and composition affect their distribution.

In this chapter, we briefly present the thermodynamic features of solvent extraction. Then, we focus on solvent extraction kinetics. Thus, we discuss the effect of diffusion and chemical transport on the overall rate transfer. In addition, we present the available experimental tools to study the extraction kinetics. Particular attention is given to chemical limitations that may determine the rate of metal transfer. Therefore, we shed light on the rate laws and the possible extraction mechanisms. Finally, we review the properties of malonamides and their use in actinide/lanthanide partition and PGMs recovery and previous reported kinetic studies using these ligands.

I. Thermodynamic aspects

A. Distribution ratio

Consider a mass transfer of a solute 'S' between two immiscible liquids, an aqueous solution, and an organic solution containing an extractant. The extraction takes place when the two phases are brought into contact. The difference of the chemical potentials drives the molecular transport 'μ' in each phase. The value of 'μ' is defined as the free energy change when 1 mol of the component is added to an infinite amount of the given solvent. At equilibrium, the chemical potentials of the extractable particles in both phases are equal, and the mass transfer is stopped.

Therefore,

$$\mu_{S,aq} = \mu_{S,org} \quad (1)$$

Where aq and org subscripts denote the aqueous and organic phases respectively.

And,

$$\mu^0_{S,aq} + RTln a_{S,aq} = \mu^0_{S,org} + RTln a_{S,org} \quad (2)$$

Where, $\mu^0_{S,aq}$ and $\mu^0_{S,org}$ are the standard chemical potentials of the solute in the selected standard states, R is the gas constant, T is the absolute temperature and $a_{S,aq}$ and $a_{S,org}$ are the activities of the solute in the solution.

The activity of the solute 'S' in the solution is expressed as follows:

$$a_S = \gamma_S \frac{C_S}{C^0} \tag{3}$$

Where, γ_S is the activity coefficient of the solute, C_S is the concentration of the solute and C^0 is the standard concentration.

In dilute solutions, when the concentration of the solute $C_S \rightarrow 0$, the activity coefficient of the solute $\gamma_S \rightarrow 1$.

Therefore,

$$P_S = \frac{a_{S,org}}{a_{S,aq}} = \frac{C_{S,org}/C^0}{C_{S,aq}/C^0} = \frac{C_{S,org}}{C_{S,aq}} \tag{4}$$

Where, P_S is the partition constant of the solute. It is defined as the ratio of the concentrations of S in the organic and the aqueous phases at equilibrium when these concentrations approach zero. Thus, P_S reflects the difference of the energies of interactions of the solute with both the aqueous and the organic phases.

When it comes to the solvent extraction of metals, the distribution of the metals in both phases is expressed differently. In general, significant amounts of chemical forms of the metals M_i exists simultaneously in equilibrium in both phases, especially in the aqueous phase. Therefore, the distribution ratio D_M is used to express the metal extraction efficiency:

$$D_M = \frac{\sum_i [M_i]_{org}}{\sum_i [M_i]_{aq}} \tag{5}$$

Where, $[M_i]_{org}$ and $[M_i]_{aq}$ represent the concentrations of the total chemical forms of the metal in the organic and in the aqueous phase, respectively.

B. Separation factor

Consider now the presence of two metals M_A and M_B. Selectivity of the separation of M_A from M_B is expressed using their separation factor, SF_{M_A/M_B}, which is equal to the ratio of their distribution ratios:

$$SF_{M_A/M_B} = \frac{D_{M_A}}{D_{M_B}} \quad (6)$$

II. Kinetics of liquid/liquid extraction

A. Introduction

In general, the kinetics of solvent extraction of metal species from aqueous solutions is a function of the rate of chemical reactions occurring in the system and the diffusion rate of the species present in the two phases. Chemical reactions can occur in the bulk phases or in the two-dimensional region called the interface. These reactions can be slow enough to determine the rate of solvent extraction. Moreover, since mass transfer occurs from one phase to another, the diffusion rate is an additional factor to consider through the diffusion films. This implies that the diffusion processes may also be rate determining. Thus, the extraction kinetics relies on the slowest step.

For instance, if the chemical reactions are fast enough, the diffusion process determines the extraction rate and the system is said to be in a diffusional regime. On the other hand, if the diffusional processes are fast enough to be considered instantaneous compared to the chemical reactions, the system is said to be in a kinetic regime. In this case, information on reaction rates is needed to describe the system thoroughly. Finally, an extraction process can be in a mixed regime. This regime is obtained when both chemical and diffusional rates are comparable.

B. Diffusion

Diffusion is a process by which matter moves spontaneously from a higher concentration region to a lower concentration region (Figure 1). The diffusion flux, J (mass.cm^{-2}.s^{-1}), of a chemical species represents the amount of material passing perpendicularly across a surface of a unit area during a unit of time.

The flux of matter through a linear dimension x is linked to the concentration gradient by Fick's first law:

$$J = -D \frac{\partial C}{\partial x} \quad (7)$$

Where, D (cm^2.s^{-1}) the diffusion coefficient is constant, characteristic of each diffusing species and independent of concentration in a given media at a given temperature.

Fick's first law is useful in a steady-state, *i.e.* the concentration gradient is constant over time. However, when a steady-state cannot be assumed, the evolution of the concentration over time must also be taken into account. Fick's second law of diffusion describes this evolution:

$$\frac{\partial C}{\partial t} = \mathcal{D}\frac{\partial^2 C}{\partial x^2} \tag{8}$$

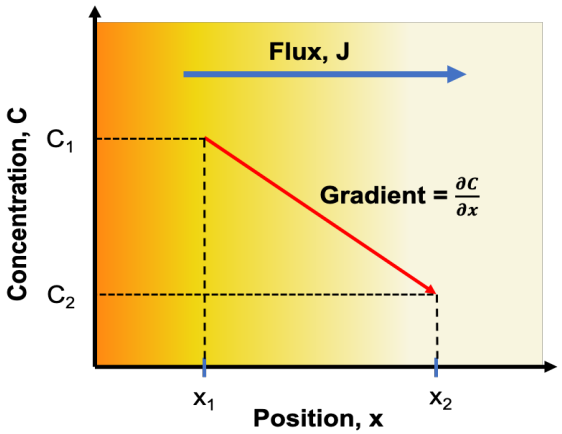

Figure 1: Diffusion of a solute between two zones.

Because a full physical description of diffusion requires the development of theories of molecular interactions and to solve complex differential equations[1–4], this complex phenomenon is usually simplified to the steady-sate occurring through thin diffusion films, where only one dimension can be taken into account.

Assuming that the concentration profile is linear between two points x_1 and x_2, within the diffusion film of thickness δ,

$$\delta = x_2 - x_1 \tag{9}$$

Equation 7 can be simplified, and the diffusional flux J is expressed as follows:

$$J = -\mathcal{D}\int_{x_2}^{x_1}\frac{\partial C}{\partial x} = -\mathcal{D}\frac{(C_2 - C_1)}{\delta} = \frac{C_1 - C_2}{\Delta} \tag{10}$$

Where,

$$\Delta = \frac{\mathcal{D}}{\delta} \tag{11}$$

is a diffusional parameter ($cm^{-1}.s$) depending on the thickness of the diffusion film δ (cm) and the diffusion coefficient.

It is crucial to distinguish between diffusion in the bulk phases and diffusion through adjacent thin films at the interface. Almost all solvent extraction processes require efficient stirring of the organic and aqueous phases. This leads to neglect of the diffusion in the bulk phases and an instantaneous transport of matter to a region very close to the interface. However, diffusional processes affect the extraction kinetics considerably. For instance, interfacial diffusion can be described even when the phases are vigorously stirred. This is possible by assuming the existence of two stagnant thin layers of finite thickness located on the organic and aqueous sides of the interface (Figure 2). This model is known as the two-film theory[5,6] and usefully describes the diffusion-driven extraction kinetics occurring near the interface. Other more complex theories have also been established to describe diffusion transfer in proximity to the interface[1,2] *e.g.* surface renewal, penetration.

C. Double film theory

According to the double film theory (Figure 2) proposed by Lewis and Whitmann in 1924,[5] diffusional transfer from an aqueous phase to an organic phase relies on the following steps:

- Diffusion in the aqueous phase brings the solute to be extracted close to the interface. This leads to a boundary layer of a thickness δ_{aq} located in the aqueous phase
- Diffusion into the organic phase of the solute leads to a boundary layer of a thickness δ_{org} located in the organic phase

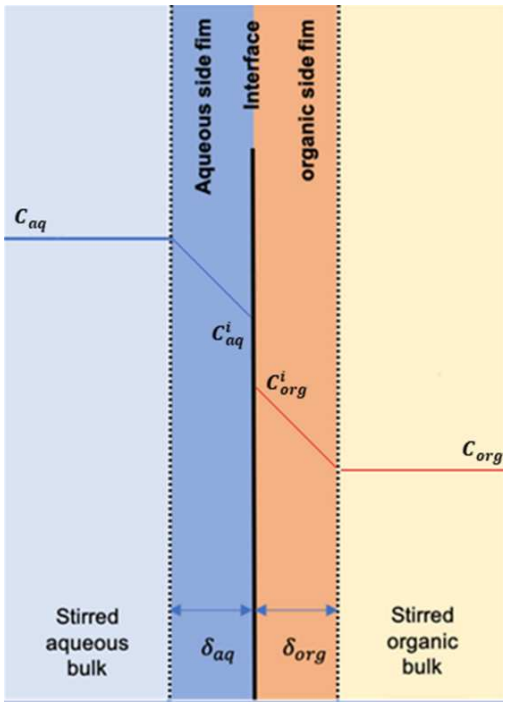

$\boldsymbol{\delta_{aq}}$: Thickness of the aqueous side film

$\boldsymbol{\delta_{org}}$: Thickness of the organic side film

$\mathbf{C_{aq}}$: Concentration of the solute in the aqueous phase

$\mathbf{C_{org}}$: Concentration of the solute in the organic phase

$\mathbf{C^i_{aq}}$: Concentration of the solute at the aqueous interface

$\boldsymbol{C^i_{org}}$: Concentration of the solute at the organic interface

Figure 2: Interfacial diffusion films following the double film theory.

The double film model is based on two assumptions:

- Each phase is sufficiently agitated so that there is no concentration gradient outside the boundary layers
- The concentration profile inside the diffusion films is stationary, so that C_{aq}^{i} and C_{org}^{i} are constant

Considering a stationary regime, the transfer flux is written in the aqueous phase for a unidirectional diffusion:

$$J = -\mathcal{D}_{aq}\frac{\partial C}{\partial x} = -\mathcal{D}_{aq}\frac{C_{aq} - C_{aq}^{i}}{\delta_{aq}} \quad (12)$$

$\mathcal{D}_{aq}$ is the diffusion coefficient in the aqueous phase.

$$J = k_a(C_{aq} - C_{aq}^{i}) \quad (13)$$

By analogy, the transfer flux in the organic phase can be written:

$$J = k_o(C_{org}^{i} - C_{org}) \quad (14)$$

Where, k_a and k_o are the single transfer coefficients in the aqueous and organic phases, respectively.

D. Chemical reaction in solvent extraction

The dependence of the extraction rate on the chemical reaction is evident, considering that the chemical state of the final products is different from that of the initial unreacted species. Depending on the type of the extractant and, subsequently, its chemical interactions with the metal, extraction reactions have been classified into solvation, cation exchange or anion exchange extractions.[7] For solvation extraction, a neutral extractant extracts the metal and its counterions into the organic phase. Several extractants present this type of extraction, namely esters, trialkyl phosphates like tributyl phosphate (TBP), monoamide like *N,N*-di-2-ethylhexyl-isobutyramide (DEHiBA) and diamide as *N,N'*-dimethyl,N,N'-dioctylhexylethoxymalonamide (DMDOHEMA). Extraction by cation exchange involves the acidic extractants. As examples of these extractants, hydoxyoximes, as 5,8-diethyl-7-hydroxydodecan-6-oxime (LIX 63). Finally, the extraction by anion exchange involves the amines and quaternary ammonium salts, as *N,N*-dioctyl-1-octanamine (Alamine 336) and tricaprylmethylammonium chloride (Aliquat 336).

Furthermore, the extraction of metallic species from the aqueous phase can be accompanied by eliminating some of the hydration water molecules and forming a new compound in the organic phase. The exchange of aqua (H_2O) ligands for any other ligand is referred to as the Irving-Williams series,

which reference the relative stabilities of complexes by transition metals.[8] The stability of the complexes formed by divalent first-row transition metal ions generally increases to maximum stability at copper. The series follow this order: Mn(II) < Fe(II) < Co(II) < Ni(II) < Cu(II) > Zn(II). In addition, a similar trend of stabilities can be noted in the second transition series with Pd(II) > Cd(II), and in the third transition series, the order of stability is Pt(II) > Hg(II).

The kinetics of complex formation from aquo cations relies strongly on the rate of solvent molecules between the primary solvation shell of a cation and the bulk solvent.[9] The charge, the radius and particularly the electronic structure of metal ions affect the rate of this reaction, mainly water exchange in the aqueous solutions (Figure 3). Indeed, it has been reported that solvent exchange and complex formation are special cases of nucleophilic substitution reactions.[10] This was based on the consideration that the formation of a new complex by breaking a coordination bond with the first ligand or water can occur at different rates and through the formation of short-lived intermediates, in which the coordination number of the metal is either lower (dissociative mechanism, S_N1) or higher (associative mechanism, S_N2) than in the initial species. Therefore, aquo-complexes that exchange fast their inner sphere molecules, including water, are called labile (alkaline-earth metals), while inert aquo-complexes (Cr(III), Rh(III)) are the ones that exchange the ligands very slowly. Helm and Merbach reported in their review that lifetimes of a water molecule in the first coordination sphere (τ_{H_2O}) of Ru^{3+} and Rh^{3+} are more significant than one day and three years, respectively, while that of Pd^{2+} is 10^{-3} s.[9] Therefore, the slow extraction kinetics of Ru(III) and Rh(III) should be ascribed of their inertness in ligand substitution reactions. Honaker and Freiser first demonstrated this approach in their kinetic study of zinc dithizonate extraction. [11]

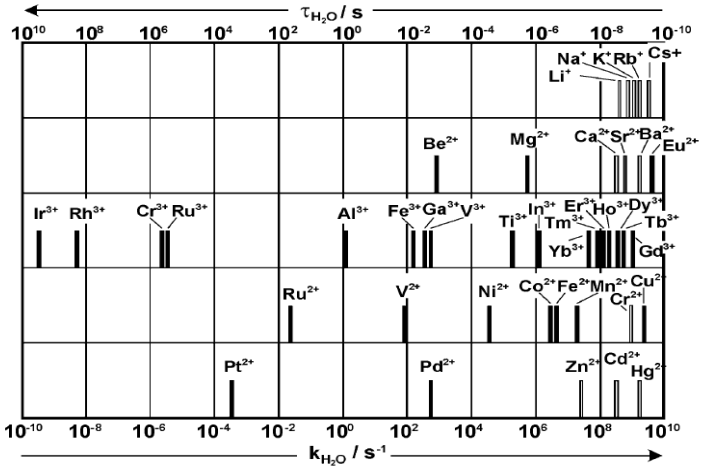

Figure 3: Mean lifetimes, τ_{H_2O} of a water molecule in the first coordination shell of a given metal ion and the associated water exchange rate, k_{H_2O}. Solid bars indicate directly determined values, and empty bars indicate values deduced from ligand substitution studies.[9]

McClellan and Freiser[12] have also established that the rate of extraction for several metal ions (Ni(II), Co(II), Zn(II) and Cd(II)) was paralleled by the rate of exchange of water molecules between the inner coordination sphere of the aquo-complexes and the bulk solvent (water).

Moreover, the extractant can undertake changes in the organic phase due to dimerization, acid extraction. In general, a chemical reaction occurs through several steps. Each step has its rate. It happens that a single step is slow enough so that its rate determines the rate of the overall extraction reactions. In the literature, many investigations report that the kinetics of the chemical reaction plays a significant role in the overall extraction kinetics.[13–21] Thus, from the chemist's point of view, when dealing with the extraction kinetics, the main goal is to elucidate the rate law that defines an extraction reaction for a given system and describe the extraction mechanism. However, this is only possible if the diffusion limitations are completely suppressed and only the chemical reaction limits the transfer.

E. Determination of the extraction kinetics regime

Different criteria can be used to distinguish the extraction kinetics regime.[10] The effect of the hydrodynamic parameters, especially the stirring speed (Figure 4) on the extraction rate, is the most used one.[22–30] The reasoning behind this criterion is that an increase in the agitation speed induces a decrease in the thickness of the diffusion films. As long as the process is controlled by diffusion, even partially, the extraction rate will increase with the stirring speed. When, finally, the thickness of the diffusion films is reduced to zero, only chemical reactions can control the rate, and the extraction becomes independent of the stirring speed.[10]

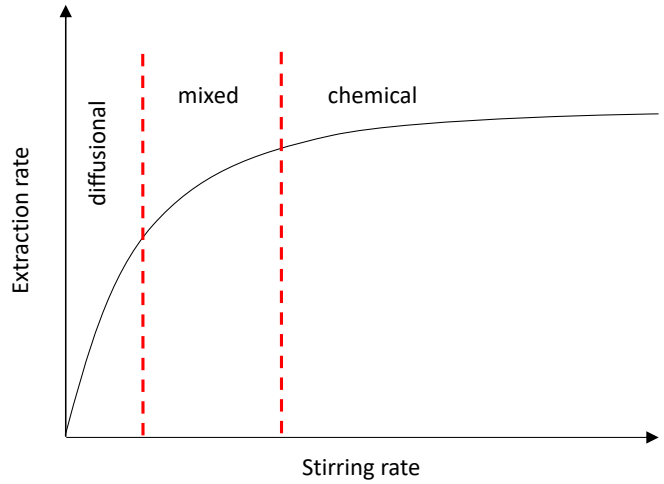

Figure 4: Curve representing the extraction kinetic regime in function of the stirring speed for constant interfacial-area stirred cell for a given temperature.

However, this rationale can sometimes lead to erroneous conclusions, both with constant interfacial-area stirred cells and vigorously stirred flasks. A non-dependence of the reaction rate on the stirring speed can sometimes result from the 'slip effect'.[31] In this case, the thickness of the diffusion films never decreases below a value, small enough for the diffusion to be neglected compared to the chemical reaction rate.

The experimental determination of the activation energy (E_a) by changing the temperature, can also be used to identify the extraction kinetics regime. In general, the activation energy of a chemical controlled rate reaction is higher than that of a diffusion-controlled process. The activation energy would be lower than 20 kJ.mol^{-1} in the diffusional regime and higher than 40 kJ.mol^{-1} in the chemical regime. Finally, for a mixed regime, the activation energy lies between $20 < E_a < 40$ kJ.mol^{-1}. However, this criterion is not considered very relevant since many chemical reactions occurring in solvent extraction processes have an activation energy of only a few kJ.mol^{-1}, which may indicate an incorrect diffusion process.[31]

In conclusion, in their review, Danesi et al.[31] reported that the experimental determination of the extraction kinetics regime could not be solved by relying on only one set of measurements. In fact, for some extraction systems, the extraction rate may show the same dependence on the hydrodynamic parameters (viscosity and density of the liquids, geometry of the apparatus, geometry of the stirrers or stirring rate) and the concentrations of the chemical species involved in the extraction reaction. Therefore, it was strongly recommended to supplement kinetic investigations with information concerning the biphasic system, *i.e.* interfacial tension measurements, the solubility of the extractant in the aqueous phase, the composition of the species in solution.

In addition, the chemical reactions that control the rate of extraction in a kinetic regime can take place at the interface or in any of the two bulk phases.[31] The investigation of the dependence of the initial rate on the interfacial area and on the volume of the phases from which metals are extracted permits to distinguish between these types of reactions. This volume is aqueous for water to organic extractions and organic for organic to water back extractions. Therefore, if the slow chemical reaction occurs in one of the bulk phases, the initial rate will be independent of the volume and the interfacial area. On the contrary, a reaction occurring at the interface will show a direct proportionality between the rate and the interfacial area. In general, the interfacial area and the volume of the phases are often considered together in the specific interfacial area, which is the ratio of total interfacial area to the volume of the phases. In addition, the hydrophobicity and the extent of the solubility of the extractant in the aqueous phase should be considered too. In the case of a highly hydrophobic extractant with high adsorption capacities at the interface, an interfacial reaction is very likely. In this regard, interfacial tension measurements are extremely useful to investigate the interfacial activity of the extractant.

F. Determination of the mass transfer resistance

The equations and the models described in this section refer to the theses of V. Toulemonde,[22] M. Dal Don.[23] The experimental determination of the flux J is delicate because of the difficulty to measure the interfacial concentrations. However, it is possible to do so by expressing the global transfer flux, which gives access to measurable quantities as shown by the following equation:

$$J = K_{aq}^{g}\left(C_{aq} - C_{aq}^{*}\right) = K_{org}^{g}(C_{org}^{*} - C_{org}) \quad (15)$$

Where,

$$D = \frac{C_{org}^{*}}{C_{aq}} = \frac{C_{org}}{C_{aq}^{*}} \quad (16)$$

- K_{aq}^{g} and K_{org}^{g} correspond to the global transfer coefficients concerning the aqueous and the organic phases, respectively
- C_{aq} and C_{org} are the average concentrations of the metal in the aqueous and organic phases, respectively. These concentrations are directly issued from experiments.
- C_{aq}^{*} and C_{org}^{*} are the concentrations of the solute in the aqueous and organic phases, in equilibrium with the average concentration in the organic and aqueous phases, respectively
- D is the distribution ratio of the metal et equilibrium

1. Mass transfer without a chemical reaction

In the absence of a chemical reaction, the flux J can be expressed in terms of the global transfer coefficients, as well as in function of the single transfer coefficients:

$$J = K_{aq}^{g}\left(C_{aq} - C_{aq}^{*}\right) = K_{org}^{g}\left(C_{org}^{*} - C_{org}\right) = k_{aq}\left(C_{aq} - C_{aq}^{i}\right) = k_{org}(C_{org}^{i} - C_{org}) \quad (17)$$

Considering that the metal concentration at the interface is in thermodynamic equilibrium, the distribution coefficient can be defined as depending on the interfacial concentration:

$$D = \frac{C_{org}^{i}}{C_{aq}^{i}} \quad (18)$$

In parallel, we have:

$$C - C^{*} = \left(C - C^{i}\right) + \left(C^{i} - C^{*}\right) \quad (19)$$

The global transfer coefficient with respect to the aqueous phase is:

$$\frac{1}{K_{aq}^{g}} = \frac{1}{k_{aq}} + \frac{1}{D}\left(C_{org}^{i} - C_{org}\right) = \frac{1}{k_{aq}} + \frac{1}{k_{org}D} \tag{20}$$

By analogy, the global transfer coefficient concerning the organic phase is written:

$$\frac{1}{K_{org}^{g}} = \frac{1}{k_{org}} + \frac{D}{k_{aq}} \tag{21}$$

The inverse of the global transfer coefficient is referred to as the global transfer resistance R_g:

$$R_g = \frac{1}{K_g} \tag{22}$$

Where, K_g can be K_{aq}^{g} or K_{org}^{g}, depending on the studied case.

By considering the global transfer resistance concerning the aqueous phase (refer to Eq. 20),

$$R_g = (R_{diff})_{org} + (R_{diff})_{aq} \tag{23}$$

Where, in the organic phase, the resistance is,

$$(R_{diff})_{org} = \frac{1}{k_{org}D} \tag{24}$$

In addition, in the aqueous phase, the resistance is,

$$(R_{diff})_{aq} = \frac{1}{k_{aq}} \tag{25}$$

This law of resistance additivity allows expressing the transfer kinetics either in relation to the organic phase or in relation to the aqueous phase.

2. Mass transfer with an interfacial chemical reaction

Assume a transfer from the aqueous phase to the organic phase, with a chemical reaction localized at the interface. Consider the following extraction reaction of a solute A_{aq} in the aqueous phase, with an extractant B_{org} in the organic phase,

$$A_{aq} + B_{org} \underset{k_r}{\overset{k_f}{\rightleftharpoons}} AB_{org} \tag{26}$$

With k_f and k_r, the kinetic constants associated to the forward and backward reactions, respectively.

Assuming that the kinetics of the chemical reaction brought to the interfacial are of pseudo-first order concerning the solute, the interfacial reaction rate 'r_i' can be written as follows:

$$r_i = -\frac{d[A]_{aq}}{dt} = \frac{d[AB]_{org}}{dt} = A\,(k_f C_{aq}^i - k_r C_{org}^i) \tag{27}$$

The flux resulting from the chemical reaction J_{chem} is written:

$$J_{chem} = k_f C_{aq}^i - k_r C_{org}^i \tag{28}$$

In order to describe the mass transfer flux in the presence of an interfacial reaction, two new terms are introduced, C_{aq}^{i*} and C_{org}^{i*}.

- C_{aq}^{i*} is the solute concentration at the aqueous interface, in equilibrium with the solute concentration at the organic interface C_{org}^i
- C_{org}^{i*} is the solute concentration at the organic interface, in equilibrium with the solute concentration at the aqueous interface C_{aq}^i

The presence of an interfacial reaction slows down the transfer, and two cases can be described:

$$C_{aq}^{i*} > C_{aq}^i \tag{29}$$

And,

$$C_{org}^{i*} < C_{org}^i \tag{30}$$

Therefore, the interfacial concentrations of the solutes are not in equilibrium,

$$D = \frac{C_{org}^{i*}}{C_{aq}^{i}} = \frac{C_{org}^{i}}{C_{aq}^{i*}} \tag{31}$$

The flux can be written as follows:

$$J = k_f\left(C_{aq}^{i} - C_{aq}^{i*}\right) = k_r(C_{org}^{i*} - C_{org}^{i}) \tag{32}$$

The following equation can describe the concentration evolution:

$$C - C^{*} = \left(C - C^{i*}\right) + \left(C^{i*} - C^{i}\right) + (C^{i} - C^{*}) \tag{33}$$

It follows the expression of the global kinetics in the aqueous phase,

$$\frac{1}{K_{aq}^{g}} = \frac{1}{k_{aq}} + \frac{1}{k_{org}D} + \frac{1}{k_f} \tag{34}$$

And in the organic phase,

$$\frac{1}{K_{org}^{g}} = \frac{1}{k_{org}} + \frac{D}{k_{aq}} + \frac{D}{k_f} \tag{35}$$

Therefore, the global transfer resistance is,

$$R_g = (R_{diff})_{org} + (R_{diff})_{aq} + R_{chem} \tag{36}$$

Where, R_{chem} is the chemical mass transfer resistance

In the aqueous phase, the resistance is,

$$R_{chem,aq} = \frac{1}{k_f} \tag{37}$$

And, in the organic phase, the resistance is,

$$R_{chem,aq} = \frac{D}{k_f} \tag{38}$$

III. Experimental techniques for the extraction kinetics study

The experimental study of extraction kinetics requires the design of devices that operate in a kinetically limited regime or allow calculation of the diffusional component of the overall mass transfer rate. Herein, we will summarize the available measurement techniques and draw attention to the hydrodynamics of each technique and the associated diffusional problems. We will divide these techniques into two groups: (i) techniques with direct contact between the organic and the aqueous phases (ii) techniques involving a third medium.

A. Techniques with direct contact between the organic and the aqueous phases

1. Single drop technique

Nitsch first described this technique in 1965.[32] It was already employed to study of metals transfer in liquid-liquid extraction by different solvents[33-35]. This method consists in dispersing one of the phases, namely the dispersed phase, in the form of drops (spherical shape) in another phase, called the continuous phase, in a thermostated column (Figure 5). During the formation of the drop, as well as during its trajectory, and until its collection by a funnel, the mass transfer occurs. The analysis of the solute concentration gradient into the drop as a function of its travel time leads to the determination of a global transfer coefficient, K_g. Indeed, the funnel is mobile, which allows for varying the travel time of the drop and to avoid end-effects. The main advantage of this technique is that interfacial area can be determined quite accurately. However, hydrodynamic control of the single drops can be difficult due to the lack of circulation or the presence of oscillations inside the drop. In addition, the hydrodynamics of the drops is variable and depends on the chemical system used. Furthermore, this technique is not suitable for fast reactions ($K_g > 10^{-4}$ m.s^{-1}) , as the extraction will essentially occur at the drop formation. Likewise, it is unsuitable for slow reactions ($K_g < 10^{-7}$ m.s^{-1}), as longer columns will be required to increase the contact time between the phases.

Depending on the ratio of the considered phases, the experimental setup has two possible configurations: The rising drop configuration (continuous aqueous phase-CAP) and the falling drop configuration (continuous organic phase-COP) (Figure 5).

- **The rising drop configuration (continuous aqueous phase-CAP)**

The dispersed phase in the form of drops in the organic phase, generally of lower density than the continuous phase (the aqueous phase). In this case, the injection of drops through a capillary is done at the bottom and the collection through a funnel at the top.

- **The falling drop configuration (continuous organic phase-COP)**

The dispersed phase is the aqueous phase, and the continuous phase corresponds to the organic phase.

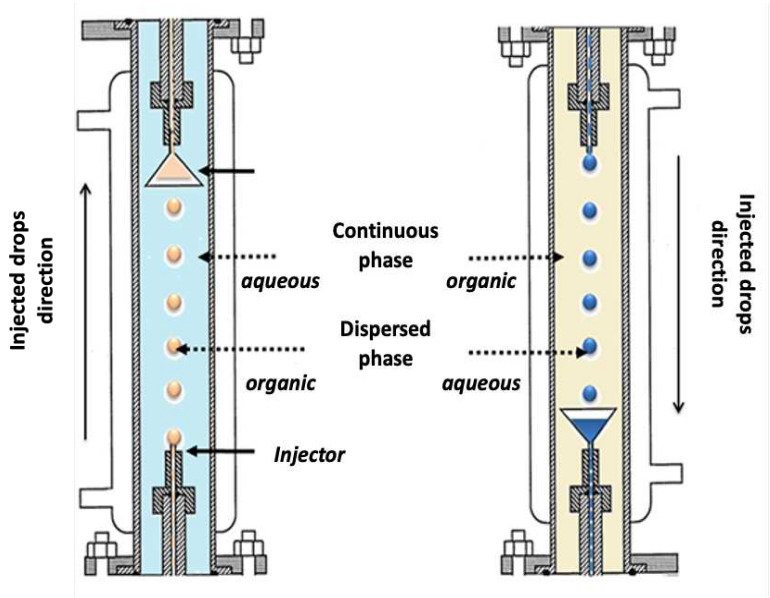

Figure 5: Single drop technique in CAP mode (left) and COP mode (right).[35]

a. Transfer of matter from the continuous phase to the dispersed phase

The transfer within the drops is modelled according to the double film theory for this technique. Thus, the single drop technique allows determining a global transfer constant in one of the two phases. During the transfer of matter between an aqueous phase and an organic phase, the relative balance of the transfer between the instants t and t+dt is expressed by:

$$V_{org}.\,C_{org}(t+dt) = V_{org}.\,C_{org}(t) + J.\,A.\,dt \qquad (39)$$

With,

- V_{org}: Volume of the organic phase
- C_{org}: Concentration of the solute in the organic phase
- t: Flight time of the drop
- A: Interfacial area
- J: Transferred matter flux

Where,

$$J = K_{aq}^{g}\left(C_{aq} - C_{aq}^{*}\right) = K_{org}^{g}\left(C_{org}^{*} - C_{org}\right) \quad (40)$$

And,

$$C_{aq}^{*} = \frac{C_{org}}{D_M} \quad (41)$$

$$C_{org}^{*} = D_M C_{aq} \quad (42)$$

Where,

- K_{aq}^{g}: Global transfer coefficient relative to the aqueous phase
- K_{org}^{g}: Global transfer coefficient relative to the organic phase
- C_{aq}: Average concentration of the solute in the aqueous phase
- C_{org}: Average concentration of the solute in the organic phase
- C_{aq}^{*}: The solute concentration in the aqueous phase in equilibrium with the average concentration C_{org} in the organic phase
- C_{org}^{*}: The solute concentration in the organic phase in equilibrium with the average concentration C_{aq} in the aqueous phase
- D_M: Distribution ratio at equilibrium

Hence,

$$C_{org}(t + dt) - C_{org}(t) = J\frac{A}{V_0}dt \quad (43)$$

And,

$$dC_{org} = \frac{A}{V_{org}}K_{org}^{g}\left(C_{org}^{*} - C_{org}\right)dt \quad (44)$$

So,

$$\frac{dC_{org}}{C_{org}^{*} - C_{org}} = \frac{A}{V_{org}}K_{org}^{g}dt \quad (45)$$

By integration of the equation (45), the following expression is obtained:

$$\ln\left(\frac{C^*_{org} - C_{org}}{C^*_{org}}\right) = \ln\left(1 - \frac{C_{org}}{C^*_{org}}\right) = -\frac{A}{V_{org}} K^g_{org} t \quad (46)$$

The transfer efficiency E for the drop is the ratio of the solute concentration to its concentration when in equilibrium with the continuous phase.

Thus,

$$E = \frac{C_{org}}{C^*_{org}} \quad (47)$$

And,

$$\ln\left(1 - \frac{C_{org}}{C^*_{org}}\right) = \ln(1 - E) = -\frac{A}{V_{org}} K^g_{org} t \quad (48)$$

Assuming that the drops are spherical so the volume V_{org} and the surface A of the drops are expressed as follows:

$$V_{org} = \frac{4}{3}\pi r^3 \quad (49)$$

$$A = 4\pi r^2 \quad (50)$$

Thus, the following expression can be deducted:

$$\frac{A}{V_{org}} = \frac{3}{r} = \frac{6}{d} \quad (51)$$

Where d is the diameter of the drop and r is its radius.

Thus, equation (48) can be expressed as follows:

$$\ln(1 - E) = -\frac{6}{d} K^g_{org} t \quad (52)$$

Experimentally, it is necessary to determine the time of flight of each droplet for each chosen height, *i.e.* the time it takes for a drop to detach from the injector and merge in the funnel.

b. Hydrodynamics of the droplets.

Mass transfer occurs at the interface of each drop during its trajectory in the column. The physical properties of the dispersed and continuous phases as well as the interface properties, control the fluid dynamic behaviour of a single particle.[36] Thus, mass transfer and fluid dynamics cannot be separated from interfacial properties and the related interfacial phenomena such as oscillation, deformation, Marangoni effect, adsorption of surfactants or impurities.

It was demonstrated by Clift et al.[37], that the shape of the drops, the Reynolds number, the ratio of viscosities, the ratio of densities of the dispersed phase and the continuous phase and the Eötvös number play a role in the drop flow.

The Eötvös number (E_0) is a dimensionless number used to measure the magnitude of gravitational forces in relation to surface tension forces. This number is used to characterize the shape of drops in a surrounding fluid.

$$E_0 = \frac{g\,\Delta\rho\,d^2}{\sigma} \tag{53}$$

σ: The interfacial tension

g: Gravitational acceleration

d: Droplet diameter

$\Delta\rho$: Density difference between the two phases

Reynolds number (Re) is a dimensionless quantity that helps predict flow models in various fluid flow conditions. For example, at low Reynolds numbers (up to 2300), flows tend to be mainly by laminar flow, while at high Reynolds numbers (Re > 4000), flows tend to be turbulent.

$$Re = \frac{u_d\,d}{\nu_c} = \frac{\rho_c\,u_d\,d}{\eta_c} \tag{54}$$

u_d: Droplet velocity

d: Droplet diameter

ν_c: Kinematic viscosity of the continuous phase

ρ_c: Density of the continuous phase

η_c: Dynamic viscosity of the continuous phase

In addition, drops with different diameters have different terminal velocities. Figure 6 summarizes the relationship between the drop terminal velocity and its diameter. Hence, four regimes of drops can be obtained. These regimes are called rigid, circulating, oscillating and deformed drops. In addition, the drop formation step plays a crucial in determining the drop size, and thus the initial velocity.

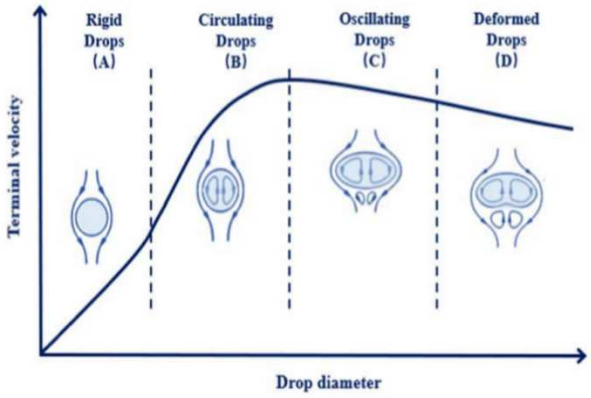

Figure 6: Terminal velocity and behaviour of the drop in function of the diameter.[38]

In general, droplets that show a diameter lower than 1 mm behave as rigid drops. The increase in the drop diameter (2 mm < d < 3 mm) induces intern circulation inside the drop associated with surface mobility. This circulation is mainly due to shear forces located at the interface. When the diameter exceeds 3 mm, the drop follows a sinusoidal trajectory accompanied by oscillation. Beyond 4 mm, the drop deforms and its speed stabilizes. Sometimes the drops separate into two when their diameter is large enough.[39]

In addition to the drop deformation, interfacial instabilities may enhance the internal mixing within the droplets, leading to a meaningful mass transfer improvement.[40,41] This phenomenon is called the Marangoni effect (Figure 7), which arises from interfacial tension gradient. Moreover, the adsorption of impurities that possess a surfactant behaviour may reduce the internal circulation of the droplet and minimize the interfacial turbulence.[42,43]

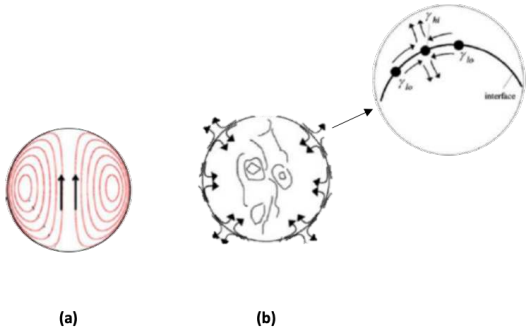

Figure 7: Schematic of flow patterns in rising drops without Marangoni effect (a) and with Marangoni effect (b).[36]

2. Constant interfacial area stirred cell

Lewis first proposed the stirred cell in 1954.[44] In fact, Lewis was the first to recognize the need to improve interfacial measurements and proposed an apparatus to solve this problem. The Lewis cell ensured direct contact between the two phases with a well-defined interfacial area and agitation, always keeping the interface quiescent.

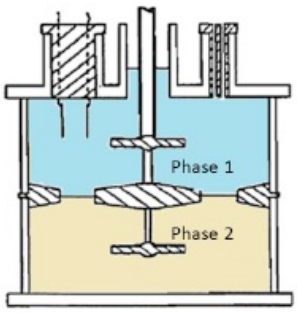

Figure 8: Lewis Cell (1954).[44]

Lewis cell had a major inconvenience since the hydrodynamics were poorly defined. Stirring of the upper and lower phases was carried out at the same rates, which produced different Reynolds numbers in each compartment. Suppose that the convective transfer in each compartment is different because of the physical parameters of the phases, *i.e*. density and viscosity.

Hence, the diffusional contributions are different on each side. In addition, this cell did not allow an efficient stirring of the fluid near the interface, which resulted in the appearance of diffusion films.[45] Modifications were made to this technique to improve its utility. Nitsch and Hillekamp carried the first one.[46] Their upgrade consisted of adding screens on either side of the interface and a separate and opposite direction stirring of each phase. In addition, the stirring speed was adjusted to equal the Reynolds number in each phase. Although, calibration measurements must be done when using this cell to work in the proper regime. The second major modification was done by Danesi et al.[26] The device was named ARMOLLEX (ARgonne MOdified Lewis cell for Liquid-liquid EXtraction). This device permits the use of smaller volumes (about 100 mL) while the Nitsch cell has a capacity of 1 L, and continuous monitoring of the variations of the concentration.

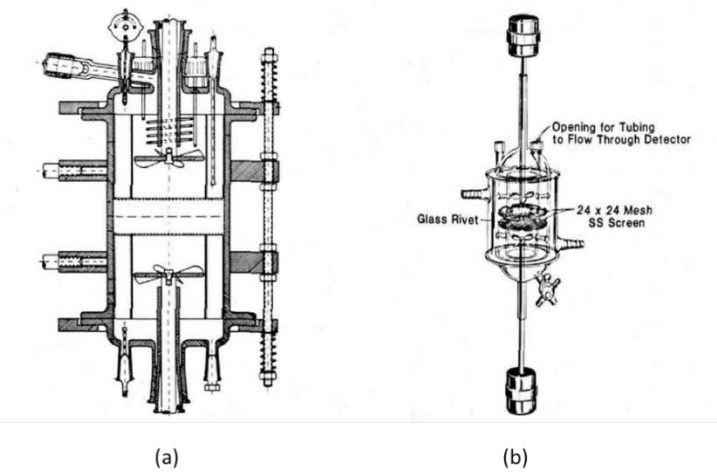

Figure 9: Contacting cell developed by Nitsch[46] (a) and ARMOLLEX cell developed by Danesi (b).[26]

Another modification was done in the framework of Toulemonde's thesis,[22] where the ARMOLLEX cell was replaced by a cell of the same design with magnetic and not mechanical agitation. And the last modification to the ARMOLLEX cell was made by Dal Don,[23] who built the AMADEUS cell (Atalante Modified Armollex Design for Extraction USes). Dal Don modified the inter-grid distance and consequently the distance between the stirring blade and the grid.

This technique allows to control the interfacial exchange surface and to work with a different degree of perturbation in the two phases for liquids of different viscosities thanks to the separate stirring of both phases. In addition, this technique minimises the diffusional limitations on the transfer by setting high agitation speed. Therefore, the chemical regime plateau can be obtained, which permits the identification of the reaction mechanism by studying the dependence of the extraction rate on the chemical composition. However, using these cells is not very suitable to slow kinetics because the interfacial surface is limited by the geometry of the cell (need to reduce the exchange surface for the precision of measurements). In addition, the presence of the grid makes the kinetic study delicate because the hydrodynamics of the fluid near the interface remains poorly known, which can directly affect the mass transfer.

- **Transfer of matter in a stirred cell**

The extraction cells allow the determination of the overall transfer coefficient in both the aqueous and the organic phases. The kinetic model applied to the extraction is also based on the double film theory. The transfer is subject to a diffusional regime in both phases, coupled with a chemical regime due to the chemical transfer reaction at the interface.

The mass balance of the solute to be extracted in the aqueous phase between the instants t and t+dt is expressed by:

$$V_{aq}.\,C_{aq}(t+dt) = V_{aq}.\,C_{aq}(t) + J.\,A.\,dt \tag{55}$$

V_{aq}: Volume of the aqueous phase
C_{aq}: Concentration of the solute in the aqueous phase
t: Contact time
A: Interfacial area
J: Transferred matter flux

Where,

$$J = K_{aq}^{g}\left(C_{aq} - C_{aq}^{*}\right) = K_{org}^{g}\left(C_{org}^{*} - C_{org}\right) \tag{56}$$

And,

$$C_{aq}^{*} = \frac{C_{org}}{D_M} \tag{57}$$

$$C_{org}^{*} = D_M C_{aq} \tag{58}$$

K_{aq}^{g}: Global transfer coefficient relative to the aqueous phase
K_{org}^{g}: Global transfer coefficient relative to the organic phase
C_{aq}: Average concentration of the metal in the aqueous phase
C_{org}: Average concentration of the metal in the organic phase
C_{aq}^{*}: Concentration of the metal in the aqueous phase in equilibrium with the average concentration C_{org} in the organic phase
C_{org}^{*}: Concentration of the metal in the organic phase in equilibrium with the average concentration C_{aq} in the aqueous phase
D_M: Distribution ratio of the metal at equilibrium

The variation of the concentration can be written as follows:

$$-\frac{dC_{aq}}{dt} = \frac{dC_{org}}{dt} = K_{aq}^{g}\frac{A}{V_{aq}}\left(C_{aq} - \frac{C_{org}}{D_M}\right) = K_{org}^{g}\frac{A}{V_{org}}\left(D_M C_{aq} - C_{org}\right) \tag{59}$$

The global mass balance allows us to write:

$$V_{aq}C_{aq,0} + V_{org}C_{org,0} = V_{aq}C_{aq} + V_{org}C_{org} = V_{aq}C_{aq,eq} + V_{org}C_{org,eq} \qquad (60)$$

$C_{aq,0}$: The initial concentration of the metal in the aqueous phase
$C_{org,0}$: The initial concentration of the metal in the organic phase
$C_{aq,eq}$: The concentration of the metal in the aqueous phase.at equilibrium
$C_{org,eq}$: The concentration of the metal in the organic phase.at equilibrium
V_{org}: Volume of the organic phase

Hence,

$$-\frac{dC_{aq}}{dt} = \frac{dC_{org}}{dt} = K_{aq}^{g}\frac{A}{V_{aq}}\left(1 + \frac{1}{D_M}\right)(C_{org,eq} - C_{org}) \qquad (61)$$

After integration and considering that only the aqueous phase initially contains the metal ($C_{org,0} = 0$), the following equation is obtained:

$$\ln\left(\frac{C_{org,eq} - C_{org}}{C_{org,eq} - C_{org,0}}\right) = \ln\left(1 - \frac{C_{org}}{C_{org,eq}}\right) = -\frac{A}{V_{aq}}K_{aq}^{g}(1 + \frac{1}{D_M})t \qquad (62)$$

If the plot of this equation leads to a straight line, then the overall aqueous phase transfer coefficient K_{aq}^{g} can be determined from the slope.

3. High-speed stirring apparatus

This apparatus was first developed by Carter and Freiser.[47] to eliminate the erratic behaviours of the fast reactions while working in batch shakers, previously reported.[11,12,48] It consists of a 500 mL Morton flask fitted with a high-speed vacuum stirrer (0-20000 rpm) (Figure 10). The concept of this methodology relies on the fact that under a high specific interfacial area, the solute can adsorb at the interface. This can result in a decrease in the bulk phase concentration. This decrease in concentration in the organic or aqueous phase caused by interfacial adsorption can be measured spectrophotometrically after continuous phase separation. The total interfacial amount is calculated from the decrement in the absorbance of the bulk phase. Under stirring, the interfacial area can be evaluated by dividing the total interfacial amount at saturation by the saturated interfacial excess determined from an independent measurement of interfacial tension. This device was further improved by Watarai et al.[49] A Teflon phase separator was introduced, as well as an online minicomputer was installed, which permit continuous monitoring of the rate of extraction and instantaneous data analysis.

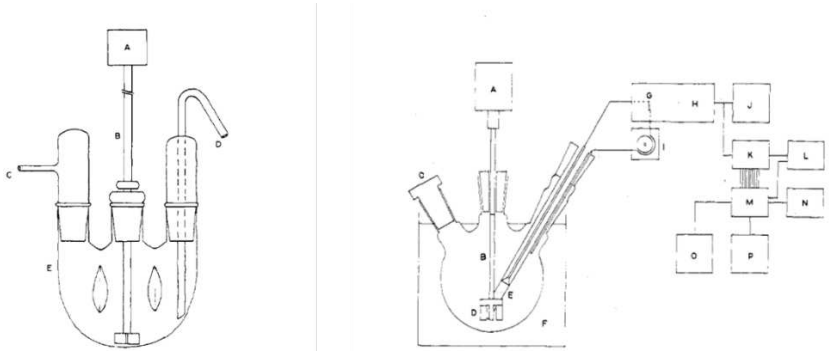

Figure 10: Carter and Freiser version of the high-speed stirrer apparatus[47] (On the left) and Morton flask apparatus with high-speed-stirrer[49] (on the right).

B. Techniques involving a third medium

1. Rotating Diffusion Cell (RDC)

Electrochemists have used the rotating disc electrode for many years.[45] After successfully adaptating of a Stokes diffusion cell for interfacial kinetic measurements, Albery et al.[50] created the rotating diffusion cell (RDC).

The RDC is derived from the Lewis cell, however, in contrast to the latter, it includes two separate compartments into which the two solution phases are placed. A porous membrane filter mounted at the lower open end of the inner cylinder separates an inner rotating cylinder containing the organic solution phase, and an outer non-rotating reaction vessel, containing the aqueous solution phase (Figure 11). The mounted porous membrane is treated with clearing solvent to selectively reduce the porosity around the membrane while maintaining a central porous disc.[51] This disc provides a defined surface interface between the two phases, through which species transport can be studied.

We mention that the study of coupled interfacial-mass transfer kinetics of several organic extractants, *i.e.* TBP, TODGA, has been carried out using this technique.[51,52]

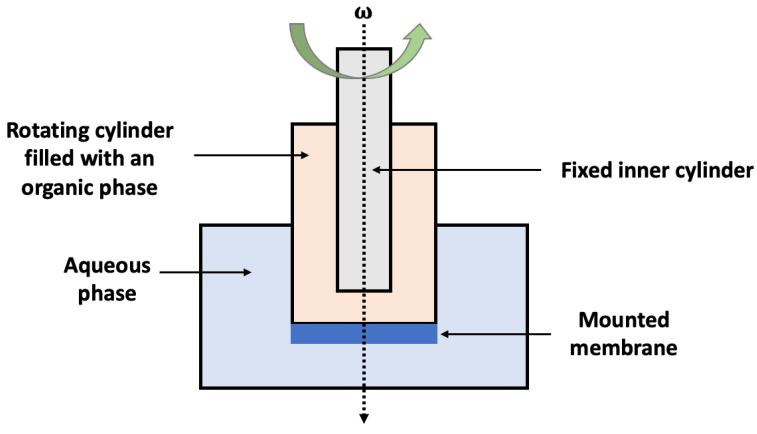

Figure 11: Rotating diffusion cell.

2. Rotating Stabilized Cell (RSC) and Rotating Membrane Cell (RMC)

Inspired by the short contact methods promoted by the Soviet School, Simonin first developed the RSC (Rotated Stabilized cell), replacing the RDC with a capillary filled with an aqueous phase gelled with polyacrylamide gel.[53] This technique allows the determination of the species transferred upon contact by analyzing the polyacrylamide gel in the capillary by radiometry. However, it was found that the gel could modify the interfacial transfer of species.

In this respect, Simonin developed the rotating membrane cell (RMC), which is a method that involves a membrane impregnated with an aqueous or organic phase in which a microporous membrane immobilizes this phase.[54] To better control the hydrodynamics of the cell and to avoid possible interactions due to the amide type gel, the latter was replaced by a hydrophilic membrane of about 120 µm thickness glued to the base of the rotating cylinder.

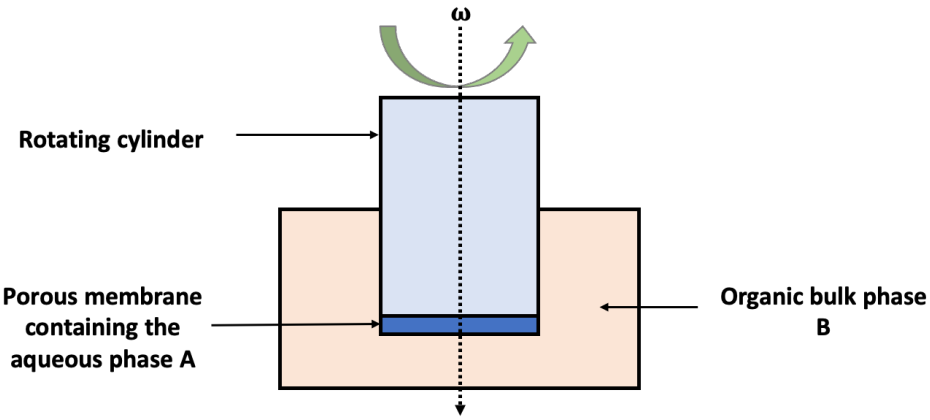

Figure 12: Sketch of the RMC technique.

The principal characteristic of RMC is that transport is controlled in both phases. In the aqueous phase A, the transport is purely diffusive. It follows the classical Fick's law with a diffusion coefficient that considers the membrane's tortuosity. In the organic phase B, a convective transport process is created, which is favoured by the hydrodynamics in this phase. The diffusion coefficients in both phases are necessary to determine the transport contributions.

- **Modelling**

Assuming that the complexation reaction is strictly interfacial, the ratio of extracted matter as a function of time can be written as:[54]

$$P(t) = 1 - \exp\left(-t/\tau\right) \qquad (63)$$

Where τ is the average-passage time of the solute in the overall A to B transfer process,

$$\tau = \tau_A + \tau_i + \tau_B \tag{64}$$

Where, τ_A is the average diffusion time in phase A (membrane), τ_i is the characteristic time for the interfacial reaction (from A to B), and τ_B is the average residence time of the solute in the diffusion layer.

These times are expressed as follows,

$$\tau_A = {}^{L^2\theta}/_{(3\mathcal{D}_B)} \tag{65}$$

$$\tau_i = {}^{L}/_{k_f} \tag{66}$$

$$\tau_B = {}^{\sigma L\delta_B}/_{(K\,\mathcal{D}_B)} \tag{67}$$

Where L is the membrane thickness, θ is the tortuosity, $\mathcal{D}_A$ and $\mathcal{D}_B$ are the solute diffusion coefficients in the bulk of phases A and B, respectively, k_f is the forward kinetic rate constant (from A to B) σ is the membrane porosity, and δ_B is the diffusion layer thickness in phase B.

The distribution ratio K satisfies the relation:

$$K = \frac{k_f}{k_r} \tag{68}$$

With k_r is the kinetic constant for the reverse B to A chemical reaction.

In the case of infinitely fast interfacial kinetics, k_f and $k_r \to \infty$ with K unchanged, the process becomes diffusion controlled, and Eq. 64 reduces to,

$$\tau = \tau_A + \tau_B \tag{69}$$

According to Eq. 63, a fit of the experimental results for $-\ln(1-P)$ versus time yields a curve and its slope τ^{-1}.

In the case of diffusional limitation, this curve has a maximum slope equal to τ_∞^{-1} reflecting the diffusional limit.

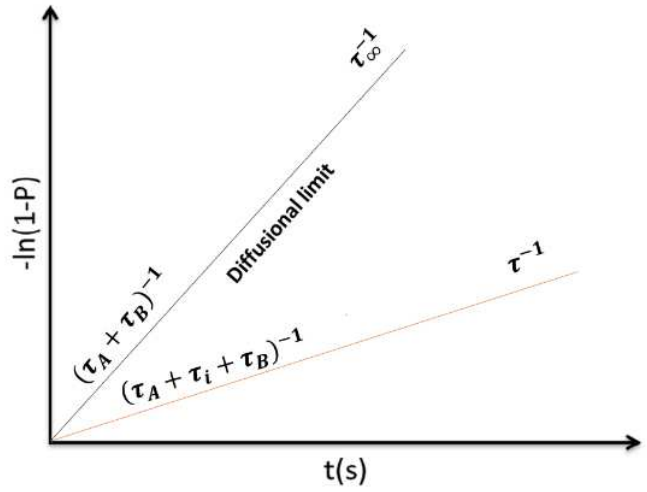

Figure 13: -ln(1-P) in function of time for the experiments with RMC.[54]

The main features of the RMC are the control of hydrodynamic in the two phases, simplicity of the setup, and transfer occurring in a transient regime, limited by the kinetics of the chemical reactions at the beginning of the transfer process. It also requires small volumes (Few microliters of the phase A deposited on the membrane and 5 ml of the phase B). Therefore, this technique constitutes a simple tool for the identification of purely interfacial reactions. However, the relative uncertainty of using this technique lies in the presence of the membrane, of which the molecular composition is poorly known (protected by the Millipore patent). It may intervene in the extraction of the solute (affinity with the extractant, the solute and the sulfonate groups grafted on the Teflon skeleton of the membrane). In parallel, the macroscopic pore size of about 0.5µm strongly limits the potential effect of the membrane on transfer. Moreover, this type of membrane has very poor adsorption properties. Finally, the small amount of phase deposited on the membrane requires sensitive analytical techniques.

C. Conclusion and choice of the technique for our study

As we presented in the section above, several techniques have been developed to study the extraction kinetics. In general, when choosing a technique, one should find a compromise between these parameters:

- Accurate evaluation and control of the interfacial area
- Perfect control of the hydrodynamics
- Precise determination of the extraction kinetics regime (diffusional or chemical)
- Sufficient agitation to suppress the diffusional limitations and reach the chemical extraction kinetics regime (case of stirred cells)
- Low consumption of organic and aqueous phases, and time-saving techniques

In Table 1, we summarize some of the pros and cons of some of the most used techniques for studying the extraction kinetics.

Table 1: Summary of the pros and cons of the most used techniques to study experimentally the extraction kinetics.

	Pros	**Cons**
Single drop technique	• Droplet size control and known interfacial area • Easy to use equipment • Possible analysis of the phases at the exit of the column *i.e.* UV-Vis	• Difficult to know the hydrodynamics at the surface and inside the droplets • Not suitable for very fast and very slow reactions (ideally 10^{-4} m.s^{-1} < K_g < 10^{-7} m.s^{-1})
Modified Lewis type cells (Nitsch Cell, ARMOLLEX cell, AMADEUS cell)	• Mastering the interfacial area • Independent phase stirring and Reynolds number control • Minimization of the contribution of diffusion	• The movement of the fluid in the interface vicinity is poorly understood (presence of grid) • Not suitable for neither fast nor slow extraction kinetics (order of magnitude not defined)
RMC	• Good control of hydrodynamics • Good characterization of the chemical reaction taking place • Easy assembly technique and low consumption of materials • Minimization of the contribution of diffusion	• Presence of a membrane (possible interaction) • Pores size of the membrane may be limiting • Requirement of sensitive analytical techniques

According to the experience already mastered at the CEA, the choice was made for the single drop technique for the kinetic characterization in our research. This technique presents a compromise between diffusional and chemical effects since an apparent global transfer constant is determined. In addition, precise knowledge of the interfacial area is possible, which is a must for our study. On the other hand, this technique is the most representative of the hydrodynamic phenomena occurring in industrial contactors. Furthermore, using models and empirical correlations makes it possible to characterize the molecular diffusion coefficient in each phase, which seems interesting for further identification of the extraction kinetics regime.

IV. The interfacial activity of the extractants

Having outlined the experimental tools for the study of the extraction kinetics, it is time to start shedding light on the comprehension of the chemical contributions to the extraction rate. If the diffusional contribution can be controlled (totally or not) with the experimental technique used (agitation, known size pores, *etc*.), understanding the chemical contribution is more subtle. This one is related to several parameters that must be taken into account. A major difficulty in the field of extraction kinetics is the localization of the rate-limiting step for the extraction reaction. Indeed, it can take place at the interface or in one of the bulk phases. In this regard, the interfacial activity of the extractants remains a crucial parameter to study in order to apprehend a more fundamental understanding of the extraction systems. Therefore, in this section, we detail the interfacial activity of the extractants, how surface tension measurements can serve to characterize it, as well as the parameters affecting it. Finally, we give some insights into the interfacial extraction reactions.

Osseo-Assare was the first to review the micellization phenomena for solvent extraction in 1991, where similarities between surfactant and extractant molecules were explained.[55] Almost all types of hydrophobic extractants of metals show an amphiphilic behaviour, due to the presence of long hydrophobic groups, usually an alkyl chain, and some hydrophilic moieties responsible for the extraction of the metals.[56] The supramolecular organization of extractants in organic solvent was evidenced in several publications.[57–60] The similarities between surfactant and extractant range from the molecular to the macroscopic level. At the molecular scale, the presence of a polar chelating part and an alkyl chain confer an amphiphilic behaviour for the molecule. At the macroscopic scale, the presence of extractants decreases the water-oil surface tension. In a similar way to more classical amphiphilic molecules, when the concentration of extractant molecules is increased, several states of aggregation are encountered with the extractant in organic solvent:[61]

- When the chemical potential is beyond a certain threshold, the molecules are present mainly as monomers.
- Above a certain threshold known as the critical micellar concentration (CMC), progressive aggregation occurs in distinct aggregates containing an average number N of the extractants.

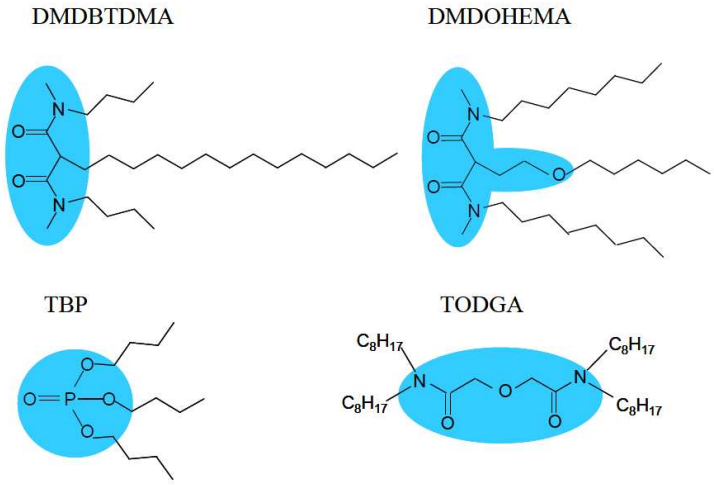

Figure 14: Amphiphilic structure of some extractants, the presumed polar groups are coloured in blue.

A. Surface tension

The interfacial tension characterizes the asymmetry of the forces exerted on a molecule at the interface compared to the force it would experience in the bulk of the solution. These forces oppose the increase of the interfacial area.[62,63]

Consider an enclosure of volume V, containing components i, separated into two phases I and II, with an area of the surface that separates them equal to A. The surface energy σ is defined by:[63]

$$\sigma_{I-II} = \left(\frac{\partial F}{\partial A}\right)_{T,V} \quad (70)$$

The interfacial tension has the dimension of energy divided by a surface. It is expressed in J/m^2. It can also be seen as a force per unit length, expressed in $mN.m^{-1}$.

The interfacial tension measurements serve to estimate various adsorption parameters. The most important parameters are the interfacial concentration and the molecular area of the molecule in the adsorption layer.[56]

The amount of surfactant adsorbed at a liquid/liquid interface can be described by the Gibbs adsorption isotherm:

$$\Gamma = \frac{-1}{RT}\left(\frac{\partial \sigma_i}{\partial \ln_C}\right)_T \quad (71)$$

Γ: The surface excess (mol/m^2)
σ_i: The interfacial tension ($mN.m^{-1}$)
R: The gas constant ($J.K^{-1}.mol^{-1}$)
T: The absolute temperature (K)
C: The bulk organic phase concentration (mol/m^{-3})

The plot of σ_i against the concentration of the surfactant (lnC) yields a curve, which its slope at any point permits the estimation of the surface excess. This surface excess can be assimilated to the surface concentration in the case of dilute solutions and for sufficiently surface-active compounds.

The area available per molecule at the interface 'a_i (m^2/molecule)' is calculated from the surface excess concentration:

$$a_i = \frac{1}{N_A \Gamma} \tag{72}$$

Where, N_A denotes the Avogadro number.

However, for the discussion of interfacial kinetics, the excess surface isotherm is needed. This isotherm can be obtained from empirical, semi-empirical or theoretical equations of the relation $\sigma = f(\ln C)$.[56]

Among the several equations often used, we cite Szyszkowski and Langmuir-Gibbs equation.[56]

1. The Szyszkowski equation

$$\sigma = \sigma_0[1 - B_{sz} \ln\left(\frac{C_0}{A_{sz}} + 1\right)] \tag{73}$$

Where, σ_0 is the interfacial tension at the aqueous/organic interface in the absence of the extractant, σ is the interfacial tension at the aqueous/organic interface for a given concentration of the ligand in the organic phase. A_{sz} and B_{sz} are Szyszkowski parameters. These parameters allow the calculation of the extractant interfacial adsorption equilibrium constant K_{ads}, and solute surface excess concentrations Γ^{∞}:

$$K_{ads} = \frac{1}{A_{SZ}} \tag{74}$$

$$\Gamma^{\infty} = \sigma_0 B_{SZ}/RT \tag{75}$$

The interfacial activity can also be defined in function of the interfacial pressure. Therefore, the semi empirical Szyszkowski can also be written as follows:

$$\Pi = \sigma_0[B_{SZ} \ln\left(\frac{C_0}{A_{SZ}} + 1\right)] \tag{76}$$

Where Π (mN.m^{-1}) is the interfacial pressure, defined as follows:

$$\Pi = \sigma_0 - \sigma \quad (77)$$

2. The Langmuir-Gibbs equation

$$\sigma = \sigma_0 + RT\Gamma^{\infty}\ln\left(1 - \frac{\Gamma}{\Gamma^{\infty}}\right) \quad (78)$$

Where, Γ^{∞} denotes the surface excess at the saturated interface. This equation is equivalent to Szyszkowski isotherm when $B_{sz} = \Gamma^{\infty}$, $A_{sz} = {}^{1}/_{K_{ads}}$ and ${}^{\Gamma}/_{\Gamma^{\infty}}$ is given by the Langmuir isotherm,

$$\Gamma = \Gamma^{\infty}\left[\frac{K_{ads}C}{K_{ads}C + 1}\right] \quad (79)$$

Where, K_{ads} is the adsorption constant.

In addition, coupling the nonlinear optical technique with the tensiometry has proved promising for better characterizing the interface.[62,63] Furthermore, the structure of the interface can be studied from a theoretical point of view by molecular dynamics that allows simulating of atomic trajectories from the forces exerted on each atom.[64]

B. Parameters affecting the interfacial activity of extractants

The extractant hydrophobicity and the alkyl chain's length directly influence the distribution of the extractant and its adsorption at the interface.[65] Thus, this affects the interfacial properties, including the interfacial tension, the interfacial concentration of the extractants and their orientation at the interface. For instance, in the case of *N,N'*- dialkylamides, it was found that the increase in the chain length for both the acyl chain and the nitrogen side chain increased the hydrophobicity, which increased the interfacial tension.[66]

Besides the extractant's structure, the extractant's hydrophobicity and its interfacial activity depend on the nature of the environment in both the organic and the aqueous phases. The length and the structure of the hydrocarbon chain and the diluent aromaticity affect the penetration of the adsorption layers with the diluent.[67] Thus, hydrocarbons with short and straight chains penetrate more easily the interfacial layers than those with long branched alkyl groups. In parallel, aromatics show a strong affinity for the aqueous phase, so a competitive interaction with water molecules with the hydrophobic extractants takes place at the interface. Thus, the interfacial zone is swollen with aromatics, with a decrease in the interfacial concentration of the molecules, and the hydrophilic molecules are dragged out

from the aqueous interfacial layer. The extractant molecules in such cases are less oriented to the interface than the system comprising an aliphatic diluent.[65] For instance, the interfacial activity of hydroxyoximes at the toluene/water interface is lower than at the octane/water interface.[56] In addition, the interfacial activity of D2EHP was higher at heptane/1M HNO_3 interface than that at toluene/1M HNO_3 interface.[68] And faster extraction of nickel, cobalt and copper with HDEHP was observed when using heptane as diluent instead of benzene or toluene.[28]

In addition, the composition of the aqueous phase affects the hydration, protonation and dissociation of the polar groups, as well as a change in the interfacial pH. It has been reported that these factors increase the polarity of the extractant molecules.[65] As a result, this makes the extractant species less compatible with the nonpolar organic phase on the one hand and enhances the attractive interaction between extractant and water molecules on the other. Therefore, an increase in adsorption is obtained due to the increase in forces that attract extractant molecules from the bulk organic phase to the interfacial region.

The effect of acidity on the surface tension was reported for several extractants. However, different observations were reported. For instance, the increase in nitric acid concentration in the aqueous phase induced a decrease in the interfacial tension of DEHiBA in dodecane.[69] The authors explained that HNO_3 strongly perturbs the interface due to the chaotropic behaviour of the nitrate anions. In parallel, the surface tension of a series of *N,N'*-dialkylamides increased when the aqueous equilibrium phase was nitric acid instead of water. This was related to the increase of polarity of the extractant after its protonation.[66] However, for the case of D2HPA in heptane, the increase of acidity decreased the interfacial activity.[68] The authors explained that this was induced by forming the weak polar adduct P=O…HNO_3. In the case of diamides, their protonation increases their surface-active properties and a decrease in the monomer concentration.[60] However, the contrary was observed with TBP, where the CMC increases with increasing nitric acid concentration. It was also reported that the functional P=O group of neutral organophosphorus compounds bound to HNO_3 are less surface-active than the P=O groups coordinated to the water molecules.[70]

Bulky, heavily substituted extractant molecules would be expected to occupy more interfacial area per molecule than unsubstituted ones. Therefore, the extraction rate should increase with diminishing interfacial area per molecule, increasing bulk phase extractant concentration and decreasing solvency of the diluent.[71]

C. Interfacial reaction

There has been an agreement about the interfacial nature of the rate-determining step for many commercial extractants.[16,25,72] This conclusion was derived from the interfacial activity and the very low

aqueous distributions of the extractants, and the dependence of the extraction rate on the volume of the phases and the interfacial area.

Some authors reported that the formation of metal complexes by an interfacial pathway proceeds through an intermediate metal complex at the interface. For instance, it was reported that the extraction of Am(III) and Eu(III) with HDEHP consisted of a series of interfacial reactions, where the metal cation reacts with the interfacially adsorbed ligand to form an interfacial complex.[73] In addition, the formation of the copper (II) complex with 5-nonyl-2-hydroxybenzaldoximes (P50) was explained by a fast formation of an intermediate $[Cu(P50)]^+$, which lifetime is long enough to enable a second extractant to react with it, to form a neutral complex.[25] Therefore, at low bulk extractant concentration, the rate-determining step is the diffusion of the second extracting molecule from the bulk organic phase to a position in the interfacial region adjacent to the cationic intermediate. In parallel, some authors elucidated some differences in the interfacial behaviour of the intermediate complexes. Where interfacial tension measurements at different pH and different metal concentrations revealed that the copper extraction with D2EHPA, non-surface-active 1:2 intermediate complexes were formed and dissolved rapidly into the organic phase. Whereas for iron, surface-active 1:2 intermediate complexes were formed and adsorbed at the interface, which resulted in slowing the extraction rate.

D. Conclusion

In this section, we explained the interfacial activity of the extractants at the liquid/liquid interface. Despite the several tools available to characterize the interfacial activity of the extractants, particular attention was given to the surface tension measurements. Therefore, several models predicting the interfacial behaviour of the ligands were presented. In our research, we were interested in identifying the interfacial behaviours of the employed ligands. These investigations were conducted through surface tension measurements. The identification of the interfacial activity of the ligands provides insights into the location of the rate-limiting step, which could be helpful for the description of the extraction mechanism, which will be presented below.

V. Rate laws and extraction mechanisms

In general, after defining the interfacial behaviour of the ligands being studied, the kinetic study is completed with a determination of the extraction rate law and then the extraction mechanism. As a general rule, when describing solvent extraction reaction mechanism, one should consider that the solute transfer takes place between two phases through an extractant across the interface. Thus, a careful study of the mechanisms of chemical reactions that either could occur in the two bulk phases or at the interface must be carried out.

In this section, we explain the extraction rate law, and then we present some of the relevant extraction mechanisms reported in the literature.

A. Rate law

Consider a reaction with the stoichiometric equation:

$$aA + bB = cC + dD \tag{80}$$

The rate of the reaction is expressed as follows:

$$v = -\frac{1}{a}\frac{d[A]}{dt} = -\frac{1}{b}\frac{d[B]}{dt} = \frac{1}{c}\frac{d[C]}{dt} = \frac{1}{d}\frac{d[D]}{dt} \tag{81}$$

The rate law of a chemical reaction arises from a mathematical equation that represents how the reaction rate relies on the concentration of each reactant, and it is expressed as follows:[73]

$$-\frac{d[A]}{dt} = k[A]^{\alpha}[B]^{\beta} \tag{82}$$

Where α, β represent the partial orders of the reaction. These partial orders values can whether an integer or not. This depends on the complexity of the reaction mechanism.

Several methods can be used to determine the rate law experimentally *i.e.* initial rate method, integration method, graphical method, *etc.*

After determining of the rate law, the correlation with a correspondent mechanism is the next step. There should be no surprise when more than one mechanism are proposed for a given reaction when proposing a mechanism. Indeed, any new information on the studied system may lead to a new conclusion and a better understanding of the description of the reaction.

B. Mechanisms in solvent extraction

In their review, Danesi et al.[31] gave a detailed explanation about the different extraction mechanisms that can take place in solvent extraction systems depending on the nature of the extractant. Hence, insights about the possible extraction mechanisms for acidic, basic and neutral extractants were given. Besides the nature of the extractant, its solubility in the aqueous phase is an important criterion to take into account. The limiting extraction reaction could take place in the aqueous phase for an extractant soluble in the aqueous phase. Likewise, interfacial tension measurements and the ability of a ligand to adsorb at the interface are also key parameters to investigate. High amphiphilic properties of an extractant leads to a saturation of the interface with the ligand even at a low concentration in the bulk

phase. As a result, the complexation reaction will take place at the interface. This may result that the limiting step being the complexation itself at the interface or the adsorption-desorption of the complexing reagent at and from the interface.

Herein, we will present some of the proposed mechanisms with an acidic extractant.

1. Slow step in the aqueous phase

This mechanism is possible when the extractant is soluble in the aqueous phase. Thus, consider an acidic extractant HB and metal ion with an oxidation state +III.

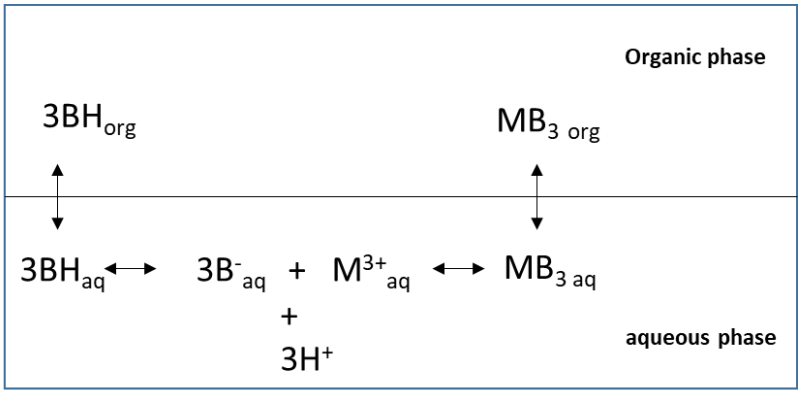

Figure 15: Extraction of the metal M^{3+} with HB, with a slow step in the aqueous phase.

The extraction system will be described with the following equations:

$$HB_{org} \underset{k_{-1}}{\overset{k_1}{\rightleftharpoons}} HB_{aq} \qquad \textit{(Fast)} \qquad (83)$$

$$D_{HB} = \frac{[HB]_{org}}{[HB]_{aq}} \qquad (84)$$

$$M^{3+}_{aq} + HB_{aq} \underset{k_{-2}}{\overset{k_2}{\rightleftharpoons}} MB^{2+}_{aq} + H^{+}_{aq} \qquad \textit{(Slow)} \qquad (85)$$

$$K_2 = \frac{[MB^{2+}]_{aq}[H^{+}]_{aq}}{[M^{3+}]_{aq}[HB]_{aq}} \qquad (86)$$

$$MB^{2+}_{aq} + 2HB_{aq} \underset{k_{-3}}{\overset{k_3}{\rightleftharpoons}} MB_{3\ aq} + 2H^{+}_{aq} \qquad \textit{(Fast)} \qquad (87)$$

$$K_3 = \frac{[MB_3]_{aq}[H^+]^2_{aq}}{[MB^{2+}]_{aq}[HB]^2_{aq}} \tag{88}$$

$$MB_{3\,aq} \underset{k_{-4}}{\overset{k_4}{\rightleftharpoons}} MB_{3\,org} \qquad (\textit{Fast}) \tag{89}$$

$$K_4 = \frac{[MB_3]_{org}}{[MB_3]_{aq}} \tag{90}$$

Thus, the rate law that describes the extraction kinetics is:

$$v = -\frac{d[M^{3+}]_{aq}}{dt} = \frac{k_2}{D_{BH}}[M^{3+}]_{aq}[HB]_{org} - \frac{k_{-2}D^2_{HB}}{K_3K_4}\frac{[MB_3]_{org}[H^+]^3_{aq}}{[HB]^2_{org}} \tag{91}$$

If the hydrolyzed ion metal has been extracted, then the following rate law will be written as follows:

$$M^{3+}_{aq} + OH^- \underset{k_{-5}}{\overset{k_5}{\rightleftharpoons}} M(OH)^{2+}_{aq} \qquad (\textit{Fast}) \tag{92}$$

$$K_5 = \frac{[M(OH)^{2+}]_{aq}}{[M^{3+}]_{aq}[OH^-]_{aq}} \tag{93}$$

$$M(OH)^{2+}_{aq} + HB_{aq} \underset{k_{-6}}{\overset{k_6}{\rightleftharpoons}} MB^{2+}_{aq} + H_2O \qquad (\textit{Slow}) \tag{94}$$

$$K_6 = \frac{[MB^{2+}]_{aq}}{[M(OH^{2+})]_{aq}[HB]_{aq}} \tag{95}$$

Therefore,

$$v = -\frac{d[M^{3+}]_{aq}}{dt} = \frac{k_6K_6}{D_{BH}}\frac{[M^{3+}]_{aq}[HB]_{org}}{[H^+]_{aq}} - \frac{k_{-6}D^2_{HB}}{K_3K_4}\frac{[MB_3]_{org}[H^+]^2_{aq}}{[HB]^2_{org}} \tag{96}$$

If the extraction reaction occurs with the dissociated form of the extractant, the rate law will be as follows:

$$HB_{aq} \underset{k_{-6}}{\overset{k_6}{\rightleftharpoons}} B^-_{aq} + H^+_{aq} \qquad \textit{(Fast)} \qquad (97)$$

$$K_a = \frac{[B^-]_{aq}[H^+]_{aq}}{[HB]_{aq}} \qquad (98)$$

Thus,

$$v = -\frac{d[M^{3+}]_{aq}}{dt} = \frac{k_2 K_4}{D_{BH}} \frac{[M^{3+}]_{aq}[HB]_{org}}{[H^+]_{aq}} - \frac{k_{-2} D^2_{HB}}{K_3 K_4} \frac{[MB_3]_{org}[H^+]^2_{aq}}{[HB]^2_{org}} \qquad (99)$$

In this case, the extraction reaction rate is independent of the interfacial area and the volume of the phases.

2. Slow steps at the interface

Extractants with low solubility in the aqueous phase and high adsorption capacity at the interface often result in slow interfacial reactions mechanisms.

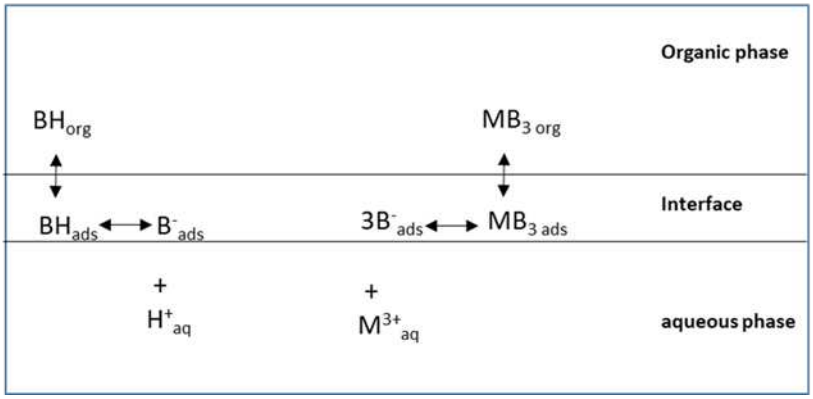

Figure 16: Extraction of the metal M^{3+} with BH with a slow step at the interface.

By applying the Langmuir adsorption isotherm, we obtain:

$$HB_{org} \underset{k_{-7}}{\overset{k_7}{\rightleftharpoons}} HB_{ads} \qquad (100)$$

Where,

$$[HB]_{ads} = \frac{\Gamma^{\infty} K_{ads}[HB]_{org}}{1 + K_{ads}[HB]_{org}} \quad (101)$$

We distinguish two cases: Ideal adsorption and complete saturation.

- **Ideal adsorption**

$$1 \gg K_{ads}[HB]_{org} \quad (102)$$

Then,

$$[HB]_{ads} = \Gamma^{\infty} K_{ads}[HB]_{org} \quad (103)$$

- **Complete saturation of the interface**

$$1 \ll K_{ads}[HB]_{org} \quad (104)$$

Then,

$$[HB]_{ads} = \Gamma^{\infty} \quad (105)$$

We limit our explanation just for the description of the mechanism that takes place if the reaction of complexation of the metal with the adsorbed extractant is slow.

$$M^{3+}_{aq} + HB_{ads} \underset{k_{-8}}{\overset{k_8}{\rightleftharpoons}} MB^{2+}_{ads} + H^{+}_{aq} \quad (\textit{Slow}) \quad (106)$$

$$K_8 = \frac{[MB^{2+}]_{ads}[H^{+}]_{aq}}{[M^{3+}]_{aq}[HB]_{ads}} \quad (107)$$

$$MB^{2+}_{ads} + HB_{ads} \underset{k_{-9}}{\overset{k_9}{\rightleftharpoons}} MB^{+}_{2\,ads} + H^{+}_{aq} \quad (\textit{Fast}) \quad (108)$$

$$K_9 = \frac{[MB^{+}_{2}]_{ads}[H^{+}]_{aq}}{[MB^{2+}]_{ads}[HB]_{ads}} \quad (109)$$

$$MB_{2\,ads}^{+} + HB_{ads} \underset{k_{-10}}{\overset{k_{10}}{\rightleftharpoons}} MB_{3\,ads} + H_{aq}^{+} \qquad (\textit{Fast}) \qquad (110)$$

$$K_{10} = \frac{[MB_3]_{ads}[H^+]_{aq}}{[MB_2^+]_{ads}[HB]_{ads}} \qquad (111)$$

$$MB_{3\,ads} + 3HB_{org} \underset{k_{-11}}{\overset{k_{11}}{\rightleftharpoons}} MB_{3\,org} + 3HB_{ads} \qquad (\textit{Fast}) \qquad (112)$$

Therefore, the rate law is expressed as follows:

$$-\frac{d[M^{3+}]_{aq}}{dt} = k_8 \frac{A}{V_a}[M^{3+}]_{aq}[HB]_{ads} - \frac{k_{-8}}{K_9K_{10}K_{11}} \frac{A}{V_o} \frac{[MB_3]_{org}[H^+]_{aq}^3[HB]_{ads}}{[HB]_{org}^3} \qquad (113)$$

- **For ideal adsorption**

$$-\frac{d[M^{3+}]_{aq}}{dt} = k_8 \frac{A}{V_a}[M^{3+}]_{aq}\Gamma^{\infty}K_{ads}[HB]_{org} - \frac{k_{-8}}{K_9K_{10}K_{11}} \frac{A}{V_o} \frac{[MB_3]_{org}[H^+]_{aq}^3\Gamma^{\infty}K_{ads}[HB]_{org}}{[HB]_{org}^3} \qquad (114)$$

- **For a saturated interface**

$$-\frac{d[M^{3+}]_{aq}}{dt} = k_8 \frac{A}{V_a}[M^{3+}]_{aq}\Gamma^{\infty} - \frac{k_{-8}}{K_9K_{10}K_{11}} \frac{A}{V_o} \frac{[MB_3]_{org}[H^+]_{aq}^3\Gamma^{\infty}}{[HB]_{org}^3} \qquad (115)$$

C. Various reported extraction mechanisms

In the literature, extensive data is present about the extraction kinetics and the determination of the extraction mechanisms. It is worth mentioning that the authors claimed that their kinetic investigations were carried out in a kinetic regime for the reported data. In this section, we will present some of the extraction mechanisms found in the literature. We were interested in the case of the rate-limiting step in the aqueous phase and at the interface.

1. Extraction of Zn(II) with thiocarbazones

Starting in the early ’60s, the group of Freiser recognized the vital role of kinetics aspects of extraction processes.[11] They could demonstrate that the rate determining step involved chemical reactions rather than mass transfer and diffusion processes for the metal chelate extraction systems. The

extraction reaction kinetics of Zn(II) with dithizone was studied, and the results indicated the importance of the role of zinc-water bond breaking in the rate-determining step, which has been found to be in the aqueous phase.[11] The kinetic study was carried out by agitating the samples in separatory funnels mounted on a Burrell shaker. The determination of the extraction rates was performed in the plateau region, for which an increase in agitation had no significant effect on the extraction rate. The following rate law has been obtained:

$$-\frac{d[Zn^{2+}]_{aq}}{dt} = k[Zn^{2+}]_{aq}[HDz]_{org}[H^{+}]_{aq}^{-1} \quad (116)$$

McClellan et al.[12] further developed this study. Their investigation aimed to detail the extraction kinetics of Zn(II), Ni(II), Co(II) and Cd(II) with other dithizones, in which the substituents are located such that steric hindrance is a contributing factor to the overall chelate structure. Thus, diphenylthiocarbazone, di-o-tolylthiocarbazone and di-α-naphthylthiocarbazone were chosen for this study. The authors concluded that several steps are involved in the chelate formation, *i.e.* loss of water of the octahedral zinc hexahydrate, the addition of the first ligand and second ligands and change in the structure from the octahedral hexahydrate to the tetrahedral zinc dithizonate. Based on the water removal rate from zinc ion, which was reported by Eigen et al.,[75] the authors expected the step involving the removal of water molecules to be the limiting step. Hence, they proposed this mechanism:

$$HD_{z\,org} \underset{k_{-1}}{\overset{k_1}{\rightleftharpoons}} HDz_{aq} \quad \textit{(Fast)} \quad (117)$$

$$K_{DR} = \frac{[HDz]_{org}}{[HDz]_{aq}} \quad (118)$$

$$HD_{z\,aq} \underset{k_{-2}}{\overset{k_2}{\rightleftharpoons}} H_{aq}^{+} + Dz_{aq}^{-} \quad \textit{(Fast)} \quad (119)$$

$$K_a = \frac{[H^{+}]_{aq}[Dz^{-}]_{aq}}{[HDz]_{aq}} \quad (120)$$

$$Zn(H_2O)_{6\,aq}^{+2} + Dz_{aq}^{-} \underset{k_3}{\overset{k_3}{\rightleftharpoons}} Zn(H_2O)_4Dz_{aq}^{+} + 2H_2O \quad \textit{(Slow)} \quad (121)$$

$$K_3 = \frac{[Zn(H_2O)_4Dz^+]_{aq}}{[Zn(H_2O)_6{}^{2+}]_{aq}[Dz^-]_{aq}} \quad (122)$$

$$Zn(H_2O)_4Dz^+_{aq} \underset{k_{-4}}{\overset{k_4}{\rightleftharpoons}} Zn(H_2O)_2Dz^+_{aq} + 2H_2O \quad \textit{(Fast)} \quad (123)$$

$$K_4 = \frac{[Zn(H_2O)_2Dz^+]_{aq}}{[Zn(H_2O)_4Dz^+_{aq}]_{aq}} \quad (124)$$

$$Zn(H_2O)_2Dz^+_{aq} + Dz^-_{aq} \underset{k_{-5}}{\overset{k_5}{\rightleftharpoons}} Zn(Dz)_{2\,aq} + 2H_2O \quad \textit{(Fast)} \quad (125)$$

$$K_5 = \frac{[ZnDz_2]_{aq}}{[Zn(H_2O)_2Dz^+]_{aq}[Dz^-]_{aq}} \quad (126)$$

The authors explained that the increase in the reaction rate of substituted dithizone with zinc comes from the fact that bulky groups facilitate the removal of water molecules after the addition of the first ligand, relieving steric hindrance by the change from octahedral to a tetrahedral structure.

Thus, the rate law can be written as follows:

$$-\frac{d[Zn^{2+}]_{aq}}{dt} = \frac{K_a k_3 k_4 [Zn^{2+}]_{aq}[HDz]_{org}}{K_{DR}[H^+]_{aq}} \quad (127)$$

It is worth mentioning that the second orders rate constants followed the order observed in the rate of water exchange of the hydrated metal ion, Cd > Zn > Co > Ni, which indicates the importance of the role of the metal-water bond in the mechanism of the formation of the chelates again.

2. Extraction of Fe(III) with TOPO: Reaction of hydrolyzed species

The extraction kinetics of Fe(III) from aqueous perchloric solutions into hexane of trioctylphosphine oxide (TOPO) was investigated.[24] The kinetic study was carried out using test tubes shaken at a speed where the extraction rate was independent of the stirring speed (plateau regime). The authors explained their results in terms of a kinetic extraction regime governed by slow reactions in the aqueous phase. Furthermore, the authors studied the influence of accelerating water-soluble anions (X^-), such as nitrate, chloride and bromide ions. The rate Fe(III) extraction was found to be first order and inverse first order with respect to TOPO and proton concentrations, respectively. Both orders were derived by plotting the logarithm of Fe(III) concentration as a function of time. It is worth mentioning

that the same authors have reported in previous papers a dependence of the rate on $[HA][H^+]^{-1}$ for the extraction of Fe(III) with thenoyltrifluoroacetone (TTA)[76] and with β-diketones. In the case of TTA, this was explained by the following controlling reaction:

$$M^{n+} + A^- \rightleftharpoons MA^{(n-1)+} \tag{128}$$

Whereas, in the case of β-diketones, this was explained by the following controlling reaction:

$$MOH^{(n-1)+} + HA \rightleftharpoons MA^{(n-1)+} + H_2O \tag{129}$$

However, since TOPO is not an acidic extractant, the authors attributed the inverse order of $[H^+]$ to the reactivity of the hydrolyzed species of Fe(III), namely $FeOH^{2+}$, stressing that no conclusion can be drawn from the kinetic data alone. Similarly, the acceleration effect produced by the water-soluble anions (X^-), with the fast formation of the more reactive FeX^{2+} species. Therefore, the rate equation of the extraction reaction was written as follows:

$$-\frac{d[Fe^{3+}]_{aq}}{dt} = k_0[TOPO]_{org}[H^+]_{aq}^{-1} + k_X K_{D,R}^{-1}[FeX^{2+}]_{aq}[TOPO]_{org} \tag{130}$$

Where,

$$K_{D,R} = \frac{[TOPO]_{org}}{[TOPO]_{aq}} \tag{131}$$

3. Extraction of U(VI) with DEHDMBA: Interfacial reaction

The extraction kinetics of U(VI) with DEHDMBA in dodecane was studied using the ARMOLLEX cell.[22] This study was carried out under neutral conditions, where the aqueous phase contained only lithium nitrate, and under acidic conditions, the aqueous phase was nitric acid medium. It was found in both mediums that the extraction reaction was limited by the chemical reaction at the interface. The partial order of the metal was of the first order in both conditions. In parallel, the partial order of NO_3^- decreased from 2.4 in neutral conditions to 1.7 in acidic ones. In addition, a change of the order of the ligand was reported in acidic conditions, where for $[DEHDMBA]_{org} \leq 1$ mol/L, the order was 1.4, and for a higher concentration of DEHDMBA, the partial order was 0. Surface tension measurements showed that, in acidic media, the interfacial tension is lower than that in neutral media, and for the former, a sharp decrease in the surface tension was observed when the concentration of DEHDMBA was greater than 1 mol/L. This was explained that when reaching a concentration of 1 mol/L for the extractant, the interface was saturated.

Therefore, for neutral conditions, the rate law was:

$$r = k[UO_2^{2+}]_{aq}[NO_3^-]_{aq}^{2.4}[DEHDMBA]_{org}^{1.6} \quad (132)$$

And for acidic conditions, the following rate laws were obtained:

- **For $[DEHDMBA]_{org} \leq 1$ mol/L:**

$$r = k[UO_2^{2+}]_{aq}[NO_3^-]_{aq}^{1.7}[DEHDMBA]_{org}^{1.4} \quad (133)$$

- **For $[DEHDMBA]_{org} > 1$ mol/L:**

$$r = k[UO_2^{2+}]_{aq}[NO_3^-]_{aq}^{1.7} \quad (134)$$

Furthermore, the addition of a cationic surfactant cetylmethylammonium bromide ($C_{16}H_{25}SO_3Na$), decreased the transfer of U(VI) upon extraction with DEHDMBA into dodecane. This proved the interfacial localization of the reaction, seeing that the adsorption of the surfactant limited the transfer of the solute.

An absorption-desorption mechanism was supposed to take place at the interface, which consisted of the following steps:

- Adsorption of the surface-active species at the interface
- Formation of an interfacial complex between the metallic cation and the adsorbed extractant molecules at the interface
- Transfer of the interfacial complex to the organic phase and the simultaneous replacement of the vacant site with extractant molecules

For the following equations, M, S and $\bar{a}$ denote the metallic specie $UO_2(NO_3)_2$, the extractant DEHDMBA and the specific interfacial area, respectively. Two major cases were identified: (a) The adsorption reaction takes place at the interface through one single step (b) The adsorption reaction takes place at the interface through two steps.

- **Case 1: Adsorption reaction in one single step**

The adsorption reaction can be written as follows:

$$M_{aq} + 2S_{ads} \underset{k_{-1}}{\overset{k_1}{\rightleftharpoons}} (MS_2)_{ads} \quad (135)$$

$$v_1 = \bar{a} * (k_1[M]_{aq}[S]_{ads}^2 - k_{-1}[MS_2]_{ads}) \quad (136)$$

And then, the desorption of the complex takes place from the interface to the bulk organic phase,

$$(MS_2)_{ads} + 2S_{org} \underset{k_{-2}}{\overset{k_2}{\rightleftharpoons}} MS_{2\,org} + 2S_{ads} \quad (137)$$

$$v_2 = \bar{a} * (k_2[MS_2]_{ads}[S]_{org}^2 - k_{-2}[MS_2]_{org}[S]_{ads}^2) \quad (138)$$

By applying the quasi-stationary state on the adsorbed species:

$$-\frac{d[S]_{ads}}{dt} = +\frac{d[MS_2]_{ads}}{dt} = 0 \quad (139)$$

$$-\frac{d[S]_{ads}}{dt} = \bar{a} * (k_1[M]_{aq}[S]_{ads}^2 - k_{-1}[MS_2]_{ads} - k_2[MS_2]_{ads}[S]_{org}^2 + k_{-2}[MS_2]_{org}[S]_{ads}^2) \quad (140)$$

- **For an ideal adsorption**

If one considers ideal adsorption, then,

$$[S]_{ads} = \Gamma^{\infty} K_{ads}[S]_{org} \quad (141)$$

$$-v_1 = \bar{a} * \left(\frac{k_1 k_2 (\Gamma^{\infty} K_{ads})^2 [M]_{aq}[S]_{org}^4 - k_{-1}k_{-2}(\Gamma^{\infty} K_{ads})^2 [MS_2]_{org}[S]_{org}^2}{k_{-1} + k_2[S]_{org}^2}\right) \quad (142)$$

If the complex formation reaction (Eq. 135) is the rate-limiting step, then,

$$v_1 = \bar{a} * (k_1[M][S]_{ads}^2) = \bar{a} * (k_1(\Gamma^{\infty} K_{ads})^2 [M][S]_{org}^2) \quad (143)$$

If the desorption reaction (Eq.137) is the rate-limiting step, then,

$$v_2 = \bar{a} * (k_2[MS_2]_{ads}[S]_{org}^2) = \bar{a} * \left(\frac{k_1 k_2 (\Gamma^{\infty} K_{ads})^2 [M]_{aq}[S]_{org}^4}{k_{-1} + k_2[S]_{org}^2}\right) \quad (144)$$

➢ **For a saturated interface**

If one considers a saturated interface, then,

$$[S]_{ads} = \Gamma^{\infty} \tag{145}$$

$$v_1 = \bar{a} * (\frac{k_1 k_2 (\Gamma^{\infty})^2 [M]_{aq} [S]_{org}^2 - k_{-1} k_{-2} (\Gamma^{\infty})^2 [MS_2]_{org}}{k_{-1} + k_2 [S]_{org}^2} \tag{146}$$

If the complex formation reaction (Eq.135) is the rate-limiting step, then,

$$v_1 = \bar{a} * (k_1 (\Gamma^{\infty})^2 [M]_{aq}) \tag{147}$$

In parallel, if the desorption reaction (Eq.137) is the rate-limiting step, the authors suggested that the rate also tends to,

$$v_2 = \bar{a} * (k_1 (\Gamma^{\infty})^2 [M]_{aq}) \tag{148}$$

- **Case 2: Adsorption reaction takes place in two steps**

$$M_{aq} + S_{ads} \underset{k_{-3}}{\overset{k_3}{\rightleftharpoons}} (MS)_{ads} \tag{149}$$

$$v_3 = \bar{a} * (k_3 [M]_{aq} [S]_{ads} - k_{-3} [MS]_{ads}) \tag{150}$$

$$(MS)_{ads} + S_{ads} \underset{k_{-4}}{\overset{k_4}{\rightleftharpoons}} (MS_2)_{ads} \tag{151}$$

$$v_4 = \bar{a} * (k_4 [MS]_{ads} [S]_{ads} - k_{-4} [MS_2]_{ads}) \tag{152}$$

And then, the desorption of the complex takes place from the interface to the bulk organic phase,

$$(MS_2)_{ads} + 2S_{org} \underset{k_{-2}}{\overset{k_2}{\rightleftharpoons}} MS_{2\,org} + 2S_{ads} \tag{153}$$

$$v_2 = \bar{a} * (k_2[MS_2]_{ads}[S]^2_{org} - k_{-2}[MS_2]_{org}[S]^2_{ads}) \quad (154)$$

If the first adsorption reaction (Eq. 149) is fast, and the second adsorption (Eq. 151), as well as the transfer of the complex from the interface to the organic phase (Eq. 153), are slow, then,

$$v_4 = \bar{a} * (k_4[MS]_{ads}[S]_{ads}) \quad (155)$$

And,

$$v_2 = \bar{a} * (k_2[MS_2]_{ads}[S]^2_{org}) \quad (156)$$

$$\frac{d[MS]_{ads}}{dt} = 0 = \bar{a} * (k_3[M]_{aq}[S]_{ads} - k_{-3}[MS]_{ads} - k_4[MS]_{ads}[S]_{ads}) \quad (157)$$

$$\frac{d[MS_2]_{ads}}{dt} = 0 = \bar{a} * (k_4[MS]_{ads}[S]_{ads} - k_{-2}[MS_2]_{org}[S]^2_{ads}) \quad (158)$$

Then, v_2 can be written as follows,

$$v_2 = \bar{a} * \frac{k_2 k_3 k_4 [M]_{aq}[S]^2_{ads}}{k_{-3} + k_4[S]_{ads}} \quad (159)$$

- **For an ideal adsorption:**

$$v_2 = \bar{a} * \frac{k_2 k_3 k_4 ((\Gamma^{\infty} K_{ads})^2 [M]_{aq}[S]^2_{org}}{k_{-3} + k_4(\Gamma^{\infty} K_{ads})[S]_{org}} \quad (160)$$

- **For a saturated interface:**

$$v_2 = \bar{a} * \frac{k_2 k_3 k_4 (\Gamma^{\infty})^2 [M]_{aq}}{k_{-3} + k_4(\Gamma^{\infty})} \quad (161)$$

It is worth mentioning that when considering the adsorption steps taking place simultaneously (case 1) and for a saturated interface, the reaction rate was always dependent on the concentration of extractant in the organic phase. However, when considering that the adsorption took place in two steps (case 2) and for a saturated interface, the reaction rate was constant. In conclusion, the authors pointed

out the difficulty of concluding on a single mechanism, which could better describe the interfacial reactions of the extraction of U(VI) with DEHDMBA.

D. Classical techniques for the determination of the reaction rate law

Beyond providing access to the extraction rate, classical contactors have essentially been used to determine the extraction reaction rate laws. The main advantages of these techniques lie in the elimination of the diffusion limitations and in the accurate estimation of the interfacial area. However, the substantial consumption of reagents is considered an important drawback of these techniques.

In addition to the classical contactors, some authors used some 'unconventional techniques' for their kinetic studies. For instance, Albazi and Freiser[77] used vials to study the extraction kinetics of Pd(II) with dioctyl sulfide. In addition, Sekine et al.[24,76,78] used stoppered glass tubes (20mL), with mechanical agitation, for several kinetic investigations. Besides, Honaker and Freiser[11] used separatory funnels to study the extraction kinetics of Zn(II) with dithizone. In addition to determining the partial orders with respect to the present reactants, the authors determined absolute rate constants. It is worth mentioning that for all these studies, the authors have claimed to collect kinetic data in the plateau regime. However, in their review, Danesi et al.[31] pointed out that the lack of hydrodynamics control for the extraction systems could induce some ambiguities in the reported results by considering that the chemical regime was not accurately reached.

In Table 2, we summarize some of the reported studies using classical contactors, with a focus on the volumes of phases used to accomplish the investigation. We mention the indicated volumes are the volumes of each phase used.

Table 2: Various reported rate laws using classical contactors.

Authors	Solute	Extractant	Device	Feeds volumes	rate law
Toulemonde[22]	U(VI)	DEHDMBA in dodecane	ARMOLLEX	75 mL	In lithium nitrate medium: ($[LiNO_3]_{aq}$ 1M) $r = k[UO_2^{2+}]_{aq}[NO_3^-]_{aq}^{2.4}[DEHDMBA]_{org}^{1.6}$ In nitric acid medium: ($[HNO_3]_{aq}$ 4M) For [DEHDMBA]org ≤ 1mol/L $r = k[UO_2^{2+}]_{aq}[NO_3^-]_{aq}^{1.7}[DEHDMBA]_{org}^{1.4}$ For [DEHDMBA]org > 1mol/L $r = k[UO_2^{2+}]_{aq}[NO_3^-]_{aq}^{1.7}$
Dal Don[23]	Nd(III)	DBMA in HTP	AMADEUS	35 mL	$r = k[Nd^{3+}]_{aq}[NO_3^-]_{aq}^{2.9}[DBMA]_{org}^{1.1}$
Komasawa et al.[28]	Cu(II) Co(II) Ni(II)	HDEHP in heptane, benzene and toluene	Lewis cell	265 mL	$r = k_1[Cu^{2+}]_{aq}[H^+]_{aq}^{-2}[HDEDHP]_{org}^{2}$ $r = k_2[Co^{2+}]_{aq}[H^+]_{aq}^{-2}[HDEDHP]_{org}^{2}$ $r = k_3[Ni^{2+}]_{aq}[H^+]_{aq}^{-2}[HDEDHP]_{org}^{3}$ $[NO_3^-]_{aq}^{-0.57}$
Daoud et al.[27]	U(IV)	TBP in kerosene	Lewis cell	20 mL	$r = k[TBP]_{org}$
Lou et al.[79]	Re(VII) Mo(VI)	Triakylamine in heptane	Lewis cell	98 mL	$r = k_1[ReO_4^-]_{aq}[RNH_3Cl]_{aq}^{0.91}[Cl^-]_{aq}^{-0.71}$ $r = k_2[Mo_7O_{24}^{6-}]_{aq}[RNH_3Cl]_{aq}^{0.71}[Cl^-]_{aq}^{-0.74}$
Fuerstenau et al.[80]	Cu(II)	Aliquat 336 in xylene	Lewis cell	125 mL	$r = k[CuCl_4^{2-}]_{aq}[R_4NCl]_{org}$
Zhao et al.[81]	Ce(IV)	D2EHPA in heptane	Lewis cell	105 mL	$r = k[Ce^{4+}]_{aq}[[NO_3^-]_{aq}^{-0.57}$
Baba et al.[82]	Pd(II)	DHS in toluene	Batch type stirred glass cell	300 mL	At low concentration of DHS $r = k[Pd^{2+}]_{aq}[DHS]_{org}^{2}$ At high concentration of DHS $r = k'[DHS]_{org}$
Inoue et al.[83]	Pd(II)	Hydroxyoxime in MSB 210 (Shell chemical)	Batch type stirred glass cell	250 mL	$r = k[Pd^{2+}]_{aq}[Oxime]_{org}[H^+]_{aq}^{-1}[Cl^-]_{aq}^{-2}$
E El-Hefny et al.[84]	Gd(III)	HDEHP in kerosene	Single drop technique	Large volumes*	$r = 2.24 * 10^{-3}[Gd^{3+}]_{aq}[NO_3^-]_{aq}[H^+]_{aq}^{-1}$
Awwad et al.[85]	Ti(IV) Fe(III) V(V) Cr(III	D2EHPA in Kerosene	Single drop technique	Large volumes*	r= $k_1[Ti^{4+}]_{aq}[HCl]_{aq}[D2EHPA]_{org}$ $r = k_2[Fe^{3+}]_{aq}^{0.4}[HCl]_{aq}[D2EHPA]_{org}^{0.49}$ $r = k_3[V^{5+}]_{aq}^{0.37}[HCl]_{aq}[D2EHPA]_{org}^{0.48}$ $r = k_4[Cr^{3+}]_{aq}^{0.05}[HCl]_{aq}[D2EHPA]_{org}^{0.5}$
Awwad et al.[86]	U(VI)	Triphenylphosphine in toluene	Single drop technique	Large volumes*	$r = k[U^{6+}]_{aq}[HNO_3]_{aq}[TPPO]_{org}$
Preston et al.[87]	Cu(II)	Ortho-hydroxyoxime in toluene	Single drop technique	Large volumes*	r = $k[Cu^{2+}]_{aq}[HA]_{ads}^{2}[H^+]_{aq}^{-1}$
Biswas et al.[88]	Mn(II)	D2EHPA in kerosene	Single drop technique	Large volumes*	$r = 10^{-6.35}[Mn^{2+}]_{aq}[H_2A_2]_{org}[H^+]_{aq}^{-1}$

*Large volumes (V > 500 mL)

E. Conclusion

In conclusion, numerous mechanisms have been reported in the literature. However, we have presented some of them, focusing on the rate-limiting step in the aqueous phase or at the interface. As shown in the section above, in some cases, the authors were able to propose an extraction mechanism that can explain the rate law, based on certain assumptions made either for the nature or the localization of the rate-limiting step. In contrast, in other cases, the authors could not propose a plausible mechanism for the studied extraction reactions. This confirms the subtlety of this study and the versatility of proposing extraction mechanisms. The reason for presenting this section is that in our research, we were interested in explaining the extraction mechanisms of the studied systems, and different cases were discussed following the literature.

On the other hand, we have emphasized the use of macroscopic tools to determine rate laws, which is commonly reported in the literature. However, using these tools could sometimes be limiting due to the large volumes needed to perform the study. Indeed, this criterion was essential and was mainly considered in our research, which has led us to find an alternative for determining the rate laws for the systems studied.

VI. Enhancement of the extraction rate of metal ions

Slow extraction kinetics can limit the extraction performance of any system. However, identifying the rate-limiting step of an extraction reaction can be an asset in improving the extraction performance. Hence, in this section, we show some of the reported studies to enhance of the extraction kinetics of some given systems.

The change of the composition of the system, by introducing some additives in order to accelerate the rate-limiting step, has proven to be very efficient for the enhancement of the extraction rate. The extraction rate of Fe(III) with TTA from perchloric acid was reported to be slow, and that the rate-determining step was the formation of Fe-TTA complex in the aqueous phase.[89] The addition of thiocyanate was found to enhance the rate of extraction of $Fe(TTA)_3$ significantly. This was attributed to the replacement of the slow formation of Fe-TTA complex in the aqueous phase by a fast formation reaction of Fe-SCN complex. A synergistic effect was suggested as responsible for this phenomenon. However, the authors could not prove this assumption until replacing benzene with a mixture of benzene-MIBK diluent. Indeed, thiocyanate complex had a very low distribution coefficient in benzene, which caused a lowering of the forward distribution ratio and competitive reaction between the formation of thiocyanate and TTA complex.[90]

The extraction of Pd(II) with LIX 63 was documented.[91,92] The authors focused on the thermodynamic and kinetic aspects of the effect of additives on the extraction of Pd(II) with this oxime ligand. The addition of Aliquat 336 improved the extraction kinetics. The thermodynamic characterization of the system revealed the presence of a synergy between the extractants. This was demonstrated by identifying a mixed complex [$PdCl_3$(LIX)Aliquat] in the organic phase, in addition to complexes involving the individual extractants. This was possible by means of distribution isotherms and UV-visible spectrophotometry. In parallel, the kinetic study revealed the interfacial nature of the rate-limiting step, and a phase transfer catalysis mechanism was then proposed. Similarly, the extraction kinetics of Pd(II) from chloride media with dialkyl sulfides was accelerated by adding thiocyanate, amines or quaternary ammonium salts.[93]

Likewise, the approach of using phase transfer catalyst was successfully achieved to accelerate the slow extraction kinetics of Am(III) and Eu(III) from nitrate media with $CyMe_4$-BTP (Figure 17) by adding DMDOHEMA.[94] The authors explained the kinetic acceleration by the fact that DMDOHEMA, which is surface-active, would complex the metals on the interface. A fast ligand exchange would occur between DMDOHEMA and $CyMe_4$-BTP in the organic phase since the extraction is favoured thermodynamically with $CyMe_4$-BTP.

In addition, studies on the replacement of some of the coordinating water molecules with other ligands were carried out to elucidate the effect on the rate of formation of the zinc and nickel chelates with diphenylthiocarbazone.[48] In fact, the rate-limiting step of the formation of 1:1 chelate between the hydrated metal and the ligand anion was closely related to the rate of loss of coordinated water from the hydrated metal.[12,95] The addition of acetate ions was found to increase the rate of extraction of zinc dithizonate. Thus, $ZnOAc^+$ was found to react 25 times as fast as Zn^{2+}, whereas the formation of $NiOAc^+$ did not accelerate the nickel dithizonate extraction. This led to propose a further improvement of the kinetic based separation procedure of Ni and Zn.

In parallel, some authors were interested in the difference in structural organization of donor atoms in the free and coordinated molecules of several polydentate extractants. Therefore, a relationship between the rates of metal ion complexation and the degree to which the ligand is pre-organized for metal binding was established, considering that this preorganization not only requires energy but also is a time-consuming process. This has led to a molecular design of a *cis*-locked phenanthroline-derived quadridentate bis-triazine ($CyMe_4$-BTPhen) (Figure 17) for a more selective and faster separation of actinides(III) from lanthanides (III) compared to its 2,2'-bipyridine counterpart ($CyMe_4$-BTBP) (Figure 17).[96] The extraction kinetics of lanthanides (III) was found to be slower with $CyMe_4$- BTBP than with $CyMe_4$-BTPhen.[97] That was explained that $CyMe_4$- BTBP must overcome a significant (ca. 12 $kcal.mol^{-1}$) energy barrier of rotation around the central biaryl C-C axis in order to achieve cis

conformation, which is required to form a complex, whereas the cis-cis conformation is already fixed in the $CyMe_4$-BTPhen.

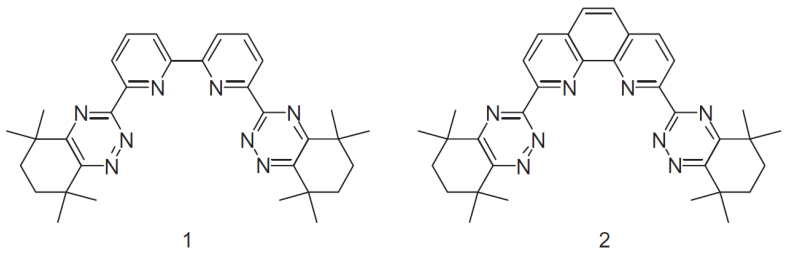

1 2

Figure 17: Structures of the ligands $CyMe_4$-BTBP (1) and $CyMe_4$-BTPhen (2).[97]

VII.Solvent extraction of transition metals

Having outlined the generalities of extraction kinetics in the previous sections, we now begin to focus on the systems that have been studied in our research. There has been considerable work in our study on the selective extraction of some transition metals, mainly Pd(II) and, to a lesser extent Pt(IV). Therefore, in this section, we present generalities on the extraction of some transition metals, then we focus on the extraction of Pd(II) and Pt(IV) from chloride and nitrate media using several extractants. Finally, we present the extraction kinetics of PGMs and some of the reported mechanisms in the literature.

Several extractants have been proposed for the extraction of transition metals. Dithizone and its derivatives have been used for the extraction of Zn(II), Ni(II), Co(II) and Cd(II).[12,48,95] In addition, the extraction of Cu(II) with oximes ligands is well reported in the literature.[17,18,87] Tetrasubtituted malonamides are very selective for the extraction of Fe(III) from hydrochloric acid media.[98] TBP is a very good extractant for the recovery of Zn(II).[99] Bis-2-ethyl hexyl phosphoric acid (D2EHPA) 2-ethyl hexyl phosphonic acid mono 2-ethyl hexyl ester are also excellent extractants for Fe(III).[100,101] In addition, a quantitative separation of Fe(III) was performed with Cyanex-923[102] and with a mixture of 70%vol TBP 30%vol MIBK.[103]

Before discussing the solvent extraction of Pd(II), we would like to present the HSAB theory that can explain the affinity of this metal to bind to soft bases.

A. HSAB theory

Pearson introduced the concept of chemical hardness and softness in 1963, which is known as the HSAB theory.[104] Lewis acids and bases were divided into two categories: hard acids and bases, soft acids and bases.

For the soft base, the donor atom has high polarizability and low electronegativity is easily oxidized and is associated with empty low lying orbitals. Whereas, for a hard base, the donor atom is of low polarizability and high electronegativity, hard to oxidize, and associated with empty orbitals of high energy. In parallel, a soft acid, the acceptor atom has a low positive charge and large size and several easily excited outer electrons. Whereas, for a hard acid, the acceptor atom is of high positive charge and small size and does not have easily excited outer electrons. The hard-soft classification of acids and bases gave rise to the postulate of the HSAB theory: Hard acids bind strongly to hard bases, and soft acids bind strongly to soft bases. In addition, it was concluded that hard-hard interactions are largely ionic and that soft-soft interactions are largely covalent. Some of the bases and acids were classified to be on the borderline, seen they present intermediate properties.[105] As a result of the HSAB theory, sulfur-containing compounds can effectively and selectively extract Pd(II), which is a soft acid, with a strong affinity towards ligands that contain donating sulfur atoms as soft bases, *i.e*. dihexylsulfide (DHS) and dioctylsulfide (DOS).[106]

Table 3: List of some of the hard, soft and borderline acids and bases.

Hard acids	Soft acids	Hard bases	Soft bases	Borderline acids	Borderline bases
Li^+, Ca^{2+}, Ba^{2+}, Sc^{3+}, Ti^{4+}, Zr^{4+}, Cr^{3+}, Fe^{3+}, Co^{3+}	Pd^{2+}, Pt^{2+}, Pt^{4+}, Ag^+, Cd^{2+}, Cu^+	NH_3, RNH_2, H_2O, NO_3^-, SO_4^{2-}, F^-	RS^-, SH^-, R_2S, CN^-, SCN^-, CO^-,	Fe^{2+}, Co^{2+} Ni^{2+}, Cu^{2+} Zn^{2+}, Pb^{2+} Rh^{3+}, Ir^{3+} Ru^{3+}, Os^{2+}	Br^-, N_3^-, NO_2^-

B. Extraction of Pt and Pd from chloride media

Two kinds of extractants have been commercialized for the PGMs refining, namely dialkylsulfide DOS/DHS and oximes LIX 64N/LIX 84 I.[106] Despite their excellent selectivity for Pd(II) in low acidic solutions compared to Pt(IV), these extractants suffer from slow kinetics.[107,108] In addition, DOS and DHS are prone to be oxidized during Pd extraction, and LIX 64 N and LIX 84 I are unstable during contact with high acidic and oxidative solutions.[106] The extraction kinetics of Pd(II) with LIX 63 was enhanced by adding a quaternary ammonium salt, which promoted a synergistic effect, and the equilibrium was then reached in 10 min.[91,92]

Dialkyl sulfides: The rate of Pd(II) extraction with dialkyl sulfides can be increased by the presence of thiocyanate ions in the aqueous phase,[93] or by adding amine derivatives in the organic phase as a phase

transfer catalyst.[107,109] Alternatively, introducing a hydrophilic hydroxyl group to the dialkyl sulfide has proven to enhance both the interfacial activity and the aqueous solubility, and therefore, the extraction rate of Pd. A typical example of such modified sulphides is 2-hydroxyethyldecylsulfide.[110] Moreover, introducing a highly fluorinated hydrophobic part to 2-hydroxyethyldecylsulfide increased the efficiency and the extraction rate of Pd(II) compared to the non-fluorinated analogues.[111] The topology of the extracting molecule also influenced the extraction kinetics of Pd(II) from chloride media.[110] For instance, Pd(II) extraction was faster when asymmetric dialkyl sulfides, *i.e.* dodecylmethylsulfide (DMS) were used instead of symmetric ones, *i.e.* dihexyl sulfide (DHS) (Figure 18). This increase in the extraction rate was attributed to different states of the hydrophile-lipophile balance of symmetric and asymmetric sulphides. The asymmetric dialkylsulfide was less hydrophobic than the symmetric one. This was also reflected by a difference in their interfacial activities, where DMS was more interfacial active than DHS and adsorbed better at the interface.[107]

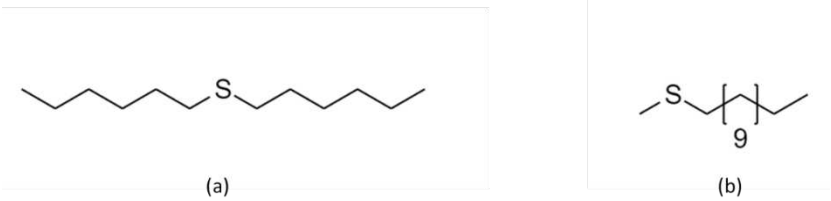

Figure 18: Chemical structure of dihexyl sulfide (DHS) (a) and dodecylmethyl sulfide (DMS) (b).

Dialkylsulfoxides: These are oxidation products of dialkylsulfides, which are more stable during contact with high acidic solutions. Dibutylsulfoxide (DBSO) showed very good and fast extraction of Pd(II) (>99.5% for 1M DBSO in kerosene in 5 min).[112] The extraction of Pt(IV) was slower than that of Pd(II) and reached its maximum 89.6% for 3M DBSO. Therefore, separation of Pd(II) from Pt(IV) was possible by controlling the contact time and the content of extractant in the organic phase.

***Monothioether compounds*:** The extraction of Pd(II) and Pt(IV) with 3,7-dimethyl-5-thianonane-2,8-dione was investigated.[113] At HCl concentration range of 0.1-2M, the extraction efficiency of Pd(II) was higher than 99.5%. However, the extraction of Pt(IV) decreased from 40% to lower than 20%. Efficient separation of Pd(II) over Pt(IV) (SF ~ 10^4) was achieved by controlling extraction time.

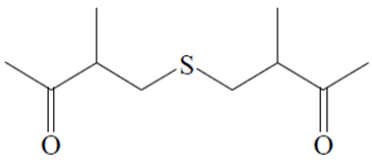

Figure 19: Chemical structure of 3,7-dimethyl-5-thianonane-2,8-dione.

Sulfide containing monoamide: The effect of the structure of the extractant on the extraction of Pd(II) was investigated with four different sulfide containing monoamides (Figure 20) in chloroform:[114] *N*-methyl-*N*-*n*-octyl-4-thiapentanamide (A), *N*-methyl-*N*-*n*-octyl-3-thiapentanamide (B) *N*-methyl-*N*-*n*-octyl-phenyl-3-thiapentanamide (C) and *N,N*-di-*n*-octyl-3-thiapentanamide (D). Results were compared with those obtained with DHS. All ligands showed excellent extraction of Pd(II) (>99%), however, the rate of extraction was different, and it followed this order: A > B > C > D > DHS. Pt(IV) was hardly extracted with these ligands.

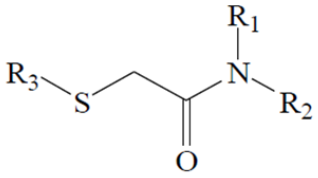

Figure 20: Sulfide-containing monoamide compound. (A) R_1= methyl R_2 = n-octyl R_3 = methyl, (B) R_1 = methyl, R_2 = n-octyl, R_3= ethyl, (C) R_1 = methyl, R_2 = n-octyl, R_3 = benzyl, (D) R_1 = R_2 = n-octyl, R_3 = ethyl.

Thiourea derivatives: Nonylthiourea (NTH) dissolved in chloroform extracted Pd(II) and Pt(II) very rapidly (less than 10 min), whereas it took much longer to reach extraction equilibrium for Pt(IV), Rh(III), Cu(III) and Fe(III).[115] In addition, the extraction of Pd(II) was very efficient., $D_{Pd} = 10^3$ for 5.10^{-4}M NTH.

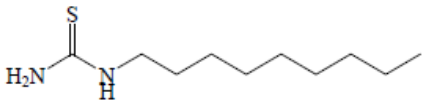

Figure 21: Chemical structure of nonylthiourea.

Amides and thioamides: N,N,N',N'-tetra-alkyl-(di)thiodiglycolamides have strong affinity for Pd(II) and fast extraction kinetics (5 min for N,N'-dimethyl-N,N'-dibutylthiodiglycolamide)[116]. In addition, *N,N,N',N'*-tetra-*n*-octyl-thiodiglycolamide showed excellent selectivity for Pd(II) over Pt(IV) and Rh(III) and other base metals.[117]

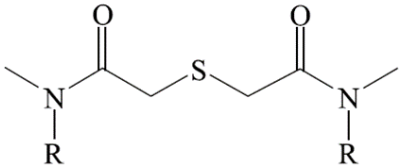

Figure 22: Chemical structure of N,N'-dimethyl-N,N'-dialkylthiodiglycolamide.

Acidic organic phosphorous extractants: Di-(2-ethylhexyl)thiophosphoric acid (DEHTPA) dissolved in kerosene, extracted quantitatively and selectively Pd(II) from a wide range of acidities (0.5-10M HCl).[118] The extraction of Pd(II) with these ligands is faster than that of Pt(IV), which allowed a complete Pd/Pt separation by controlling contact time.

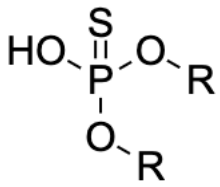

Figure 23: Chemical structure of DEHTPA.

Amines derivatives: The basicity of amines determines their extractability, and this follows the order: quaternary ammonium salts > tertiary amines > secondary amines > primary amines.[106] Since amines extract with an anion exchange mechanism, they can extract Pt(IV) efficiently, and even better than Pd(II).[119]

C. Extraction of Pd and Pt from nitrate media

Neutral organophosphorus compounds: The distribution ratio of Pd(II) with TBP is low, and it reaches a maximum of 1.3 in pure TBP, and is only 0.2, in the usual conditions of 30% TBP in TPH.[120] In parallel, triisobutylphophine sulfide (Cyanex-471X) extracts Pd(II) quantitatively with a nitric acid concentration between 2 and 6M. Nitric acid in the range of 2 to 5M does not affect the extractant for at least 71 hours.[121] In addition, palladium is highly extracted with triphenylphosphine dissolved in chloroform,[122] or benzene.[123] On the contrary, it is not extracted with triphenylphosphine oxide dissolved in chloroform.[122] Phosphine oxides can also be used: The trialkylated (butyl, isoamyl, octyl) in benzene, extract better palladium nitrate than TBP, for 0.2M < $[HNO_3]$ < 4M. However, increasing acidity decreased the extractability of Pd(II), which is only important for low acid concentration ($[HNO_3]$ <1M).[124]

Dialkylsulfide: As in chloride media, dialkylsulfides are very efficient for extracting Pd(II). For example, diheptyl sulfide in benzene (0.25M) extracts palladium with distribution ratios of the order of a hundred from $[HNO_3]$ = 1M. The main drawback remains in the equilibrium time, which is reached after 8-10 hours. Despite this, D_{Pd} = 5 was obtained after five minutes even if an equilibrium is not yet reached, provided that the extractant concentration is high (> 0.6M). Very high palladium distribution ratios ($D_{Pd} > 10^3$) can be obtained with DHS, 0.42M in *n*-dodecane, and for $[HNO_3]$=0.1-6M.[125] In addition, dioctyl sulfide (DOS) is a very good extractant even at low concentrations.[121]

Amide derivatives: *N,N,N',N'*-tetra(2-ethylhexyl) thiodiglycolamide extracts Pd(II) quantitatively, with a D_{Pd} >100 for 4M HNO_3 and an extraction equilibrium reached in 5 min.[126]

Quinolinol derivatives: Despite that the extraction of Pd(II) with LIX 34 (8-(alkarysulfonamido) quinolone is slow, low concentrations of the extractant are required to perform a quantitative extraction.[127]

D. Extraction kinetics of PGMs

The effects of the solution chemistry of PGMs chloro-complexes on their separation through ion exchange and solvent extraction methods were summarized by Albazi and Chow.[128] The differences in the kinetics behaviours of PGMs chloro-complexes to form extractable species and the strength of their electrostatic interactions with liquid-ion exchangers have also been emphasized. The separation of PGMs relies essentially on the difference of their kinetic behaviour due to their difference in lability. The lability and the exchange mechanisms of d-transition metal ions are affected by the occupancy of their d-orbitals. Square planar stereochemistry, which is primarily conferred to d^8 transition metals. Pd^{2+} and Pt^{2+} are the most investigated. The labile character of the platinum metals decreases in the order Pd > Pt > Ru > Rh >Ir.

The different processes for separating the common binary mixtures, namely, Pd/Pt, Rh/Ir, Ru/Os, were also reviewed. For example, the kinetically labile character of palladium towards several hydrophobic anions allows a fast formation of highly extractable anionic complexes at room temperature. Therefore, a separation may be possible from platinum, which reacts slowly under the same conditions. Similarly, the extractable neutral complexes of Pd(II) are formed rapidly even at room temperature, whereas Pt(II) complexes form more slowly, and Pt(IV) complexes require heating or the use of a catalyst. In addition, the relatively labile character of rhodium compared to iridium [Rh(III)>Ir(III)>Ir(IV)] in the formation of the extractable anionic or neutral complexes plays a major role in their separation. In addition, the reactivity of PGMs depends on their oxidation state and the nature of the reactant ligands.[130]

Table 4: Lability of the chlorocomplexes of the PGMs and Au(III) to ligand substitution.[129]

Metal	lability
Os(IV) Pt(IV) Ir(II)	Inert
Pt(II) Rh(III), Ir(IV)	Moderately unreactive
Ru(III), Ru(IV)	Moderately labile
Pd(II), Au(III)	labile

Several studies on the extraction kinetics of Pd(II) from chloride media have been conducted, using several types of extractants, *i.e.* dialkylsulfide,[77,82,131,132] dialkylsulfoxide,[133] hydroxyoximes,[83,134,135] hydroxyquinolinol derivatives,[136] N,N'-dicotylglycine,[137] dialkylmonothio phosphoric acid,[138,139] 2-(5-bromo-2-pyridylazo)-5-diehylaminophenol,[140] dithizone.[141] For these studies, the extraction mechanisms have been described in terms of an interfacial limiting step or a homogeneous rate determining-step in the aqueous phase.

1. Extraction kinetics of Pd(II) with sulphur containing extractants

The extraction kinetics of Pd(II) from chloride media was documented with sulfur-containing ligands namely, dihexylsulfide (DHS)[131], 1,2-bis(tert-hexylthio)ethane (*t*-BHTE)[132], triisobutylphosphine (TIBPS)[82] and bis(2-ethyl) sulfoxide (DEHSO).[133] It was concluded that the extraction mechanism of Pd(II) with these ligands were mainly affected by the solubility and the interfacial activity of the extractant. For *t*-BHTE, which is highly soluble in the aqueous phase and not surface-active, the extraction of Pd(II) was interpreted based on a homogeneous reaction in the aqueous phase. In parallel, the extraction mechanisms of Pd(II) with TIBPS, DHS and DEHSO (all of them are surface-active molecules) were interpreted based on interfacial mechanisms. In the case of TIBPS, the elementary reactions between the extractant molecules adsorbed at the interface, and the aquatrichloro and tetrachlorcomplexes of Pd(II) in the aqueous phase were identified as the rate-determining steps. However, the authors pointed out that the extraction mechanism with DHS was found to be rate controlled by a complicated reaction involving complex formation between the intermediate complex adsorbed at the interface and a free extractant molecule in the aqueous phase. Finally, in the case of DEHSO, the rate-determining step was identified as the reaction between the interfacial complex $PdCl_3(DEHSO)^-$ and the aqueous DEHSO molecules to produce the final extracted complex $PdCl_2(DEHSO)_2$.

We present only the extraction mechanism with 1,2-bis(tert-hexylthio)ethane (*t*-BHTE) in toluene. The extraction kinetics of Pd(II) from chloride media with 1,2-bis(tert-hexylthio)ethane (*t*-BHTE) in toluene was studied using a batch-type stirred glass cell. In addition, the partition of the extractant between the organic and aqueous phases, as well as its interfacial adsorption, was determined. In addition, it was found that Pd(II) was extracted as $PdCl_2R$ (1:1 complex).

In their investigation, the authors considered that over the whole concentration of chloride ions, Pd(II) essentially existed as tetrachlorocomplex $PdCl_4^{2-}$ and in a small amount as $PdCl_3(H_2O)^-$, and the stability constant β_i of the i^{th} chloro complex was defined as follows:

$$\beta_i = \frac{[PdCl_i]^{(i-2)-}}{[Pd^{2+}][Cl^-]^i} \quad (162)$$

The effects of the concentrations of chloride ions and the extractant on the observed rate constants were determined. It was found that at low chloride ion concentration, the extraction rate was inverse first order with respect to chloride ion concentration, whereas it was zero at high chloride ion concentration. In addition, the extraction rate was first order with respect to the extractant concentration. In parallel, the experimental results showed that *t*-BHTE was not interfacially active and had high solubility in the aqueous phase. Therefore, the kinetic data were analyzed based on a heterophase homogeneous reaction model of complexation in the aqueous phase, with the following reaction scheme:

$$R_{org} \underset{k_{-1}}{\overset{k_1}{\rightleftharpoons}} R_{aq} \quad (\textit{Fast}) \quad (163)$$

$$K_{DR} = \frac{[R]_{org}}{[R]_{aq}} \quad (164)$$

$$PdCl_3(H_2O)^-_{aq} + R_{aq} \underset{k_{-2}}{\overset{k_2}{\rightleftharpoons}} PdCl_2R_{aq} + Cl^-_{aq} + H_2O \quad (\textit{Slow}) \quad (165)$$

$$PdCl_4^{2-} + R_{aq} \underset{k_{-3}}{\overset{k_3}{\rightleftharpoons}} PdCl_2R_{aq} + 2Cl^- \quad (\textit{Slow}) \quad (166)$$

$$PdCl_2R_{aq} \underset{k_{-4}}{\overset{k_4}{\rightleftharpoons}} PdCl_2R_{org} \quad (\textit{Fast}) \quad (167)$$

By assuming that the parallel reactions of $PdCl_3(H_2O)^-_{aq}$ and $PdCl_4^{2-}$ with t-BHTE were the rate-determining steps, the rate expression was described as follows:

$$-\frac{d[Pd^{2+}]_{aq}}{dt} = k_2[PdCl_3(H_2O)^-]_{aq}[R]_{aq} + k_3[PdCl_4^{2-}]_{aq}[R]_{aq} \quad (168)$$

Similarly,

$$-\frac{d[Pd^{2+}]_{aq}}{dt} = \{\frac{k_2\beta_3[Cl^-]^3_{aq} + k_3\beta_4[Cl^-]^4_{aq}}{\beta_3[Cl^-]^3_{aq} + \beta_4[Cl^-]^4_{aq}}\}K_{DR}[Pd^{2+}]_{aq}[R]_{org} \quad (169)$$

This was further approximated by,

$$-\frac{d[Pd^{2+}]_{aq}}{dt} = \{k_2(\frac{\beta_3}{\beta_4})[Cl^-]^-_{aq} + k_3(K_{DR}[Pd^{2+}]_{aq}[R]_{org}\} \quad (170)$$

Therefore, from the Eq. 170, the rate equation was first order with respect to both *t*-BHTE and Pd^{2+}, and was inverse first order with respect to chloride ion in its low concentration region and zero order in its high concentration region.

2. Extraction kinetics of Pd(II) with oxime based ligands

The extraction kinetics of Pd(II) from chloride media using hydroxyoximes was also reported. For these studies, the authors were interested in determining the orders for the reactants and the rate law of the extraction reaction. Ma and Freiser[135] conducted a quantitative investigation on the equilibrium and kinetics of extraction of palladium from aqueous chloride media with LIX 65N, an aromatic hydroxyoxime, in chloroform. According to the authors, the complexation took place in the aqueous phase, with the formation of the intermediate 1:1 complex $PdCl_2(LIX65N)$, as the limiting step. The rate of the reaction was described as follows:

$$v = k\frac{[Pd^{2+}]_{aq}[LIX65N]_{org}}{[Cl^-]_{aq}} \quad (171)$$

In parallel, Inoue and Maruuchi,[83] investigated the extraction kinetics of Pd(II) from chloride media using anti-2-hydroxy-5-nonylacetopheneone oxime (SME 529) in MSB 210 diluent (Shell chemical) with a batch-type glass stirred cell. It is worth mentioning that the extraction was extremely slow, and equilibrium was reached after 72 hours. Interestingly, quite different results were obtained. The reaction orders were as follows: first-order with respect to hydroxyoxime concentration, and inverse first-order and inverse second-order with respect to proton and chloride ion concentrations, respectively. Therefore the rate law was:

$$v = k'\frac{[Pd^{2+}]_{aq}[SME]_{org}}{[H^+]_{aq}[Cl^-]^2_{aq}} \quad (172)$$

The authors explained the obtained extraction rate expression based on an interfacial reaction, considering that hydroxyoximes are highly interfacially active. Therefore, in their proposed mechanism, the limiting step was the reaction between an intermediate 1:1 complex ($Pd(SME)Cl_2^-$) and the hydroxyoxime molecule in the aqueous layer for the formation of the final chelate at the interface $Pd(SME)_{ads}$.

This study was further investigated by Szymanowski et al.[134] The authors tried to predict the orders of the reactions based on interfacial tension measurements, which depended upon the reaction assumed as rate-limiting. An exhaustive description of the multitude of possible rate-limiting steps was given. The reaction orders predicted from the interfacial tension data were in a good agreement with those determined experimentally when the limiting step was assumed to be the reaction between an intermediate 1:1 complex ($Pd(SME)Cl_2^-$) and the hydroxyoxime molecule in the aqueous layer. Therefore, their investigation supported the interfacial mechanism proposed by Inoue and Marruchi.[83] It is worth mentioning that the first-order with respect to hydroxyoxime was predicted from the interfacial tension data, which was not in disagreement with the findings of Ma and Freiser.[135] Therefore, it was concluded that the surface activity of extractants cannot be considered alone as proof of an interfacial mechanism.

3. Extraction kinetics of Pd(II) oxine and other ligands

The extraction kinetics of Pd(II) from chloride media with an 8 hydroxyquinolinol derivative (KELEX 100) in chloroform was carried out.[136] The extraction mechanism was described based on homogeneous reactions in the aqueous phase. The reaction between the intermediate 1:1 complex and the protonated ligand was identified as the rate-limiting step. As a result, the extraction rate constant was found equal to $3.63*10^2$ $mol.L^{-1}.s^{-1}$, which was smaller than that with LIX 65N[135] ($3.51*10^3$ $mol.L^{-1}.s^{-1}$) and DOS ($3.51*10^4$ $mol.L^{-1}.s^{-1}$).[77]

The extraction kinetics of Pd(II) from chloride media with o-xylene bis(diethyldithiocarbamate) (o-XEDTC), 3-mercapto-1,5-diphenylformazan (dithizone, Hdz) and 1,10-phenanthroline was studied.[141] The rate-limiting steps with these ligands were the competitive substitution reaction of each ligand with $PdCl_4^{2-}$ (rate constant k_1) and $PdCl_3(H_2O)^-$ (rate constant k_2), in the aqueous phase. It was found that the rate constants increased in the following order: Dithizone > o-XEDTC > 1,10-phenanthroline. The larger reactivity of dithizone compared to 1,10-phenanthroline, was ascribed to the larger softness of dithizone as a Lewis acid. However, the smaller reactivity of o-XEDTC was linked to the large steric effect of the ligand.

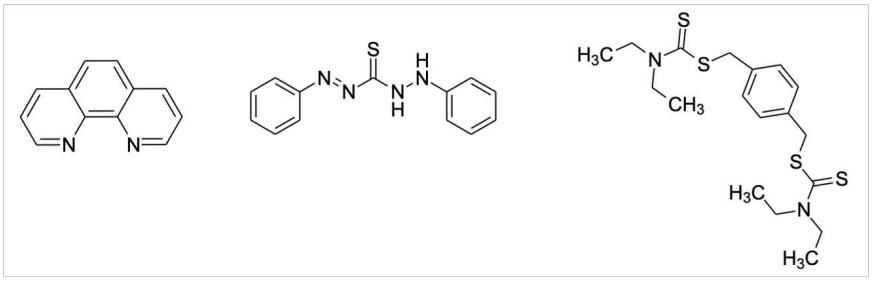

Figure 24: Chemical structures of 1,10-phenanthroline (a), dithizone (b) and o-XEDTC (c).

E. Conclusion

As shown in this section, several extractants were used for the selective extraction of Pd(II) from nitrate and chloride media. Besides the search for a selective extractant, researchers also focused on the stability of the latter in highly acidic media, avoiding so the formation of degradation products, which are a new source of waste. Accordingly, the choice was made for malonamides as extractants for our research, which are known for their highly stable amide moiety in highly acidic and oxidizing media. The properties of these ligands and their capacity to extract Pd(II) will be detailed hereafter.

On the other hand, while the extraction kinetics of Pd(II) from chloride media is well documented in the literature, a complete and detailed study for its extraction kinetics from nitrate media has not been presented so far. Few studies with malonamides (DMDOHEMA and DBMA),[142,143] reported that the extraction equilibrium of Pd(II) from nitrate media was reached in less than 1 hour, which is much faster than that with dialkylsulfides ligands in chloride media. In this regard, nitrate media was primarily chosen for our kinetic study.

VIII. Malonamides for liquid/liquid extraction

The long-term radiotoxicity of spent fuel from power plants is governed by its composition of several long-lived radioelements. The most important are plutonium and the so-called minor-actinides, neptunium, americium and curium. The separation of trivalent minor actinides (americium and curium) from the lanthanides is a key step that remains to be under investigation owing to the chemical similarity of the two groups of elements.[144] The preference of actinide ions for soft donor ligands is the common basis for the successful chemical separations of trivalent actinides from the trivalent lanthanides.[144]

Among the several synthesized and designed extractants for the f elements, diamide molecules have shown very promising results for actinide lanthanide coextraction.[145–148] In fact, these molecules contain only carbon, oxygen, hydrogen and nitrogen (CHON principle), so they are fully incinerable.

The extraction properties of *N,N,* dialkylamides for the hexa and tetravalent actinides were first reported by Siddall et al.[149]. Since then, several studies have been published dealing with the extraction abilities of malonamides for long-lived actinides.[145,150–156] In France, the DIAMEX process for the extraction of lanthanides and actinides has been developed. Recently, DMDOHEMA was chosen as the new reference molecule, replacing DBMA, the previously used molecule.[157]

The structure of the malonamide has a great influence on the metal extraction.[150,156] The chemical properties of the solvent depend on the nature of the substituents on the nitrogen and the central carbon atoms.[146] Solubilities, electronic effects and steric hindrance together impact the degree of extraction.[150] Moreover, the bulkiness of substituents on the nitrogen and the central carbon lowers the rotation barriers of malonamides, which impacts the interactions with the metal.[158]

In this section, we will present some of the phycsico-chemical properties of malonamides, as well as their extraction properties for actinides, lanthanides and PGMs.

A. Properties of malonamides

The general structure of malonamide molecule is represented in Figure 25. Malonamides have two amide functions. These chemical functions have the structural characteristics to be located in a plane due to the delocalization of electrons on the O-C-N atoms.[159] This O-C-N conjugated π system gives C=N double bond character inducing a high rotational barrier, which leads to different or less stable conformations.

1. Amphiphilic and surfactant properties

The supramolecular organization of malonamides in organic phases has been reported.[57,58,60] Due to their amphiphilic properties, malonamides molecules in an alkane are organized in reverse micelle type aggregates, composed of a polar core formed by the malonamide polar heads and the extracted solutes. In addition, the surfactant behaviour of malonamides was evidenced by several authors.[23,60,62,160,161]. The interfacial activity of the malonamide depended mainly on the substituents and the length of the diluent chain. For instance, *N,N'*-dimethyl-*N,N'*-dicyclohexylmalonamide (DMDCHMA) in 1,2 DCE was more surface-active than *N,N'*-dimethyl-*N,N'*-diphenymalonamide (DMDPHMA).[160] In parallel, it was found that micelles were formed easily when the central chain was changed from tetradecyl to octadecyl for dimethyldibutyltetradecylmalonamide (DBMA) and dimethyldibutyloctadecylmalonamide (DMDBODMA).[58] However, when decreasing the alkyl chain of the diluent (from hexane to hexadecane), the CMC increased. Furthermore, it was reported that micellization is favoured in the presence of an extracted solute such as nitric acid or neodymium nitrate.[60]

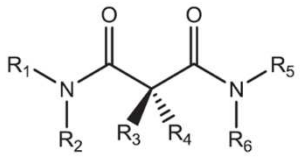

Figure 25: General structure of a malonamide.

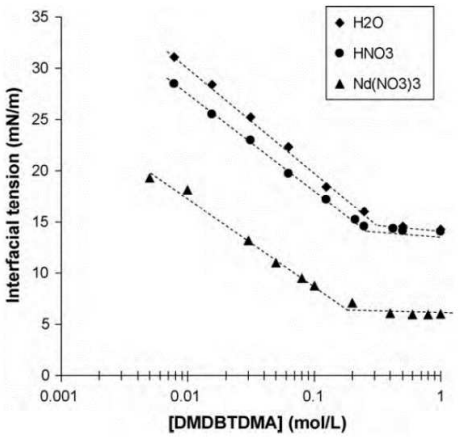

Figure 26: Variation of the interfacial tension in the function of the concentration of DBMA in dodecane, for different organic/aqueous interfaces: water, 0.2M $Nd(NO_3)_3$ 1M $LiNO_3$ 0.01M HNO_3, and 2M HNO_3.[60]

2. Acid uptake

Due to their basicity, malonamides can extract acid. Studied by many authors,[34,145,150,162–164] the extraction of nitric acid by malonamides implies various stoichiometries of extracted complexes:

- $MA(HNO_3)_y$ with $1 \leq y \leq 4$,
- $MA_2(HNO_3)$
- $MA(HNO_3)_3$ and $MA(HNO_3)_4$ were observed at very high acidities ([$HNO_3 \geq$ 5M and 12M)

Based on IR spectroscopic studies performed on DBMA and dimethyldioctylmalonamide (DMDOMA), HNO_3 has been proven to bind to malonamide by hydrogen bonding to the oxygen of a carbonyl group of the diamide. The latter would then be protonated by a covalent bond between the proton and the oxygen of one of the two C=O bonds and a hydrogen bond with the second carbonyl group.[145,165]

The effect of the substitution on the central carbon on the basicity of malonamide extractants was also documented. Cuillerdier et al.[146] reported that the presence of a substitute (alkyl chain) on the central carbon decreases the basicity of the malonamide molecule, and that it decreases further if the substitute is an oxyalkyl chain. However, Martinet[166] studied the effect of the central hydrocarbon chain and the length of the chain of the diluent on the basicity of different malonamides type $(CH_3(C_4H_9)NCO)_2CHR$.

The author reported that the acid extraction increased with the increase of the central hydrocarbon chain of the extractant in a given diluent, and with the decrease of the diluent chain for a given extractant.

B. Extraction of lanthanides and actinides

Malonamides extract light lanthanides better than heavy ones (Figure 27), and have a better affinity for actinides than for lanthanides.[23,167]

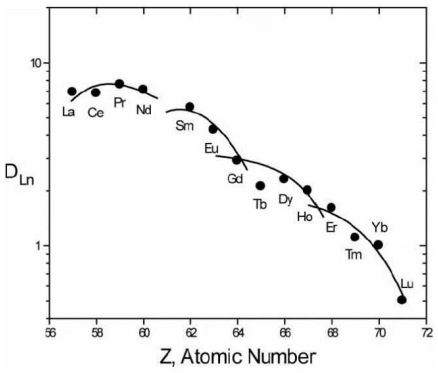

Figure 27: Distribution ratio of lanthanide ions for the extraction by 0.7M DMDOHEMA in n-dodecane from 1M HNO_3 and 2M $LiNO_3$ at 23°C.[167]

In general, malonamides are good extractants of U(VI).[145,168,169] The distribution ratios of U(VI) and Pu(IV) with 0.5M DBMA in TPH increased with the increase of nitric acid concentration, and the extraction of both metals was quantitative for [HNO_3] > 2M. In addition, DBMA in normal paraffinic hydrocarbon diluent, extracted metal cations from 3 to 4M nitric acid following this order: Pu(IV) > U(VI) >Am(III)-Eu(III) ~Fe(III) ~Tc(VII) > Zr(IV).[170] In parallel, it was found that Pu(IV) and Am(III) formed complexes with three DBMA ligands, while the complex with UO_2^{2+} consisted of only two DBMA ligands.[148]

The new reference molecule DMDOHEMA in *n*-dodecane has similar extraction properties to DBMA, except that the former has a preference for U(VI) over Pu(IV).[171] The distribution ratios obtained with DMDOHEMA for different metals followed the order: U(VI) > Nd(III) > La(III) > Eu(III).[172]

The extraction of trivalent cations (Eu(III), Am(III) and Nd(III)) from a nitric acid medium with DMDOHEMA in *n*-dodecane was investigated.[167] It was demonstrated by the slope method that for all the trivalent cations, a 1:2 metal:ligand complex was formed. In addition, DMDOHEMA was more selective for Am(III) over the two other lanthanide metals. And the separation factor of Am(III)/Eu(III) was ~ 2.

Cuillerdier et al.[146] have reported the extraction of actinides with tetraalkyl malonamides with an oxyalkyl group at the central carbon. These molecules showed very good results in the extraction of the actinides (III, IV, VI). However, they showed poor solubility in *n*-dodecane, which is the process diluent.

Furthermore, the extraction of U(VI), Pu(IV) and Am(III) from nitrate medium with *N,N'*-dimethyl-*N,N'*-dibutylmalonamide (DMDBMA) in benzene was investigated.[147] The extracted species (metal:ligand) of U(VI) and Pu(IV) were 1:2 and 1:3 for Am(III). In parallel, DBMA has shown very good results for the extraction of actinides. This ligand dissolves in *n*-dodecane and does not form a third phase when in contact with 3-4M HNO_3.[148]

The effect of the diluent and the length of the substituent chain on the extraction of some trivalent lanthanides were reported.[173] First, it was concluded that malonamides substituted at the central carbon atom have a greater Ln(III) extraction capacity than the unsubstituted ones on the central chain. Then, it was found that the distribution ratios of trivalent lanthanides were higher when using aliphatic diluents, and these values decreased when shifting to aromatic diluents. This is in agreement with the study conducted by Poirot et al.[174] The authors demonstrated that the extraction of Nd(III) with DMDOHEMA is driven by aggregation, which is more promoted in aliphatic diluents than in aromatic ones.

The effect of alkyl substitution on the central carbon for the extraction of Eu(III) was investigated with a series of malonamides: *N,N,N',N'*-tetrahexylmalonamide (THMA), *N,N,N',N'*-tetrahexyl-2-methylmalonamide (THEMMA) and *N,N,N',N'*-tetrahexyl-2,2-dimethylmalonamide (THDMMA).[175] A single methylation of the central carbon resulted in a decrease of the distribution ratio of Eu(III) by nearly one order of magnitude. While double methylation inhibited the extraction of Eu(III).

Furthermore, the effect of changing the basicity of malonamides, by changing the alkyl chain substituents, on the extraction of Eu(III) and Am(III) into tertbutylbenzene was reported.[176] The highest distribution ratios of these metal ions were obtained with the malonamides having the lowest basicity values.

C. Malonamides for transition metals extraction

Besides their ability to extract actinides and lanthanides, malonamides have shown very interesting features in the extraction of PGMs and Fe(III) from chloride and nitrate media.

1. Chloride media

Recently, some malonamide derivatives have been considered for solvent extraction of PGMs from hydrochloric acid solutions. The extraction of Rh(III) and Pt(IV) and Pd(II) from chloride media

by N,N'-dimethyl-N,N'-diphenyltetraecylmalonamide (DMDPHTDMA) in 1,2-DCE was studied.[177,178] The addition of a labilizing agent, *e.g.,* tin chloride ($SnCl_2$), was necessary to achieve an efficient extraction of metals (>95%). In the absence of $SnCl_2$, the maximum extraction of Rh(III) did not exceed 25% at 0.1M HCl, and that of Pt(IV) was 30% at 5M HCl, whereas the maximum for Pd(II) was 15% at 1M HCl.

N,N'-dimethyl-*N,N'*-dicyclohexylmalonamide (DMDCHMA) in 1,2-DCE was examined for the extraction of Ru(III), Ru(IV), Rh(III), Pt(IV), Ir(III) and Ir(IV) from chloride media.[179] Interestingly, this ligand showed good Pd(II) extraction at 7M HCl (79% extraction yield) without the addition of any labilizing agent. However, the extraction of Pt(IV), Ir(III) and Ir(IV) could not be evaluated due to third phase formation.

N,N'-dimethyl-*N,N'*-dicyclohexyltetradecylmalonamide (DMDCTHTDMA) in 1,2-DCE showed very promising results for the extraction of Pt(IV).[180] A fast and efficient extraction of Pt(IV) could be achieved without adding tin chloride: The extraction yield is over 88% from 6 to 8M HCl. Furthermore, the use of different diluents was tested, and only *n*-octanol was the best alternative to 1,2-DCE. Whereas, the extraction yield was very low for aromatic and commercial diluents, *i.e.* toluene, xylene, kerosene, Shellsol D70, Escaid 100.

In addition, the efficient extraction of Pd(II) and Pt(IV) without the addition of tin chloride was reported when using *N,N'*-dimethyl-*N,N'*-dibutylmalonamide (DMDBMA) in 1,2-DCE.[181] The extraction of Pt(IV) increased with the aqueous HCl concentration, reaching 91% at 6M HCl. In contrast, Pd(II) extraction decreased with HCl concentration, and the maximum was 63% at 1M HCl. Interestingly, the extraction outcome of Pd(II) was different between DMDBMA and DMDHMA, which both share a fairly similar skeleton. Whereas for DMDHMA, Pd(II) extraction was very low up to HCl < 4M and reached 79% at 8M HCl. Finally, chlorinated diluents were vital for these systems, as solubility problems were encountered with commercial diluents, and low extraction yields with aromatic diluents.

2. Nitrate media

The extraction of PGMs from nitrate media using malonamides was carried out exclusively with Pd(II). The extraction of Pd(II) with DMDOHEMA in *n*-heptane was characterized in detail.[142] The extraction equilibrium was reached in less than 1 hour. Good distribution ratios were obtained with high nitrate concentration in the aqueous phase or high DMDOHEMA in the organic phase (D_{Pd} = 12 for 0.5M DMDOHEMA and 3M HNO_3). The extracted species were identified using the slope method and were $Pd(NO_3)_2(DMDOHEMA)_2$.

In addition, the authors identified the different conditions leading to solid third phase apparition resulting from poor solubility of Pd(II) complexes in heptane organic phase. Third phase formation was prevented by using chlorinated or aromatic diluent in parallel. Furthermore, coordination chemistry (complexation) was shown to be the driving force for Pd(II) extraction with DMDOHEMA, and there was no impact from the organization of the organic phase.[174] Thus, when using toluene as a diluent, a ca. 10-fold increase in Pd/Nd selectivity was obtained since the extraction of the latter was governed by aggregation of the organic phase in addition to metal coordination. The selective extraction of Pd(II) in the presence of different +II and +III cations metals (Al(III), Fe(III), Nd(III), Cu(II), Co(II), Ni(II) and Zn(II)) using DMDOHEMA in heptane was studied.[143] Negative impact on $S_{Pd/Nd}$ was obtained when increasing both DMDOHEMA and aqueous nitric acid concentrations. In parallel, it was found that the extraction of Fe(III) was important only when the aqueous concentration of HNO_3 was higher than 3M. Otherwise, no noticeable extraction of other metals was found.

In parallel, DBMA in toluene showed better extraction of Pd(II) compared to DMDOHEMA, and the distribution ratios were about twice higher; D_{Pd} reached 5 for 0.3M DMDOHEMA and 4M HNO_3, whereas for 0.3M DBMA, D_{Pd} reached 12.[143] Furthermore, Fe(III) extraction showed the same trend with DBMA, where D_{Fe} increased with the increase of aqueous nitric acid concentration, while D_{Nd} was lower with DBMA than with DMDOHEMA, and increased with the increase of DBMA concentration. Based on these results, a process for the selective extraction of Pd(III) from Fe(III) was developed. It is worth mentioning that the slow extraction kinetics of Fe(III) with DBMA can lead to a kinetically controlled separation process, which was the case for the separation of Fe(III) from Am(III) using DBMA in *n*-dodecane.[148]

Finally, the effect of the ramification on the central chain on the extraction of Pd(II) was studied using two different malonamides, N,N-dimethyl-N,N-dioctylmalonamide (DMDOMA) and N,N-dimethyl-N,N-dioctyltetradecylmalonamide (DMDOTDMA).[182] The study was carried out using a mixture of 75 vol% n-dodecane-25 vol% n-octanol as a diluent to avoid third phase formation. Despite the extraction kinetics of Pd(II) from 5M HNO_3 with both malonamides (0.05M each) was similar (10 min to reach equilibrium), the extraction efficiency of Pd(II) increased when the central chain was alkylated. The same trend was noticed in a hydrochloric medium. In addition, increasing the concentration of nitric acid up to 5M HNO_3 increased the extraction of Pd(II). Thereafter, a decrease in D_{Pd} was observed for both malonamides. The extracted species were identified for both malonamides through the slope method as $Pd(MA)_2(NO_3)_3$, which was in agreement with the species identified in the case of DMDOHEMA.[142] (MA denotes malonamide). Furthermore, DMDOTDMA has shown a very selective extraction of Pd(II) when using multicomponent mixtures of metals, *e.g.* Zn(II), Ni(II), Mn(II), Cu(II) and Pb(II).

D. Kinetic studies using malonamides

The extraction kinetics studies using malonamides have been reported in the literature.[22,23,34,183-187] These studies mainly focused on the extraction kinetics of lanthanides and actinides. In parallel, a detailed study of the extraction kinetics of transition metals with malonamides has never been reported so far. Unless some preliminary results on the time needed to reach the extraction equilibrium for Pd(II) and Fe(III) are reported in the literature.[142,148,188] Indeed, it has been reported that the extraction equilibrium of Pd(II) from nitrate media in extraction with DMDOHEMA in toluene was reached in 30 minutes. [142] Whereas, it has been reported that the extraction of Fe(III) equilibrium from nitrate media with DBMA in *n*-dodecane was reached for extended extraction durations, revealing its slow extraction kinetics.[148,188]

This section will summarize the kinetic studies carried out on the extraction of some actinides and lanthanides. Thus, we will present the primary parameters studies: The effects of metal, ligand topology, diluent and acidity. In addition, we will present the experimental tools employed for the kinetic investigations in each case.

The extraction kinetics studies for actinides and lanthanides using malonamides have been investigated by Toulemonde,[22] Dal Don,[23] Charbonnel et al.,[183] Weigl et al.,[184] Bosland[34] and Simonin et al.[185].These studies were carried out using ARMOLLEX cell, AMADEUS cell, RSC, RMC and single drop technique. One of the main issues in the extraction kinetics studies is the control, or at least, the minimization of the diffusive contribution to the overall process. Here, the delicacy that a kinetic study requires is emphasized since several authors investigated almost the same system, yet their results were divergent. This was strongly related to the control of hydrodynamics, which led to a total elimination or not of the diffusive limitations.

Toulemonde was the first to report the extraction kinetics of actinides Am(III) and lanthanides Eu(III) and Ce(III) with DBMA in dodecane.[22] This study was carried out using the RSC cell. It was found that the transfer was controlled by a slow interfacial reaction. The extraction kinetics of Am(III) and Eu(III) was nearly similar. However, the extraction kinetics of Am(III) was 1.15 higher than that of Ce(III). Moreover, the extraction kinetics of Am(III) and Eu(III) were enhanced with the increase in nitric acid concentration in the aqueous phase (Table 5). However, the studies carried out with the RSC were not complete because the problems of chemical affinity encountered between the gel support and the species to be extracted, were considered limiting the use of the cell. This is why the rotating membrane cell was developed. Some of the reported results are summarized in Table 5.

Table 5: Chemical mass transfer constants k_f for the extraction of Am(III) and Eu(III) with DBMA using the RSC cell,[22] [DBMA] 1M in dodecane, T = 21°C.

$[HNO_3]$ (mol/L)	K_f (10^{-6} m/s) Am(III)	K_f (10^{-6} m/s) Eu(III)	regime
2	0.8	0.7	**Thought as kinetic**
4	1.0	1.4	
6	1.2	2.0	

In addition, Dal Don investigated the extraction kinetics of Nd(III) with DBMA in TPH using AMADEUS cell.[23] The determination of the global transfer coefficients (Table 6) was performed under conditions where no further increase in the extraction rate was observed at a high Reynolds number (Re > 600). This methodology allowed estimating the chemical extraction rate constant that was found to be controlled by a slow interfacial reaction. Furthermore, increasing the concentration of Nd(III) in the aqueous feed did not induce any change in the extraction rate. In parallel, the extraction rate was enhanced with increasing temperature and the increase of nitric acid concentration in the aqueous phase. However, the latter, was more likely related to the increase in nitrate ions concentrations since the partial order concerning proton concentration was zero.

Table 6: Nd(III) extraction kinetics with DBMA using AMADEUS cell,[23] [DBMA] 0.5M in TPH, $[HNO_3]$ 2M, T = 25°C.

$[HNO_3]$ (mol/L)	$[Nd^{3+}]_{aq}$ (10^{-2} mol/L)	K_f (10^{-7} m.s^{-1})	regime
2	3	4.2	**Thought as kinetic**
	6	4.5	
	9	4.84	
3	6	8.2	
4		10	

Furthermore, the extraction kinetics of Nd(III) remained invariant when DBMA was replaced with another malonamide, bearing an oxygen atom on the central chain (*N,N'*-dimethyl-*N,N'*-dibutyl-dodecylethoxymalonamide DMDBDDEMA), while the distribution ratio increased by a factor of 2.

The extraction kinetics of other lanthanides(III) was investigated.[23] The kinetic extraction rate constant decreased along with the series of 4f elements. For the beginning of the series (lanthanum, cerium and praseodymium), k_f was 18.10^{-7} m.s^{-1}, while it decreased to 6.10^{-7} m.s^{-1} for the middle

elements of the series (neodymium, samarium and gadolinium). Finally, k_f was 1.10^{-7} m.s^{-1} for dysprosium and lutetium, which are placed at the end of the series of 4f elements. Furthermore, the extraction kinetics of Am(III) and Cm(III) was also carried out, and the results obtained were comparable to those obtained with Toulemonde using RSC.[22]

The kinetic studies performed by Dal Don were carried out using a Lewis type cell, which is a stirred cell with a constant interfacial area. According to Danesi,[10] when using these devices, a non-dependence of the reaction rate on the stirring speed can sometimes arise from the 'slip effect' of the fluids on the blades of the propellers when their rotation speed is increased above some critical speed. In this case, the thickness of the diffusion films never decreases below a sufficiently small value. Thus, although the extraction flux attains a plateau, the diffusion cannot be completely neglected compared to the rate of the chemical reaction. Therefore, Weigl et al.[184] investigated the extraction kinetics of lanthanides(III) and actinides(III) with DBMA using a Nitsch cell to clearly identify the extraction kinetics regime. This cell was designed to overcome the deficiencies of the Lewis cell with a more efficient stirring. The linear increase of the extracted metals flux with stirring speed indicated that the rate of extraction was governed by diffusion, which contradicted the results of Dal Don.[23] It is worth mentioning that the cell was tested with systems operating in a diffusional regime (toluene transfer into water), which confirmed the capability of the used device in discriminating between chemical and diffusional regimes. Furthermore, the extraction rates at 3.5M [HNO_3] of La(III), Ce(III) and Pr(III) were about 50% higher than for the heavier lanthanides, Nd(III), Sm(III) and Eu(III). This difference was explained by larger driving concentration gradients between bulk and interfacial concentrations, corresponding to the higher distribution ratios of La(III), Ce(III) and Pr(III). The results obtained with Weigl et al.[184] are summarized in Table 7.

Table 7: Extraction kinetics of Ce(III), Eu(III) and Am(III) with DBMA using Nitsch cell, [DBMA] 0.5M in HTP, [HNO_3] 3.5M, [M^{3+}] $1.66*10^{-4}$ M.[184]

metal	K (10^{-5} m.s^{-1})	regime
Ce^{3+}	1.9	
Eu^{3+}	1.2	**diffusional**
Am^{3+}	1.9	

Given these opposite conclusions, the extraction kinetics of Eu(III) with DBMA and DMDOHEMA in TPH was further investigated by Simonin et al. using RMC cell.[185] First, the extraction of Eu(III) with DBMA at 22°C was very fast and was controlled by diffusion. This finding was in agreement with the observation made by Weigl et al.[184] and in contradiction with the result of Dal Don.[23]

In parallel, the extraction kinetics of Eu(III) with DMDOHEMA was slower than that with DBMA at 22°C, and became fast at 33°C. The results obtained with Simonin et al.[185] are summarized in Table 8.

Table 8: Extraction kinetics of Eu(III) with DBMA and DMDOHEMA in TPH using RMC cell, [DBMA] 0.5M, [DMDOHEMA] 0.5M, [HNO_3] 2M.[185]

Ligand	T (°C)	K (10^{-7} m.s^{-1})	k_f (10^{-5} m.s^{-1})	Regime
DBMA	22	8.8	-	**Diffusional**
DMDOHEMA	22	-	5.58	**Combined**
DMDOHEMA	33	-	20.9	

Bosland investigated the extraction kinetics of Nd(III) with DMDOHEMA in TPH, using ARMOLLEX cell and single drop technique.[34] The experimental results of both devices indicated that a mixed regime governed the extraction. More interesting in this study was the use of two different ARMOLLEX cells, which had different geometries, where the plateau was not reached for one of them, proving the effect of the device on the results of extraction kinetics again. In parallel, increasing the temperature lowered the extraction kinetics of Nd(III). The effect of the metal, the diluent, the ligand and the organic phase viscosity were also assessed. First, the effect of the metal was investigated by replacing Nd(III) with Eu(III). The same trend was observed when increasing the temperature. Moreover, the extraction kinetics of Nd(III) was the same in TPH and dodecane, although the aggregation state of DMDOHEMA was different in both diluents. In addition, the extraction kinetics of Nd (III) with DBMA was similar to that with DMDOHEMA. The effect of viscosity of the organic phase was investigated by using pentane as a diluent, which is less viscous than TPH. The author indicated that DMDOHEMA presented the same aggregation state in both diluents. The extraction kinetics of Nd(III) in both diluents were quite similar. Finally, the effect of temperature was assessed. It was concluded that the decrease in the extraction kinetics with temperature was more likely due to the decrease in the affinity of DMDOHEMA to adsorb at the interface when increasing the temperature. In Table 9, we summarize the results obtained with Bosland using ARMOLLEX cell and the single drop technique.[34]

Table 9: Extraction kinetics of Nd(III) and Eu(III) with DBMA and DMDOHEMA using ARMOLLEX cell and single drop technique at different temperatures and for different diluents, K: global mass transfer constant, [DMDOHEMA] 0.65M [DBMA] 0.65M [Nd^{3+}] 0.01M [Eu^{3+}] 0.01M.[34]

Device	T (°C)	Metal	Ligand	diluent	K (10^{-5} m.s^{-1})	regime
ARMOLLEX	15	Nd^{3+}	DMDOHEMA	TPH	1.4	**mixed**
					0.4	
	35		DBMA		1.0	
					0.4	
	15	Eu^{3+}	DMDOHEMA		1.0	
		Nd^{3+}		Dodecane	1.3	
Single drop	15			TPH	4.0	
	25				3.7	

In addition to classical contactors, the extraction kinetics of Eu(III) by DBMA was studied using microchannels with parallel flows[186] and segmented flows.[187] For the latter study, the authors determined the pseudo-kinetic coefficient, defined as a lower bound limit for the kinetic forward coefficient. Moreover, a model was proposed for the evolution of this pseudo-kinetic coefficient with the velocity of the droplets, analogous to the stirring rate. The maximum value of the pseudo-kinetic coefficient was $k_f = 6.6 * 10^{-5}$ m.s^{-1}. This value was compared to values reported in the literature, rendering the obtained ones of the mass transfer in segmented flows in microsystems very efficient, not only compared to traditional contactors, but also to laminar flows in microchannels.[186]

IX. Conclusion

In this bibliographic study, we presented an overview of the extraction kinetics of metal ions, focusing on the rate of the chemical reaction. The different chemical properties of the metals, the structure of the ligands and the resulting lability of complexes play a central role in their extraction kinetics.

Knowing that the extraction process involves the transfer of matter between two immiscible phases, the rate-limiting step can take place in one of the bulk phases or at the interface. Interfacial reactions are more likely when a surface-active and highly hydrophobic extractant is used. In contrast, the use of an extractant that has low surface activity and partial or total solubility in the aqueous phase often leads to a homogeneous reaction, which takes place in the aqueous phase.

A thorough understanding of the extraction kinetics can be provided by establishing a detailed mechanistic study. In this respect, we reviewed some of the reported mechanisms in the literature, focusing on cases where the rate-limiting step is in the aqueous phase and cases where the rate-limiting step is at the interface. We mention that there is a good agreement between authors for the latter that the adsorption of the surface-active ligands follows Langmuir isotherm. It is interesting to note the different rate laws of Pd(II) extraction when using two different oximes, which illustrates the direct impact of the ligand on the extraction kinetics.

Particular attention was given to the available experimental tools to study the extraction kinetics. It was found that the extraction kinetics results are highly dependent on the experimental tool used, which is governed by the extent to which hydrodynamics were controlled, and diffusion processes were suppressed. The use of classical tools has been extended to screen the effect of the concentrations of the reactants on the extraction rate in order to determine the rate laws. However, it turned out that large volumes were required to accomplish the study.

Although extraction kinetic studies using malonamides is extensively reported in the literature, these studies focused primarily on the extraction kinetics of lanthanides and actinides. In particular, the extraction kinetics of lanthanides including Nd(III) with malonamides is reported to be fast and diffusion controlled. On the other hand, no detailed information is available to date on the extraction kinetics of transition metals from nitrate media with malonamides, despite a few publications depicting the required time to reach extraction equilibrium of Pd(II) and Fe(III). Indeed, it is reported that 30 minutes were necessary to reach the extraction equilibrium of Pd(II) with DMDOHEMA. In contrast, the extraction equilibrium of Fe(III) with DBMA required more extended time.

Therefore, for our study, we were interested in characterizing the extraction kinetics of Pd(II), Nd(III) and Fe(III) from nitrate media which we considered to be representative of metals with different kinetic behaviours, with malonamide of different topologies. Finally, we mention that the single drop technique was selected for studying the mass transfer kinetics in our research. This technique presents a compromise between diffusional and chemical effects since an apparent global transfer constant is determined. In addition, precise knowledge of the interfacial area is possible, which is essential for our study.

Chapter 2: Selection of malonamides and thermodynamic characterization

The extraction of metals using malonamides has been the subject of numerous studies.[1-9] These studies have proven that several parameters impact the extraction behaviours of malonamides, as well as their extraction efficiencies towards metals. The organization of malonamides[174,189,190] and their affinity to form third phases are among these parameters. In addition, the geometry of the molecule, and implicitly the length of the substituents, largely dictate the ability of the molecule to extract metals.[172,173,176] In general, this feature is a crucial parameter for designing new molecules to improve metals extractability.

The amphiphilic structure of malonamide extractants gives them surface-active properties (Refer to Chapter 1 § XII-A-1). The main consequence of these properties is the aggregation of malonamides in apolar solvents. The aggregation is the result of a subtle balance between Vander Waals attraction acting between the alkyl chains of the extractant and the solvent, and dipole-dipole attraction forces between the polar parts of the extractant molecules.[191]

In a previous study performed on the extraction of Pd(II) and Nd(III) with *N,N'*-dimethyl-*N,N'*-dioctylhexylethoxymalonamide (DMDOHEMA), it was reported that the extraction of Nd(III) is driven by aggregation, which is more likely to occur in aliphatic diluents, rather than aromatic ones.[174] In parallel, the extraction of Pd(II) was found to be driven by coordination and that the aggregation of the organic phase has no impact on its extraction.

In this regard, three different ligands were investigated for the extraction of Pd(II), Fe(III) and Nd(III) from nitrate media. These malonamides are *N,N,N',N'*-tetrahexylmalonamide (THMA), *N,N,*-dimethyl-*N'-N'*-dibutyltetradecylmalonamide (DBMA) and *N,N,N',N'*-tetramethylmalonamide (TDMA) (Figure 28).

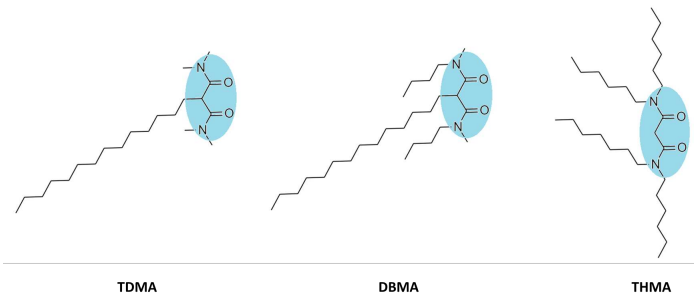

Figure 28: Chemical structure of diamides employed in this study with the presumed hydrophilic part coloured in blue.

The choice of these ligands was made according to their different structures, which implicitly affect their organization in the organic phase. The bulkiness of the head affects the assembly of the polar core of the ligands when organized, which can affect their aggregation ability. THMA, DBMA and TDMA differ in the length of their central and lateral chains, as shown in Figure 28. Indeed, TDMA presents the smallest head with a long tail, suggesting a higher affinity for aggregation than DBMA, which also has a long tail, but a bulkier head than the former, due to the presence of two butyl chains. Finally, THMA presents the largest head due to the presence of four hexyl chains, suggesting a lower aggregation capacity.

For this thesis work, we were interested in assessing the extraction kinetics of Pd(II), Nd(III) and Fe(III) with these three ligands. In this respect, understanding the characteristics of the chosen systems was necessary before any extraction kinetics investigation.

Hence, in this chapter, we focused on the thermodynamic characterization of the extracting systems. This characterization comprised the choice of the diluent and third phase formation, characterization of the basicity of the molecules and the determination of the stoichiometry of the extracted complexes with the different metals.

I. Synthesis of ligands

The synthesis of tetrasubstituted malonamides is well reported in the literature.[149,154] Two main routes have been considered for the synthesis of tetrasubstituted malonamides. These are the reaction of secondary amines with acid esters (**route I,** Figure 29) and the reaction of secondary amines with acyl chlorides (**route II,** Figure 29). DBMA was kindly provided for this work by CEA Marcoule, whereas TDMA and THMA were synthesized.

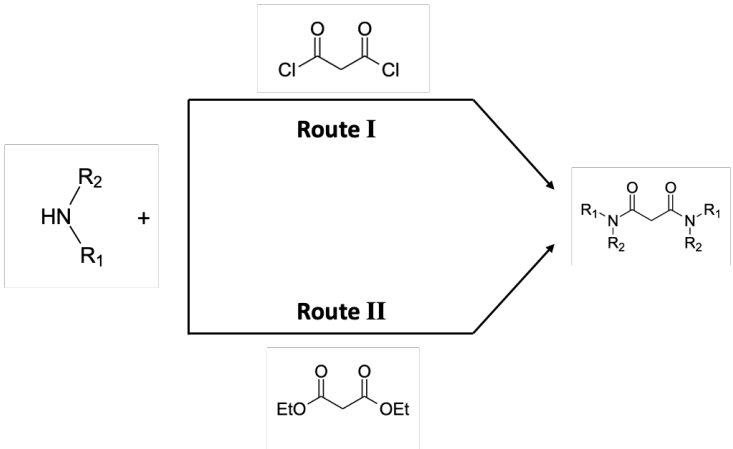

Figure 29: Synthesis of tetrasubstituted malonamides extractants: Route I starting from diethyl malonate, Route II from malonyl chloride.

A. Synthesis of TDMA

TDMA was synthesized following a procedure described in the literature.[192] It was prepared by alkylation of the central carbon of the commercially available tetramethylmalonamide dissolved in tetrahydrofuran (THF) by the reaction with sodium hydride and with bromotetradecane (Figure 30).

This synthesis was prepared on a small scale (0.5g). The resulting product was washed and recrystallised in a chloroform/pentane mixture, then concentrated *in vaccuo.* The final product was obtained as a white powder with a yield of 64%. The purity of the ligand was verified with ^{1}H and ^{13}C NMR, and it was more than 98%.

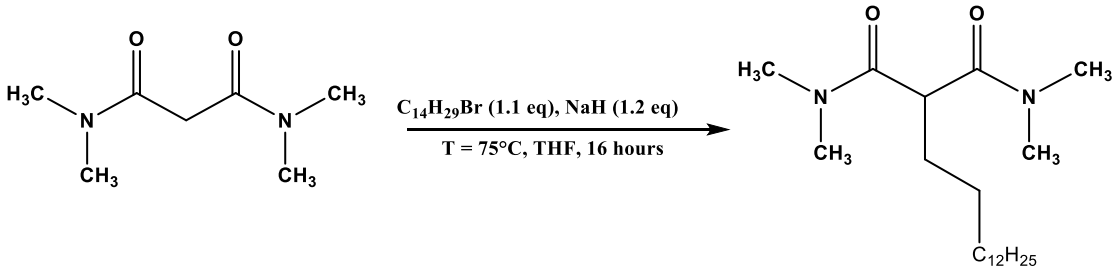

Figure 30: Scheme of the synthesis of TDMA.

B. Synthesis of THMA

The synthesis of THMA from the reaction of diethyl malonate with dihexylamine, and the reaction of malonyl chloride with dihexylamine is documented in the literature.[175,193] One major problem we faced with THMA was the effect of the purity of the final product on the extraction performance of Pd(II). This will be explained in details later in Chapter 5. Thus, besides the necessity to obtain high product yields, the challenge was to optimize both the experimental conditions and setup, to obtain a batch of THMA with high purity.

1. Synthesis of THMA using malonyl chloride (Route I)

The synthesis of THMA was performed as reported in the literature.[194] A mixture of dihexylamine, malonyl chloride and triethylamine used as an HCl scavenger, was diluted in chloroform at 0°C and refluxed at 40°C during 4 hours (Figure 31). This synthesis route was abandoned since low product yields were obtained (less than 40%).

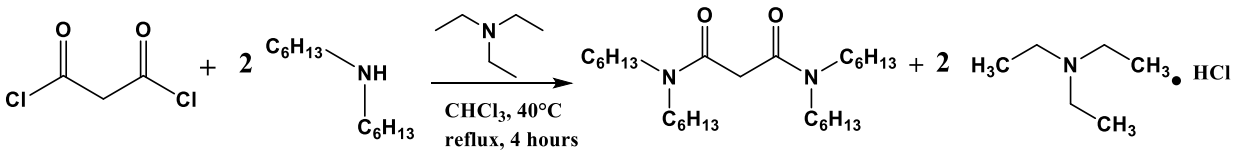

Figure 31: Synthesis of THMA by reaction of malonyl chloride with dihexylamine, in the presence of triethyl amine as HCl scavenger.

2. Synthesis of THMA using diethyl malonate (Route II)

The thermal synthesis of THMA from diethyl malonate and dihexylamine was carried out (Figure 32). A screening on several experimental parameters led to optimize better the experimental conditions as well as the experimental setup for the synthesis. This optimization was necessary to obtain high reaction yields and high purity of the final product. Herein, we present the set of experiments performed that permitted us to elaborate the final synthesis procedure, which is now adopted in our laboratory.

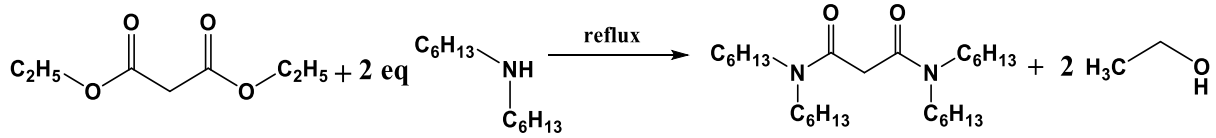

Figure 32: Synthesis of THMA by reaction of diethylmalonate with dihexylamine.

The synthesis of THMA was first carried out by heating a mixture of diethyl malonate and dihexylamine under reflux. The experimental setup is presented in Figure 33. It is worth mentioning that preliminary tests showed that the evacuation of ethanol was essential to avoid a low conversion rate, and thus ensuring a good yield of the reaction. Therefore, an argon flow was flushed continuously in the vessel during the reaction, which improved the reaction yield. This flow can be realized with nitrogen however, it is not available at the laboratory.

Despite the argon flush, diethyl malonate, dihexylamine, and mono-adduct product residues were present in the final product, indicating that the reaction was not complete. We point out that the synthesis was performed under reflux at 200°C, for 4 hours, using an excess of dihexylamine (2.05 molar equivalent). Therefore, several hypotheses were made:

1- The heating time was not sufficient
2- The heating temperature was not well adapted
3- The dihexylamine to diethyl malonate molar ratio was not suitable

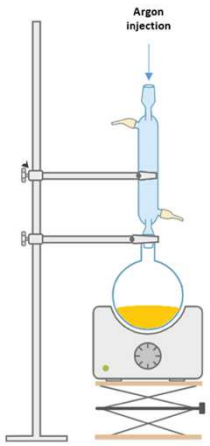

Figure 33: Reflux setup for the synthesis of THMA.

In this regard, kinetic monitoring through NMR analysis of the synthesis was performed to estimate the required heating time to complete the reaction. For this follow-up, we decided to study the effect of three parameters simultaneously: Temperature, dihexylamine to diethyl malonate molar ratio and the heating time. In Table 10 we summarize the selected experimental conditions.

Table 10: Summary of the experimental conditions tested for the synthesis of THMA.

Dihexylamine to diethyl malonate molar ratio	Time of heating	Temperature
2 eq. < ratio < 2.2 eq.	0 hour < t < 8 hours	180°C < T < 200°C

Despite modifying several experimental conditions, the starting and the mono-adduct products were still present in the final product. However, signal integration showed that their amounts were the lowest when using 2.1 molar equivalent of dihexylamine and heating at 180°C for 5 hours. In parallel, the obtained spectra revealed the presence of ethanol for all the synthesized THMA, regardless of the experimental conditions. We, therefore, assumed that if ethanol is totally removed from the medium, the reaction would further proceed in the direction of reactants consumption, which is generally in agreement with Le Chatelier's principle. Therefore, we concluded that the optimization of the synthesis procedure should be based on total elimination of ethanol from the reaction mixture

With this in mind, we proposed a distillation-reflux setup for the synthesis of THMA, which is presented in Figure 34. This setup is also provided with an argon flow.

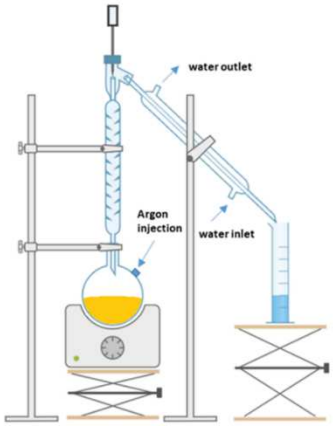

Figure 34: Reflux distillation setup for the synthesis of THMA.

Kinetic monitoring by NMR analysis showed that the reaction was complete after 7 hours of heating. We point out that for this setup, an argon flow is applied for 1 min every single 30 min, for the first 4 hours of reaction, and then a continuous flow is applied for 3 hours, until a total elimination of ethanol. The final product was washed to remove unreacted dihexylamine, and then dried over Mg_2SO_4. For the purification, the obtained product, which is diluted in diethyl ether, was mixed with activated charcoal and silica gel. The mixture was vigorously shaken for 10 minutes and then filtered through Celite. The final product was obtained after concentration *in vaccuo* as a viscous pale yellow oil with 98% yield. The purity was verified through ^{1}H and ^{13}C NMR and was over 99% (Refer to Chapter 6, § II - A).

3. Synthesis of THMA with microwave assistance:

The use of microwave assisted synthesis for malonamide is reported in the literature.[195] In general, this synthesis route proved to be very efficient, where the synthesis of tetraethylmalonamide was achieved in 30 min. In addition, large yields were obtained, and side products were avoided.

In this regard, the synthesis of THMA was performed using a microwave hydrothermal reactor. Several trials were conducted by varying the heating time from 30 min to 1 hour and increasing the temperature from 185°C to 200°C. However, NMR analysis showed an incomplete reaction, with the formation of side products

According to the results obtained with reflux setup, eliminating ethanol is mandatory to complete the reaction, which is not the case when using microwave since closed vessels are used. This synthesis route was therefore abandoned.

4. Conclusion

In conclusion, for this work, the synthesis of THMA was carried out using a reflux-distillation setup (Figure 34), following the reaction scheme illustrated in Figure 35.

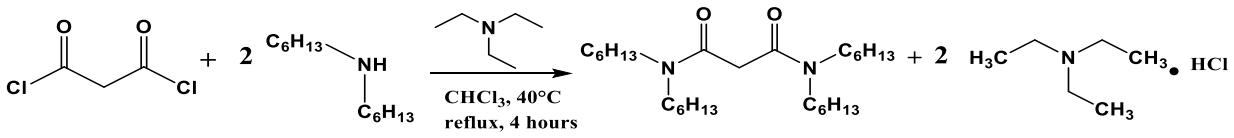

Figure 35: Optimized synthesis of THMA by reaction of diethyl malonate with dihexylamine

II. Determination of the extraction system

A. Absence of organization in toluene

In addition to the ligand structure, the organization of malonamides in the organic phase is dictated by the nature of the diluent.[196] In a previous study conducted with *N,N'*-dimethyl-*N,N'*-dioctylhexylethoxymalonamide (DMDOHEMA), it was demonstrated that no organization of the organic phase was found when using toluene as a diluent.[174] However, it was more likely when using heptane. We add that the organization of malonamides in other aliphatic diluents, *i.e.* dodecane is reported in the literature.[58,60]

The absence of organization of the organic phase when using THMA and DBMA in toluene was also verified by SAXS measurements (Figure 36). The recorded spectra revealed that for both ligands and for 3M and 5M HNO_3, no increase in intensity at low q-values was observed. Therefore, no supramolecular correlation signature was visible. This is in perfect agreement with the results reported with DMDOHEMA.

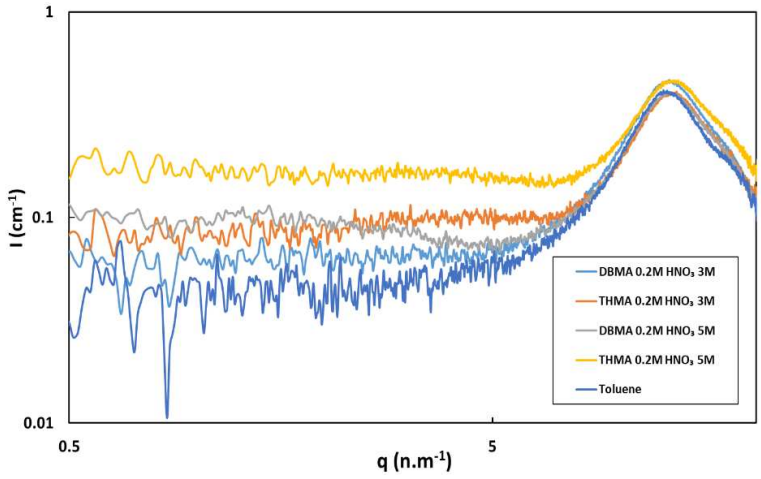

Figure 36: SAXS spectra of 0.2M THMA and 0.2M DBMA in toluene, pre-equilibrated with 3M and 5M aqueous nitric acid solutions.

Therefore, the effect of the structure of the chosen ligands, THMA, DBMA and TDMA, cannot be observed in aromatic diluents, such as toluene. Instead, aliphatic diluents are needed for that. However, third phase formation could be limiting. In this respect, the experimental conditions for the appearance of third phase formation should be adequately defined.

B. Third phase formation

One major problem in designing a solvent extraction system is third phase formation,[161] which corresponds to the splitting of the organic phase into heavier and lighter phases when the metal or acid loadings reach a specific limiting organic concentration (LOC). The supramolecular organization of the organic phase is at the origin of this phenomenon.[55] It was demonstrated that the Van der Waals attractions between the cores of reverse micelles is the key factor for understanding and modelling the apparition of the third phase.[58] The Baxter sticky hard-sphere model can be applied to describe the interactions between the reverse aggregates.[58]

Third phase formation is influenced by many parameters, namely, the nature and concentration of the metal, acid, diluent, extractant structure and temperature. We add that third phase formation is often eliminated by adding diluent modifiers with a hydrocarbon chain containing a polar atom such as long-chain aliphatic alcohols *i.e. n*-octanol.[190]

- **Diluent**: It is a crucial factor in the occurrence of this phenomenon.[196] The attenuation of binding between the aggregates is due to the increase in stabilizing steric repulsions between the hydrophobic chains of the diamide. The presence of a 'penetrating' diluent, namely toluene, hexane, octanol, delays or avoids the formation of the third phase. The term penetrating reflects the affinity of the diluent for the hydrophobic chains of the extracting molecule.[197] Similarly, branching can delay the onset of the third phase.[198]
- **Structure of the extracting molecule:** The longer the hydrophobic chains, the greater the inter aggregate distance, and the weaker the attraction force. The longer hydrophobic chains of the extractants will therefore delay the appearance of the third phase
- **Temperature:** An increase in temperature decreases the aggregation of the molecules into reversed micelles, which delays the appearance of the third phase.

This study started with a screening of the influence of the diluent, the concentration of the ligand in the organic phase and the acidity of the aqueous phase on third phase formation. To do so, a series of experiments were performed at T = 21°C, varying the nature of the ligand and its concentration (0.1M and 0.2M), the diluent, and the acidity in the aqueous phase (3M and 5M). Four diluents were chosen for this study, toluene, heptane, cyclohexane and iso-octane. We specify that these experiments were

carried out by bringing into contact the various organic phases with the different aqueous phases of nitric acid during 1 hour.

The first series of experiments was performed with THMA. The occurrence of the third phase with THMA for the different experimental conditions used is summarized in Table 11. First, using toluene as a diluent, no third phase formation was encountered, regardless of the ligand and nitric acid concentrations in the organic and aqueous phases, respectively. The same was true when using cyclohexane as a diluent. However, when using heptane, third phase formation was more governed by the concentration of nitric acid in the aqueous phase rather than the concentration of the extractant in the organic phase. Hence, third phase was more likely for [HNO_3].5M. Whereas, when using iso-octane as a diluent, third phase appeared for both nitric acid and ligand concentrations.

Table 11: Third phase occurrence using THMA as an extractant with different diluents and aqueous nitric acid concentrations.

	THMA 0.1M		**THMA 0.2M**	
	HNO_3 3M	**HNO_3 5M**	**HNO_3 3M**	**HNO_3 5M**
Toluene	×	×	×	×
Heptane	×	✓	×	✓
Cyclohexane	×	×	×	×
Iso-octane	✓	✓	✓	✓

The second set of experiments was performed with DBMA. The occurrence of third phase formation with DBMA is summarized in Table 12. As with THMA, third phase apparition was not encountered when using toluene as a diluent. Whereas for heptane, it appeared when 0.2M of DBMA in the organic phase was in contact with a 5M aqueous nitric acid solution. Finally, by using iso-octane, third phase appeared for all the studied conditions.

Table 12: Third phase occurrence using DBMA as an extractant with different diluents and aqueous nitric acid concentrations.

	DBMA 0.1M		**DBMA 0.2M**	
	HNO_3 3M	**HNO_3 5M**	**HNO_3 3M**	**HNO_3 5M**
Toluene	×	×	×	×
Heptane	×	×	×	✓
Iso-octane	✓	✓	✓	✓

Finally, the experiments with TDMA were limited to toluene only since the ligand is insoluble in neither heptane nor cyclohexane (Table 13). Like the two previous ligands, by using toluene, no third phases appeared with TDMA. It is worth mentioning that the maximum concentration of TDMA that can be solubilized in toluene is 0.4M; by exceeding this concentration, precipitation of the ligand occurs.

Table 13: Third phase occurrence using TDMA as an extractant with different diluents and aqueous nitric acid concentrations.

	TDMA 0.1M		**TDMA 0.2M**	
	HNO_3 3M	**HNO_3 5M**	**HNO_3 3M**	**HNO_3 5M**
Toluene	×	×	×	×
Heptane	insoluble	insoluble	insoluble	insoluble
Cyclohexane	insoluble	insoluble	insoluble	insoluble

According to this screening, and despite some extractions trials were performed using other diluents, toluene was chosen for the suite of this PhD thesis, seen that no third formation was encountered for the three ligands, regardless of the concentrations of the ligand and nitric acid in the aqueous phase.

III. Extraction of metals using different diluents

Bearing in mind that toluene was chosen for the suite of this work, we characterized rapidly the scope of extraction of Pd(II), Nd(III) and Fe(III) with THMA, DBMA and TDMA using different diluents, *i.e.* toluene, heptane and cyclohexane. As a result, we characterized the effect of the diluent, nitric acid and ligand concentrations on the extraction of the three metals with the three ligands briefly. We mention that this study was carried out after defining conditions for which third phases occurred.

The first set of experiments was performed with THMA. As shown in Figure 37, THMA shows excellent and selective extraction of Pd(II) over Fe(III) and Nd(III). On the other hand, Nd(III) extraction is extremely poor with THMA, especially when using toluene or heptane as diluents. The same is true for Fe(III). However, by using cyclohexane, an increase of Fe(III) extraction is observed. In addition, an increase in acidity slightly favours the extraction of Fe(III), especially with toluene and cyclohexane, which is in complete agreement with the results reported by Mastretta et al.[142] Moreover, for 0.2M THMA and constant HNO_3 concentration, the extraction yields of Nd(III) and Fe(III) were slightly higher with heptane, compared to cyclohexane then to toluene.

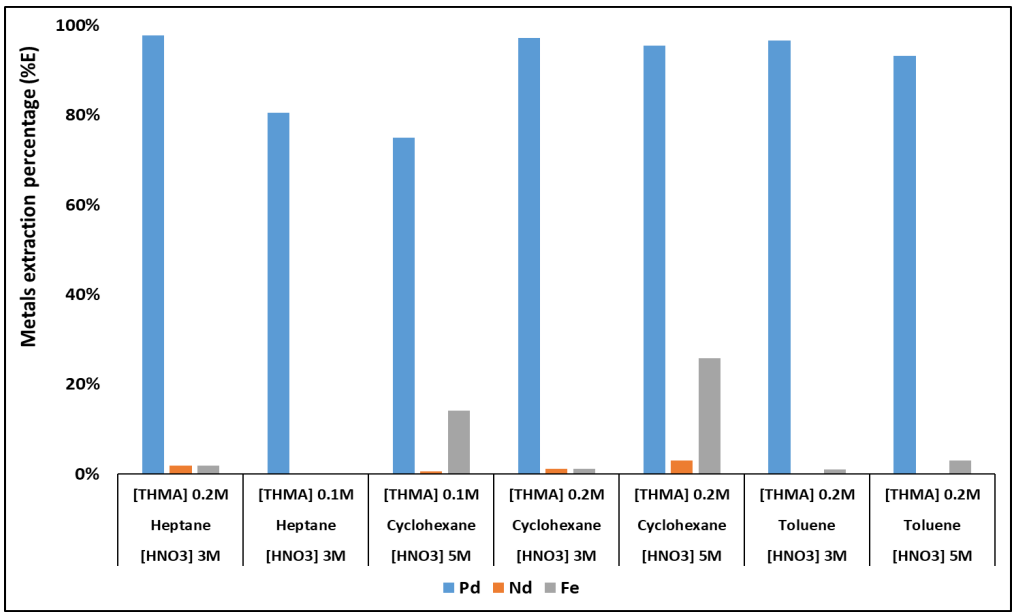

Figure 37: Extraction of Pd(II), Nd(III) and Fe(III) with THMA using different diluents. T=21°C, A/O=1, [Pd] 100 mg.L^{-1}, [Nd] 200 mg.L^{-1}, [Fe] 200 mg.L^{-1}.

In addition, the effect of the diluent on the extraction of Pd(II), Nd(III) and Fe(III) with DBMA was performed. As for THMA, the extraction of Pd(II) with DBMA is the highest, compared to that of Nd(III) and Fe(III), for both diluents. However, DBMA shows better extraction for Fe(III) and Nd(III) than THMA by using heptane, or by increasing the concentration of nitric acid in the aqueous phase, in the case of toluene as a diluent as depicted in Figure 38.

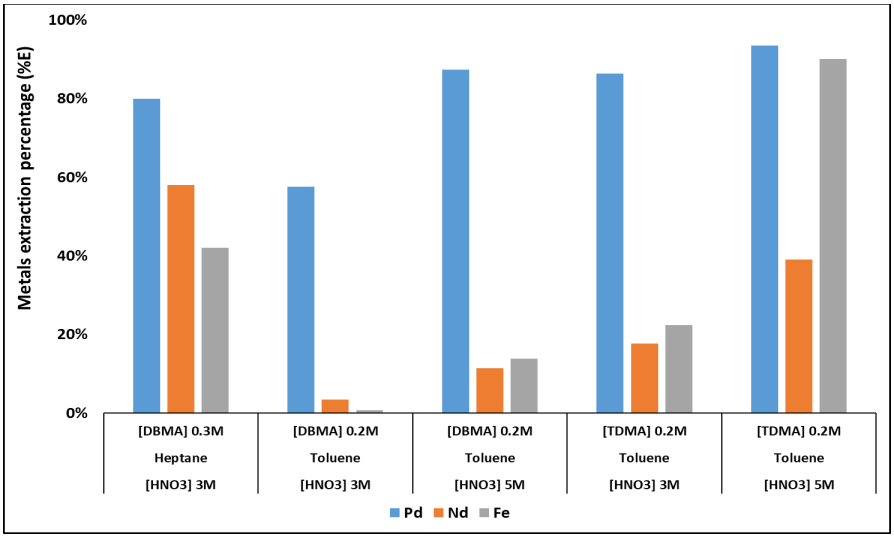

Figure 38: Extraction of Pd(II), Nd(III) and Fe(III) with DBMA and TDMA using different diluents. T=21°C, A/O=1, [Pd] 100 mg.L^{-1}, [Nd] 200 mg.L^{-1}, [Fe] 200 mg.L^{-1}.

Finally, for TDMA, the extraction was limited by using toluene as a diluent since this ligand is insoluble neither in cyclohexane nor in heptane. Conversely to the other malonamides, TDMA showed less selective extraction for Pd(II). A well visible enhancement of Fe(III) extraction was noticed when

increasing the concentration of nitric acid (Figure 38). By increasing the nitric acid concentration, the extraction of Nd(III) increased.

It appears from this screening that the extraction of the metals is strongly influenced by the nature of the ligand and its concentration, the diluent and the aqueous nitric acid concentration. THMA is a very selective extractant for Pd(II) when using toluene and heptane as diluents. In parallel, DBMA and TDMA, both showed less selective extraction for Pd(II).

IV. Acid uptake

A. Stoichiometry of the extracted species

Due to a resonance hybridization of the amide bond, a carbonyl oxygen atom of a carboxylic acid amide has an excess electron density. Therefore, the electron donor properties of this oxygen allow us to consider malonamides as Lewis bases.[176] Hence, they can coordinate with Lewis acids, such as proton ions or metals. The basicity of a malonamide molecule is influenced by its structure.[176] The introduction of substituents of different electronegativity causes changes in the basicity.

In general, malonamides (L) extract nitric acid by forming complexes in organic phases. The reaction takes place according to the following reaction:

$$\mathrm{yHNO_3} + \mathrm{x\bar{L}} \rightleftharpoons \overline{(\mathrm{HNO_3})_y\mathrm{L_x}} \tag{173}$$

$$\mathrm{K_{ext,a}} = \frac{[\overline{(\mathrm{HNO_3})_y\mathrm{L_x}}]}{[\mathrm{HNO_3}]^y[\bar{\mathrm{L}}]_{\mathrm{free}}^x} = \frac{[\bar{\mathrm{L}}]_{\mathrm{bound}}}{[\mathrm{HNO_3}]^y[\bar{\mathrm{L}}]_{\mathrm{free}}^x} \tag{174}$$

Where the bar denotes the species present in the organic phase, $[\bar{\mathrm{L}}]_{\mathrm{bound}}$ is the concentration of the ligand bound to acid, and $[\bar{\mathrm{L}}]_{\mathrm{free}}$ is the free ligand concentration.

Two different modes of acid extraction were reported for malonamides: By protonation of the extractant (Figure 39-a) or through hydrogen bond between the hydrogen of the nitric acid and the oxygen of the carbonyl group (Figure 39-b).[165,199]

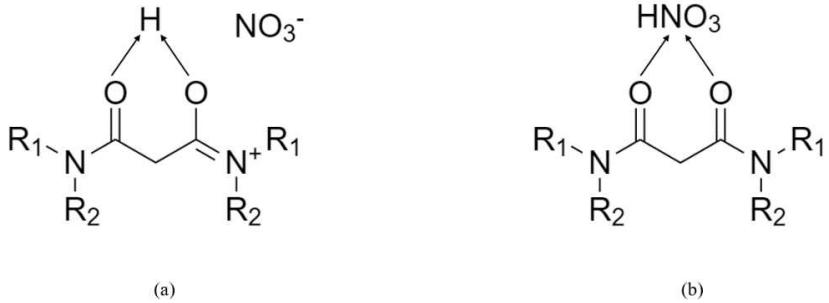

(a) (b)

Figure 39: Types of HNO_3-Malonamide adducts, (a) acid extraction by protonation, (b) acid extraction through hydrogen bond formation.

However, nitric acid titration alone of the organic phase is insufficient to predict the species present accurately. In this regard, we would like to clarify that this section is not primarily dedicated to determining the nature of the extracted species of malonamide-HNO_3. Instead, the effect of the geometry of the ligand, the concentrations of the ligand in the organic phase and of the nitric acid in the aqueous phase on the overall basicity of the ligands were investigated.

First, and for the sake of simplicity, we will consider that the acid extraction takes place according to the following equilibrium:

$$H^+ + NO_3^- + x\bar{L} \rightleftharpoons \overline{HNO_3L_x} \tag{175}$$

$$K'_{ext,a} = \frac{[\overline{HNO_3L_x}]}{[H^+][NO_3^-][\bar{L}]^x} = \frac{D_{H^+}}{([NO_3^-]_0 - D_{H^+}[H^+])[\bar{L}]^x} \tag{176}$$

Where,

$$D_{H^+} = \frac{[\overline{H^+}]}{[H^+]} = \frac{[\overline{HNO_3L_x}]}{[H^+]} \tag{177}$$

And,

$$[NO_3^-] = [NO_3^-]_0 - [\overline{HNO_3L_x}] = [NO_3^-]_0 - D_{H^+}[H^+] \tag{178}$$

By taking the log on each side,

$$LogK'_{ext,a} = Log(D_{H^+}) - Log([NO_3^-]_0 - D_{H^+}[H^+]) - xLog[\bar{L}] \tag{179}$$

So,

$$\mathrm{Log}(\mathrm{D_{H^+}}) - \mathrm{Log}([\mathrm{NO_3^-}]_0 - \mathrm{D_{H^+}}[\mathrm{H^+}]) = \mathrm{xLog}[\bar{\mathrm{L}}] + \mathrm{LogK''_{ext}} \quad (180)$$

The plot of $\mathrm{Log}(\mathrm{D_{H^+}}) - \mathrm{Log}([\mathrm{NO_3^-}]_0 - \mathrm{D_{H^+}}[\mathrm{H^+}])$ versus $\mathrm{Log}[\bar{\mathrm{L}}]$ should give a straight line with a slope of x.

Nitric acid extraction was investigated for THMA and DBMA in toluene by varying the nitric acid concentrations in the aqueous phase and ligands in the organic phase. Three concentrations were chosen for nitric acid: 1.5M, 3M and 5M. In addition, the concentrations of ligands in the organic phase ranged from 0.05M to 0.4M (Figure 40).

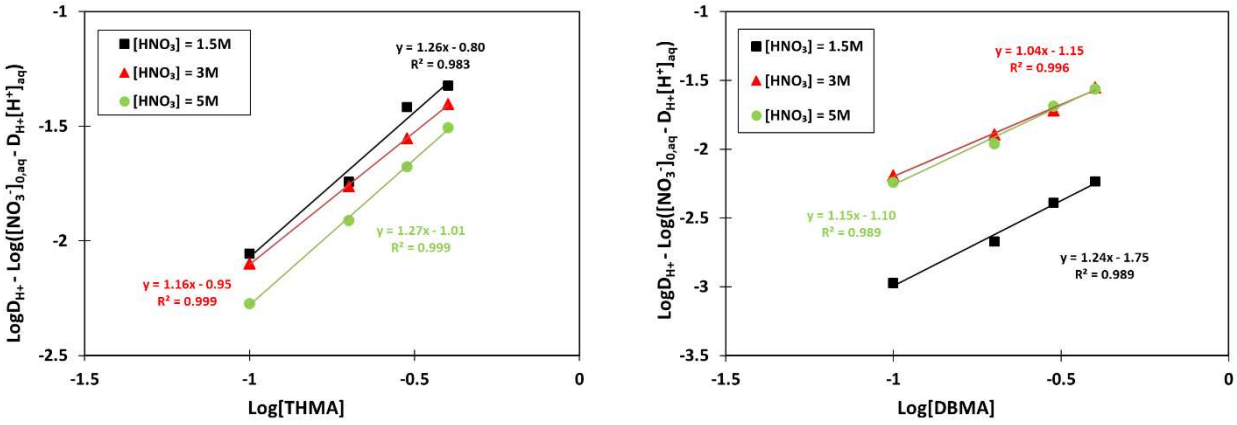

Figure 40: Nitric acid extraction with THMA and DBMA in toluene for different nitric acid concentrations in the aqueous phase.

First, the linearity of the curves confirms the coherence between the experimental findings and the proposed extraction equilibrium. The slope nearly equal to the unit reveals that the extracted species are of type $\overline{\mathrm{L(HNO_3)}}$.

In parallel, it is not forbidden to consider the slight deviation of the unit value for the slopes. For instance, adducts type $\overline{\mathrm{L_x(HNO_3)}}$ may exist in the organic phase if we consider that the slopes are slightly higher than 1, especially in the case of THMA. However, and as mentioned above, no decisive conclusion can be made about the type of the extracted species at this level of investigation.

In their study, Spjuth et al.[150] reported that for *N,N'*-dimethyl-*N,N'*-dicyclohexyltetradecylmalonamide (DMDCHTD), adducts type $\mathrm{L(HNO_3)_y}$ were formed at high nitric acid concentrations (>10M), whereas, at 1M $\mathrm{HNO_3}$, the authors reported that $\mathrm{L_x(HNO_3)}$ were formed. This statement was concluded from the slope of the curves of $\mathrm{logD_{HNO_3}}$ against

log [Malonamide], which was equal to 1 at high concentrations of nitric acid, and equal to 1.5, at 1M HNO_3.

B. The average number of extracted HNO_3 molecules

The previous experimental results presented in Figure 40 allow the determination of (α), the average number of the extracted molecules of HNO_3 per 1 molecule of ligand for both ligands, THMA and DBMA. This number (α) was calculated as follows:

$$\alpha = \frac{[\overline{HNO_3}]}{[\overline{Ligand}]_0} \tag{181}$$

Where $[\overline{HNO_3}]$, denotes the concentration of proton ions extracted in the organic phase and $[\overline{Ligand}]_0$, is the initial ligand concentration in the organic phase.

The obtained results for THMA and DBMA are presented in Table 14 and Table 15, respectively.

Table 14: Average number of HNO_3 molecules extracted per 1 molecule of THMA in toluene, at different concentrations of nitric acid and THMA.

	[THMA] 0.1M	**[THMA] 0.2M**	**[THMA] 0.3M**	**[THMA] 0.4M**
[HNO_3] = 1.5M	0.21	0.21	0.28	0.25
[HNO_3] = 3M	0.71	0.73	0.75	0.75
[HNO_3] = 5M	1.30	1.40	1.50	1.54

Table 15: Average number of HNO_3 molecules extracted per 1 molecule of DBMA in toluene, at different concentrations of nitric acid and DBMA.

	[DBMA] 0.1M	**[DBMA] 0.2M**	**[DBMA] 0.3M**	**[DBMA] 0.4M**
[HNO_3] = 1.5M	0.02	0.02	0.03	0.03
[HNO_3] = 3M	0.58	0.55	0.53	0.56
[HNO_3] = 5M	1.39	1.27	1.46	1.39

The number of extracted HNO_3 molecules is independent of the ligand concentration, for both THMA and DBMA. Rather, it depends strongly on the nitric acid concentration in the aqueous phase. In other words, the number of extracted molecules of HNO_3 per one molecule of ligand (α) is constant

for a range of ligand concentration, at a given concentration of nitric acid in the aqueous phase. This is in agreement with the results reported by Déjugnat et al.[199] in the case of DMDOHEMA, and the results reported by Spjuth et al.[150,176] The authors, reported that for several malonamides, the ratio α was constant regardless of the concentration of the ligand, and this ratio increased steadily with increasing nitric acid concentration in the aqueous phase.

In parallel, by comparing the average number of HNO_3 extracted by one molecule of ligand, we notice that values lower than 1 were obtained when nitric acid concentration was lower or equal to 3M in the aqueous phase. However, these values were higher than 1 when aqueous nitric acid concentration was 5M. This can be explained by a change of the adducts present in the organic phase. In fact, for the diamides, different adducts of ligand-nitric acid complexes were identified, for a concentration range of 0.1M to 1M of diamide in different diluents (toluene, TPH, dodecane).[34,200] These species are:

- Free ligand L
- $L_2(HNO_3)$
- $L(HNO_3)$
- $L(HNO_3)_2$
- $L(HNO_3)_3$

From these findings, we assume the presence of the following species:

- Mainly free ligand L and $L(HNO_3)$ for $[HNO_3] \leq 3M$
- Mainly $L(HNO_3)$ and $L(HNO_3)_n$ for $[HNO_3] > 3M$

C. Basicity of THMA and DBMA

If we look at the results shown in Table 14 and Table 15, we notice that the obtained values of α with THMA are higher than that obtained with DBMA, at $[HNO_3] \leq 3M$, whereas these values become approximately equal at 5M $[HNO_3]$. This shows that THMA has a more basic character than DBMA, which is particularly visible at low nitric acid concentrations. This is illustrated in Figure 41, where the concentration of the extracted nitric acid in the organic phase is plotted against the concentration of ligands at different nitric acid concentrations in the aqueous phase.

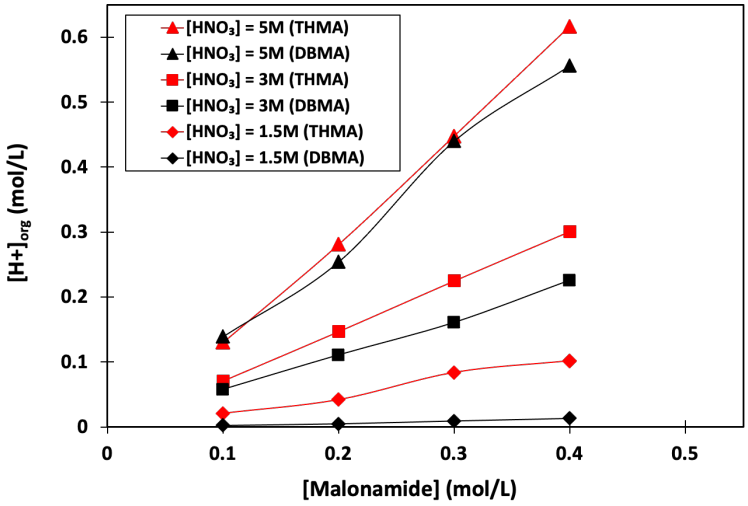

Figure 41: Extraction of nitric acid for different concentrations of THMA and DBMA in toluene, at different concentrations of aqueous nitric acid.

The results obtained above reveal the effect of the substituents on the basicity of the studied malonamides. The substitution of the central carbon with an alkyl chain decreases the basicity of the ligands since DBMA, which has a tetradecyl chain on its central carbon, is less basic than THMA, which is free of any central chain. This is in agreement with the results reported by Cuillerdier et al.[146]

V. Extraction of Pd(II)

In the light of the screening of the extraction of Pd(II), Fe(III) and Nd(III) with THMA, DBMA and TDMA in toluene, we found that the three ligands generally show better extraction of Pd(II) compared to the other two metals.

In parallel, as discussed in Chapter 1 § VIII, the extraction properties of the malonamides have been linked to their different basicities and geometries. The acid uptake showed that THMA is more basic than DBMA. In addition, the three studied malonamides present different geometries. Therefore, in this section, we will discuss the effect of the aqueous nitric acid concentration and the impact of the geometry of the ligands on the extraction of Pd(II). Finally, the selective extraction of Pd(II) with THMA will be presented.

A. Effect of nitric acid concentration on the extraction of Pd(II)

The extraction of Pd(II) with THMA and DBMA at different nitric acid concentrations in the aqueous phase was carried out (Figure 42).

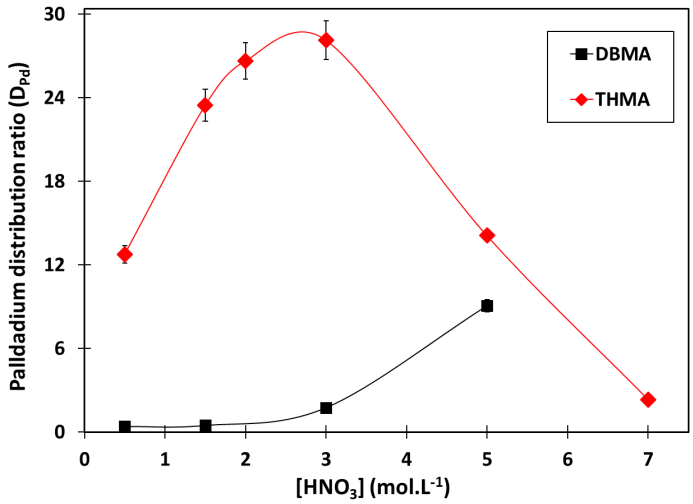

Figure 42: Effect of the concentration of nitric acid in the aqueous phase on the distribution ratios of Pd(II) in extraction with THMA and DBMA in toluene. Initial $[Pd]_{aq}$ 500 mg.L^{-1}, [THMA] 0.2M, [DBMA] 0.2M, 24 hours extraction, A/O=1, T = 21°C.

The maximum Pd(II) extraction with THMA is reached for a lower concentration of nitric acid in the aqueous phase, compared to DBMA. Due to the more basic character of THMA, the extraction competition of H^+ is more enhanced than that with DBMA. Therefore, the increase in nitric acid concentration in the aqueous phase will disturb less Pd(II) extraction with DBMA.

In general, the impact of nitric acid concentration usually implies the competition with H^+ extraction on the one hand and the influence of nitrate ions on the speciation of Pd in the aqueous phase on the other.[142] Therefore, the effect of the concentration of proton ions on Pd(II) extraction with THMA and DBMA was studied (Figure 43). The concentration of nitrate ions was fixed at 5M using lithium nitrate salt ($LiNO_3$), and only the concentration of proton ions was varied.

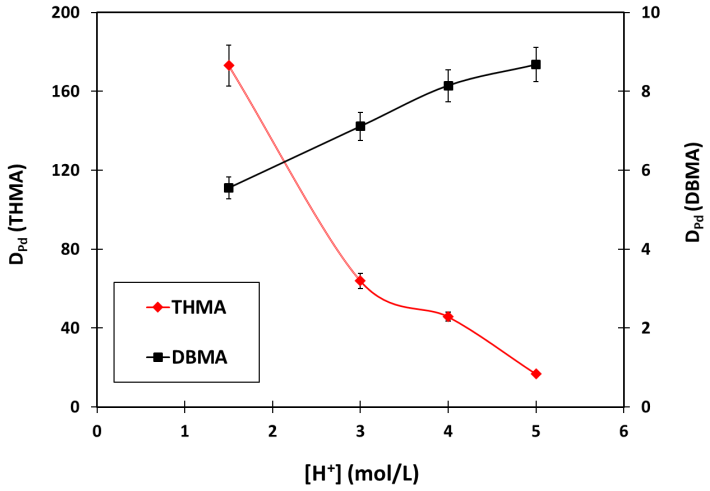

Figure 43: Extraction of Pd(II) with THMA and DBMA as a function of $[H^+]_{aq}$. Initial $[Pd]_{aq}$ 200 mg.L^{-1}, $[NO_3^-]_{aq}$ 5M, $[THMA]_{org}$ 0.2M and $[DBMA]_{org}$ 0.2M in toluene, 24 hours of extraction, A/O 1, T=21°C.

The increase in the $[H^+]$ has a different effect on Pd(II) extraction with THMA and DBMA. A continuous and steep decrease of Pd(II) extraction was noticed with THMA, whereas a continuous increase was noticed with DBMA. Thus, we conclude a strong competitive effect of H^+ in the extraction of Pd(II) with THMA, whereas a cooperative effect in the case of DBMA. These results can be related to the larger basic character of THMA compared to DBMA, where the increase of $[H^+]$ induces larger competition with the extraction of Pd(II). In the case of THMA, the extraction of acid is strongly favoured, even at a low proton concentration in the aqueous phase, which decreases the concentration of free ligand and enhances the competition between acid-binding and Pd(II) complexation. It could be interesting to study the impact of proton concentration on a more extensive range of concentrations.

B. Effect of the ligand basicity and structure on the extraction of Pd(II)

The difference in the extraction abilities of malonamides is attributed mainly to the electronic and steric effects.[150,153,172,176] The former is described with the basicity of the molecule, while the latter is related to its structure and the length of the substituents. In this section, we highlight the effect of the basicity of THMA and DBMA, as well as the effect of their structures on Pd(II) extraction.

An increase in the basicity of a malonamide may increase the competition between metals extraction and acid extraction, which may decrease the metals distribution ratio. According to Spjuth et al.[176], malonamides of lower basicity give better ion extractions since the competition between proton and metal ions is less severe than with more basic malonamides. Although THMA was found to be more basic than DBMA, the former gives a much better Pd(II) extraction than DBMA (Figure 44). This suggests that the electronic effect has more negligible effect on Pd(II) extraction, and this difference in extractability is more likely related to the steric effect.

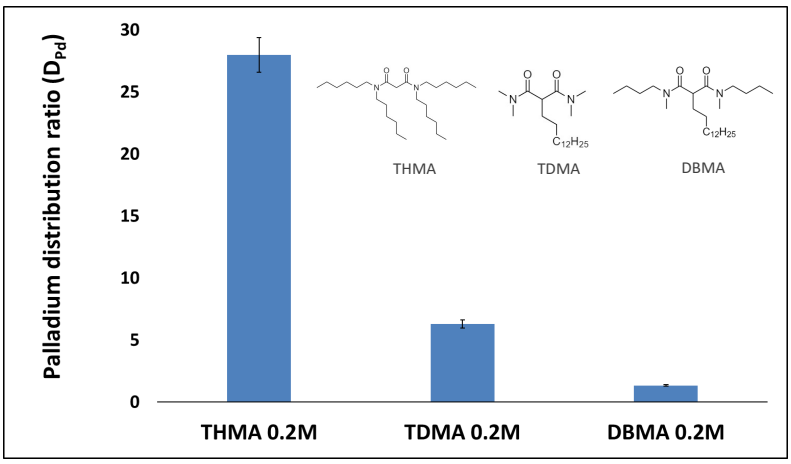

Figure 44: Extraction of Pd(II) with THMA, DBMA and TDMA in toluene. initial $[Pd]_{aq}$ 500 $mg.L^{-1}$, $[HNO_3]_{aq}$ 3M, T = 21°C, A/O = 1.

The ability of malonamides to extract metal ions is related to the structure and substituents of the molecules.[149,152,172] In general, malonamides can change their O=C…C=O torsion angle and the O…O distance between the carbonyl oxygen atoms.

The results in Figure 44 show that the central carbon substitution decreased to a greater extent the extraction of Pd(II). The distribution ratio of palladium decreased from (28 ± 1.4) with THMA to (6.3 ± 0.3) with TDMA and (1.3 ± 0.1) with DBMA. At this level of experiments, we can relate this decrease in extraction to steric hindrance imposed by the central chain on the complexation of Pd(II), since the carbonyl groups are the complexing sites for the metals. The decrease of the distribution ratio of metals with the methylation of the central carbon was reported in the case of the extraction of Eu(III) with *N,N,N',N'*-tetrahexylmalonamide (THMA), *N,N,N',N'*-tetrahexylmethylmalonamide, (MeTHMA) and *N,N,N',N'*-tetrahexyldimethylmalonamide (DiMeTHMA).[175] The authors assumed that steric hindrance caused by the presence of the central chain results in decreasing the binding affinity of the ligand to the metal.

In parallel, the effect of the lateral substituents on Pd(II) extraction was highlighted by comparing the distribution ratios of Pd(II) upon extraction with TDMA and DBMA. Both ligands have a tetra-decyl central chain. However, DBMA has two lateral butyl and methyl chains, compared to four methyl chains for TDMA. The extraction of Pd(II) is better with TDMA than with DBMA, proving that the steric hindrance is higher when two methyl and two butyl groups are present instead of four methyl groups. This is in agreement with the results reported by Mowafy et al.[172] in studying the effect of the lateral substituents on the extraction of several trivalent cations. The authors reported a decrease in metals extraction when switching from dimethyldihexylmalonamide to dimethyldioctylmalonamide. In addition, Rao et al.[153] demonstrated that the complexation constant of Eu(III) decreased with the increase

of the substitutional groups on the nitrogen atoms, and this was related to the steric hindrance and the energy required for reorganization.

Moreover, it was reported that malonamides substituted at their central carbon atom have a higher Ln(III) extraction ability than non-substituted analogues.[173] This may explain the improvement of Nd(III) extraction with TDMA compared to that with THMA, where D_{Nd} increases from 0.008 to 0.215 when using 0.2M THMA and 0.2M TDMA, respectively (Table 16). However, the same trend was not observed with DBMA, where D_{Nd} decreased again to 0.015 when using a concentration of 0.2M in toluene. This can be explained by the extra steric hindrance generated by the two butyl chains, which inhibited the extraction of Nd(III).

VI. Selective extraction of Pd(II)

In addition to their capacity to remove minor actinides, diamides have shown an affinity to extract Pd(II) from nitric acid media[142,143,182]. Accordingly, the selective extraction of Pd(II) over Nd(III) and Fe(III) was reported with DBMA,[143] and it was strongly dependent on two key parameters: The concentration of DBMA for Nd(III) and the aqueous nitric acid concentrations for Fe(III). Therefore, the optimized conditions to reach selective Pd(II) extraction with DBMA have been established at 0.5-0.6M DBMA in toluene with 3M HNO_3 solution. In this regard, we investigated the scope of the selective extraction of Pd(II) over Nd(III) and Fe(III) with the three malonamides diluted in toluene, and the results are presented in Table 16.

Table 16: Distribution ratios of Pd(II), Fe(III) and Nd(III) and Pd/Fe, Pd/Nd selectivity $S_{Pd/Fe}$, $S_{Pd/Nd}$ after extraction using THMA, TDMA and DBMA in toluene, from an aqueous 3M HNO_3 phase. Initial $[Pd]_{aq}$ 500 mg.L^{-1}, initial $[Fe]_{aq}$ 250 mg.L^{-1}, initial $[Nd]_{aq}$ 250 mg.L^{-1}.

	THMA 0.2M	TDMA 0.2M	DBMA 0.2M	THMA 0.3M	DBMA 0.3M	THMA 0.5M	DBMA 0.5M
D_{Pd}	28	6.3	1.4	>70	4	>70	10
D_{Nd}	0.008	0.215	0.015	<0.002	0.08	0.038	0.37
D_{Fe}	<0.002	0.288	0.003	0.006	0.02	0.05	0.2
$S_{Pd/Nd}$	3435	29	86	>11600	200	>1400	50
$S_{Pd/Fe}$	2442	21	378	>35000	50	>1840	27

First, THMA exhibited overall much better extraction of Pd(II) than DBMA and TDMA. Interestingly, palladium distribution ratios D_{Pd} with THMA were between 10 and 100 times higher than that with DBMA, using 0.3M THMA. Furthermore, THMA showed an impressively high selective

extraction of Pd(II) in the presence of Fe(III) and Nd(III) compared to the other malonamides. For instance, at 0.3M THMA and 3M HNO_3, $S_{Pd/Fe}$ and $S_{Pd/Nd}$ were above 11,600 and 35,000 , respectively, and Pd(II) extraction was quantitative. Experimentally, after extraction, Pd(II) could not be detected in the aqueous layer ($D_{Pd} > 70$), and Nd(III) could not be detected in the organic layer ($D_{Nd} < 0.002$). Fe(III) was barely quantified in the organic layer ($D_{Fe} = 0.006$). In comparison, for the same concentration for DBMA, $S_{Pd/Fe}$ and $S_{Pd/Nd}$ were 180 and 50, respectively, with a Pd(II) distribution ratio of 4 only.

The increase in extractant concentrations leads to a decrease in the selectivity regarding Fe(III) or Nd(III) with DBMA, as previously reported.[143] When using THMA, the distribution ratios of both Fe(III) and Nd(III) also increased with THMA concentration. However, they remained very low (below 0.1) so that $S_{Pd/Fe}$ and $S_{Pd/Nd}$ were still much higher than those obtained using the same DBMA concentration.

Although the extraction of Pd(II) was better with TDMA than with DBMA, the former showed a better affinity for the extraction of Nd(III) and Fe(III). Therefore, for a 0.2M ligand concentration, TDMA showed the least selective extraction of Pd(II) compared to THMA and DBMA. Although the extraction of Nd(III) is enhanced with the aggregation of the organic phase, however, this is not the case here since toluene is used as a diluent. Therefore, the ability of the extraction of TDMA is more likely related to the geometry of the molecule, where steric hindrance is lower in the presence of four methyl side chains, instead of two methyl and two dibutyl chains (case of DBMA).

VII.Stoichiometry of the extracted complexes

Slope analysis provides useful information on the composition of the extracted chemical species. This method consists of determining the distribution coefficients of the metal ion by varying a parameter such as pH, ionic strength or the concentration of the extractant, while keeping the other parameters constant.[201]

Considering that the extraction of a metal (M^{n+}) with a malonamide (L) from nitrate media is based on a solvation extraction mechanism, the extraction reaction is written as:

$$M^{n+} + nNO_3^- + p\bar{L} \rightleftharpoons \overline{M(NO_3)_nL_p} \quad (182)$$

Where the bar denotes the species in the organic phase.

The extraction reaction can be described by the equilibrium constant $K_{ext,M}$:

$$K_{ext,M} = \frac{[\overline{M(NO_3)_n L_p}]}{[M^{n+}][NO_3^-]^n[\bar{L}]^p} * \Pi_{Yi} = \frac{[\bar{M}]}{[M^{n+}][NO_3^-]^n[\bar{L}]^p} * \Pi_{Yi} \quad (183)$$

Where, Π_{Yi} is the product of the activity coefficients of the species involved in the reaction, which is assumed constant, at constant ionic strength.

We suppose that M^{n+} represents the significant species of metal in the aqueous phase, and therefore, the concentration of $[M^{n+}]$ is equal to $[M^{n+}]_{aq}$.

Therefore, $K_{ext,M}$ can be written as follows,

$$K_{ext,M} = \frac{D_M}{[NO_3^-]^n[\bar{L}]^p} * \Pi_{Yi} \quad (184)$$

Where, D_M is the metal distribution ratio, which is defined as follows,

$$D_M = \frac{[\bar{M}]}{[M^{n+}] + [M(NO_3)^{(n-1)+}] + [M(NO_3)_n]} = \frac{[\bar{M}]}{[M^{n+}]} \quad (185)$$

And,

$$[\bar{L}]_{total} = [\bar{L}]_{bound\ to\ acid} + [\bar{L}]_{bound\ to\ metal} + [\bar{L}]_{free} \quad (186)$$

Hence,

$$\log D_M = \log(K_{ext,M}) + n \log([NO_3^-]) + p \log [\bar{L}]_{free} - \log \Pi_{Yi} \quad (187)$$

Where $[\bar{L}]_{free}$, is the free malonamide concentration, which is the concentration of the ligand bound neither to metal nor to acid, since malonamides extract acid.

And the values of the stoichiometric equilibrium coefficients (n or p) can be determined by representing the slopes of the extraction isotherms in logarithmic coordinates.

In general, the experimental conditions allow making some assumptions to find the equation that will lead to the stoichiometric coefficients.

First, the concentration of nitrate ions in the aqueous phase is generally higher than that of metals. In our case, the maximum concentrations of metals used are:

$$[\mathrm{Pd}]_{\mathrm{aq}} \approx 2.35 * 10^{-3}\ \mathrm{mol.\,L^{-1}}$$

$$[\mathrm{Nd}]_{\mathrm{aq}} \approx 3.47 * 10^{-3}\ \mathrm{mol.\,L^{-1}}$$

$$[\mathrm{Fe}]_{\mathrm{aq}} \approx 8.95 * 10^{-3}\ \mathrm{mol.\,L^{-1}}$$

And the concentration of $\mathrm{NO_3^-}$ is at least 3 $\mathrm{mol.\,L^{-1}}$. Therefore, we can consider the following equality:

$$[\mathrm{NO_3^-}] = [\mathrm{NO_3^-}]_{\mathrm{initial}} - \mathrm{n}[\mathrm{M^{n+}}] \approx [\mathrm{NO_3^-}]_{\mathrm{initial}} \quad (188)$$

In the case of extraction from a relatively low acidic media, the acid extraction is low. Therefore, the concentration of the ligand bound to acid is negligible. Furthermore, if the total concentration of the ligand is much higher than the concentration of the metal, the concentration of the metal-bound ligand can be neglected.

Therefore, we can write:

$$[\mathrm{L}]_{\mathrm{initial}} = [\mathrm{L}]_{\mathrm{bound\ to\ acid}} + [\mathrm{L}]_{\mathrm{free}} \approx [\mathrm{L}]_{\mathrm{free}} \quad (189)$$

Thus, the simplified equation can be obtained:

$$\log \mathrm{D_M} = \mathrm{p}\ \log([\bar{\mathrm{L}}]_{\mathrm{initial}}) + \mathrm{constant} \quad (190)$$

It is worth mentioning that the discrepancy arising from conventional slope analysis often results in non-integral slopes.[202] This is possibly due to the non-ideality of the organic solution or the presence of extra amide molecules in the second coordination sphere.

A. Extraction from weakly acidic media

The stoichiometry of the extracted species was first determined from weakly aqueous acidic media. By doing so, the ligand concentration bound to acid is negligible, and the initial concentration of the ligand can be taken into account.

The effect of the concentration of DBMA, THMA and TDMA on the extraction of Pd(II), Nd(III) and Fe(III) was demonstrated by performing a series of extraction experiments using an aqueous phase containing [Pd] 250 $\mathrm{mg.L^{-1}}$, [Nd] 500 $\mathrm{mg.L^{-1}}$ and [Fe] 500 $\mathrm{mg.L^{-1}}$. The concentration of nitrate ions in

the aqueous phase was imposed with lithium nitrate salt $LiNO_3$ (2.9M). For all the systems, nitric acid concentration was fixed at 0.1M, which made the total concentration of nitrate ions equal to 3M.

1. Extraction of Pd(II)

The stoichiometry of Pd(II) extraction reactions from nitrate media with THMA, DBMA and TDMA in toluene was studied. The empirical stoichiometric coefficients in the extraction reaction of Pd(II) were determined by slope analysis (Figure 45). The log-log plots of the distribution ratios of Pd(II) *vs* the initial extractants concentrations gave for all ligands straight lines with a slope of 2. Therefore, it is assumed that 1:2 (metal:extractant) stoichiometry species are involved in the extraction of Pd(II) with DBMA and TDMA. This is consistent with the reported results of Pd(II) extraction from nitrate media with DMDOHEMA in toluene.[142] However, this statement could not be made in the case of THMA, even though the slope was also nearly 2, which is in agreement with the results obtained with DBMA and TDMA. In fact, these experiments were carried out for 1 hour of agitation. According to previously published results for the extraction of Pd(II) with DMDOHEMA in toluene, extraction equilibrium was reached in less than 1 hour.[142] This is valid for TDMA and DBMA but not for THMA. Indeed, the distribution ratios of Pd(II) with THMA for 1 hour extraction were far from the ratios obtained at equilibrium. As such, the results obtained with THMA will not be presented in this section. Finally, we point out that the kinetic limitations observed with THMA will be explained in details in the following chapters.

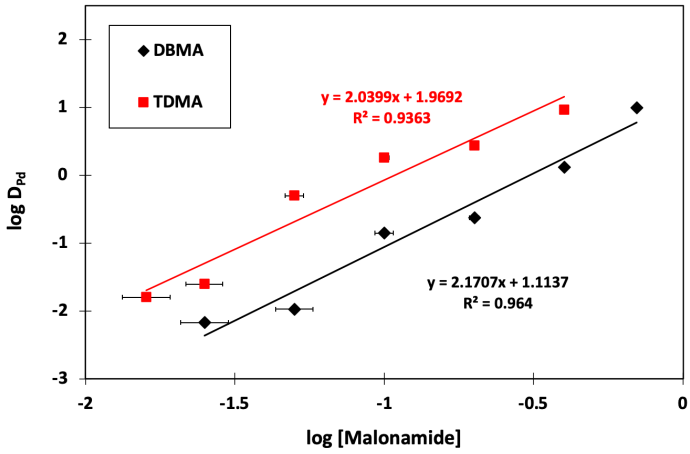

Figure 45: Distribution ratios of Pd(II) between aqueous nitrate solutions and organic solutions of TDMA and DBMA in toluene, as a function of the extractant concentrations. Initial $[Pd]_{aq}$ 250 $mg.L^{-1}$, $[HNO_3]_{aq}$ 0.1M, $[LiNO_3]_{aq}$ 2.9M, A/O=1, T=21°C.

2. Extraction of Nd(III)

The stoichiometries of the extracted complexes of Nd(III) with THMA and DBMA were determined (Figure 46). The log-log plots of the distribution ratios of Nd(III) *vs* the initial concentration for the three extractants gave straight lines, with a slope of nearly 3 with both ligands. These obtained results are consistent with the literature.[172] It is worth mentioning that the reported data in the case of Nd(III) are well at equilibrium for all the ligands. We add that the reported results were limited to a concentration of 0.2M (log[L] = - 0.69) since for a lower concentration of ligand, the concentration of Nd(III) in the organic phase was below the detection limit of the ICP-AES analysis.

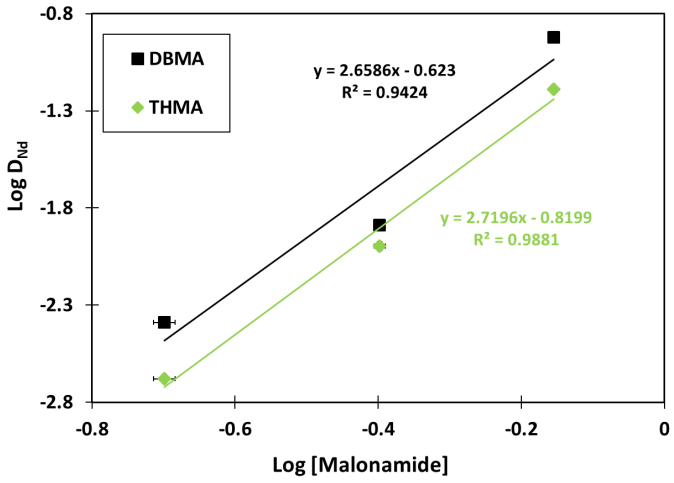

Figure 46: Distribution ratios of Nd(III) between aqueous nitrate solutions and organic solutions of THMA and DBMA in toluene as a function of the extractant concentrations. Initial [Nd] aq 500 $mg.L^{-1}$, $[HNO_3]$aq 0.1M, $[LiNO_3]$aq 2.9M, A/O=1, T=21°C.

In parallel, the stoichiometries of the extracted species could not be determined for Fe(III) from low acidic media.

B. Extraction from highly acidic media

In his thesis work, Poirot investigated the effect of the concentration of DMDOHEMA in toluene on the extraction of Pd(II) at low and high acidic media.[203] In the case of high acidic media, the effect of the total concentration of DMDOHEMA and the effect of the free concentration (not bound to acid), was reported. Interestingly, in both cases, the same dependence was obtained. In this regard, another series of experiments was conducted to get insights into the nature of the extracted species from high acidic media, with the three malonamides, especially with Fe(III), for which the nature of the extracted species could not be determined at low acidic media. For this investigation, two acidities were chosen: $[HNO_3]_{aq}$ 3M and $[HNO_3]_{aq}$ 5M.

1. Extraction of Pd(II)

The effect of the concentrations of TDMA and DBMA on the extraction of Pd(II) from 3M HNO_3 and 5M, respectively, was investigated. We note that the initial concentrations of TDMA and DBMA were used for these experiments, rather than the concentrations of the free ligands (not bound to acid).

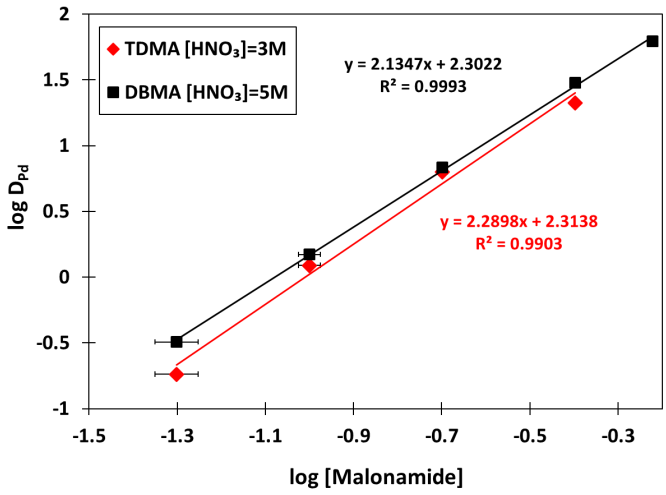

Figure 47: Pd(II) distribution ratios between aqueous nitrate solutions and organic solutions of TDMA and DBMA in toluene. $[Pd]_{aq}$ 500 $mg.L^{-1}$, $[HNO_3]_{aq}$ = 3M in the case of TDMA, and $[HNO_3]_{aq}$=5M in the case of DBMA, A/O=1, T=21°C.

The log-log plot of Pd(II) distribution ratios in the function of both TDMA and DBMA concentrations gave straight lines with a slope of nearly 2 (Figure 47). Therefore, it was assumed that 1:2 (metal:extractant) species are involved in the extraction of Pd(II) with both ligands, regardless of the concentration of nitric acid in the aqueous phase. Interestingly, these results are in agreement with the ones obtained at low acidic media in the previous section.

The effect of the concentration of THMA on the extraction of Pd(II) from 3M HNO_3 was investigated, and a slope of 2 was obtained. However, due to the same above-mentioned kinetic limitations, these results will not be presented.

2. Extraction of Nd(III)

The stoichiometry of the extracted Nd(III) complex from 5M HNO_3, with DBMA in toluene was investigated. The log-log plot of Nd(III) distribution ratios versus DBMA concentration gave a straight line with a slope of nearly 3 (Figure 48). Therefore, a 1:3 (metal:ligand) complex was extracted. This result is in agreement with the one found in extraction from low acidic media. In addition, it is consistent with the results reported in the literature.[172]

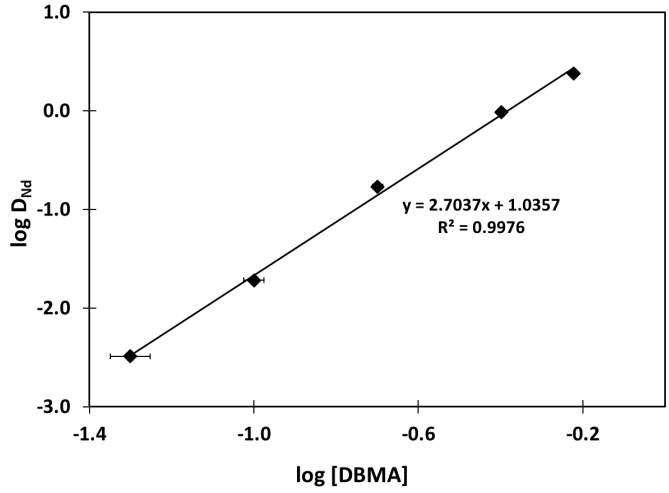

Figure 48: Distribution ratios of Nd(III) between aqueous nitrate solutions and organic solutions of DBMA in toluene, initial $[Nd]_{aq}$ 500 mg.L^{-1}, $[HNO_3]_{aq}$ 5M, A/O=1,T = 21°C.

3. Extraction of Fe(III)

The stoichiometry of the extracted species of Fe(III) from 5M HNO_3 with DBMA in toluene was investigated. The log-log plot of the distribution ratios of Fe(III) versus the concentration of DBMA gave a straight line with a slope near 3 (Figure 49). Therefore, the extracted species can be assumed to be 1:3 (metal:ligand) adducts.

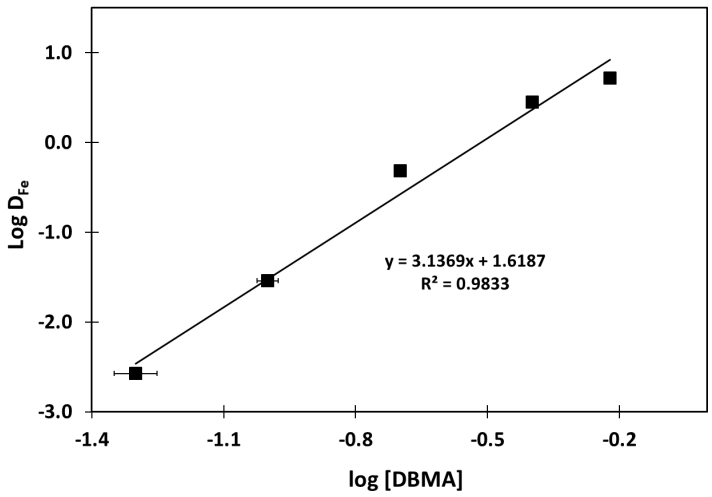

Figure 49: Distribution ratios of Fe(III) between aqueous nitrate solutions and organic solutions of DBMA in toluene, as a function of the ligand concentration. Initial $[Fe]_{aq}$ 200 mg.L^{-1}, $[HNO_3]_{aq}$ 5M, A/O=1, T=21°C.

We mention that the slope of the curve for [DBMA] < 0.2M (log[DBMA] <-0.7), is nearly 4, whereas it decreases to a value nearly 2, when [DBMA] ≥ 0.2M (log [DBMA] ≥-0.7. However, there are not enough experimental points to confirm this slope variation.

Finally, the extraction stoichiometry of Fe(III) complexes with THMA and TDMA were determined at 3M HNO_3. Fe(III) is extracted with a stoichiometry of nearly 5 with TDMA and 3 with THMA (Figure 50).

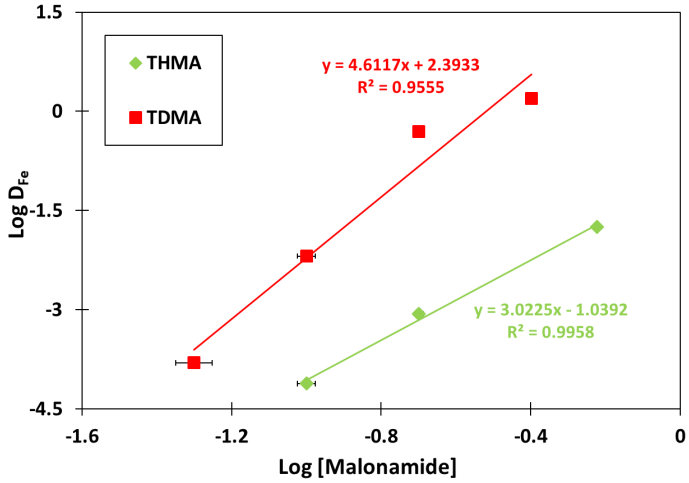

Figure 50: Distribution ratios of Fe(III) between aqueous nitrate solutions and organic solutions of THMA and TDMA in toluene, initial $[Fe]_{aq}$ 500 mg/L, $[HNO_3]_{aq}$ 3M, A/O=1, T=21°C.

C. Conclusion

In conclusion, slope analysis gave an overview of the stoichiometries of the extracted complexes for the different metals with THMA, DBMA and TDMA. The stoichiometries of the extracted complexes with Pd(II) and Nd(III) are in full agreement with the literature, where (1:2) and (1:3) stoichiometries were reported with Pd(II) and Nd(III) in extraction with DMDOHEMA in toluene from nitrate media.[142,203] Interestingly is that the various ramifications on the lateral and the central carbon did not impact the stoichiometries of the extracted complexes in the case of Pd(II), where a 1:2 (metal:ligand) stoichiometry was obtained with TDMA and DBMA, and apparently, THMA follows the same trend. In Table 17, we summarize the obtained results.

Table 17: Summary of the (metal:ligand) stoichiometries obtained with graphical slope analysis.

	Weakly acidic media			Highly acidic media		
	THMA	**DBMA**	**TDMA**	**THMA**	**DBMA**	**TDMA**
Pd(II)	-	(1:2)	(1:2)	-	(1:2)	(1:2)
Fe(III)	-	-	-	(1:3)	(1:3)	(1:5)
Nd(III)	(1:3)	(1:3)	-	-	(1:3)	-

VIII. Effect of nitrate ions concentration on Fe(III) extraction

The increase in nitric acid concentration enhances the extraction of Fe(III) with the three malonamides. This observation is in agreement with the literature.[143,156,200] In addition, Nigond.[200] reported that Fe(III) is extracted with DBMA from nitrate media under anionic species of $Fe(NO_3)_4^-$. Therefore, an increase in nitrate ions should further enhance the extraction of Fe(III).

In this regard, we investigated the effect of the concentrations of nitrate ions on the extraction of Fe(III) with THMA in toluene. This investigation was performed by keeping the concentration of proton ions constant at 1.5M and varying the concentration of nitrate ions by adding lithium nitrate to the medium.

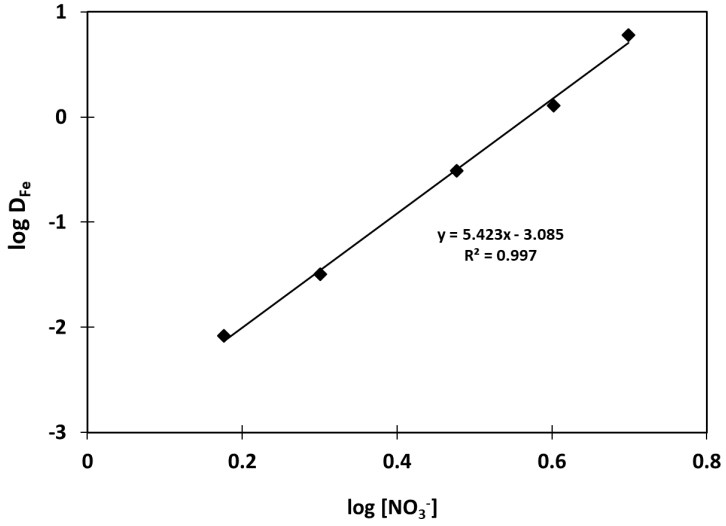

Figure 51: Effect of the concentration of nitrate ions on the extraction of Fe(III) with 0.8M THMA in toluene. Initial $[Fe]_{aq}$ 7 $g.L^{-1}$, $[H^+]_{aq}$ 1.5M, A/O =1, T=21°C.

The plot of the Fe(III) distribution ratios against the concentration of nitrate ions in the aqueous phase gives a linear curve with a slope of nearly 5. It is worth mentioning that Mastretta et al.[143] reported the variation Fe(III) distribution ratios against the concentration of nitric acid, and a slope of 6 was obtained. This suggests that Fe(III) is possibly extracted as anionic species of $Fe(NO_3)_5^{2-}$. Therefore, the formation of these anionic species can perhaps explain the enhancement of Fe(III) extraction with the increase of nitric acid concentration. Indeed, the increase of the nitric acid concentration induces a simultaneous increase in nitrate ions and protons, which are essential for electroneutrality.

In parallel, this large slope may originate from the extraction of polynuclear hydrolyzed species of Fe(III). The polymerization of iron in the aqueous phase is documented in the literature, and the

presence of polynuclear hydrolyzed iron(III) species has been evidenced.[204-207] It has been reported that the polymerization occurs mainly *via* two routes: Olation and oxolation.[208] For the olation, the polymerization takes place upon deprotonation, and only hydroxo-bridged oligomers or polymers are formed. Whereas for the oxolation, oxobridges are formed. The presence of dimer species was evidenced in nitrate solutions $Fe_2(OH)_2^{4+}$, in addition to other hydrolyzed species $Fe(OH)^{2+}$, $Fe(OH)_2^{+}$.[209] It is worth mentioning that species of $Fe_3(OH)_4^{5+}$ were also detected. In addition, in their paper, Knight and Sylva,[204] pointed out that the variation of absorbance, conductance and pH of dilute hydrolyzed iron(III) perchlorate solutions were attributed to the formation of higher molecular weight hydrolysis products (polymers). They also suggested that polymerization might occur during solution preparation due to local concentration effects while the iron salt is dissolving. Once the polymer is formed, it may exist for some time, seeing that its rate of decomposition is very slow. However, for our study, the speciation of Fe(III) in the aqueous phase was not performed to verify the validity of this hypothesis.

IX. Conclusion

This PhD thesis aimed to characterize the extraction kinetics of Pd(II), Nd(III) and Fe(III) with malonamide ligands of different topologies. Three molecules, THMA, DBMA and TDMA, were initially selected according to their different potential ability to self-organize in the organic phase. THMA, DBMA and TDMA all possess the same coordinating malonamide (1,3-diamide) moiety, and differ in the length of their central and lateral alkyl chains substituents. TDMA presents the smallest polar head with a long tail, suggesting a higher affinity for aggregation, compared to DBMA, which also has a long tail, but a bulkier head, due to the presence of two butyl chains instead of two methyl substituents. THMA presents a more hindered polar head, decorated with four hexyl chains, and was anticipated to have a lower aggregation capacity

Screenings were performed on the third phase formation when using heptane, cyclohexane and iso-octane as diluents. This study was carried out by varying the concentrations of ligands in the organic phase and nitric acid in the aqueous phase. Based on the preliminary results obtained, we realized that the evaluation of the extraction kinetics when using these aliphatic diluents could be limited. Indeed, third phase with THMA and DBMA occurred for different ligand and nitric acid concentrations. Moreover, TDMA is not soluble in either heptane or cyclohexane, and its concentration threshold cannot exceed 0.4M in toluene otherwise, the ligand will precipitate.

Therefore, we chose toluene as the diluent for the continuation of the work. By doing so, the absence of third phase formation was ensured for the considered experimental conditions. In this respect,

some of the thermodynamic aspects of the extraction systems were sought, and further kinetic characterization was followed, which will be presented in the following chapters.

First, in this chapter, we presented the optimized solvent free synthesis of THMA, as well as the synthesis of TDMA.

Then, acid uptake for THMA and DBMA in toluene was characterized for different ligands concentrations at various nitric acid concentrations in the aqueous phase. The stoichiometries of the extracted adducts were determined by graphical slope analysis. The obtained values of the slopes were nearly equal to unit, showing that adducts type $L(HNO_3)$ are formed with both ligands. A slight deviation of the slopes from unit value with THMA was observed possibly originating from $L(HNO_3)_x$. Moreover, the average number of extracted HNO_3 molecules is constant at a given ligand concentration and depends solely on the concentration of nitric acid in the aqueous phase. Finally, THMA is more basic than DBMA, and this was particularly visible at low concentrations of nitric acid in the aqueous phase ($\leq$ 3M).

The extraction of Pd(II) with THMA and DBMA at various nitric acid concentrations was investigated. Seen that THMA is more basic than DBMA, the maximum extraction of Pd(II) with the former occurs at a lower concentration of nitric acid compared to DBMA. Furthermore, the extraction of Pd(II) with THMA decreased steeply with the increase of proton ions concentration. In contrast, it increased with DBMA, revealing that proton ions are intensely competitive with THMA, whereas they play a cooperative role in the case of DBMA. In addition, the effect of the basicity of the molecule has a minor impact on the extraction of Pd(II) since THMA is more basic than DBMA. However, it gives a much better extraction of Pd(II) than DBMA.

The effect of the ligand structure on Pd(II) extraction was evidenced. The presence of a substituent on the central carbon, as well as the increase of the length of the alkyl side chains, decrease the extraction of Pd(II). In addition, THMA presents a very selective extraction of Pd(II) over Nd(III) and Fe(III) compared to the other two malonamides. The extraction of Fe(III) is enhanced with the increase of nitric acid in the aqueous phase. And TDMA has the lowest extraction selectivity towards Pd(II), which decreased further by increasing the concentration of nitric acid in the aqueous phase.

The stoichiometries of the extracted complexes of the three metals with the three ligands were determined by graphical slope analysis from weakly and highly acidic media. The stoichiometry of Pd(II) complexes was found to be 1:2 (metal ligand) with DBMA and TDMA. Three ligands are necessary to extract Nd(III) with THMA and DBMA. The stoichiometry of the extracted complexes in the case of Fe(III) was determined at highly acidic media. In general, 1:3 (metal:ligand) stoichiometries were obtained with THMA and DBMA, whereas for TDMA, a 1:5 stoichiometry was obtained.

For the extraction of Fe(III), the graphical slope analysis showed that that the former requires on average five nitrate ions. However, no decisive conclusion was made on whether Fe(III) is extracted as anionic species of $Fe(NO_3)_5^{2-}$ since polymeric species of Fe(III) could also be present.

Finally, we would like to mention the kinetic limitations encountered in the extraction of Pd(II) with THMA, where longer extraction times were required to reach equilibrium. In the following chapters, we will present in detail the study of the extraction kinetics of Pd(II) with THMA.

Chapter 3: Extraction kinetics of Pd(II), Fe(III) and Nd(III)

In the course of our study, we observed thermodynamic differences for the extraction of Pd(II), Nd(III) and Fe(III) with THMA and DBMA. The stoichiometry of the extracted Pd(II) complexes are different from that of Nd(III) and Fe(III). The effect of the malonamide structure on Pd(II) extraction was discussed in Chapter 2 § V - B. It was found that the presence of a central carbon chain decreases its extraction efficiency.

Herein, attention is drawn to the kinetic characterization of Pd(II), Nd(III) and Fe(III) extraction with DBMA and THMA. Indeed, we sought to understand the effect of metals, as well as the effect of the structure of the extractant on the extraction kinetics. This study was first carried out in small batch experiments. Then, well-defined experiments with a single drop technique were performed under selected conditions.

I. Extraction kinetics of Pd(II), Nd(III) and Fe(III) in small batch experiments

A screening of the extraction progress of Pd(II), Nd(III) and Fe(III) with DBMA was performed, using an aqueous solution of a mixture of metals (Figure 52).

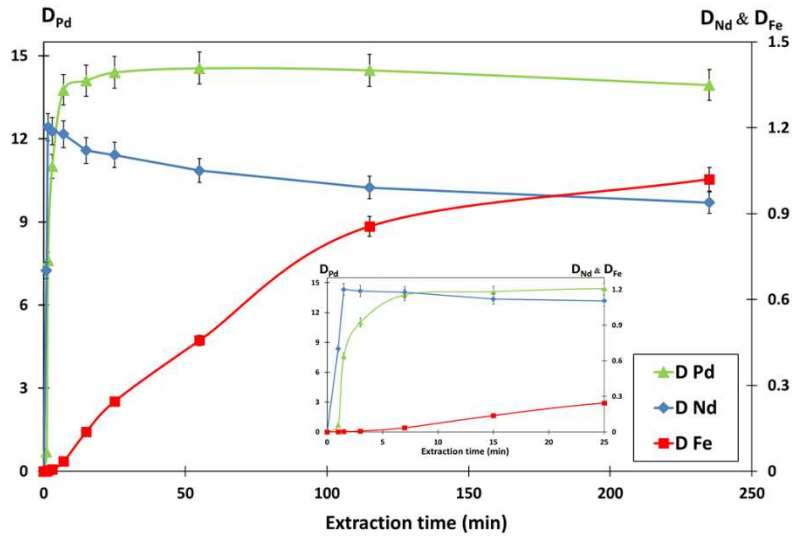

Figure 52: Extraction of Pd(II) , Fe(III) and Nd(III) with DBMA in toluene as a function of time. $[DBMA]_{org}$ 0.6M, $[HNO_3]_{aq}$ 3M, initial $[Pd]_{aq}$ 200 $mg.L^{-1}$, initial $[Nd]_{aq}$ 500 $mg.L^{-1}$, initial $[Fe]_{aq}$ 2000 $mg.L^{-1}$. The embodied diagram is an enlargement between the zero point and 25 minutes.

First of all, Pd(II), Nd(III) and Fe(III) exhibited different behaviours in terms of extraction kinetics as a function of time. The maximum extraction yield of Nd(III) was reached very quickly, in about 2 minutes. This is shown in the embodied diagram in Figure 52. In parallel, the extraction of Pd(II) increased progressively, and the extraction equilibrium was reached in about15 minutes. Finally, the extraction of Fe(III) was the slowest, where even after 100 minutes of agitation, the distribution ratio continued to increase.

After reaching its maximum, Nd(III) extraction initiated to decrease after 10 min of agitation. This decrease may reflect the different stabilities of metal-DBMA complexes, which may induce some competition with Fe(III) for the complexation at equilibrium.

Interestingly, these results demonstrate that it is possible to establish a kinetic separation between Pd(II) and Fe(III). In Table 18, the distribution ratios of Pd(II) and Fe(III) are reported and the corresponding separation factors for 3 min, 5 min and 240 min of extraction.

Table 18: Distribution ratios of Pd(II) and Fe(III) and Pd/Fe selectivity ($S_{Pd/Fe}$) for a short extraction duration with DBMA, $[DBMA]_{org}$ 0.6M in toluene, Initial $[Pd]_{aq}$ 200 mg.L^{-1}, Initial $[Fe]_{aq}$ 2000 mg.L^{-1}, $[HNO_3]_{aq}$ 3M

Extraction time	D_{Pd}	D_{Fe}	$S_{Pd/Fe}$
3 min	7.6	0.003	2227
5 min	11	0.007	1620
240 min	14	1.02	13.7

A kinetic separation is undoubtedly feasible by exploiting the slow extraction of Fe(III) with DBMA compared to Pd(II). As shown in Table 18, successful separation of Pd(II) from Fe(III) at equilibrium is not very efficient since the separation factor is about 14. However, a separation factor above 1000 can be achieved for a few minutes of extraction.

The extraction kinetics of Pd(II) from 3M HNO_3 with THMA and DBMA was also studied in batch experiments (Figure 53).

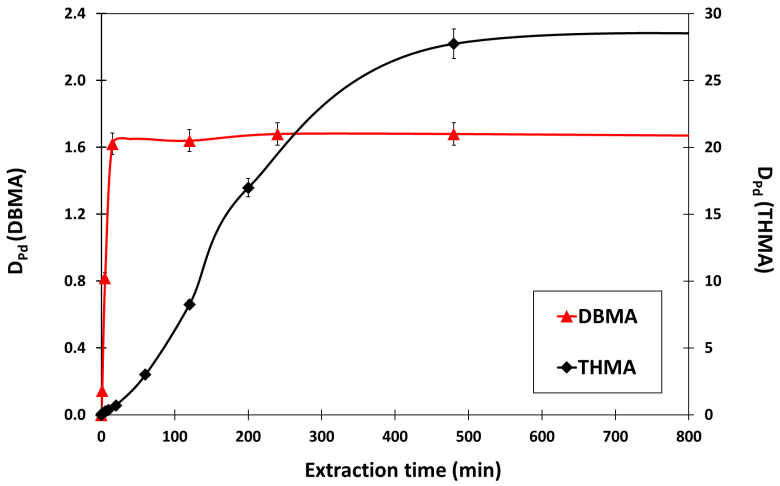

Figure 53: Extraction progress of Pd(II) with DBMA and THMA in toluene. $[DBMA]_{org}$ 0.2M, $[THMA]_{org}$ 0.2M, $[HNO_3]_{aq}$ 3M, $[Pd]_{aq}$ 500 $mg.L^{-1}$, T=21°C.

The extraction kinetics of Pd(II) with DBMA is much faster than that with THMA. Indeed, the extraction equilibrium of Pd(II) with DBMA was reached in about 15 min, whereas it took more than 8 h to reach equilibrium with THMA.

In conclusion, screening the extraction kinetics of Pd(II), Nd(III), and Fe(III) in small batch experiments revealed that the extraction of Nd(III) is the fastest compared to Pd(II) and Fe(III). In addition, the extraction of Pd(II) with DBMA is much faster than with THMA. Based on these findings, the extraction conditions were set for a well-defined characterization of the extraction kinetics of the three metals with THMA and DBMA, using the single drop technique.

II. Interfacial activity

Prior to the investigation of the extraction kinetics using the single drop technique, the interfacial activities of DBMA and THMA were characterized through interfacial tension measurements (IFTs) (Figure 54).

These measurements were performed using the spinning drop technique. We mention that this study could not be conducted with the pendant drop method because the tensiometer available in the laboratory is not equipped to perform measurements using a corrosive, highly acidic aqueous solution.

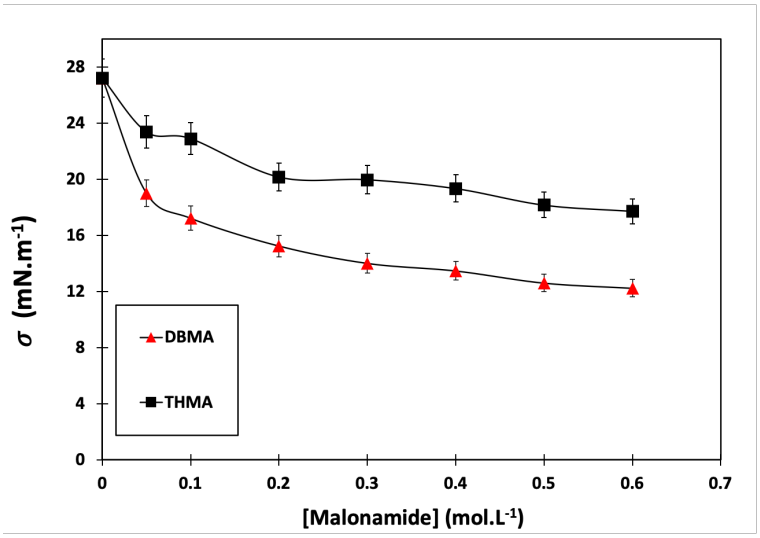

Figure 54: Interfacial tension σ (mN.m^{-1}) at the aqueous-organic interface for solutions of DBMA and THMA in toluene, $[HNO_3]_{aq}$ 3M. T=21°C.

The decrease in interfacial tension observed with increasing concentrations of DBMA and THMA corresponds to the general pattern observed for conventional surfactants.[210]

The decrease in interfacial tension is more significant with DBMA, suggesting that the latter is more surface-active than THMA. This result was expected given the different structures of both malonamides. The polar core is more hindered in the case of THMA due to the presence of four bulky lateral substituents, which may decrease the adsorption capacity of the ligand (Figure 55).

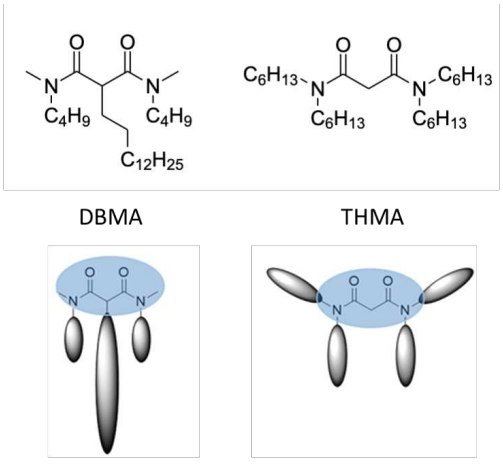

Figure 55: Chemical structure of DBMA and THMA with the presumed hydrophilic part coloured in blue.

In general, when a new surface of a surfactant solution is created, a finite time is required to reach an equilibrium between the surface concentration and the bulk concentration.[210] The dynamic adsorption is governed by an adsorption process and a mass transfer process (usually diffusion and sometimes also a degree of convection). Although the dynamic interfacial tension was not measured for THMA and

DBMA, differences in non-equilibrium surface tension were noticed between the two ligands. Thus, a stabilization of the interfacial tension was reached at shorter durations with DBMA compared to THMA.

In order to get insights into the different interfacial properties of both malonamides, as well as the evaluation of their dependence on parameters such as malonamide structure, we aimed to establish a relationship between IFTs and extractant concentrations at the L/L interface.

Different models of adsorption isotherms have been reported in the analysis of IFTs data (Refer to Chapter 1 - § VI - A). In the present study, Szyszkowski isotherms, as one of the most commonly used models, were applied to the characterization of malonamide extractants. However, we point out that Szyszkowski isotherm is restricted to ideal solutions, *i.e.* diluted solutions of surfactants. Although this is not the case for our measurements, we proceeded to fit the experimental IFTs in accordance with this isotherm.

The semi empirical Szyszkowski isotherm is expressed as follows:

$$\Pi = \sigma_0[B_{SZ} \ln\left(\frac{C_0}{A_{SZ}} + 1\right)] \quad (191)$$

Where Π, is the interfacial pressure, c_0 is the initial bulk concentration of extractant, A_{SZ} and B_{SZ} are Szyszkowski parameters. These parameters allow the calculation of the extractant interfacial adsorption equilibrium constants, K_{ads}, and solute surface excess concentrations Γ^{∞}:

$$K_{ads} = \frac{1}{A_{SZ}} \quad (192)$$

$$\Gamma^{\infty} = \sigma_0 B_{SZ}/RT \quad (193)$$

The interfacial pressure Π ($mN.m^{-1}$) was calculated for each concentration of ligand:

$$\Pi = \sigma_0 - \sigma \quad (194)$$

Where σ_0 the interfacial tension at the aqueous nitric acid/toluene interface, in the absence of the extractant, and σ is the interfacial tension at the aqueous nitric acid/toluene interface for a given concentration of the ligand in the organic phase.

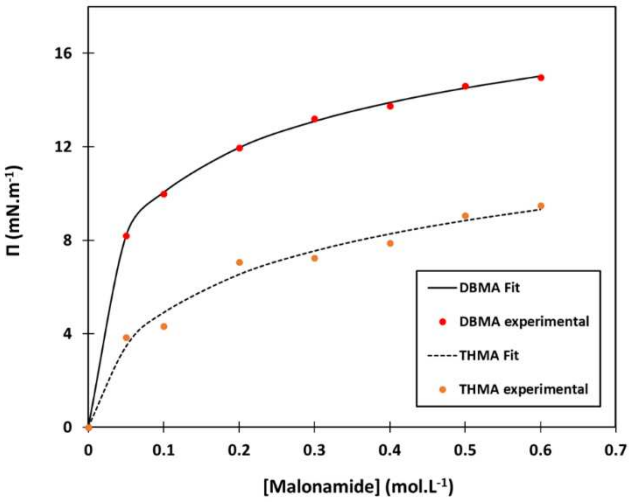

Figure 56: Interfacial pressure ($\Pi = \sigma_0 - \sigma$) *vs* concentration of DBMA and THMA in toluene, $[HNO_3]_{aq}$ 3M, T=21°C.

A_{SZ} and B_{SZ} parameters were obtained by fitting on MATLAB the experimental IFTs data. The goodness of fit was confirmed by the regression coefficients, which were 0.999 and 0.982, for DBMA and THMA, respectively.

Gibbs adsorption energy, ΔG_{ads} ($\Delta G_{ads} = RT \ln A_{SZ}$) and extractant effective surface area, a_i, at interfacial saturation ($a_i = {}^{1}/_{\Gamma^{\infty} N_A}$) were also calculated. In these equations, N_A is Avogadro constant.

In Table 19, the Szyszykowski parameters are presented.

Table 19: Szyszkowski parameters fitted to the experimental interfacial tension.

	THMA	**DBMA**
$\mathbf{B_Z}$	0.0982	0.1034
$\mathbf{A_Z}$ **(mol.dm^{-3})**	0.0190	0.0028
$\mathbf{K_{ads}}$ **(dm^3.mol^{-1})**	52	345
$\mathbf{\Gamma^{\infty}}$ **(10^{-6} mol.m^{-2})**	1.08	1.14
$\mathbf{a_i}$ **(10^{-18} m^2.molecule^{-1})**	1.54	1.46
$\mathbf{\Delta G_{ads}}$ **(kJ. mol^{-1}) T = 298K**	-9.81	-14.48

The obtained results confirm the highest interfacial activity of DBMA compared to THMA. Indeed, the adsorption constant at the equilibrium of DBMA (K_{ads} = 345 dm^3.mol^{-1}) is much larger than THMA (K_{ads} = 52 dm^3.mol^{-1}). In parallel, the values of the surface excess concentrations Γ^{∞} of both ligands are very close. We remind that the parameter Γ^{∞} is a theoretical limit, which is important but cannot be normally reached because of the constraint of a maximum concentration.[210] According to

Szymanowski,[56] the surface excess of a saturated interface is only marginally dependent on the structural changes of extractant, which means that approximately the same values of surface excess are obtained for different compounds of various structures and hydrophobicity. This may explain the close values of Γ^{∞} obtained with THMA and DBMA.

The surface excess concentrations of DBMA in several diluents using several devices are reported in the literature. These values are summarized in Table 20.

Table 20: Surface excess concentration for DBMA in different conditions.

Author	Diluent	Aqueous phase	Γ^{∞} (mol.m^{-2})	Device
Berthon et al.[60]	Dodecane	[HNO_3] 2M	$1.64*10^{-6}$	Drop-weight technique
Dal Don[23]	Dodecane	[HNO_3] 0.1M	$1.5 * 10^{-6}$	De Nouy
		[HNO_3] 1M	$1.6 * 10^{-6}$	
		[HNO_3] 4M	$1.5 * 10^{-6}$	
Lefrançois[211]	Dodecane	[HNO_3] 5.2M	$1.3 * 10^{-6}$	De Nouy
		Water	$1.5 * 10^{-6}$	
Erlinger[212]	Toluene	Water	$5.5 * 10^{-7}$	De Nouy
	Hexane	Water	$9.2 * 10^{-7}$	
	Dodecane	Water	$1.1 * 10^{-6}$	
	Hexadecane	Water	$1.5 * 10^{-6}$	
This work	Toluene	[HNO_3] 3M	$1.14 * 10^{-6}$	Spinning drop

The surface excess concentration determined by Erlinger at the toluene/water interface is $5.5*10^{-7}$ mol.m^{-2}, which is lower than the value at the aqueous toluene/3M HNO_3 interface obtained in our study. This can be related to the higher interfacial activity of the protonated DBMA at the liquid/liquid interface.

In parallel, in the case of dodecane, the excess surface concentration determined by Berthon et al.[60] for an aqueous solution of HNO_3 2M is $1.64*10^{-6}$ mol.m^{-2}, which is higher than the determined value when using toluene, in our study. Thus, DBMA is more surface-oriented when using dodecane as a diluent. This emphasizes the higher solvation of toluene and its higher penetration for the interfacial area. It is documented in the literature that aromatics show an affinity for the aqueous phase, so a competitive interaction with water molecules and with the hydrophobic extractants takes place at the interface.[65] In fact, aromatic molecules try to interact with water molecules by their π-electrons to obtain a position parallel to the interface.[213] Thus, the interfacial zone is swollen, decreasing the

interfacial concentration of the extractants at the interface.[56] In this regard, the extractant molecules in such cases are less oriented towards the interface than the systems comprising an aliphatic diluent.

III. Mass transfer kinetics

As already shown in Chapter 1, § V, numerous techniques are available to study the mass transfer kinetics. As a rule, thermodynamic studies in liquid/liquid extraction are carried out with setups where the organic and aqueous phases are sufficiently agitated so that diffusion is not limiting compared to the chemical reaction. On the other hand, kinetic studies require apparatus where the contact time between the two phases is not necessarily sufficient. It is then imperative to ensure that the diffusional component is not limiting, which will introduce complications for the kinetic characterization. Therefore, according to the experience already mastered at the CEA, the choice was made for the single drop technique for the kinetic characterization in our study. This technique presents a compromise between diffusional and chemical effects since an apparent global transfer constant is determined. In addition, precise knowledge of the interfacial area is possible, which is a must for our study, and this will be detailed in Chapter 4. Theoretical calculations for the description of the matter transfer using this technique are detailed in Chapter 1, § V-A-1-a.

First, we tried to estimate the diffusional contribution in the mass transfer using the single drop technique. To do so, we chose to work with a system for which, the mass transfer is supposed to be controlled by diffusion.

In this respect, the transfer of I_2 into cyclohexane was investigated. The experimental conditions were chosen according to the properties of iodine in the aqueous phase reported in the literature. In the absence of radiation,[214] hydrolysis of molecular iodine to form hypoiodous acid (HOI), following rapid equilibrium involving intermediate species (I_3^-, I^-, IO_3^-) is a significant reaction. On the other hand, molecular iodine is the primary specie under acidic and oxidizing conditions.[214,215]

Therefore, an aqueous solution was made up containing I_2, sodium periodate $NaIO_4$ and HNO_3. However, the analysis was complicated due to the simultaneous presence of several iodine species in the aqueous phase, and this study was not further developed.

We point out that an alternative that could be useful for the determination of the diffusion transfer constant is the transfer of a simple organic component, *i.e.* acetone or ethanol, between toluene and water.[216] However, for our study, we did not investigate these experiments further and proceeded directly to the determination of the global transfer constants for Pd(II), Nd(III) and Fe(III).

A. Single drop technique

All the experiments carried out in this study were performed in CAP configuration (continuous aqueous phase). Bearing in mind that the mass transfer occurs from the formation of the drop and continues into the collector. These are known as the end effects. Therefore, sampling of the organic phase was carried out at various heights, using a mobile funnel, which allowed to subtract the end effects and improve the accuracy of the measurements. The experimental setup and the experimental procedure for the determination of the global transfer constants are detailed in Chapter 6, § VII.

1. The exploitation of the results

As seen in Chapter 1, § V-A-1-a, this technique allows the determination of a global transfer constant related to a drop according to the following equation:

$$\ln(1 - E) = -6\frac{K_{org}^{g}}{d}t + b \tag{195}$$

Where K_{org}^{g} is the global transfer constant relative to the organic phase, b is a constant, t is the drop flight time, and E is the transfer efficiency, defined as:

$$E = \frac{C_{org}}{D_M C_{aq,ini}} \tag{196}$$

With, C_{org} is the metal concentration in the organic droplet at a time t, $C_{org,eq}$ is the concentration of the metal in the organic phase at equilibrium, D_M is the distribution ratio of the metal at equilibrium and $C_{aq,ini}$, is the initial concentration of the metal in the continuous aqueous phase.

2. Validation of the results

The validity of the experimental determination of the global transfer constants when using single drop technique is ensured by:

- A constant concentration of the continuous aqueous phase during the experiment
- Diameter drop of the order of ≥ 2 mm, which ensures a minimal circulation inside the drop (Figure 6), so that transfer of matter is not constrained by diffusional limitations
- During its flight across the column, each drop must be separated from the next by 10 times its diameter
- Terminal velocity reached

Altogether, suppose all the above conditions are met. In that case, the linearity of the plot of ln(1-E) against the flight of the drop, guarantees the validity of the experimental model, and therefore, the global transfer constant can be determined.

Special attention was paid to the determination of the distribution ratio, which must be considered to exploit the results, when using the single drop technique.

The transfer efficiency (Eq.196) can be also written as follows:

$$E = \frac{C_{org}}{C_{org,eq}} = \frac{C_{org}}{D_M C_{aq,ini}} \quad (197)$$

Where, C_{org} is the concentration of the metal in the organic droplet at a time t, $C_{org,eq}$ is the concentration of the metal in the organic phase at equilibrium.

Now, consider the case of the organic droplet that passes through a continuous aqueous phase. The question is, what would be the metal concentration in the organic droplet at equilibrium? Especially that in this case, the aqueous to organic ratio A/O is much larger than 1. Throughout its trajectory, the droplet will be confronted at each movement with a new layer of the aqueous phase. The transfer of metal from the aqueous phase to the organic phase will continue until reaching equilibrium. This equilibrium can result of:

- Classical equation observed at A/O = 1
- Saturation of the organic phase

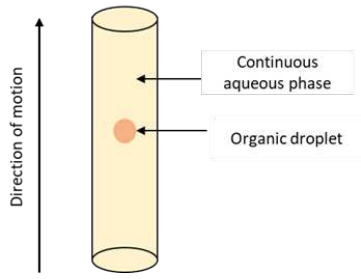

Figure 57: Sketch of the trajectory of an organic droplet through a continuous aqueous phase.

In this regard, we were interested in evaluating the distribution ratio in batch experiments for different aqueous to organic volumes A/O ratios. Thus, the extraction of Pd(II) with THMA was performed for A/O equal to 1, 10, 30 and 50 (Table 21).

Table 21: Extraction of Pd(II) with 0.2M THMA in toluene for different A/O. Initial $[Pd]_{aq}$ 1 $g.L^{-1}$, $[HNO_3]_{aq}$ 3M, 24 h extraction, T = 21°C.

	A/O = 1	**A/O = 10**	**A/O = 30**	**A/O = 50**
$\mathbf{D_{Pd}}$	20.2	12.9	10.4	6.3

As the A/O ratio increased, the distribution ratio decreased. Indeed, for A/O = 1, the distribution ratio was 20.2, while it dropped to 6.3 for A/O = 50. Thus, there was some ambiguity as to which value of the distribution ratio to consider to exploit the results since different values of the global transfer constants would be obtained by considering each of these values.

Given the discrepancy in the obtained values of the distribution ratios, all kinetic studies carried out in our study with the single drop technique, were operated using the values of the distribution ratios determined in batch experiments for A/O = 1. Finally, we mention that the approach chosen in Chapter 4 based on the analysis of flux, is independent of this choice for the determination of the chemical order.

Another uncertainty that we encountered is the variation of Pd(II) distribution ratios with THMA, where the extraction conditions are favourable for the extraction. In this case, the distribution ratio is strongly affected by the slightest variation in the concentration of the metal in the aqueous phase. Herein, we illustrate the situation with an example.

Consider an aqueous phase of a metal M, with an initial concentration equal to 200 $mg.L^{-1}$. Consider that the extraction conditions are favoured, and the analyzed concentration of the metal in the organic phase after extraction is 198 $mg.L^{-1}$. The distribution ratio is defined as follows:

$$D = \frac{C_{org}}{C_{aq,f}}$$

Where $C_{aq,f}$ is the measured aqueous metal concentration after extraction.

- For $C_{aq,f} = 1.5\ mg.\ L^{-1}$, then D would be equal to (132 ± 7)
- For $C_{aq,f} = 1.4\ mg.\ L^{-1}$, then D would be equal to (141 ± 7)
- For $C_{aq,f} = 1.6\ mg.\ L^{-1}$, then D would be equal to (123 ± 6)

Therefore, the distribution ratios employed were calculated from the average of three values.

B. Extraction kinetics of Pd(II), Nd(III) and Fe(III)

The global mass transfer constants K_{org}^{g} of the extraction of Pd(II), Nd(III) and Fe(III) with THMA and DBMA were determined in various conditions.

Thermodynamic characterization of the extraction of Fe(III) and Nd(III) showed that the extraction of both metals is low at low concentrations of DBMA and THMA (see Chapter 2, § III). In parallel, previous works on the single drop technique indicate that the contact time (drop flight time) is usually very short, in the range of a few seconds.[34,35]

Therefore, it was necessary to set the experimental conditions so that no analytical problems would be encountered to determine the metal content in the organic phase, which was accomplished using ICP-AES. In Table 22, the quantification limits for ICP-AES analysis of Pd(II), Nd(III) and Fe(III) are presented.

Table 22: Quantification limits (LoQ) for ICP-AES analysis of diluted solutions.

Metal	**Pd**	**Fe**	**Nd**
LoQ (mg.L $^{-1}$)	0.28	0.21	0.23

Given our analytical method, a minimum quantifiable concentration can be deduced from the following relationship:

$$[\mathrm{M}]_{\mathrm{min}} = \mathrm{FD} * \mathrm{LoQ} \quad (198)$$

With, $[\mathrm{M}]_{\mathrm{min}}$ is the minimum quantifiable concentration of a metal, and FD is the dilution factor.

We add that a minimum dilution factor of 10 is required to avoid matrix effects. Thus, the minimum quantifiable concentrations for Fe(III) and Nd(III) are 2.1 mg.L^{-1} and 2.3 mg.L^{-1}, respectively.

In this regard, we fixed the concentrations of THMA and DBMA at 0.6M in the organic phase, where the extraction performances are suitable for a kinetic study.

1. Extraction kinetics with THMA

The global transfer constants K_{org}^{g} of Pd(II), Nd(III) and Fe(III) were first determined with 0.6M THMA in toluene, starting of an aqueous phase containing a mixture of the three metals. In Table 23, we summarize the experimental conditions.

Table 23: Experimental conditions set for the determination of the global transfer constants of Pd(II), Nd(III) and Fe(III).

$[Pd]_{aq}$	$[Nd]_{aq}$	$[Fe]_{aq}$	$[HNO_3]_{aq}$	$[THMA]_{org}$
1 g.L^{-1}	1 g.L^{-1}	5 g.L^{-1}	3M	0.6M

We mention that for all the experiments performed with the single drop technique, the linearities of the curves were verified. In Figure 58, we present the plots of ln(1-E) for Pd(II), Nd(III) and Fe(III) in extraction with 0.6M THMA as a function of time. All other plots are presented in Appendix I.

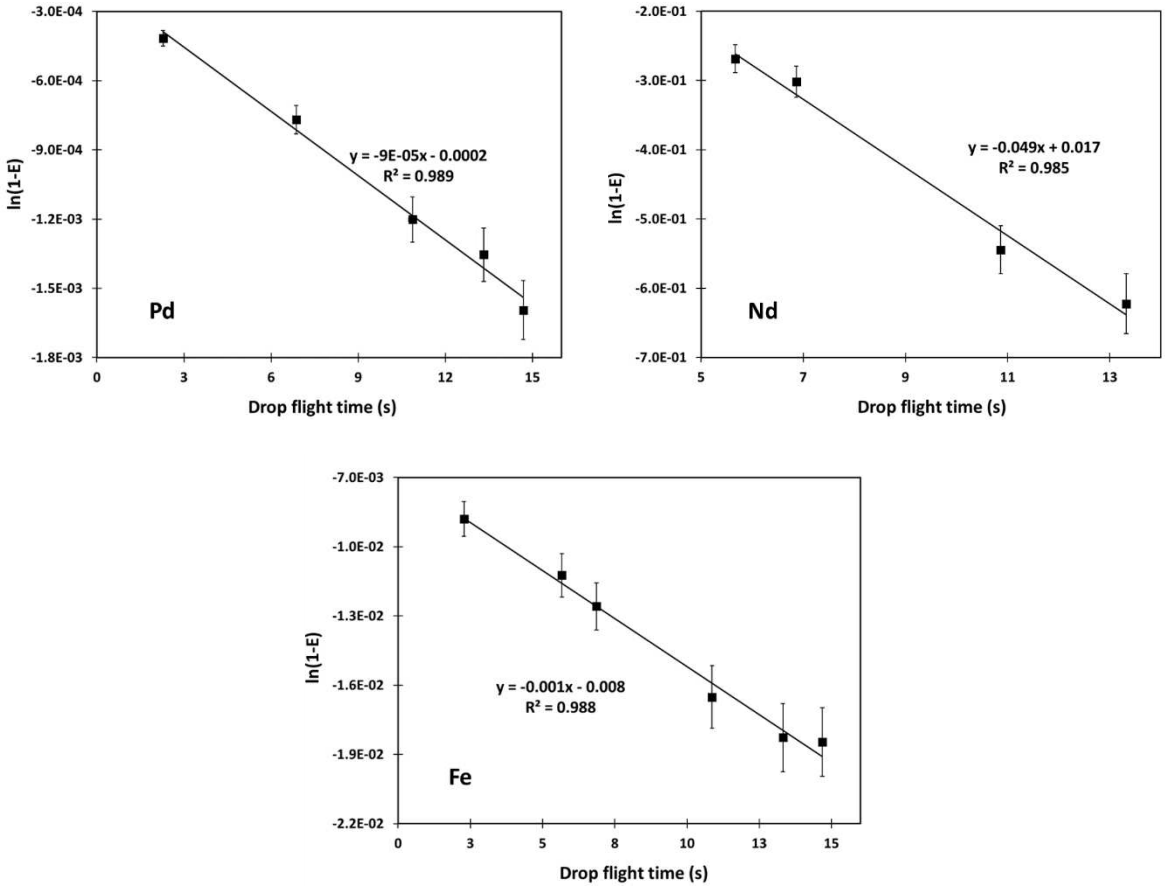

Figure 58: Dependence of ln(1-E) as a function of time for the extraction of Pd(II), Nd(III) and Fe(III) with 0.6M THMA in toluene. Initial $[Pd]_{aq}$ 1 $g.L^{-1}$,initial $[Fe]_{aq}$ 10 $g.L^{-1}$ and initial $[Nd]_{aq}$ 1 $g.L^{-1}$, $[HNO_3]_{aq}$ 3M, T = 21°C.

The strong linearity of the curves (regression coefficient > 0.98) proved the validity of the experimental model. Thus, the global transfer constants of the three metals could be calculated (Table 24).

Table 24: Global transfer constants and distribution ratios of Pd(II), Nd(III) and Fe(III) in extraction with 0.6M THMA in toluene, $[HNO_3]_{aq}$ 3M, T=21°C.

	Pd(II)	**Nd(III)**	**Fe(III)**
$\mathbf{C_{aq,\,ini}}$	1 $g.L^{-1}$	1 $g.L^{-1}$	5 $g.L^{-1}$
$\mathbf{D_M}$	$D_{Pd} = 194$	$D_{Nd} = 0.07$	$D_{Fe} = 0.08$
$\mathbf{K^g_{org}\ (m.s^{-1})}$	$(3.43 \pm 0.21)*10^{-8}$	$(1.59 \pm 0.16)*10^{-5}$	$(3.08 \pm 0.17)*10^{-7}$

First, the global transfer constant of Nd(III) is the largest compared to that of Pd(II) and Fe(III), revealing its fastest extraction kinetics compared to the other two metals. In parallel, the extraction kinetics of Pd(II) appeared to be the slowest. However, the extraction kinetics of Fe(III) should be treated with caution due to the possible extraction of hydrolyzed species, which extraction kinetics are fast. This will be discussed hereafter.

The fast extraction kinetics of Nd(III) with malonamides is documented in the literature. Indeed, Weigl et al.[184] investigated the extraction kinetics of Nd(III) with 0.5M DBMA in hydrogenated polypropylene tetramer (TPH), using Nitsch cell. As a result, the transfer was found to be diffusion controlled, and the transfer constant was equal to $2*10^{-5}$ m.s^{-1}. In addition, in the framework of his PhD thesis, Bosland[34] investigated the extraction kinetics of Nd(III) from 3M HNO_3 with 0.65M DMDOHEMA in TPH at 25°C using single drop technique, and the global transfer constant was determined equal to $(3.7\pm0.6)*10^{-5}$ m.s^{-1}. Furthermore, the same author investigated the extraction kinetics of Nd(III) from 3M HNO_3 with 0.65M DBMA in TPH at 15°C using ARMOLLEX cell, and the transfer constant was determined equal to $(1.0 \pm 0.2)*10^{-5}$ m.s^{-1}.

In parallel, the slower extraction kinetics of Pd(II) compared to Nd(III) may be related to chemical resistance to the transfer of the metal.

The second experiment involving only Nd(III) and Fe(III) was performed with 0.6M THMA. In Table 25 we summarize the experimental conditions set, the global transfer constants and the distribution ratios of Nd(III) and Fe(III) in extraction with 0.6M THMA.

Table 25: Global transfer constants and distribution ratios of Nd(III) and Fe(III) in extraction with 0.6M THMA in toluene, $[HNO_3]_{aq}$ 3M, T=21°C.

	Nd(III)	**Fe(III)**
$\mathbf{C_{aq,ini}}$	1 g.L^{-1}	10 g.L^{-1}
$\mathbf{D_M}$	$D_{Nd} = 0.07$	$D_{Fe} = 0.06^*$
$\mathbf{K^g_{org}}$ **(m.s^{-1})**	$(1.32 \pm 0.05)*10^{-5}$	$(9.40 \pm 0.91)*10^{-7}$

(*) The decrease of the distribution ratio from 0.08 (previous experiment) to 0.06 (this experiment) is related to the increase of the initial concentration of Fe(III) from 5 g.L^{-1} (previous experiment) to 10 g.L^{-1} (this experiment).

First, the extraction kinetics of Nd(III) was still the fastest, and its global transfer constant remained almost the same in the absence of Pd(II). Thus, we conclude that the presence of Pd(II) does not imply any competitive effect on the extraction kinetics of Nd(III).

In parallel, this comparison cannot be made for Fe(III) since its concentration in the two initial aqueous phases is not the same. Nevertheless, we noticed that the transfer constant of Fe(III) is ten times better than the result of the previous experiment. This improvement can be the consequence of two factors: Either the removal of Pd(II) or the increase of the initial Fe(III) concentration (from 5g.L ^{1} to 10 g.L^{-1}). However, our studies did not take into account the effect of the initial metal concentration. Furthermore, we recall that the extraction kinetics of Fe(III) can be quickly complicated due to the participation of hydrolyzed species, which present faster extraction kinetics than the aquocations of Fe(III). Thus, increasing the initial concentration of Fe(III) may also increase the concentration of the hydrolyzed species of Fe(III), which may impact the observed global transfer constant directly.

2. Extraction kinetics with DBMA

First of all, the global transfer constant of Pd(II) could not be determined from an aqueous phase containing the mixture of metals in the case of DBMA, following the set experimental conditions (0.6M DBMA). The extraction of Pd(II) was strongly enhanced, resulting in a significant decrease in its final concentration in the continuous aqueous phase. Therefore, the results obtained were not usable since the mass transfer equations between the continuous phase and the dispersed phase, postulate a constant concentration of metal in the continuous phase.

In this regard, we studied the extraction kinetics of Pd(II) separately from Nd(III) and Fe(III), by reducing the concentration of DBMA in the organic phase, in the case of Pd(II). The experimental conditions are summarized in Table 26.

Table 26: Experimental conditions set for the determination of the global transfer constants of Pd(II), Nd(III) and Fe(III) with DBMA.

	Experiment 1	**Experiment 2**	**Experiment 3**
	Pd(II)	**Nd(III)**	**Fe(III)**
$\mathbf{[DBMA]_{org}}$	0.3M	0.6M	0.6M
$\mathbf{C_{aq,ini}}$	$[Pd]_{aq,ini}$ 1 g.L^{-1}	$[Nd]_{aq,ini}$ 1 g.L^{-1}	$[Fe]_{aq,ini}$ 10 g.L^{-}
$\mathbf{[HNO_3]_{aq}}$	3M	3M	3M

In Table 27, the global transfer constants, as well as the distribution ratios of Pd(II), Nd(III) and Fe(III) upon extraction with DBMA are summarized.

Table 27: Global transfer constants and distribution ratios of Pd(II), Nd(III) and Fe(III) in extraction with DBMA in toluene. Initial $[Pd]_{aq}$ 1 $g.L^{-1}$, initial $[Nd]_{aq}$ 1 $g.L^{-1}$, initial $[Fe]_{aq}$ 5 $g.L^{-1}$, $[HNO_3]_{aq}$ 3M, T = 21°C.

	Experiment 1	**Experiment 2**	**Experiment 3**
	Pd(II)	**Nd(III)**	**Fe(III)**
	$D_{Pd} = 4.3$	$D_{Nd} = 1.2$	$D_{Fe} = 0.9$
$\mathbf{K_{org}^{g}}$ **(m.s^{-1})**	$(7.81 \pm 0.84)*10^{-7}$	$(2.26 \pm 0.30)*10^{-5}$	$(2.17 \pm 0.16)*10^{-8}$

In these experimental conditions, the global transfer constant of Nd(III) is again the highest, revealing that its extraction kinetics is the fastest compared to Pd(II) and Fe(III). Bearing in mind that the global transfer constant of Pd(II) was obtained with 0.3M DBMA, the obtained values indicate that the extraction kinetics of the three metals follow this order: Nd(III) > Pd(II) > Fe(III). Indeed, Nd(III) mass transfer is almost 1000 and 30 times faster than that of Fe(III) and Pd(II), respectively. This is in complete agreement with the results obtained in batch experiments (Figure 52).

Moreover, the extraction kinetics of Nd(III) is approximately twice as fast with DBMA than with THMA. Previous studies on the extraction of Nd(III) showed that the extraction of the latter requires organization in the organic phase.[174] Although SAXS measurements showed that no signature of supramolecular correlation was visible when using toluene as a diluent (refer to Chapter 2, § II-A), the faster extraction of Nd(III) with DBMA may indicate that the latter is more prone to be organized, even when using toluene. As discussed above, the polar core of DBMA is less hindered than THMA (see Figure 55), which affects its organization in the organic phase. Therefore, it is interesting to assess the effect of the organization of the organic phase on the extraction kinetics of Nd(III) by using an aliphatic diluent, *i.e.* heptane. However, particular attention must be given for third phase formation. We add that in the literature, differences in the extraction kinetics of Eu(III) with DBMA and DMDOHEMA are documented.[185] The extraction kinetics of Eu(III) at 22°C is reported to be very fast and controlled by diffusion with DBMA, whereas it is slower with DMDOHEMA. This again emphasizes the effect of the ligand structure on the extraction kinetics of the metal again.

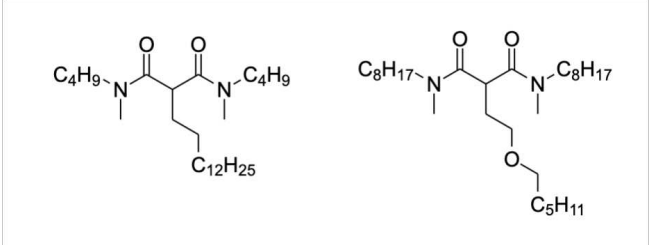

Figure 59: Chemical structure of DBMA (a), DMDOHEMA (b).

On the other hand, the slowness of the extraction of Pd(II) and Fe(III), compared to Nd(III), may be related to the additional diffusional limitations of these metals. However, the diffusion coefficients of the Pd(II), Nd(III) and Fe(III) were not determined. On the other hand, this slowness may also originate from a slow chemical reaction, which increases the chemical resistance to transfer for Pd(II) and Fe(II), compared to Nd(III).

Among the chemical reactions that an extraction reaction may require, is the loss of water molecules from the coordination sphere of the metals for their transfer from the aqueous to the organic phase. Therefore, in Table 28 the rates of the exchange of water molecules for Pd(II), Nd(III) and Fe(III) are presented.

Table 28: Rate constants of the exchange of water molecules for Pd(II), Nd(III) and Fe(III), T=25°C.[9]

	$Pd(H_2O)_4^{2+}$	$Fe(H_2O)_6^{3+}$	$Nd(H_2O)_9^{3+}$
$k(s^{-1})$	$5.6 * 10^2$	$1.6 * 10^2$	$\geq 50*10^7$

The large gap in the water exchange rate of Nd(III), Pd(II) and Fe(III) may explain the fast and diffusion controlled extraction kinetics of the former. The water exchange rate for Nd(III) is much higher than that of Pd(II) and Fe(III). Furthermore, the water exchange rate for Fe(III) is the lowest, which is in agreement with the results obtained from the kinetic characterization with DBMA. We emphasize that the differences in the extraction kinetics between Pd(II) and Fe(III) could not be clearly identified for the experimental conditions chosen in the case of THMA. Thus, we assumed that the extraction kinetics of Fe(III) can be quickly complicated due to the participation of the hydrolyzed species of Fe(III) in the extraction reaction, which will be explained hereafter.

3. Extraction kinetics of Pd(II) with THMA and DBMA

In the light of the extraction performance of Pd(II) with 0.6M DBMA, we considered varying the concentration of the extractant to establish the constants of the extraction kinetics of Pd(II). In addition, we also acquired data with THMA to better compare the influence of the extractant on the extraction kinetics of Pd(II).

The extraction kinetics of Pd(II) with THMA and DBMA were investigated, and the respective global transfer constants were determined. These studies were carried out using 0.15M and 0.3M DBMA and 0.3M and 0.6M THMA in toluene. The obtained results are presented in Table 29.

Table 29: Global transfer constants K_g and distribution ratios at equilibrium of Pd(II) in extraction with THMA and DBMA. Initial $[Pd]_{aq}$ 1 $g.L^{-1}$, $[HNO_3]_{aq}$ 3M, T=21°C.

	[THMA] 0.6M	**[THMA] 0.3M**	**[DBMA] 0.3M**	**[DBMA] 0.15M**
$\mathbf{D_{Pd}}$	194	57	4.27	1.13
$\mathbf{K_{org}^{g}}$ **($m.s^{-1}$)**	$(3.43 \pm 0.21)*10^{-8}$	$(2.74 \pm 0.21)*10^{-8}$	$(7.81 \pm 0.84)*10^{-7}$	$(1.84 \pm 0.19)*10^{-6}$

First of all, by comparing the global transfer constants of Pd(II) obtained for 0.3M DBMA and THMA, we conclude that the extraction kinetics of Pd(II) is much faster with DBMA. This is in full agreement with the results obtained in small batch experiments.

First, let us recall the expression of the global transfer constant in the presence of an interfacial reaction (refer to Chapter 1, § IV-A):

$$R_{total} = R_{chemical} + R_{diffusional} \tag{199}$$

$$\frac{1}{K_{org}^{g}} = \frac{1}{k_{org}} + \frac{D}{k_{aq}} + \frac{D}{k_f} \tag{200}$$

The first two terms, describe the diffusional resistance:

$$R_{diffusional} = \frac{1}{k_{org}} + \frac{D}{k_{aq}} \tag{201}$$

While the third term represents the resistance due to the chemical reaction:

$$R_{chemical} = \frac{D}{k_f} \tag{202}$$

Looking at the different distribution ratios of Pd(II) with the two ligands, this effect may be related to diffusion processes. Indeed, in the case of THMA, larger distribution ratios of Pd(II) are obtained compared to DBMA. Thus, the global transfer constant expression reduces to the last two terms, which are the diffusional term in the aqueous phase and the chemical term. Therefore, this slow extraction kinetics of THMA may be related to the diffusional limitations in the aqueous phase or the chemical resistance at the interface.

On the other hand, the chemical origins of the slow extraction kinetics of THMA may stem from the rotational barrier of the latter and the energy required for reorganization compared to DBMA. In their paper, Lefrançois et al.[159] reported the existence of four types of conformational changes, each type characterized by a specific rate. The formation of the metal-ligand complex through the two carbonyl groups of the malonamide ligand, may require an interconversion from a *trans* position to a nearly *cis* position of the two carbonyl groups to form chelates. Furthermore, the authors reported that the bulkiness of substituents on nitrogen atoms and the central carbon atom lowers the barriers of rotation. Therefore, it seems crucial to further investigate the conformational changes of THMA and DBMA through DFT calculations and compare the changes in the energy differences between a free and complexed ligand for both malonamides.

Second, increasing the ligand concentration in the organic phase had a different impact on the extraction kinetics of Pd(II). By doubling the concentration of DBMA from 0.15M to 0.3M, the global transfer constant decreased by half. Whereas, for THMA, when its concentration was doubled from 0.3M to 0.6M, the global transfer constant of Pd(II) was nearly equal K_g (0.6M THMA)/ K_g (0.3M THMA) ≈ 1.2. The decrease in the extraction kinetics of DBMA upon doubling its concentration in the organic phase may be related to diffusional limitations. In fact, DBMA is more surface-active than THMA. Thus, by doubling its concentration in the organic phase, its interfacial concentration is supposed to increase, which may increase the diffusional resistance since the Pd-DBMA complexes formed at the interface, have to diffuse back in the bulk of the organic phase. Furthermore, this observation may reflect the difference in the residence time of the formed complexes at the interface. It may be larger in the case of DBMA, which may imply more diffusional limitations, which are observed with a further decrease of the global transfer constant.

C. Conclusion

In conclusion, the extraction kinetics characterization of Pd(II), Nd(III) and Fe(III) with THMA and DBMA showed that the extraction kinetics of Nd(III) is the fastest with both ligands, and that is probably controlled by diffusion. While that of Pd(II) and Fe(III) were slower. This slowness may result from chemical limitations of the transfer of both metals. Finally, the extraction kinetics of Pd(II) is faster with DBMA compared to THMA.

These investigations emphasized the impact of the structure of the extractant on the extraction kinetics of Pd(II). For instance, the presence of bulky lateral alkyl chains with the absence of any central chain for THMA seems to cause a gain in the thermodynamic extraction efficiency of Pd(II), while it leads to a loss in the kinetic performance. In parallel, for DBMA, the reduction of the bulkiness of the

lateral chains, in the presence of a long central chain, cause a decrease in the thermodynamic performances of the extraction of Pd(II), while a visible gain the extraction kinetics.

IV. Extraction of Fe(III): Possible presence of hydrolyzed species

The slowness of the extraction of Fe(III) with malonamides is documented in the literature. Indeed, the separation of Fe(III) from Am(III) in extraction with DBMA was possible by controlling the extraction time.[148,200] However, because of the strong propensity of $Fe(H_2O)_{6,aq}^{3+}$ to hydrolyse to $Fe(OH)_{aq}^{2+}$,[204–207] both the hydrolyzed and the unhydrolyzed species may participate in the extraction reaction.[217,218] Furthermore, it has been reported that ligand substitution for $Fe(H_2O)_6^{3+}$follows a different mechanistic pathway than for $Fe(OH)^{2+}$, where for the former an associative character has been suggested, whereas for the latter, a dissociative character has been proposed.[219]

The extraction of the hydrolyzed species is generally faster than the aquocation $Fe(H_2O)_6^{3+}$.[218] The fast extraction of hydrolyzed iron species can be attributed to their faster water exchange rate compared to aquocations. The presence of a hydoxide ion enhances the release of the water molecules from their coordination sphere, which enhances their transfer in the organic phase. In Table 30, the rate constants for the water exchange of $Fe(H_2O)_6^{3+}$ and $Fe(OH)^{2+}$ are presented.

Table 30: Rate constant (k) for the water exchange of $Fe(H_2O)_6^{3+}$ and $Fe(OH)^{2+}$ at T = 298K.[9]

	$Fe(H_2O)_6^{3+}$	$Fe(OH)^{2+}$
$k(s^{-1})$	$1.6 * 10^2$	$1.2 * 10^5$

In our study, the extraction kinetics of Fe(III) with DBMA was found to be the slowest compared to Nd(III) and Pd(II). However, this could not be established in the case of THMA, where the global transfer constant of Fe(III) was larger than that of Pd(II) (Table 24).

Looking back at the thermodynamic extraction of Fe(III) with both ligands, we notice that the extraction of Fe(III) is higher with DBMA compared to THMA (Table 31).

Table 31: Distribution ratios of Fe(III) in extraction with 0.6M THMA and 0.6M DBMA in toluene. Initial $[Fe]_{aq}$ 10 $g.L^{-1}$, $[HNO_3]_{aq}$ 3M, T = 21°C.

	[THMA] 0.6M	**[DBMA] 0.6M**
$\mathbf{D_{Fe}}$	0.06	0.9
$\mathbf{K_{org}^{g}}$ **($m.s^{-1}$)**	$(9.40 \pm 0.20)*10^{-7}$	$(2.17 \pm 0.16)*10^{-8}$

Let us recall again the expression of the global transfer constant:

$$\frac{1}{K_{org}^{g}} = \frac{1}{k_{org}} + \frac{D}{k_{aq}} + \frac{D}{k_f} \quad (203)$$

Seen the distribution ratio of Fe(III) is very low with THMA, then the two last terms can be neglected, and in this case, the resistance is located mainly in the organic phase. In parallel, in the case of DBMA, seen that the value of the distribution ratio is not sufficiently high to eliminate the first term, the resistance to transfer may be present in the organic and the aqueous phases, which may explain the slow extraction kinetics of Fe(III) with DBMA.

In parallel, when considering the chemical term, one cannot neglect the possible participation of the hydrolyzed species in the extraction of Fe(III) in the extraction reaction. As mentioned above, Fe(III) has a propensity to hydrolyze in aqueous phases.

Thus, assuming that aquocations and hydrolyzed species are present in the aqueous phase, the total aqueous concentration of iron $[Fe]_{tot,aq}$ can be expressed as follows:

$$[Fe]_{tot,aq} = [Fe^{3+}]_{aq} + [Fe(OH)_n^{(3-n)+}]_{aq} \quad (204)$$

Where, $[Fe^{3+}]_{aq}$ is the concentration of aquocation $Fe(H_2O)_6^{3+}$ and, $[Fe(OH)_n^{(3-n)+}]$ is the concentration of the hydrolyzed species.

Thus, both species Fe^{3+} and $Fe(OH)_n^{(3-n)+}$ may participate in the extraction reaction. Since the transfer time is short when using a single drop technique, only the forward reaction will be considered. Hence, the extraction rate of Fe(III) in the organic phase can be written as follows:

$$+\frac{\mathrm{d}[\mathrm{Fe}]_{\mathrm{org}}}{\mathrm{dt}} = k_1[\mathrm{Fe}^{3+}]_{\mathrm{org}} + k_2[\mathrm{Fe(OH)}_{\mathrm{n}}^{(3-\mathrm{n})+}]_{\mathrm{org}} \quad (205)$$

Where, k_1 is the rate constant of the reaction of the extraction of the aquocations $\mathrm{Fe(H_2O)}_6^{3+}$, and k_2 is the rate constant of the reaction of the extraction of the hydrolyzed species $\mathrm{Fe(OH)}_{\mathrm{n}}^{(3-\mathrm{n})+}$.

It is worth noting that $k_2 > k_1$, since the extraction of the hydrolyzed species of Fe(III) are faster than the aquocation species.

For this discussion, we will consider two cases:

- **Case 1: $[\mathbf{Fe(OH)}_{\mathbf{n}}^{\mathbf{(3-n)+}}]_{\mathbf{org}}$ can be neglected**

First, we note that the aqueous concentration of the hydrolyzed species of Fe(III) is in general much lower than the concentration of the aquocations. So if the experimental conditions are favourable for the extraction of Fe(III), the contribution of the hydrolyzed species in the overall transfer of Fe(III) in the organic phase can be neglected.

$$[\mathrm{Fe}]_{\mathrm{org}} = [\mathrm{Fe}^{3+}]_{\mathrm{org}} + [\mathrm{Fe(OH)}_{\mathrm{n}}^{(3-\mathrm{n})+}]_{\mathrm{org}} \approx [\mathrm{Fe}^{3+}]_{\mathrm{org}} \quad (206)$$

Thus, the rate of transfer of iron in the organic phase is reduced to:

$$+\frac{\mathrm{d}[\mathrm{Fe}]_{\mathrm{org}}}{\mathrm{dt}} = k_1[\mathrm{Fe}^{3+}]_{\mathrm{org}} \quad (207)$$

In this case, the extraction rate is governed with the first term, representing the slow extraction of the aquocations species of Fe(III).

- **Case 2: The concentration of $\mathbf{Fe(OH)}_{\mathbf{n}}^{\mathbf{(3-n)+}}$ cannot be neglected**

In this case, we consider that the experimental conditions do not favour the extraction of Fe(III). Therefore, the contribution of the hydrolyzed species in the overall transfer of Fe(III) in the organic phase cannot be neglected anymore.

$$[\mathrm{Fe}]_{\mathrm{org}} = [\mathrm{Fe}^{3+}]_{\mathrm{org}} + [\mathrm{Fe(OH)}_{\mathrm{n}}^{(3-\mathrm{n})+}]_{\mathrm{org}} \approx [\mathrm{Fe(OH)}_{\mathrm{n}}^{(3-\mathrm{n})+}]_{\mathrm{org}} \quad (208)$$

In this case, the extraction rate of iron can be written as follows,

$$+\frac{\mathrm{d[Fe]_{org}}}{\mathrm{dt}} = k_2[\mathrm{Fe(OH)_n^{(3-n)+}}]_{\mathrm{org}} \quad (209)$$

In this case, the extraction rate is governed by the second term, representing the fast extraction of the hydrolyzed species.

This approach may also explain the different extraction kinetics of Fe(III) with THMA and DBMA. Thus, seen the extraction of Fe(III) is very low with THMA compared to DBMA, the contribution of the hydrolyzed species is more likely in the case of the former. Thus, a larger global transfer constant is obtained.

According to the findings collected in Chapter 2, § VIII , the extraction of Fe(III) was found to be enhanced with increasing nitrate ions concentration in the aqueous phase. Therefore, the extraction kinetics of Fe(III) was investigated under conditions where its transfer is favourable.

In this regard, the extraction kinetics of Fe(III) with THMA was investigated at a fixed concentration of acidity and by changing the concentration of nitrate ions. The concentration of H^+ was kept constant at 1.5M, and that of THMA in the organic phase was fixed at 0.8M.

A thermodynamic characterization was first carried out to determine the distribution ratios of Fe(III) for the different aqueous phases. The distribution ratios, as well as the global transfer constants of Fe(III) in extraction with THMA, are presented in Table 32.

Table 32: Determination of the distribution ratios and the global transfer constants in extraction with 0.8M THMA in toluene for different concentrations of nitrate ions in the aqueous phase. Initial $[Fe]_{aq}$ 8 $g.L^{-1}$, $[H^+]_{aq}$ 1.5M, T = 21°C.

	$[\mathbf{NO_3^-}]$ **2M** $[\mathbf{H^+}]$ **1.5M**	$[\mathbf{NO_3^-}]$ **3M** $[\mathbf{H^+}]$ **1.5M**	$[\mathbf{NO_3^-}]$ **4M** $[\mathbf{H^+}]$ **1.5M**
$\mathbf{D_{Fe}}$	0.03	0.31	1.29
$\mathbf{K_{org}^{g}}$ **(m.s^{-1})**	$(1.03 \pm 0.10)*10^{-6}$	$(1.75 \pm 0.21)*10^{-7}$	$(7.08 \pm 0.25)*10^{-8}$

First we notice that the distribution ratios of Fe(III) increase with the increase of nitrate ions, whereas the global transfer constants decrease.

For a low concentration of nitrate ions, the extraction of iron is thermodynamically low, thus the analyzed concentration of iron in the organic phase, originates from the hydolyzed species, that exhibit high extraction kinetics. Thus, the global transfer constants were the highest.

In parallel, by increasing the concentration of nitrate ions to 4M, the extraction of iron was enhanced. Thus, from a kinetic point of view, the importance of the hydrolyzed species is suppressed, since the concentration of iron analyzed in the organic phase originates primarily from the transfer of the aquocation $Fe(H_2O)_6^{3+}$, which is clear in the decrease of the global transfer constant.

Finally, for a moderate concentration of nitrate ions in the aqueous phase (3M), we suggest that the analyzed concentration of iron in the organic phase originates from both, the aquocation and the hydrolyzed species. Therefore, the contribution of the aquocations is not sufficient to suppress the fast extraction of the hydrolyzed species.

V. Conclusion

In this chapter the characterization of the extraction kinetics of Pd(II), Fe(III) and Nd(III) were detailed.

The investigation of the extraction kinetics of Pd(II), Fe(III) and Nd(III) in small batch experiments revealed that the extraction equilibrium of Nd(III) is reached very fast. On the other hand, the extraction of Fe(III) is the slowest. Furthermore, the extraction equilibrium of Pd(II) with DBMA is reached faster than that with THMA.

The interfacial properties of THMA and DBMA were characterized prior to investigating the extraction kinetics using the single drop technique. DBMA is more surface-active than THMA. The experimental IFTs were fitted using Szyszkoswki isotherm. It is worth noting that the equilibrium adsorption constant K_{ads} of DBMA is higher than that of THMA, which proves the high adsorption capacity of DBMA at the interface.

The global transfer constants of the three metals in extraction with THMA and DBMA, were determined using the single drop technique. The extraction of Nd(III) with both ligands was found to be very fast, suggesting that its extraction kinetics is diffusion controlled. The extraction kinetics of the three metals with DBMA followed this order: Nd(III) > Pd(II) > Fe(III). The slow extractions of Pd(II) and Fe(III) compared to Nd(III) were related to slow chemical reactions. Furthermore, the effect of the topology on the extraction kinetics was evidenced as the extraction kinetics of Pd(II) is much faster with DBMA than with THMA. Similarly, the extraction kinetics of Nd(III) is twice faster with DBMA than with THMA.

Finally, it was suggested that the extraction kinetics of Fe(III) depends strongly on the nature of the extracted species. The fast extraction of the hydrolyzed species of Fe(III) can lead to some

ambiguities when interpreting the results. Thus, it was concluded that when the conditions are not favoured thermodynamically for the extraction of the aquocation $Fe(H_2O)_6^{3+}$, the fast extraction of hydrolyzed species dictates the observed rate constant. Conversely, as long as the experimental conditions are favoured thermodynamically for the extraction of $Fe(H_2O)_6^{3+}$, the slow rate of transfer of Fe(III) governs the observed rate constant of the extraction.

Chapter 4: Determination of the rate laws of the extraction

A detailed study of the solvent extraction rate is of great interest to have a clear understanding of the nature of mass transfer and its limitations. It also requires a good knowledge of the rate-controlling steps and the overall extraction mechanism.

In Chapter 3, the differences in the extraction kinetics of Pd(II), Nd(III) and Fe(III) with DBMA and THMA were presented. In addition, the effect of the structure of the ligands on the extraction kinetics of Pd(II) and Nd(III) was evidenced. Therefore, we were interested in further characterizing the extraction kinetics of the three metals by determining their extraction rate laws.

The rate law of a chemical reaction usually depends on the concentration of some (or all) of the reactants. Thus, its determination involves screening for the effect of the concentration of the various reactants that may contribute to the extraction reaction. In Chapter 1, § IX, we documented some of the reported studies using classical tools to determine rate law, *i.e.* Lewis cell, Nitsch cell, single drop technique. However, the use of these techniques can be disadvantageous for a large number of screening experiments, as they require significant consumption of reagents that can be costly (DBMA) or must be synthesized (THMA).

We present here a simple calculation to illustrate the situation when using the single drop technique: Considering two ligands, THMA and DBMA, and then three metals, Pd(II), Nd(III) and Fe(III), for each one, four parameters of a minimum of three different concentrations for each, must be screened. This makes a number of experiments equal to: 2*3*4*3 = 72 experiments. However, this number is only an estimate that describes the situation in its best case, when no analytical problems are detected, and the concentrations chosen were definitely the optimum concentrations to study.

Therefore, we proposed screening the extraction kinetics in small batch experiments, using safe lock tubes, based on the initial rate method. The study of the extraction kinetics in batch experiments is documented in the literature (see Chapter 1). However, these studies have often been criticized for the lack of knowledge of the interfacial area and the control of hydrodynamics.[31] Therefore, the validity of the results obtained from batch experiments had to be confirmed by some selected single drop technique experiments, where the interfacial area is known.

In this chapter, we describe the experimental approach implemented to determine the extraction rate law. In addition, we highlight how it proved helpful in cases where the characterization of the

extraction kinetics requires screening of multiple parameters. We also show that, by relying on the results obtained in batch experiments, a mechanistic study of an extraction reaction is feasible.

We specify that the mechanistic study focused mainly on the extraction kinetics of Pd(II). Based on the extraction kinetics experiments performed with the single drop technique and in small batch experiments, we suspected the involvement of several Fe(III) species in the extraction reaction. Therefore, we assumed that the study of the extraction kinetics of Fe(III) could be complicated. In parallel, Nd(III) extraction rate law could not be determined in small batch experiments due to its fast extraction kinetics. All these details will be explained hereafter.

I. Initial rate method

Several methods can be used to determine experimentally the rate law, *e.g.* initial rate method, integration method etc. For our study, the choice was made on the initial rate method.

Many authors have reported the accuracy of this method.[220–222] On the first hand, the results obtained from the initial data are not influenced by the effect of the reverse reaction nor by side reactions. On the other hand, a simple change of the pH or the ionic strength during the reaction can be marginalized since the results treated are the ones obtained for 10% of the reaction. Providing an accurate initial data accessible for different initial concentrations of reactants, the kinetical order of each reactant can be determined in addition to the rate constant. Therefore, a mechanistic treatment is feasible. Finally, this method is often regarded as a time saver.

Despite the advantages mentioned above, this method is rarely used due to some restrictions. First, this method is only applicable if an accurate measurement of the small amount of product can be made. Second, this method has a significant dependence on the rate constant, and the largest errors when the temperature is changed. Therefore, it is necessary to keep all parameters steady, including temperature.

Consider the following reaction:

$$\mathrm{A} + \mathrm{B} + \mathrm{C} = \mathrm{D} + \mathrm{E} + \mathrm{F} \tag{210}$$

For this reaction, the rate depends on the concentrations of the three reactants A, B and C.

Therefore, a complete rate law would be:

$$\text{rate} = -\frac{\mathrm{d[A]}}{\mathrm{dt}} = -\frac{\mathrm{d[B]}}{\mathrm{dt}} = -\frac{\mathrm{d[C]}}{\mathrm{dt}} = k[\mathrm{A}]^{\alpha}[\mathrm{B}]^{\beta}[\mathrm{C}]^{\gamma} \tag{211}$$

Where k is the rate constant, α, β, γ denote the partial orders of A, B and C, respectively.

The rate law, which describes the reaction both at $t = 0$ and at later times, can be written to focus on what it predicts initially by using the subscript '0' to indicate initial concentrations values. Therefore, the initial rate can be reported as follows:

$$\text{initial rate} = v_0 = k[A]_0^{\alpha}[B]_0^{\beta}[C]_0^{\gamma} \quad (212)$$

If several experiments are performed using the same starting concentrations of B and C, but a different starting concentration of A, the terms $[B]_0^{\beta}$ and $[C]_0^{\gamma}$ would be constant. Therefore, the measure of the initial rate will only depend upon $[A]_0$, which can be expressed:

$$\text{initial rate} = v_0 = -\left(\frac{d[A]}{dt}\right)_{t=0} = k[A]_0^{\alpha} * \text{constant} \quad (213)$$

Taking logarithm on both sides:

$$\ln\left[-\left(\frac{d[A]}{dt}\right)_{t=0}\right] = \ln\left(\frac{[A]_0 - [A]_t}{t_1 - t_0}\right) = \ln k + \alpha \ln [A]_0 + \text{constant} \quad (214)$$

The slope α of the curve $\ln\left(\frac{[A]_0 - [A]_t}{t_1 - t_0}\right) = f(\ln[A])$, is the kinetical order for A.

Similarly, the kinetical orders of the other reactants B and C can be determined.

II. Small batch experiments

A. Description

Screening the extraction kinetics in small batch experiments using safe lock tubes. The extraction rate law was determined by screening the effect of the concentration of one parameter on the extraction rate, as we explained above. The studied parameters were:

- $[M]_{aq}$
- $[L]_{org}$
- $[H^+]_{aq}$ and $[NO_3^-]_{aq}$

The extraction rate of a given metal can be written as follows:

$$v = -\frac{d[M]_{aq}}{dt} = +\frac{d[M]_{org}}{dt} \quad (215)$$

And the effect of the variation of the concentration of one parameter on the extraction rate was deduced from the variation of the concentration of metal in the aqueous or organic phase. It should be noted that for this study, the organic concentration of the metal was used for the determination of the rate law.

B. Choice of the experimental conditions

In general, when applying the initial rate, a conversion rate of less than 10% is often targeted. Therefore, choosing the experimental conditions for the realization of small batch experiments was necessary, particularly the stirring speed and the extraction time. The extraction experiments were carried out in small safe lock tubes. The aqueous to organic volume ratio A/O was kept equal to 1, and the extraction time was fixed at 1 min. After extraction, tubes were centrifuged for 30 s to separate both phases.

On the other hand, when two immiscible fluids are agitated, a dispersion is formed in which a continuous breakup and coalescence of droplets co-occur. A local dynamic balance between breakup and coalescence is established after a sufficient time, which will dictate the average size of the droplets. However, in batch experiments, a precise determination of the size of the droplets is difficult like the interfacial area. In this regard, for the choice of the stirring speed, we tried to find a compromise between eliminating the diffusional limitations and exploiting the initial rate. Bearing in mind that an increase of the stirring speed induces a decrease in the size of the dispersed organic droplets, leading to an increase of the total interfacial area and thus the extraction rate.

Preliminary extraction kinetics were then performed by varying the stirring speed and fixing the extraction time for 1 min. For this screening, Pd(II) extraction from 3M and 5M HNO_3 with 0.2M THMA was performed (Figure 60).

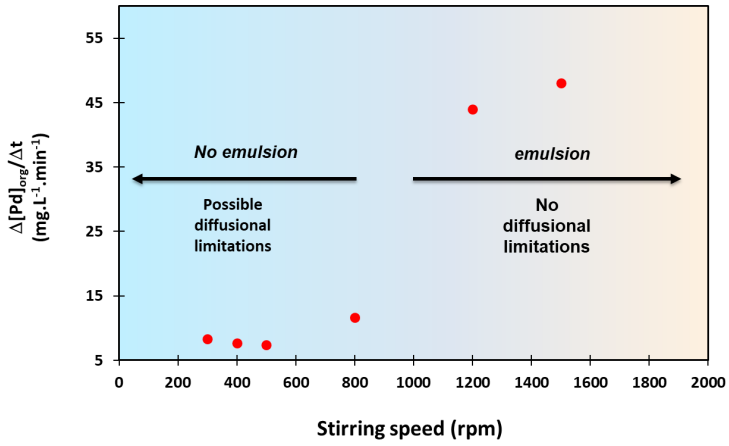

Figure 60: Effect of the stirring speed on the extraction rate of Pd(II) from 3M with 0.2M THMA in toluene. Initial $[Pd]_{aq}$ 500 $mg.L^{-1}$, T=21°C.

A visual study of the impact of the stirring speed on the mixing of both phases revealed that, for low stirring speed (<600 rpm), the aqueous/organic interface is more or less quiescent. A dispersion of the organic into the aqueous phase occurs at a stirring speed between 800 and 1000 rpm. At higher speed (>1000 rpm), emulsification of the biphasic system is well visible, and it can be assumed that the concentration in metal is homogeneous in each phase.

The stirring speed was then fixed at 1200 rpm, where emulsification of both phases was highly ensured. We mention that working at a higher stirring speed, *e.g.* 1500 rpm would be better for screening the extraction kinetics since, for this value, a plateau was observed. However, screening the extraction kinetics in batch experiments was further developed to depict the effect of adding dihexylamine on the extraction kinetics of Pd(II) with THMA, which will be detailed in Chapter 5. For these experiments, we deliberately lowered the stirring speed to investigate in detail the extraction kinetics. In order to standardize the experimental conditions for screening the extraction kinetics, the stirring speed was fixed at 1200 rpm.

According to the preliminary acquired results, following the experimental conditions set, we noticed that the extraction of Fe(III) with DBMA and THMA was very low. This was accentuated when the experimental conditions were unfavourable for Fe(III) extraction, *e.g.* low nitric acid concentration. Therefore, to avoid any analytical problem for the determination of Fe(III) concentration, due to the quantification limits (LoQ) of ICP-AES, we proposed to increase the initial volumes of the aqueous and organic phases, always keeping the ratio A/O = 1. By doing this, larger volumes of the organic phase could be sampled for back-extraction, which allowed for lower dilution factors. Thus, 5 mL Eppendorf tubes were used for the extraction experiments. However, the available shaking system at the laboratory is not equipped to increase the stirring speed above 1000 rpm, when a thermoblock of 5 mL Eppendorf

tubes is mounted. In this regard, Fe(III) extraction experiments were performed at 1000 rpm, where visual emulsification of both phases was always ensured.

From a technical point of view, the batch methodology could be applied for the extraction of Pd(II) and Fe(III) since for both metals, the equilibrium was not reached for 1 min of extraction, which permits to investigate appropriately the extraction kinetics. In contrast, this could not be applied in the case of Nd(III). Due to its fast extraction kinetics with both ligands, the extraction equilibrium is reached in less than 2 minutes (see Chapter 3). Therefore, screening the extraction kinetics is only valid for very low extraction durations. However, given the experimental setup employed for this study, reducing the extraction time was not possible since significant errors will be encountered, which will affect the accuracy of the results.

This methodology is based on the initial rate method, so a conversion percentage of less than 10% is often targeted. Therefore, it is necessary to define the experimental conditions so that the extraction percentage is not very high, as this would induce large errors in the accuracy of the results. Interestingly, for all the results presented in our study, the extraction percentage reached at most 20%.

III. Pd extraction rate law with THMA and DBMA in small batch experiments

In Chapter 2, thermodynamic characterizations of Pd(II) extraction with THMA and DBMA were presented. Based on our findings and the results reported in the case of the extraction of Pd(II) with DMDOHEMA,[142] the extraction equilibrium of Pd(II) with THMA and DBMA can be written as follows:

$$Pd^{2+}_{aq} + 2NO^{-}_{3,aq} + 2L_{org} = Pd(NO_3)_2L_{2,org} \quad (216)$$

The distribution ratios of Pd(II) extraction were shown to be dependent on the nitric acid concentration in the aqueous phase.

In this regard, for the kinetic characterization of the extraction of Pd(II) with THMA and DBMA, we investigated the effect of the concentrations of Pd(II), NO_3^-, H^+ in the aqueous phase, and the concentration of the ligands in the organic phase.

A. Pd(II) extraction rate law with DBMA

1. Partial order of the concentration of Pd(II)

The partial order of Pd(II) concentration in the extraction reaction with DBMA from 3M HNO_3 was determined (Figure 61). The studied concentrations of Pd(II) were 500 $mg.L^{-1}$, 250 $mg.L^{-1}$and 125 $mg.L^{-1}$.

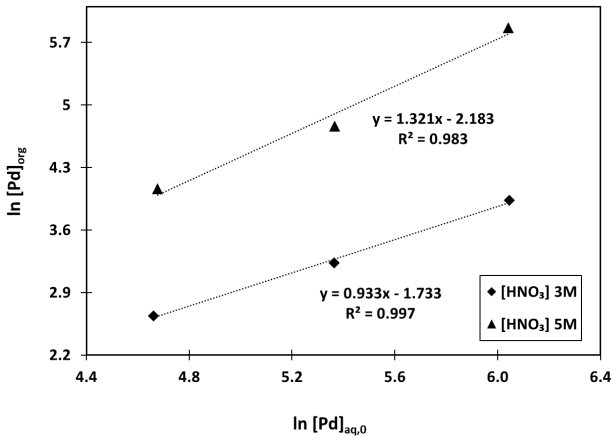

Figure 61: Dependence of $ln[Pd]_{org}$ as a function of $ln[Pd]_{aq,0}$ for $[HNO_3]_{aq}$ 3M and $[HNO_3]_{aq}$ 5M, $[DBMA]_{org}$ 0.2M in toluene, A/O 1, 1 min of extraction, stirring speed 1200 rpm, T=21°C.

The slopes of the curves reveal that the extraction rate law follows a first-order dependence on palladium concentration.

2. Partial order of the concentration of DBMA

The partial order of the concentration of DBMA in the extraction of Pd(II) was determined at different nitric acid concentrations in the aqueous phase, *i.e.* 1.5M, 3M and 5M (Figure 62).

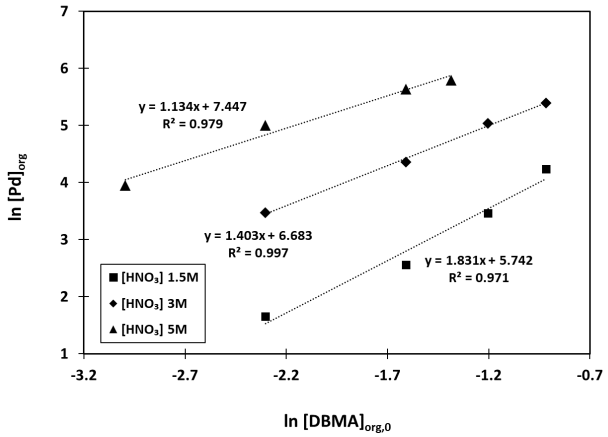

Figure 62: Dependence of $ln[Pd]_{org}$ as a function of $ln[DBMA]_{org,0}$ at different nitric acid concentrations. Initial $[Pd]_{aq}$ 500 $mg.L^{-1}$, A/O 1, 1 min of extraction, stirring speed 1200 rpm, T=21°C.

The dependence of the extraction reaction on the concentration of DBMA decreased with the increase of the concentration of nitric acid in the aqueous phase. For instance, at $[HNO_3]_{aq}$ 1.5M, the partial order was approximately 1.83, which is almost 2. By increasing the concentration of nitric acid to 3M, the partial order of DBMA decreased to a value close to 1.4. A further decrease was observed when increasing the nitric acid concentration to 5M, and the partial order of DBMA obtained was close to 1.

We mention that the DBMA concentrations studied for the experiments performed at 1.5M and 3M HNO_3 were 0.1M, 0.2M, 0.3M and 0.4M. However, at 5M HNO_3, Pd(II) extraction is highly enhanced for DBMA concentration greater or equal to 0.3M, which may pose problems on the accuracy of the results. In this regard, the partial order of DBMA at 5M HNO_3 was determined for a reduced range of DBMA concentrations, *i.e.* 0.05M, 0.1M, 0.2M and 0.025M.

As shown in Chapter 2, the average number of HNO_3 molecules extracted per 1 molecule of DBMA increases with the increase of nitric acid concentration in the aqueous phase. Thus, the decrease in the partial order of DBMA concentration upon increasing acidity may be related to the reduction in the free ligand concentration in the organic phase due to the formation of DBMA-HNO_3 adducts.

3. Partial order of nitric acid concentration

The partial order of the nitric acid concentration in the extraction of Pd(II) with DBMA was determined, and the studied concentrations were 1.5M, 3M, 5M and 7M (Figure 63).

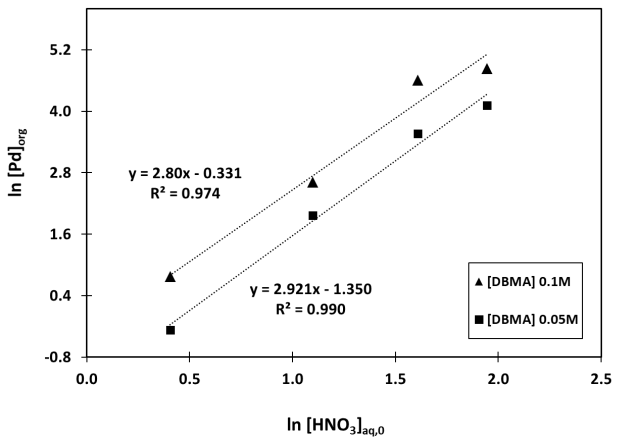

Figure 63: Dependence of $\ln[Pd]_{org}$ as a function of $\ln[HNO_3]_{aq,0}$ for 0.05M DBMA and 0.1M DBMA. Initial $[Pd]_{aq}$ 500 $mg.L^{-1}$, A/O 1, 1 min of extraction, stirring speed 1200 rpm, T=21°C.

The slopes of the curves reveal that the extraction reaction of Pd(II) is third-order dependent on HNO_3 concentration for the two DBMA concentrations studied.

We emphasize that the organic phases were contacted with an aqueous phase of the corresponding acidity for both studies prior to the extraction experiment. Thus, we investigated the effect of the pre-equilibration of the organic phases on determining the partial orders of HNO_3 in the extraction reaction of Pd(II) with DBMA. For this purpose, we determined the partial order of HNO_3 in the extraction reaction of Pd(II), using 0.05M and 0.1M DBMA, without prior contact with an acidic aqueous phase.

Interestingly, for the non-pre-equilibrated DBMA organic solutions, the partial orders of the concentration of HNO_3 were also of the third order.

4. Partial order of the concentration of NO_3^-

The partial order of the concentration of nitrate ions in the extraction of Pd(II) with DBMA was determined for the range of 1.5M, 2M, 3M and 3.5M $[NO_3^-]$.

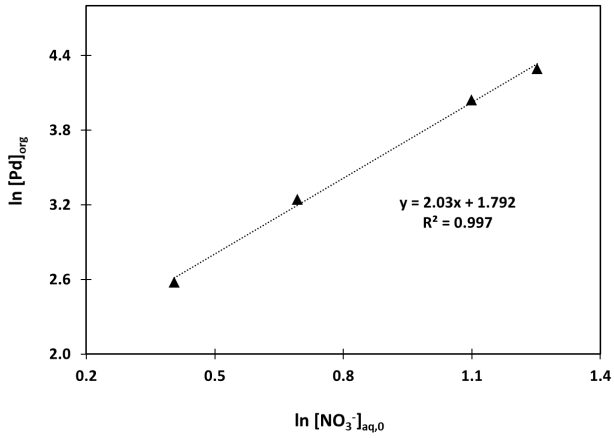

Figure 64: Dependence of $\ln[Pd]_{org}$ as a function of $\ln[NO_3^-]_{aq,0}$, $[Pd]_{aq}$ 500 $mg.L^{-1}$, $[H^+]_{aq}$ 1.5M, $[DBMA]_{org}$ 0.2M. A/O 1, 1 min of extraction, stirring speed 1200 rpm, T=21°C.

The curve slope reveals that the extraction reaction of Pd(II) with DBMA is second-order dependent on the concentration of nitrate ions in the aqueous phase.

5. Partial order of the concentration of H+

The partial order of the concentration of proton ions in the extraction reaction of Pd(II) was determined with 0.05M and 0.1M DBMA. The studied concentrations of H^+ were: 1.5M, 3M and 5M (Figure 65).

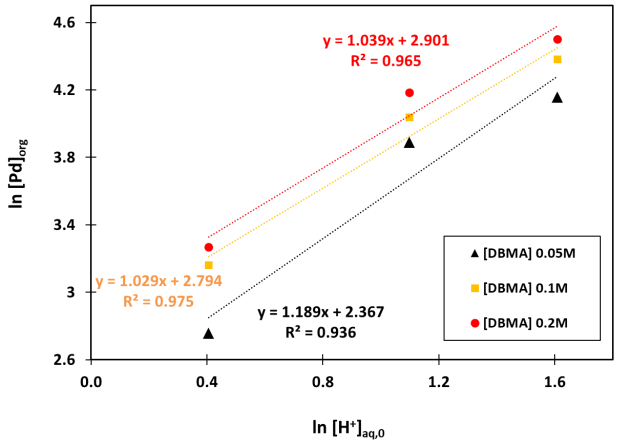

Figure 65: Dependence of $\ln[Pd]_{org}$ as a function of $\ln[H^+]_{aq,0}$ for 0.1M DBMA and 0.2M DBMA in the organic phase. Initial $[Pd]_{aq}$ 300 $mg.L^{-1}$, $[NO_3^-]_{aq}$ 5M, A/O 1, 1 min of extraction, stirring speed 1200 rpm, T = 21°C.

The slopes of the curves were approximately 1, which reveal that the extraction reaction of Pd(II) is first-order dependent on the concentration of proton ions.

6. Conclusion

The results obtained from batch experiments suggest that the extraction rate law of Pd(II) with DBMA is first-order dependent on the concentrations of Pd(II) and proton ions and second-order dependent on the concentration of nitrate ions. In parallel, a decrease of the partial order of DBMA was noticed when increasing the concentration of nitric acid in the aqueous phase. The extraction reaction is nearly second-order dependent on the concentration of DBMA at 1.5M HNO_3. At 3M HNO_3, the partial order was found to decrease to a value of about 1.5, whereas at 5M HNO_3, it further decreased to 1. This may be related to the decrease in the free ligand concentration for complexation due to the acid extraction, which is promoted by the increase in the acidity of the aqueous phase.

Therefore, the rate law of the extraction of Pd(II) can be expressed as follows:

$$-\frac{d[Pd]_{aq}}{dt} = k_1[Pd^{2+}]^1_{aq}[DBMA]^n_{org}[H^+]^1_{aq}[NO_3^-]^2_{aq} \quad (217)$$

Where,

- $n \approx 2$ for $[HNO_3] \leq 1.5M$
- $n < 2$ for $[HNO_3] > 1.5M$

B. Pd(II) extraction rate law with THMA

1. Partial order of the concentration of Pd(II)

The partial order of the concentration of Pd(II) in the extraction reaction with THMA from 3M and 5M HNO_3 was determined, and the studied concentrations of Pd(II) were 500 $mg.L^{-1}$, 250 $mg.L^{-1}$and 125 $mg.L^{-1}$(Figure 66).

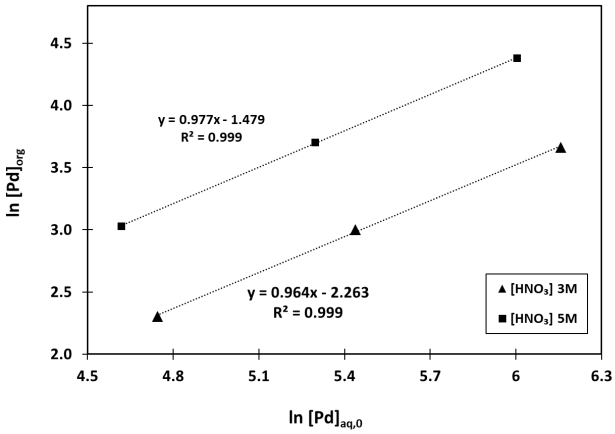

Figure 66: Dependence of $ln[Pd]_{org}$ as a function of $ln[Pd]_{aq,0}$ at 3M HNO_3 and 5M HNO_3. $[THMA]_{org}$ 0.2M in toluene, A/O 1, 1 min of extraction, stirring speed 1200 rpm, T=21°C.

The slopes of the curves reveal that palladium extraction rate law follows a first-order dependence on palladium concentration.

2. Partial order of the concentration of THMA

The partial order of the concentration of THMA was determined at various aqueous nitric acid concentrations, *i.e.* 1.5M, 3M and 5M (Figure 67).

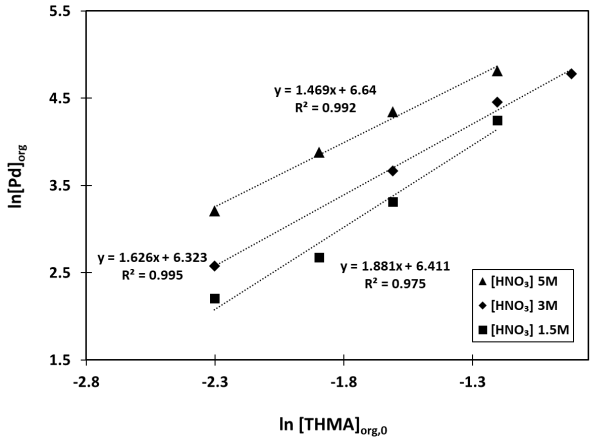

Figure 67: Dependence of $ln[Pd]_{org}$ as a function of $ln[THMA]_{org,0}$, $[Pd]_{aq}$ 500 $mg.L^{-1}$, $[HNO_3]_{aq}$ 1.5M, 3M and 5M, A/O 1, stirring speed 1200 rpm, T=21°C.

Similarly to the results obtained with DBMA, the partial order of the concentration of THMA decreased with the increase of the concentration of nitric acid. For instance, at $[HNO_3]_{aq}$ 1.5M, the partial order was 1.88, which is almost 2. A slight decrease was noticed at 3M HNO_3, and the partial order of THMA was almost 1.6. The partial order further decreased at 5M HNO_3 and reached 1.5.

With the same reasoning suggested for DBMA, the decrease in the partial order of THMA concentration with increasing aqueous nitric acid concentration, can be related to the formation of THMA-HNO_3 adducts, causing the free THMA concentration to decrease.

3. Partial order of the concentration of HNO_3

The partial order of the concentration of HNO_3 in the extraction of Pd(II) with THMA was determined, and the studied concentrations were 1.5M, 3M and 5M (Figure 68).

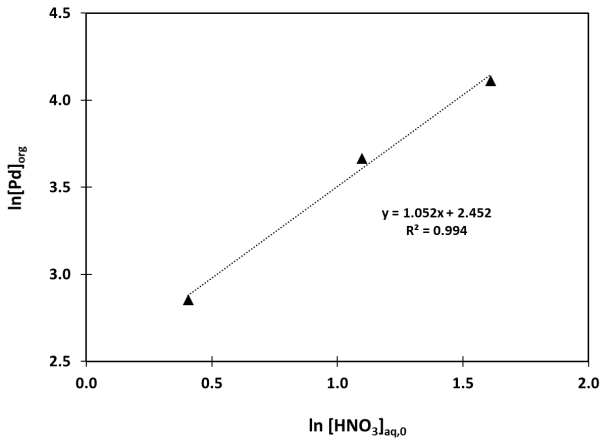

Figure 68: Dependence of $\ln[P]_{org}$ as a function of $\ln[HNO_3]_{aq,0}$. $[THMA]_{org}$ 0.2M in toluene, $[Pd]_{aq}$ 500 $mg.L^{-1}$, A/O 1, 1 min of extraction, stirring speed 1200 rpm, T=21°C.

From the slope of the curve, the extraction rate law of Pd(II) with THMA seems to be first-order dependent on the concentration of HNO_3.

4. Partial order of the concentration NO_3^-

The partial order of the concentration of nitrate ions in the extraction of Pd(II) with THMA was determined, and the studied concentrations were 1.5M, 2M and 3M (Figure 69).

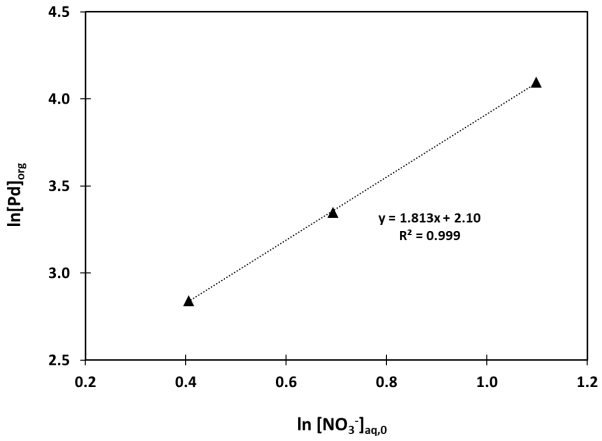

Figure 69: Dependence of $\ln[Pd]_{org}$ as a function of $\ln[NO_3^-]_{aq,0}$. $[THMA]_{org}$ 0.2M in toluene, $[Pd]_{aq}$ 500 $mg.L^{-1}$, $[H^+]_{aq}$ 1.5M. A/O 1, stirring speed 1200 rpm, T=21°C.

The slope of the curve has nearly a slope of 2, which reveals that the partial order of the concentration of NO_3^- in the extraction of Pd(II) with THMA is of the second-order.

5. Partial order of H+

Based on the findings obtained for the partial orders of the concentrations of nitric acid and nitrate ions, an inverse first-order dependence was expected for the concentration of proton ions in the aqueous phase.

The partial order of the concentration of proton ions in the extraction reaction of Pd(II) with 0.2M THMA was determined, and the studied concentrations of H^+ were 1.5M, 3M and 5M (Figure 70).

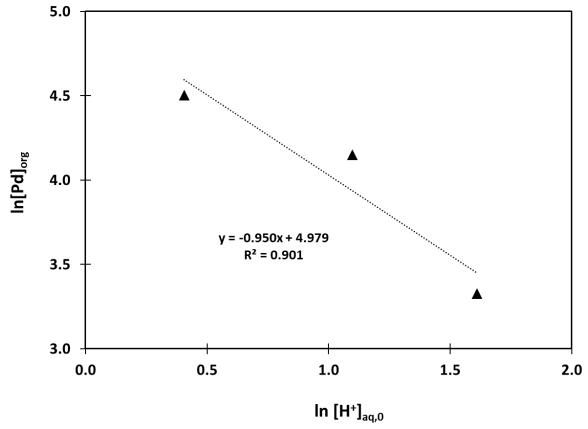

Figure 70: Dependence of $\ln[Pd]_{org}$ as a function of $\ln[H^+]_{aq,0}$. $[THMA]_{org}$ 0.2M in toluene, $[Pd]_{aq}$ 300 $mg.L^{-1}$, $[NO_3^-]_{aq}$ 5M, A/O 1, stirring speed 1200 rpm, T=21°C.

From the curve slope, we suggest that the extraction reaction rate follows an inverse first-order with respect to the concentration of proton ions in the aqueous phase.

6. Conclusion

The results obtained in batch experiments suggest that the rate law is first-order dependent on the concentration of Pd(II), inverse first-order dependent on the concentration of proton ions and second-order dependent on the concentration of nitrate ions. Similarly to DBMA, a decrease of the partial order of THMA was noticed when increasing the concentration of nitric acid in the aqueous phase. The partial order of THMA was nearly 2 for 1.5M HNO_3, and it decreased to 1.6 at 3M HNO_3, whereas it reached nearly 1.5 at 5M HNO_3. As suggested for DBMA, this decrease may be related to the acid uptake of THM, which results in a drop in the concentration of free THMA for complexation.

Therefore, the rate law of the extraction of Pd(II) can be expressed as follows:

$$-\frac{d[Pd]_{aq}}{dt} = k_1[Pd^{2+}]_{aq}^{1}[THMA]_{org}^{m}[H^+]_{aq}^{-1}[NO_3]_{aq}^{2} \quad (218)$$

Where,

- $m \approx 2$ for $[HNO_3] \leq 1.5M$
- $m < 2$ for $[HNO_3] > 1.5M$

C. Conclusion

In Table 33, we summarize the obtained results for the extraction rate laws of Pd(II) with DBMA and THMA.

Table 33: Summary of the partial orders of the reactants involved in the extraction reaction of Pd(II) with THMA and DBMA.

	DBMA	**THMA**
Pd^{2+}	1	1
NO_3^-	2	2
H^+	1	-1
Ligand	≈ 2 for $[HNO_3]_{aq} \leq 1.5M$ < 2 for $[HNO_3]_{aq} > 1.5M$	

IV. Fe(III) extraction with THMA and DBMA in batch experiments

The thermodynamic and kinetic characterizations of Fe(III) extraction, presented in Chapters 2 and 3, have shown that polymeric hydrolyzed species are supposed to participate in the extraction reaction. In this regard, we assumed that a mechanistic study of the extraction of Fe(III) could be complicated, and that requires a deep characterization of the speciation of Fe(III) in the aqueous phase.

In this section, we present some of the obtained results for Fe(III) extraction with DBMA and THMA, in different conditions, and the conclusions that could be drawn.

It is worth mentioning that the extraction of Fe(III) is lower with THMA compared to DBMA. Thus, these kinetic screenings were carried out using 0.2M DBMA and 0.3M THMA, unless stated differently in the text.

A. Extraction of Fe(III) with DBMA

1. Partial order of the concentration of Fe(III)

The partial order of Fe(III) concentration in the extraction reaction with DBMA was determined by fixing the concentration of Fe(III) at 250 mg.L^{-1} and that of HNO_3 at 3M in the aqueous phase. The concentration of DBMA was fixed at 0.2M. The studied concentrations of Fe(III) were 250 mg.L^{-1}, 125 mg/L and 60 mg.L^{-1}.

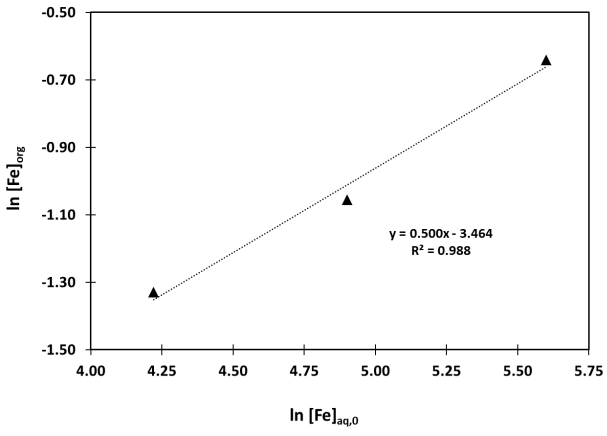

Figure 71: Dependence of $\ln[Fe]_{org}$ as a function of $\ln[Fe]_{aq,0}$, $[HNO_3]_{aq}$ 3M, $[DBMA]_{org}$ 0.2M in toluene, A/O 1, 1 min of extraction, stirring speed 1000 rpm, T = 21°C.

The slope of the plot of $\ln[Fe]_{org}$ against $\ln[Fe]_{aq,0}$ is 0.5, which suggests that the extraction rate is half order dependent on the concentration of Fe(III). This non-integer partial order may originate from

complex mechanisms involving the participation of other species than the aquocations, *e.g.* dimer species of Fe(III).

2. Partial order of the concentration of NO_3^-

The partial order of the concentration of nitrate ions in the extraction of Fe(III) with 0.2M DBMA was determined, and the studied concentrations of nitrate ions were 3M, 3.5M, 4M and 5M (Figure 72).

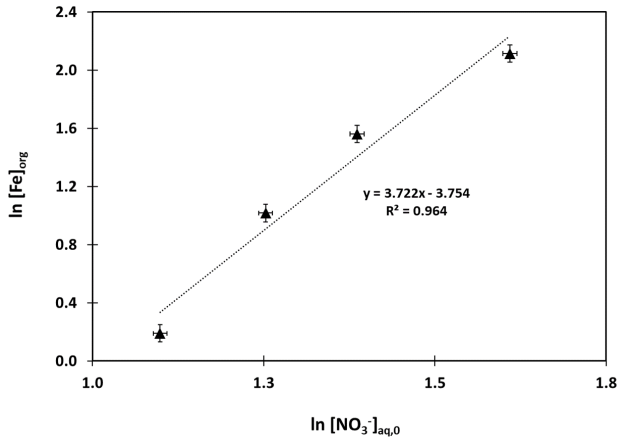

Figure 72: Dependence of $\ln[Fe]_{org}$ as a function of $\ln[NO_3^-]_{aq,0}$.Initial $[Fe]_{aq}$ 250 $mg.L^{-1}$, $[H^+]_{aq}$ 1.5M, $[DBMA]_{org}$ 0.2M, A/O 1, 1 min of extraction, stirring speed 1000 rpm, T = 21°C.

The slope of the curve suggests that the extraction reaction of Fe(III), for the studied conditions, follows an order of 4 with respect to the concentration of nitrate ions. A fine observation of the slope variation shows that the latter decreases from 5 to 3 with the increase of the concentration of nitrate ions in the aqueous phase (Figure 73).

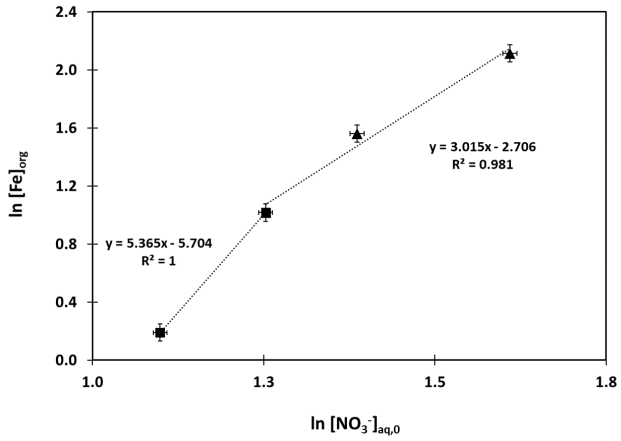

Figure 73: Dependence of $\ln[Fe]_{org}$ as a function of $\ln[NO_3^-]_{aq,0}$, at low and high concentrations of nitrate ions. Initial $[Fe]_{aq}$ 250 $mg.L^{-1}$, $[H^+]_{aq}$ 1.5M, $[DBMA]_{org}$ 0.2M, A/O 1, 1 min of extraction, stirring speed 1000 rpm, T = 21°C.

We suppose that the high partial order obtained at low nitrate ions concentrations may arise from the participation of hydrolyzed species of Fe(III) in the extraction reaction. As presented in Chapter 2, hydrolyzed species of Fe(III) type $Fe(OH)^{2+}$, $Fe(OH)_2^+$ $Fe_2(OH)_2^{4+}$ and even $Fe_3(OH)_4^{5+}$ have been detected in the literature.

For a concentration of nitrate ions equal to or higher than 3.5M, the extraction rate of Fe(III) seems to be third order dependent on the concentration of nitrate ions in the aqueous phase, which is in agreement with the extraction of aquocation species of Fe(III).

3. Partial order of the concentration of H^+

The partial order of the concentration of proton ions in the extraction of Fe(III) with 0.2M DBMA was determined, and the studied concentrations were 1.5M, 3M and 5M (Figure 74).

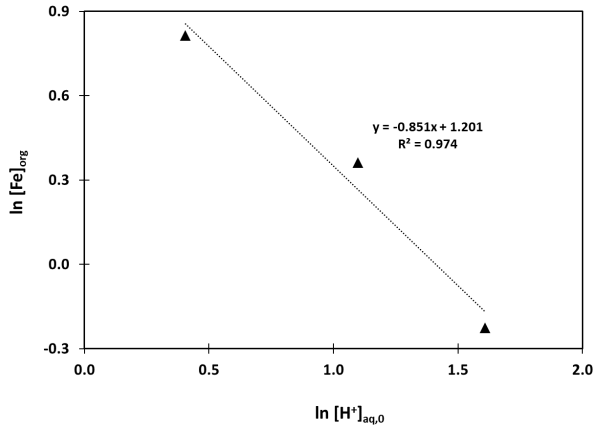

Figure 74: Dependence of $\ln[Fe]_{org}$ as a function of $\ln[H^+]_{aq,0}$, Initial $[Fe]_{aq}$ 250 $mg.L^{-1}$, $[NO_3^-]_{aq}$ 5M, $[DBMA]_{org}$ 0.2M, A/O 1, 1 min of extraction, stirring speed 1000 rpm, T = 21°C.

The slope of the plot of $\ln[Fe]_{org}$ as a function of $\ln[H^+]_{aq,0}$ is nearly -1, which suggests that the extraction rate of Fe(III) follows an inverse first-order with respect to the concentration of proton ions.

In the light of the ambiguities regarding the involved species in the extraction reaction and the possible involvement of hydrolyzed species in the extraction mechanism, the inverse first order with respect to the concentration proton, may also originate from the participation of hydrolyzed species.

Consider the reaction of hydrolysis of Fe(III) into $Fe(OH)^{2+}$:

$$Fe_{aq}^{3+} + H_2O \underset{k_{-1}}{\overset{k_1}{\rightleftharpoons}} Fe(OH)_{aq}^{2+} + H^+ \qquad (219)$$

$$K_1 = \frac{[Fe(OH)^{2+}]_{aq}[H^+]_{aq}}{[Fe^{3+}]_{aq}} \quad (220)$$

If $Fe(OH)^{2+}$ species are the main extracted species, then the extraction can be written as follows:

$$Fe(OH)^{2+}_{aq} + nNO^-_{3,aq} + mDBMA_{org} \underset{k_{-2}}{\overset{k_2}{\rightleftharpoons}} FeOH(NO_3)_n(DBMA)_m \quad (221)$$

The rate of the reaction can be expressed in function of $Fe(OH)^{2+}_{aq}$,

$$-\frac{d[Fe(OH)^{2+}]_{aq}}{dt} = k_2[Fe(OH^{2+})]_{aq}[NO_3^-]^n_{aq}[DBMA]^m_{org} \quad (222)$$

With,

$$[Fe(OH)^{2+}]_{aq} = \frac{K_1[Fe^{3+}]_{aq}}{[H^+]_{aq}} \quad (223)$$

Thus, considering the reaction of $Fe(OH)^{2+}$, an inverse first-order with respect to H^+ is obtained.

B. Extraction of Fe(III) with THMA

1. Partial order of Fe(III)

The partial order of the concentration of Fe(III) in the extraction reaction with THMA was determined, and the studied concentrations were 250 mg.L^{-1}, 125 mg.L^{-1}, and 60 mg.L^{-1}.

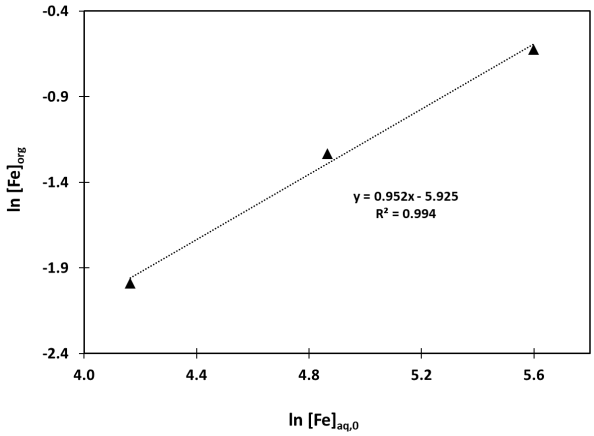

Figure 75: Dependence of $\ln[Fe]_{org}$ as a function of $\ln[Fe]_{aq,0}$, $[HNO_3]_{aq}$ 3M, $[THMA]_{org}$ 0.3M, A/O 1, 1 min of extraction, stirring speed 1000 rpm, T = 21°C.

The curve slope suggests that the extraction of Fe(III) with THMA is first-order dependent on the concentration of Fe(III) in the aqueous phase. We add that the partial order of Fe(III) was also determined at 5M HNO_3, and an order of 1.4 was found.

2. Partial order of the concentration of THMA

The partial order of the concentration of THMA in the extraction reaction of Fe(III) from 5M HNO_3 was determined, and the studied concentrations were 0.2M, 0.3M and 0.4M (Figure 76).

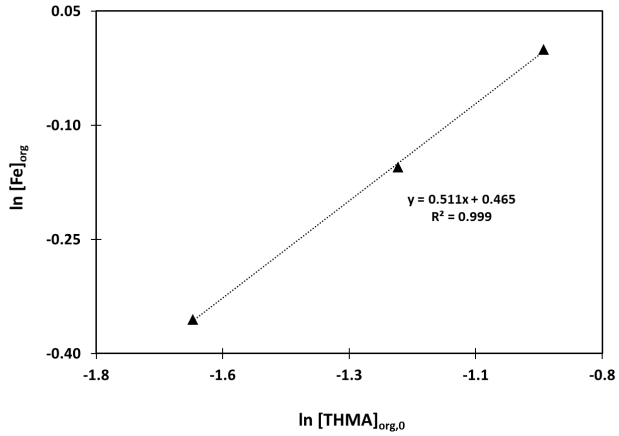

Figure 76: Dependence of $\ln[Fe]_{org}$ as a function of $\ln[THMA]_{org,0}$. $[Fe]_{aq}$ 250 $mg.L^{-1}$, $[HNO_3]$ 5M, A/O 1, 1 min of extraction, stirring speed 1000 rpm, T = 21°C.

From the curve slope, we suggest that the partial order of THMA in the extraction of Fe(III) is 0.5. Similarly to what we assumed for the partial order of Fe(III) with DBMA, the apparition of non-integer partial orders may indicate a complex mechanism, involving other species than aquocations in the extraction reaction, *e.g.* dimer species of Fe(III).

3. Partial order of the concentration of NO_3^-

The determination of the partial order of the concentration of nitrate ions in the extraction rate of Fe(III) was carried out under two different conditions (Table 34):

Table 34: Summary of the experimental conditions set for the determination of the partial order of $[NO_3^-]$.

$[Fe]_{aq,0}$	$[H^+]_{aq,0}$	$[THMA]_{org}$	$[NO_3^-]_{aq,0}$
250 $mg.L^{-1}$	1.5M	0.3M	1.5M, 2M, 3M and 3.5M

For this experiment, the analyzed concentration of Fe(III) for 1.5M and 2M $[NO_3^-]$ was lower than the detection limit of the ICP-AES. However, the slope of the curve taking only into account 3M

and 3.5M [NO_3^-] was nearly 6, suggesting that the partial order of nitrate ions is 6. Seen that this curve is based on only two points, it will not be presented.

In this regard, another attempt was made to determine the partial order of nitrate ions. For this investigation, the experimental conditions were chosen, such as the extraction of Fe(III) is higher, to avoid any analytical problem. We mention that the classical operation mode was applied in this case (stirring speed 1200 rpm / 2 mL Eppendorf tubes) since the chosen experimental conditions were sufficient to ensure Fe(III) extraction without any analytical problem. These conditions are summarized in Table 35.

Table 35: Summary of the experimental conditions set for the determination of the partial order of [NO_3^-].

$[Fe]_{aq,0}$	$[H^+]_{aq,0}$	$[THMA]_{org}$	$[NO_3^-]_{aq,0}$
7 $g.L^{-1}$	1.5M	0.8M	1.5M, 2M, 3M, 4M and 5M

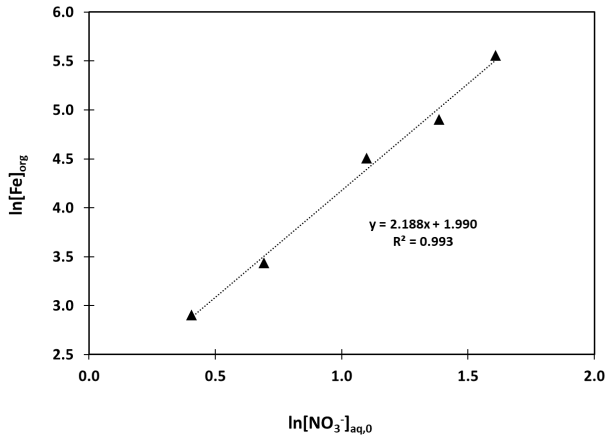

Figure 77: Dependence of $\ln[Fe]_{org}$ as a function of $\ln[NO_3^-]_{aq,0}$. $[Fe]_{aq}$ 7 $g.L^{-1}$, $[H^+]_{aq}$ 1.5M, $[THMA]_{org}$ 0.8 M in toluene, A/O 1, 1 min of extraction, stirring speed 1200 rpm, T = 21°C.

The plot of ln $[Fe]_{org}$ against ln $[NO_3^-]_{aq,0}$ shows a slope of 2, which suggests that the extraction reaction of Fe(III) is second-order dependent on the concentration of nitrate ions in the aqueous phase.

4. Partial order of the concentration of H^+

The partial order of the concentration of THMA in the extraction reaction of Fe(III) was determined, and the studied concentrations were1.5M, 3M and 5M (Figure 78).

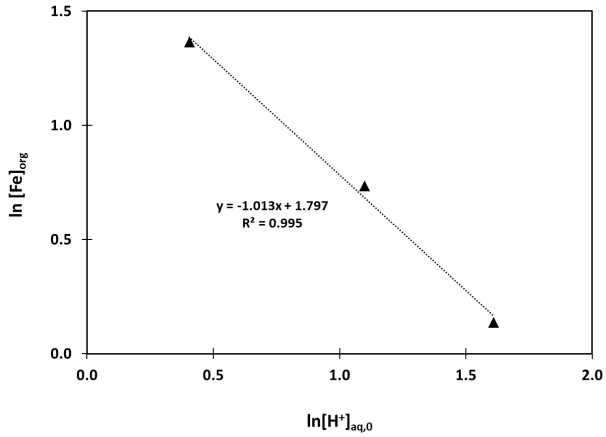

Figure 78: Dependence of $\ln[Fe]_{org}$ as a function of $\ln[H^+]_{aq,0}$. $[Fe]_{aq}$ 250 $mg.L^{-1}$, $[NO_3^-]_{aq}$ 5M, $[THMA]_{org}$ 0.3M, A/O 1, 1 min of extraction, stirring speed 1000 rpm, T = 21°C.

The plot of $\ln[Fe]_{org}$ against $\ln[H^+]_{aq}$ shows a slope of -1, which suggests that the extraction rate of Fe(III) follows an inverse first-order dependence on the extraction of proton ions in the aqueous phase.

Similarly to DBMA, the inverse first order with respect to H^+, may originate from the participation of hydrolyzed species of Fe(III).

C. Conclusion for the extraction of Fe(III)

The few experiments performed with Fe(III) revealed the possible participation of other species than the aquocation species in the extraction reaction. According to the experimental conditions, this was assumed based on the deviation of the partial order of nitrate ions. Also, non-integer partial orders were obtained, suggesting that complex mechanisms occur, with the possible involvement of dimeric species of Fe(III). However, a thorough understanding of the reactions taking place requires complete and detailed speciation of Fe(III) in the aqueous phase for the studied conditions, which was not performed in the framework of this thesis work.

According to the findings obtained, we suggest that the extraction kinetics can be investigated in conditions where the extraction of aquocations is favoured, *i.e.* high concentration of nitrate ions. However, in our study, we did not further investigate the extraction kinetics of Fe(III) with THMA and DBMA. Finally, we point out that the partial order of nitrate ions was also determined using the single drop technique, and the results will be discussed hereafter.

V. Validation of the methodology by single drop technique experiments

First, we recall that our aim for this work was to implement an experimental approach that can enable a fast screening of the extraction kinetics, without using sophisticated macroscopic tools. Thus, an experimental approach based on the initial rate method was established in small batch experiment to determine the extraction rate laws. However, the main drawback of this method is the lack of insights into the interfacial area.

Therefore, it was necessary to validate the main experimental results in conditions where the interfacial area is known. For this purpose, we elected to perform some experiments using the single drop technique, which main advantages are the knowledge of the interfacial area and the short contact time between the phases.

A. Choice of the extraction systems

According to the batch experiments, the extraction rate laws of Pd(II) with THMA and DBMA can be written as follows:

With THMA,

$$v = k_1[Pd^{2+}]_{aq}^{1}[THMA]_{org}^{n}[H^+]_{aq}^{-1}[NO_3^-]_{aq}^{2} \quad (224)$$

And with DBMA,

$$v = k_2[Pd^{2+}]_{aq}^{1}[DBMA]_{org}^{m}[H^+]_{aq}^{+1}[NO_3^-]_{aq}^{2} \quad (225)$$

The first order and second-order dependence of the extraction reactions on the concentrations of Pd(II) and NO_3^-, respectively, did not strike us as very surprising. The same was true for the partial orders of THMA and DBMA, where the same trend was observed with both ligands. In contrast, the change of the partial order from +1 to -1, with respect to the proton ion concentration, received much attention, and we considered it worth validating.

B. Determination of the partial order using single drop technique

The forward extraction rate of a metal (M) from an acid solution (Acid) by an extractant (E) can be presented at constant drop volume and constant temperature as follows:[86,223–225]

$$R_f = k_f[M]^a[Acid]^b[E]^c \quad (226)$$

Where R_f is the forward extraction rate per unit area ($mol.m^{-2}.s^{-1}$), k_f is the forward reaction rate constant, and a, b, c are the corresponding reaction orders. They can be obtained by plotting $\ln(R_f)$ as a function of ln [variable] under investigation while keeping the other variables constant.

R_f is assimilated to a flux, and is calculated from the experimental results using the following equation:

$$\frac{dn}{A} = R_f\, dt \quad (227)$$

Where n is the transferred number of moles, and A is the interfacial area of the drop.

Thus, R_f can be expressed:

$$R_f = \frac{V_{org}}{A}\frac{dC_{org}}{dt} \quad (228)$$

Where, C_{org} is the concentration of the metal in the organic phase, V_O is the volume of the organic drop, and A is the interfacial area of the drop defined as follows:

$$V_{org} = \frac{4}{3}\pi r^3 \quad (229)$$

$$A = 4\pi r^2 \quad (230)$$

With r, the radius of the drop.

$$\frac{V_{org}}{A} = \frac{r}{3} = \frac{d}{6} \quad (231)$$

Thus, Eq (228) can be written as follows,

$$R_f = \frac{d}{6}\frac{dC_{org}}{dt} \quad (232)$$

A straight line should be obtained by plotting C against the contact time t and R_f can be calculated from its slope. We add that the mean diameter value of the organic droplet is considered for to determine R_f.

C. Partial order of $[H^+]$ in the extraction reaction of Pd(II) for the validation of the methodology

The partial orders of the concentration of H^+ in the extraction of Pd(II) with DBMA and THMA were determined using the single drop technique. In Table 36 we summarize the experimental conditions set.

Table 36: Experimental conditions for the determination of the order of the concentration of H^+ in the extraction reaction of Pd(II) with THMA and DBMA, T = 21°C.

$[Extractant]_{org}$	$[Pd]_{aq}$	$[NO_3^-]_{aq}$	Studied $[H^+]_{aq}$
$[THMA]_{org}$ 0.2M $[DBMA]_{org}$ 0.2M	200 $mg.L^{-1}$	5M	1.5M, 3M and 5M

The determination of R_f in each case was determined by plotting the concentration of Pd(II) in the organic phase as a function of the extraction time. In the present section, we only present the determination of R_f for the extraction of Pd(II) with 0.2M DBMA, for $[H^+]_{aq}$ 1.5M (Figure 79). All the other curves are presented in Appendix III.

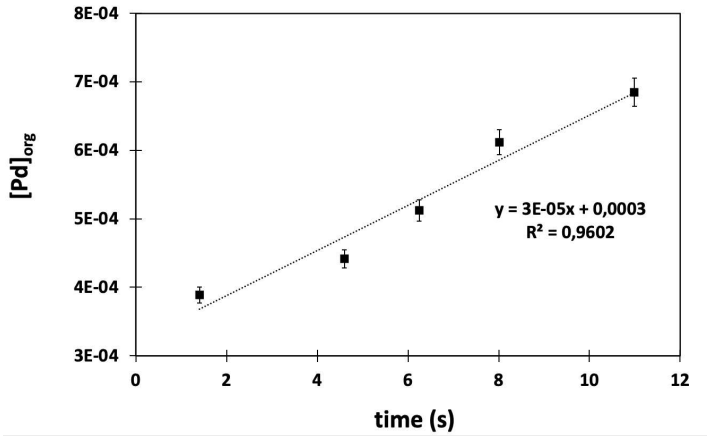

Figure 79: Dependence of $[Pd]_{org}$ as a function of time for the extraction of Pd(II) with 0.2M DBMA in toluene. Initial $[Pd]_{aq}$ 200 $mg.L^{-1}$, $[H^+]_{aq}$ 1.5M, $[NO_3^-]_{aq}$ 5M, T=21°C.

R_f was determined from the slope of the curve and by taking into account the mean value of the diameter 'd' of the organic droplets (Table 37).

Table 37: Determination of R_f for the extraction of Pd(II) with 0.2M DBMA in toluene. Initial $[Pd]_{aq}$ 200 mg.L^{-1}, $[H^+]_{aq}$ 1.5M, $[NO_3^-]_{aq}$ 5M, T=21°C.

Slope	d (m)	R_f (mol.m^{-2}.s^{-1})
$(3.29 \pm 0.38)*10^{-5}$	$2.27*10^{-3}$	$(1.24 \pm 0.14)*10^{-8}$

By analogy, we determined R_f for all $[H^+]_{aq}$ with DBMA and THMA. The plots of ln R_f against ln $[H^+]_{aq}$ with THMA and DBMA, reported in Figure 80, show strong linearities, with a slope of nearly +1 and -1, respectively, for DBMA and THMA. Therefore, the extraction of Pd(II) is first-order and inverse first-order dependent on the concentration of H^+ with DBMA and THMA, respectively, which is in full agreement with the results obtained in small batch experiments.

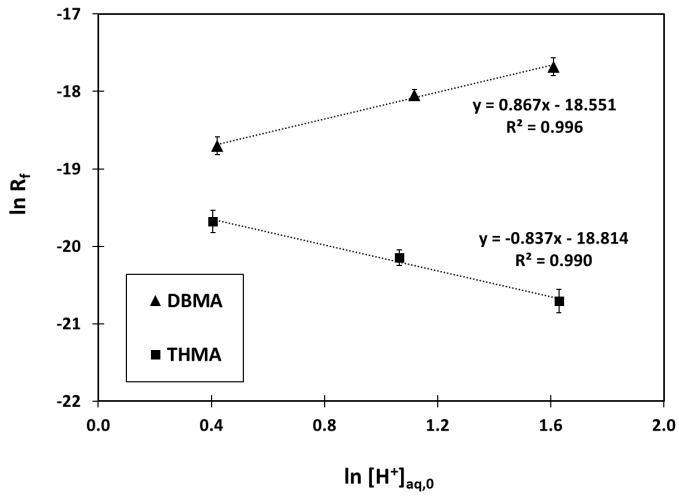

Figure 80: Dependence of lnR_f as a function of ln$[H^+]_{aq}$ for the extraction of Pd(II) with 0.2M DBMA and 0.2M THMA in toluene. Initial $[Pd]_{aq}$ 200 mg.L^{-1}, $[NO_3^-]_{aq}$ 5M, T=21°C.

Based on the results obtained from the single drop technique, we can assume that the experimental methodology is valid and that all the results obtained in batch experiments are correct. These results are summarized in Table 38.

Table 38: Summary of the partial orders of the reactants involved in the extraction reaction of Pd(II) with THMA and DBMA.

	DBMA	THMA
Pd^{2+}	1	1
NO_3^-	2	2
H^+	1	-1
Ligand	≈ 2 for $[HNO_3]_{aq} \leq 1.5M$ < 2 for $[HNO_3]_{aq} > 1.5M$	

D. Determination of the partial order of $[NO_3^-]$ in the extraction of Fe(III) using single drop technique

The screening of the extraction kinetics of Fe(III) in small batch experiments showed that the participation of the hydrolyzed species of Fe(III) could not be neglected. Discrepancies in the partial orders of the nitrate ions concentration were observed, depending on the experimental conditions employed.

In this regard, we were interested in determining the partial order of the concentration of nitrate ions in the extraction of Fe(III) with THMA using the single drop technique. We point out that these experiments were carried out under the same experimental conditions as the ones performed in batch experiment Table 39.

Table 39: Experimental conditions set for the determination of the partial order of $[NO_3^-]_{aq}$ in the extraction reaction of Fe(III) with THMA using the single drop technique. T=21°C.

$[THMA]_{org}$	Initial $[Fe]_{aq}$	$[H^+]_{aq}$	Studied $[NO_3^-]_{aq}$
0.8M	7 $g.L^{-1}$	1.5M	1.5M, 2M, 3M, 4M and 5M

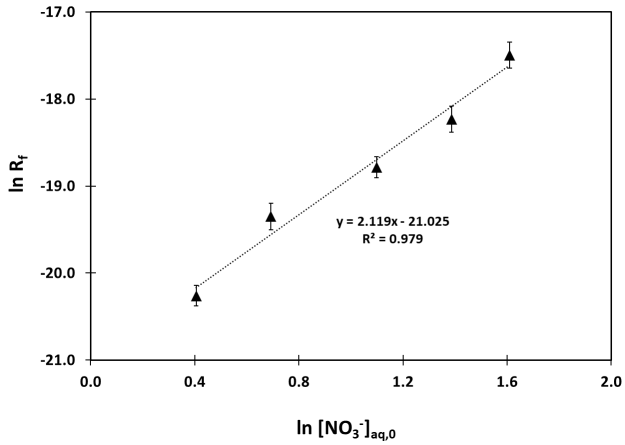

Figure 81: Dependence of $\ln R_f$ as a function of $\ln[NO_3^-]_{aq,0}$ for the extraction of Fe(III) with 0.8M THMA in toluene, Initial $[Fe]_{aq}$ 7 $g.L^{-1}$, $[H^+]_{aq}$ 1.5M, T=21°C.

The slope of the plot of $\ln R_f$ against $\ln [NO_3^-]_{aq,0}$ is nearly 2, which suggests that the partial order of the concentration of nitrate ions in the extraction rate is of the second order. This fully agrees with the result obtained in small batch experiment under the same conditions.

A fine observation of the slopes of the curves of the dependence of the rate on the concentration of nitrate ions in small batch experiments, suggest a deviation of the slopes from 2 to 3 when shifting from low to high nitrate ions concentrations (Figure 82).

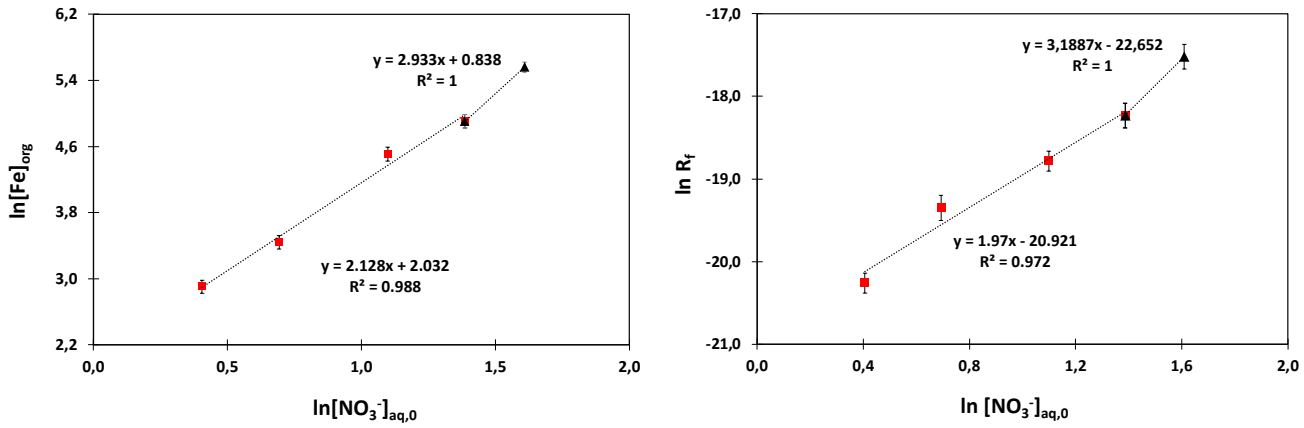

Figure 82: Dependence of $\ln[Fe]_{org}$ and $\ln R_f$ as a function of $\ln[NO_3^-]_{aq,0}$ for the extraction of Fe(III) at low and high concentrations of nitrate ions. 0.8M THMA in toluene, Initial $[Fe]_{aq}$ 7 $g.L^{-1}$, $[H^+]_{aq}$ 1.5M, T=21°C **(a)** Small batch experiment, **(b)** Single drop technique.

We were aware that an accurate slope cannot be obtained based only on two points. Additional experiments for higher concentrations of nitrate ions were not performed to confirm these trends of the curves obtained in small batch experiments and using the single drop technique. However, we strongly suggest that different species may contribute to the extraction reaction. This reasoning is based on the

dependence of the order of nitrate ions following the experimental conditions, which was observed in the case of DBMA as well as THMA, and which was also depicted when using the single drop technique.

In this respect, we highlight the potential for screening the extraction kinetics in small batch experiments. Indeed, the same results were reproduced when using the single drop technique, again confirming the validity of the methodology and the accuracy of the results.

E. Conclusion

In conclusion, this methodology proves helpful for a fast and reliable screening of the extraction kinetics. First of all, the extraction kinetics of Pd(II) with THMA and DBMA could be successfully studied. Although in the case of Fe(III), this methodology gave insights into the extraction kinetics, the study was not completed, due to the possible participation of several species, which may complicate the investigation.

In parallel, this methodology has some limitations, including that it is not adapted for fast extraction systems. For instance, the extraction kinetics of Nd(III) could not be studied due to its fast extraction kinetics. Therefore, from a technical point of view, reducing the extraction time is impossible, as large error on the latter would be encountered.

Moreover, the lack of adequacy of the experimental conditions could also be limiting. This methodology is based on the initial rate method, so a conversion percentage of less than 10% is often targeted. Therefore, it is necessary to define the experimental conditions in such a way that the extraction percentage is not very high, as this would induce large errors in the accuracy of the results. We add that for the systems studied, the separation of the phases was very fast, where 30 s of centrifugations were largely sufficient for a complete separation of the organic and aqueous phases.

VI. Pd(II) extraction mechanisms

To complete the extraction rate laws of Pd(II) with THMA and DBMA, we aimed to propose the correspondent extraction mechanisms. The determination of the extraction mechanisms was based on the following data that were collected in the course of this study:

- DBMA is more surface-active than THMA
- THMA is more basic than DBMA
- H^+ is cooperative for the extraction of Pd(II) with DBMA, whereas it is competitive in the case of THMA

For the propositions of the mechanisms, we will consider the case of ideal solutions. Hence, the concentrations of the active species are used instead of their activities.

A. Pd(II) extraction mechanism with DBMA

The characterization of the interfacial activity of DBMA showed that the latter is adsorbed at the water-oil interface. Consequently, its surface activity will enhance the probability of having extraction kinetics determined by interfacial chemical reactions.

According to the experimental results, the rate equation for the extraction of Pd(II) with DBMA, for $[HNO_3]_{aq} \leq 1.5M$, can be written as follows:

$$R_f = -\frac{d[Pd^{2+}]_{aq}}{dt} = k_f[Pd^{2+}]_{aq}[DBMA]^2_{org}[H^+]_{aq}[NO_3]^2_{aq} \quad (233)$$

The proposed mechanism consists of the following steps:

1- When in contact with an acidic solution, DBMA (L) undergoes protonation to form LH^+ species.

$$L_{org} + H^+_{aq} \underset{k_{-1}}{\overset{k_1}{\rightleftharpoons}} LH^+_{org} \quad \text{(Fast)} \quad (234)$$

$$K_1 = \frac{[LH^+]_{org}}{[L]_{org}[H^+]_{aq}} \quad (235)$$

Thus,

$$[LH^+]_{org} = K_1[L]_{org}[H^+]_{aq} \quad (236)$$

These species, LH^+ are polar and are highly adsorbed at the interface, following the Langmuir adsorption isotherm:

$$LH^+_{org} \rightleftharpoons LH^+_{ads} \quad \text{(Fast)} \quad (237)$$

With,

$$[LH^+]_{ads} = \frac{\Gamma^\infty K_{ads}[LH^+]_{org}}{1 + K_{ads}[LH^+]_{org}} \quad (238)$$

Where, ads denotes the term adsorbed and K_{ads} is the adsorption constant.

2- The adsorbed protonated species of DBMA react with $Pd(NO_3)_3^-$ anions at the interface, resulting in the formation of adsorbed species of $LHPd(NO_3)_3$.

$$LH^+_{ads} + Pd(NO_3)^-_{3,aq} \underset{k_{-2}}{\overset{k_2}{\rightleftharpoons}} LHPd(NO_3)_{3,ads} \quad \text{(Fast)} \qquad (239)$$

$$K_2 = \frac{[LHPd(NO_3)_3]_{ads}}{[LH^+]_{ads}[Pd(NO_3)^-_3]_{aq}} \qquad (240)$$

With,

$$Pd^{2+}_{aq} + NO^-_3 \rightleftharpoons Pd(NO_3)^+_{aq} \qquad (241)$$

$$\beta_1 = \frac{[Pd(NO_3)^+]_{aq}}{[Pd^{2+}]_{aq}[NO^-_3]_{aq}} \qquad (242)$$

And,

$$Pd(NO_3)^+_{aq} + NO^-_3 \rightleftharpoons Pd(NO_3)_{2,aq} \qquad (243)$$

$$\beta_2 = \frac{[Pd(NO_3)_2]_{aq}}{[Pd(NO_3)^+]_{aq}[NO^-_3]_{aq}} \qquad (244)$$

And,

$$Pd(NO_3)_{2,aq} + NO^-_3 \rightleftharpoons Pd(NO_3)^-_{3,aq} \qquad (245)$$

$$\beta_3 = \frac{[Pd(NO_3)^-_3]_{aq}}{[Pd(NO_3)_2]_{aq}[NO^-_3]_{aq}} \qquad (246)$$

With β_1, β_2, and β_3, the constant stabilities of the formation of $Pd(NO_3)^+_{aq}$, $Pd(NO_3)_{2,aq}$ and $Pd(NO_3)^-_{3,aq}$, respectively.

Thus,

$$[Pd(NO_3)_3^-]_{aq} = \beta_1\beta_2\beta_3[Pd^{2+}]_{aq}[NO_3^-]_{aq}^3 \quad (247)$$

And,

$$[LHPd(NO_3)_3]_{ads} = \beta_1\beta_2\beta_3K_2[LH^+]_{ads}[Pd^{2+}]_{aq}[NO_3^-]_{aq}^3 \quad (248)$$

3- The interfacial complex releases HNO_3 molecule into the aqueous phase and an interfacial complex $LPd(NO_3)_2$ is formed.

$$LHPd(NO_3)_{3,ads} \underset{k_{-3}}{\overset{k_3}{\rightleftharpoons}} LPd(NO_3)_{2,ads} + HNO_{3,aq} \quad \text{(Fast)} \quad (249)$$

$$K_3 = \frac{[LPd(NO_3)_2]_{ads}[HNO_3]_{aq}}{[LHPd(NO_3)_3]_{ads}} \quad (250)$$

Taking into account that the acid constant dissociation is,

$$K_a = \frac{[H^+]_{aq}[NO_3^-]_{aq}}{[HNO_3]_{aq}} \quad (251)$$

Thus,

$$[LPd(NO_3)_2]_{ads} = \frac{1}{[H^+]_{aq}}\beta_1\beta_2\beta_3k_aK_2K_3[LH^+]_{ads}[Pd^{2+}]_{aq}[NO_3^-]_{aq}^2 \quad (252)$$

4- The formed complex reacts again with an adsorbed protonated specie of DBMA (LH^+), resulting in the formation of an interfacial $PdL_2(NO_3)_2$ complex. This step is considered to be the rate-determining step.

$$LPd(NO_3)_{2,ads} + LH^+_{ads} \underset{k_{-4}}{\overset{k_4}{\rightleftharpoons}} PdL_2(NO_3)_{2,ads} + H^+_{aq} \quad \text{(Slow)} \quad (253)$$

Considering only the forward reaction, the rate of extraction is given by the following equation:

$$v_4 = -\frac{d}{dt}[LPd(NO_3)_2]_{ads}] = k_4[LPd(NO_3)_2]_{ads}[LH^+]_{ads} \quad (254)$$

By applying the quasi-steady state to the adsorbed species, we can write:

$$-\frac{d}{dt}[LPd(NO_3)_2]_{ads}] = +\frac{d}{dt}[PdL_2(NO_3)_2]_{ads} = 0 \quad (255)$$

Therefore, the rate of extraction can be written as follows:

$$v = -\frac{d}{dt}[Pd^{2+}]_{aq} = \frac{A}{V}v_4 = \frac{A}{V}k_4[LPd(NO_3)_2]_{ads}[LH^+]_{ads} \quad (256)$$

Where,

$$V\frac{d}{dt}[Pd^{2+}]_{aq} - A\frac{d}{dt}[LPd(NO_3)_2]_{ads} = 0 \quad (257)$$

5- A protonated DBMA specie replaces the interfacial $PdL_2(NO_3)_2$ complex, which is transferred fast to the organic phase.

$$PdL_2(NO_3)_{2,ads} + LH^+_{org} \underset{k_{-5}}{\overset{k_5}{\rightleftharpoons}} PdL_2(NO_3)_{2,org} + LH^+_{ads} \quad \text{(Fast)} \quad (258)$$

$$K_5 = \frac{[PdL_2(NO_3)_2]_{org}[LH^+]_{ads}}{[LHPd(NO_3)_2]_{ads}[LH^+]_{org}} \quad (259)$$

DBMA is surface active, and it was reported that for many surfactants, their adsorption is well described by Langmuir adsorption isotherm.[31] When considering the latter, two cases have to be taken into account: The ideal adsorption and the complete interfacial saturation.

- **Ideal adsorption**

Considering an ideal adsorption, the concentration of LH^+_{ads} is written as follows:

$$[LH^+]_{ads} = \Gamma^{\infty}K_{ads}[LH^+]_{org} = \Gamma^{\infty}K_{ads}K_1[L]_{org}[H^+]_{aq} \quad (260)$$

And Eq. (252) becomes,

$$[LPd(NO_3)_2]_{ads} = \Gamma^{\infty}\beta_1\beta_2\beta_3k_aK_{ads}K_1K_2K_3[L]_{org}[Pd^{2+}]_{aq}[NO_3^-]^2_{aq} \quad (261)$$

And Eq. (256) becomes,

$$v = -\frac{d[Pd^{2+}]_{aq}}{dt} = \frac{A}{V} k_4 \Gamma^{\infty} K_{ads} K_1 [LPd(NO_3)_2]_{ads} [L]_{org} [H^+]_{aq} \quad (262)$$

Therefore, the rate of the reaction can be written as follows,

$$-\frac{d[Pd^{2+}]_{aq}}{dt} = \frac{A}{V} k_4 K [L]^2_{org} [H^+]_{aq} [Pd^{2+}]_{aq} [NO_3^-]^2_{aq} \quad (263)$$

With,

$$K = (\Gamma^{\infty} K_{ads})^2 \beta_1 \beta_2 \beta_3 k_a (K_1)^2 K_2 K_3 \quad (264)$$

In conclusion, considering an ideal adsorption, the proposed mechanism can explain the experimental results, seen that the rate expression is in perfect agreement with the experimental partial orders obtained with DBMA (refer to § V- A).

- **Complete saturation**

In the case of a complete saturation, the concentration of LH^+_{ads} is written as follows,

$$[LH^+]_{ads} = \Gamma^{\infty} \quad (265)$$

And Eq (252) becomes,

$$[LPd(NO_3)_2]_{ads} = \frac{\Gamma^{\infty}}{[H^+]_{aq}} \beta_1 \beta_2 \beta_3 k_a K_2 K_3 [Pd^{2+}]_{aq} [NO_3^-]^2_{aq} \quad (266)$$

And Eq (256) becomes,

$$-\frac{d[Pd^{2+}]_{aq}}{dt} = \frac{A}{V} k_4 (\Gamma^{\infty} [LPd(NO_3)_2]_{ads}) \quad (267)$$

Therefore, the rate of the reaction can be written as follows,

$$-\frac{d[Pd^{2+}]_{aq}}{dt} = \frac{A}{V} k_4 \, K' \left(\frac{1}{[H^+]_{aq}} [Pd^{2+}]_{aq} [NO_3^-]^2_{aq}\right) \quad (268)$$

With,

$$K' = (\Gamma^{\infty})^2 \beta_1 \beta_2 \beta_3 k_a K_2 K_3 \quad (269)$$

According to the proposed mechanism, and for a complete saturation of the interface, the reaction rate shows an inverse first order dependence on the concentration of proton ions and zero dependence on the concentration of DBMA, which is not consistent with the experimental results.

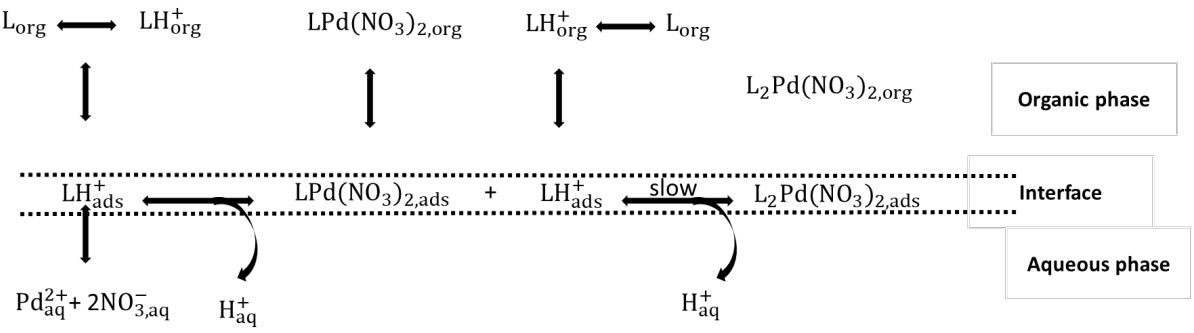

Figure 83: Detailed proposed mechanism of the extraction reaction of Pd(II) with DBMA.

We point out that according to the interfacial characterization of DBMA, the surface pressure of the latter showed no saturation, which indicates that DBMA follows an ideal adsorption (Figure 56).

Moreover, the decrease of the partial order of the concentration of DBMA when increasing the concentration of nitric acid in the aqueous phase can be related to a deviation from an ideal adsorption of DBMA towards a saturation of the interface. In fact, a decrease of the interfacial tension was observed for 0.2M DBMA when increasing the concentration of nitric acid in the aqueous phase Table 40.

Table 40: Interfacial tension measurements at the nitric acid/DBMA in toluene interface, $[DBMA]_{org}$ 0.2M in toluene, T=21°C.

	$[HNO_3]$ 1.5M	**$[HNO_3]$ 3M**	**$[HNO_3]$ 5M**
σ (mN.m^{-1})	19.52	15.24	12.14

In addition, this decrease of the partial order of the ligand can also be related to the decrease of the concentration of the free ligand for complexation. In fact, when determining the partial order of the concentration of DBMA in the extraction rate of Pd(II), we considered the initial ligand concentration in the organic phase. However, this does not relate the actual situation, since the concentration of $[L]_{org}$

represents the concentration of the free ligand, which is different from the initial concentration of DBMA:

Considering the equilibrium of protonation of DBMA:

$$L_{org} + H^+_{aq} \underset{k_{-1}}{\overset{k_1}{\rightleftharpoons}} LH^+_{org} \quad (270)$$

Thus, the total ligand concentration $[L]_{tot}$ in the organic phase can be expressed as follows:

$$[L]_{tot} = [L]_{ini} = [L]_{org} + [LH^+]_{org} \quad (271)$$

Where, $[L]_{ini}$ is the initial concentration of DBMA

And,

$$[L]_{tot} = \alpha[L]_{ini} \qquad (0 < \alpha < 1) \quad (272)$$

Increasing the concentration of H^+ leads to a more significant shift of the equilibrium towards the formation of LH^+, making the concentration of L_{org} decrease, which is manifested in the rate law, by a decrease of the order of the ligand. We emphasize that the estimation of the free ligand cannot be made solely based on experimental results of acid uptake. This value can be determined from modelling taking into account all the protonation equilibria taking place.

Finally, we would like to mention that for this proposed mechanism, we considered the anionic species $Pd(NO_3)_3^-$ in the step reactions, the same applies when considering the species of Pd^{2+}. In other words, this mechanism is independent of the species of Pd(II) in the aqueous phase.

B. Pd(II) extraction mechanism with THMA

First, we recall that THMA exhibited lower interfacial activity than DBMA. In addition, the acid uptake characterization showed that THMA is more basic than DBMA (Chapter 2, § IV - C).

According to the experimental results, the rate equation for the extraction of Pd(II) with THMA can be written as follows:

$$R_f = -\frac{d[Pd^{2+}]}{dt} = k_f[Pd^{2+}]_{aq}[THMA]^2_{org}[H^+]^{-1}_{aq}[NO_3]^2_{aq} \quad (273)$$

In a first attempt, we tried to propose a similar stepwise mechanism for THMA as with DBMA, with a different limiting step.

The protonation of THMA can be written as follows:

$$L_{org} + H^+_{aq} \underset{k_{-1}}{\overset{k_1}{\rightleftharpoons}} LH^+_{org} \quad \text{(Fast)} \quad (274)$$

$$K_1 = \frac{[LH^+]_{org}}{[L]_{org}[H^+]_{aq}} \quad (275)$$

Thus,

$$[LH^+]_{org} = K_1[L]_{org}[H^+]_{aq} \quad (276)$$

Considering the same stepwise mechanism with DBMA as shown in Figure 84, the possible slow steps may be:

a- The adsorption of a protonated THMA at the interface **(a)**
b- The desorption of $LPd(NO_3)_{2,ads}$ from the interface **(b)**
c- The desorption of $PdL_2(NO_3)_{2,ads}$ from the interface **(c)**

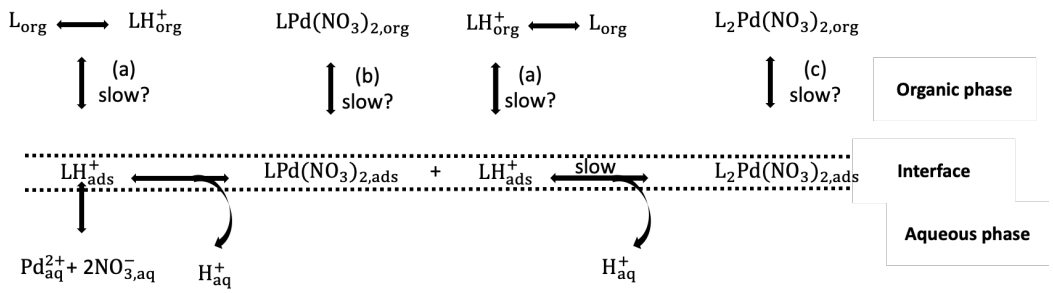

Figure 84: Stepwise mechanism for Pd(II) extraction with THMA.

1. Slow step (a)

Considering that the adsorption of a protonated THMA at the interface is the rate-limiting step, the rate of the reaction would be expressed as follows:

$$v = -\frac{d[Pd^{2+}]_{aq}}{dt} = \frac{A}{V}\frac{d[LH^{+}]_{ads}}{dt} = \frac{A}{V}k_f[LH^{+}]_{ads} \quad (277)$$

- **Ideal adsorption**

Considering an ideal adsorption, Eq. (277) becomes,

$$v = -\frac{d[Pd^{2+}]_{aq}}{dt} = \frac{A}{V}\frac{d[LH^{+}]_{ads}}{dt} = \frac{A}{V}k_f\Gamma^{\infty}K_{ads}K_1[L]_{org}[H^{+}]_{aq} \quad (278)$$

This step cannot be the rate-limiting one, since the rate is first-order dependent on the concentration of THMA and first-order dependent on the concentration of proton ions, which is not consistent with the experimental results. Even if considering a complete saturation, the obtained rate expression would not explain the experimental results.

2. Slow step (b)

Considering the desorption of $LPd(NO_3)_{2,ads}$ from the interface is the rate-limiting step. Then, the rate of the reaction would be expressed as follows:

$$v = -\frac{A}{V}\frac{d[LPd(NO_3)_2]_{ads}}{dt} = \frac{A}{V}k_f\frac{1}{[H^{+}]_{aq}}\beta_1\beta_2\beta_3k_aK_2K_3[LH^{+}]_{ads}[Pd^{2+}]_{aq}[NO_3^{-}]_{aq}^2 \quad (279)$$

- **Ideal adsorption**

In the case of an ideal adsorption, Eq (279) becomes,

$$v = -\frac{A}{V}\frac{d[LPd(NO_3)_2]_{ads}}{dt} = \frac{A}{V}k_f\beta_1\beta_2\beta_3k_aK_1K_2K_3[L]_{org}[Pd^{2+}]_{aq}[NO_3^{-}]_{aq}^2 \quad (280)$$

The obtained rate cannot explain the experimental results, since a first-order and zero-order dependence were obtained for THMA and protons ions concentrations, respectively.

- **Complete saturation**

In the case of a complete saturation, Eq (279) becomes,

$$v = -\frac{A}{V}\frac{d[LPd(NO_3)_2]_{ads}}{dt} = \frac{A}{V}k_f\frac{1}{[H^+]_{aq}}\Gamma^{\infty}\beta_1\beta_2\beta_3k_aK_2K_3[Pd^{2+}]_{aq}[NO_3^-]_{aq}^2 \quad (281)$$

Although we could obtain an inverse first-order dependence with respect to the concentration of proton ions, the obtained rate could not explain the experimental results, since zero-order dependence was obtained with respect to THMA concentration.

3. Slow step (c)

Since THMA is not highly surface-active, the adsorption of a protonated THMA to desorb the interfacial complex is not very likely. Then, the desorption of $PdL_2(NO_3)_{2,ads}$ from the interface may be considered as the rate-limiting step. Thus, once the interfacial complex is formed, it must desorb by itself from the interface to the organic phase.

In this case, the rate-limiting step can be written as follows:

$$v = -\frac{d[Pd^{2+}]_{aq}}{dt} = -\frac{A}{V}\frac{d[PdL_2(NO_3)_2]_{ads}}{dt} \quad (282)$$

Where,

$$[PdL_2(NO_3)_2]_{ads} = \frac{1}{[H^+]_{aq}^2}\beta_1\beta_2\beta_3K_aK_2K_3K_4[LH^+]_{ads}^2[Pd^{2+}]_{aq}[NO_3^-]_{aq}^2 \quad (283)$$

- **Ideal adsorption**

In the case of an ideal adsorption, Eq (283) becomes,

$$[PdL_2(NO_3)_2]_{ads} = \beta_1\beta_2\beta_3K_aK_1^2K_2K_3K_4[L]_{org}^2[Pd^{2+}]_{aq}[NO_3^-]_{aq}^2 \quad (284)$$

And Eq (282) becomes,

$$v = -\frac{A}{V}\frac{d[PdL_2(NO_3)_2]_{ads}}{dt} = \frac{A}{V}k_f\beta_1\beta_2\beta_3K_aK_1^2K_2K_3K_4[L]_{org}^2[Pd^{2+}]_{aq}[NO_3^-]_{aq}^2 \quad (285)$$

The obtained extraction rate cannot explain the experimental results, since the concentration of H^+ does not influence the rate expression.

- **Complete saturation**

In the case of a complete saturation, Eq (283) becomes,

$$[PdL_2(NO_3)_2]_{ads} = \beta_1\beta_2\beta_3K_aK_2K_3K_4(\Gamma^\infty)^2[Pd^{2+}]_{aq}[NO_3^-]_{aq}^2 \quad (286)$$

And Eq (282) becomes,

$$v = -\frac{A}{V}\frac{d[PdL_2(NO_3)_2]_{ads}}{dt} = \frac{A}{V}\frac{1}{[H^+]_{aq}^2}k_f\beta_1\beta_2\beta_3K_aK_2K_3K_4(\Gamma^\infty)^2[Pd^{2+}]_{aq}[NO_3^-]_{aq}^2 \quad (287)$$

The obtained extraction rate is also inconsistent with the experimental results, since neither the THMA concentration nor the H^+ concentration, appear in the rate expression.

It is worth mentioning that the extraction rate law, including a second-order dependence on the ligand concentration and inverse first order on the proton concentration, is documented in the literature, for the extraction of copper Cu(II) with ortho hydroxyoximes.[86] However, in this case, the extractant is intrinsically protonated, since it is an acidic extractant, and the release of the proton ion occurs upon complexing the metal. However, this is not supposed for THMA. Adopting such a mechanism in our case, let us consider that protonated adducts of THMA participate in the extraction reaction, and these species are not in equilibrium with the free THMA in the organic.

In fact, THMA is protonated according to the following equilibrium:

$$THMA_{org} + HNO_{3,aq} \underset{k_{-1}}{\overset{k_1}{\rightleftharpoons}} THMA\ HNO_{3,org} \quad (288)$$

Assuming that protonated species of THMA are not in equilibrium with the free THMA, let us suggest that the acid extraction is very slow. However, this cannot be true since acid extraction is known to be very fast. In parallel, the rate of HNO_3 exchange between two THMA ligands could be slow,

making it possible that the rate of exchange of HNO_3 between two THMA ligands is slow, which makes the protonated THMA, not in equilibrium with its analogues.

$$THMA_1HNO_{3,org} + THMA_2 \underset{k_{-2}}{\overset{k_2}{\rightleftharpoons}} THMA_1 + THMA_2HNO_3 \quad (289)$$

However, no detailed information on the rate of HNO_3 exchange is available so far.

In conclusion, considering the same stepwise mechanism of Pd(II) with THMA, as with DBMA, we could not explain the experimental results. However, the possibility of having a different mechanism for the extraction of Pd(II) with THMA cannot be eliminated. To explain the results, we considered that the extraction mechanism takes place at the interface. Nevertheless, it is quite possible that the extraction reaction of Pd(II) occurs in one of the bulk phases, *i.e.* the aqueous bulk phase or the organic bulk phase.

C. Comparison of the extraction rate of Pd(II) in batch experiments and single drop technique

When proposing the extraction mechanism of Pd(II) with THMA, we assumed that the rate-limiting step might be located in one of the bulk phases. The dependence of the extraction rate on the specific area, which is the ratio of the interfacial area over the volume of the bulk phase is often used to identify interfacial reactions.[31] If the chemical reactions occur in the bulk phases, the extraction rate would be independent of the specific interfacial area. In contrast, if the chemical reactions occur at the interfacial zone, the extraction rate would be directly proportional to the specific interfacial area.

The validation of the batch methodology for the determination of the extraction rate laws, allowed us to compare the results obtained in batch experiments and with the single drop technique. The extraction rates of Pd(II) extraction at different H^+ concentrations, obtained with both setups, were then compared to each other.

Bearing in mind that the specific surface area in batch experiments was not determined. However, we strongly suggest that its value is different from that when using the single drop technique.

The extraction rates of Pd(II) with THMA and DBMA can be expressed in both setups, as follows:

$$R_f, R_f' = \frac{V_{org}}{A}\frac{d[Pd]_{org}}{dt} \quad (290)$$

Where, A is the interfacial area, V_{org} is the volume of the organic phase. And, R_f corresponding to the single drop results and R_f' for the batch experiments.

In the following, the extraction rates, expressed as the variation of the concentration of Pd(II) as a function of time, in both set-ups, with THMA and DBMA, are compared. The obtained slopes are shown in Table 41 and Table 42. For the comparison of the extraction rates in both set-ups, with both ligands, we define the ratio of the extraction rates as:

$$\text{ratio} = \left(\frac{d[Pd]_{org}}{dt}\right)_{\text{single drop}} / \left(\frac{d[Pd]_{org}}{dt}\right)_{\text{batch}} \quad (291)$$

Table 41: Extraction rates of Pd(II) extraction with THMA using single drop technique and in batch experiments. Initial $[Pd]_{aq}$ 300 mg.L^{-1} (batch experiment), Initial $[Pd]_{aq}$ 200 mg.L^{-1} (for single drop technique), $[NO_3^-]_{aq}$ 5M, $[THMA]_{org}$ 0.2M in toluene.

	$[H^+]$ 1.5M	**$[H^+]$ 3M**	**$[H^+]$ 5M**
$\left(\frac{d[Pd]_{org}}{dt}\right)_{\text{THMA,single drop}}$	1.49 * 10^{-5}	0.94 * 10^{-5}	0.47 * 10^{-5}
$\left(\frac{d[Pd]_{org}}{dt}\right)_{\text{THMA,batch}}$	1.50 * 10^{-5}	1.05 * 10^{-5}	0.46 * 10^{-5}
ratio	0.99	0.9	1.02

Table 42: Extraction rates of Pd(II) extraction with DBMA using single drop technique and in batch experiments. Initial $[Pd]_{aq}$ 300 mg.L^{-1} (batch experiment), Initial $[Pd]_{aq}$ 200 mg.L^{-1} (for single drop technique), $[NO_3^-]_{aq}$ 5M, $[DBMA]_{org}$ 0.2M in toluene.

	$[H^+]$ 1.5M	**$[H^+]$ 3M**	**$[H^+]$ 5M**
$\left(\frac{d[Pd]_{org}}{dt}\right)_{\text{DBMA,single drop}}$	3.50 * 10^{-5}	7.25 * 10^{-5}	10.52 * 10^{-5}
$\left(\frac{d[Pd]_{org}}{dt}\right)_{\text{DBMA,batch}}$	0.44 * 10^{-5}	1.01 * 10^{-5}	1.45 * 10^{-5}
ratio	7.95	7.17	7.25

First, we conclude that the ratio of the rate constants of the single drop technique and that in batch experiments is constant for each ligand. Interestingly, the rate constants obtained in batch experiments and using the single drop technique are approximately equal in the case of THMA. In contrast, for DBMA, the rate constants obtained using the single drop technique are around 7 times higher.

Although the specific surface area was not determined in the case of batch experiments, we strongly assume that its value is quite different for the two experimental setups. In this regard, these

results suggest that the extraction of Pd(II) with THMA is likely to be independent of the specific surface area, whereas this is not the case for DBMA. In other words, these findings let us suggest that the extraction reaction of Pd(II) with DBMA is more likely to be interfacial. In contrast, for THMA, the possibility of complexation in the bulk phases is not precluded. This reinforces our hypothesis that the rate-limiting step of THMA may not be interfacial, which is what we put forth when proposing an extraction mechanism.

We emphasize that these results were interesting to show, but we do not adopt any decisive conclusion regarding the reaction zone based on them. When using the single drop technique, changing the interfacial area can be envisioned by changing the drop diameter. However, for our study, we did not investigate the effect of the size of the drops on the extraction rate of Pd(II) with both ligands.

VII. Conclusion

In this chapter, an experimental approach based on the initial rate method was implemented for studying the extraction kinetics in small safe lock tubes. This experimental methodology proves to be extremely useful for rapid and reliable screening of several parameters on the extraction kinetics without the need to use sophisticated tools, making 'time-saving' one of its main advantages. In addition, the reduction of reagent consumption, and thus waste volumes, can be regarded as crucial points.

The screening of the extraction kinetics in batch experiments of Pd(II) with THMA and DBMA showed that the extraction rate laws of Pd(II) are of first-order dependence on the concentration of Pd(II), second-order dependence on the concentrations of nitrate ions, THMA and DBMA. In parallel, the extraction rates were found to be first-order and inverse first-order dependent on the concentration of H^+, with DBMA and THMA, respectively.

In this respect, the validation of the experimental results obtained in batch experiments was successfully performed using the single drop technique considering the partial order of the concentration of proton ions as a reference. Indeed, a first-order and inverse first-order dependence were also acquired.

In addition, in this Chapter, we discussed some of the limitations of this methodology, which lies mainly in its unsuitability for fast extraction systems. For instance, the extraction kinetics of Nd(III) could not be studied due to its fast extraction kinetics. Therefore, from a technical point of view, reducing the extraction time is impossible, as significant error on the latter would be encountered. Moreover, the lack of adequacy of the experimental conditions could also be limiting. Therefore, it is necessary to define the experimental conditions in such a way that the extraction percentage is not very high, as this

would induce large errors in the accuracy of the results. We mention that for all the results presented in this study correspond to a conversion rate which was at most 20%.

The study of the extraction kinetics of Fe(III) proved to be complicated due to the possible participation of the hydrolyzed species of Fe(III) in the extraction reaction, which may pose some ambiguities regarding the reactions taking place. Based on the findings obtained in batch experiments and using the single drop technique, we noticed a change of the partial order of the concentration of nitrate ions in the rate equation depending on the experimental conditions imposed. Two cases were discussed, the extraction kinetics of Fe(III) under favourable conditions for extraction and the extraction kinetics under non-favourable conditions for extraction. In this regard, we suggested that the extraction kinetics of Fe(III) is not driven by the aquocation species $Fe(H_2O)_6^{3+}$, unless the experimental conditions are favourable for the extraction of the latter. Otherwise, the extraction of hydrolyzed species will govern the observed extraction kinetics of Fe(III). Although speciation of Fe(III) in the aqueous phase was not studied to confirm this hypothesis, we were able to elaborate these ideas from the change in the partial order of nitrate ions in the extraction rate of Fe(III) as a function of the experimental conditions imposed, using batch experiments and with the single drop technique.

The investigation of the extraction kinetics of Pd(II) with THMA and DBMA was further developed, and the extraction mechanism was proposed in the case of DBMA. An interfacial mechanism was proposed for the extraction of Pd(II) with DBMA, and the rate-limiting step was considered as the adsorption of a second ligand at the interface. The proposed mechanism could explain the experimental results.

In parallel, with THMA, we first tried to consider that it follows the same stepwise mechanism as with DBMA, with a different limiting step. First, we proposed that the rate-limiting step is the adsorption of protonated species of THMA at the interface. However, considering this, the extraction rate cannot explain the experimental results. Then, we proposed that the formed interfacial complex has to desorb by itself from the interface and that this step constitutes the rate-limiting step. However, considering this, we could neither explain the experimental results, since the inverse first-order dependence with respect to the concentration of proton does not appear in the extraction rate. Finally, it is worth mentioning that when proposing the extraction mechanism with THMA, we limited our investigation for the case of an interfacial reaction. Nevertheless, THMA may follow a completely different stepwise mechanism than DBMA, and the limiting steps could be located in the bulk phases. Altogether, we could not identify a plausible mechanism so far for the extraction of Pd(II) with THMA.

Chapter 5: THMA a promising candidate for the extraction of PGMs

The challenges imposed by increasing demand and scarcity of primary resources have led to great interest in urban mining.[226–228] Urban mining involves recovering critical metals from the waste of electronic and electrical equipment (WEEE) through a sustainable recycling process. The latter could improve the production of critical metals while addressing environmental concerns related to hazardous waste and exhaust emissions. The reuse and recirculation of products and materials are the basis of the circular economy concept. The circular economy originates from eco-industrial development theory and thought.[229] It is based on the 'win-win' philosophy that a healthy and environmental health can co-exist[230], and on eliminating the linear model of production based on a *take, make and dispose* approach.[231] In Europe, this has emerged after the financial crisis in 2010, when Europe presented its decade-long 'Europe 2020' strategy to improve and boost EU competitiveness and employment.[232]

Platinum group metals (PGMs) include the lighter metals ruthenium, rhodium and palladium, as well as osmium, iridium and platinum, which are known as the heavy platinoids. With gold and silver, PGMs are classified as precious metals thanks to their high corrosion and oxidation resistance.[233,234] Indeed, they play a pivotal role in modern society, being of particular importance for clean technologies and other high-tech equipment, *i.e.* chemical process catalysts, catalytic converters for vehicle emission control, fuel cells, and electronic components

However, the supply of PGMs solely from primary sources could come under pressure due to the increasing demand and, at the same time, the laborious, energy-intensive and costly processes for the treatment of PGMs ores. It is important to mention that the Covid crisis in 2020 has further revealed the weaknesses in the supply chain in most developed countries. The pandemic disrupted mining in South Africa and caused prolonged outages at Anglo American Platinum's converter plant (ACP). For instance, platinum and rhodium production fell by 18%, and that of palladium fell by 13%.[235]

Hence, secondary raw materials play a major role in the security of supply. WEEE represents one of the largest sources of waste globally with the highest growth per year.[236] The consumer items that are mass produced, such as computer motherboards, contain 200-250 grams per ton ($g.t^{-1}$) of gold and about 80 $g.t^{-1}$ of palladium, mobile phone handsets hold up to 350 $g.t^{-1}$ of gold and 130 $g.t^{-1}$ of palladium and automotive catalytic converters may contain up to 2000 $g.t^{-1}$ PGMs in the ceramic catalyst brick. This very high inherent value of metals makes recycling attractive from an economic and environmental standpoint, as the metal content of the waste is higher than that of gold or PGMs ores (< 10 grams per ton on average).[237]

Therefore, the recovery of PGMs from secondary resources has been the subject of several studies.[238–241] High selectivity is required to recycle PGMs from secondary sources. Indeed, various complementary solutions have been proposed, based on either pyrometallurgical or hydrometallurgical processes.[242,243] Hydrometallurgical refining is less costly than pyrometallurgical one. Nevertheless, final isolation and purification of PGMs generally rely on a solvent extraction stage, whatever the technology employed.[244] In fact, the synthesis of new robust extractants faces several critical challenges such as the use of expensive reagents, multiple synthesis steps, sophisticated purification methods, sustainability and difficulties in back extraction and reuse. Consequently, several organic molecules have been developed after molecular design and synthesis route selection.[105] Amide compounds play a central role, as the amide moiety is very stable in the highly acidic and oxidizing media employed.[245] Among these compounds, malonamides proved to lead to very stable Pd(II) complexes, and efficient extraction from nitrate media.[142,143,174]

As shown in Chapter 2, § VI, THMA presents high selective extraction for Pd(II) compared to DBMA. However, as explained in Chapter 3, § III - B -3, the extraction kinetics of Pd(II) with THMA is very slow. A detailed kinetic study conducted in small batch experiments revealed that the slow extraction kinetics of Pd(II) with THMA can be addressed by using an excess of dihexylamine (DHA) in the synthesis reaction. Furthermore, this study enabled an extraction solvent formulation, based on optimized addition of DHA. Therefore, in this Chapter, we present the effect of DHA addition on the extraction kinetics performance of THMA. Finally, the extraction performance of THMA was extended to chloride media for the extraction of Pd(II) and Pt(IV).

We mention that the results presented in this Chapter have been published in Separation and Purification Technology 276 (2021) 119293.

I. Variation of the extraction performance of Pd(II)

According to previously published studies on Pd(II) extraction with DMDOHEMA and DBMA, the extraction equilibrium is reached in less than 1 h.[142,143] Therefore, for our early experiments, we initially considered that 1 h is more than sufficient to reach the extraction equilibrium of Pd(II) with THMA, regardless of its concentration in the organic phase. However, we noticed a fluctuation in the performance of Pd(II) extraction with THMA. Moreover, we were surprised to notice a sudden drop in performance when lowering THMA concentration to 0.2M or below. This fluctuation could not be related to the operating mode since the same was adopted for all the investigations. We then suspected the extractant synthetic pathway, especially as low Pd(II) distribution ratios were sometimes obtained, depending on the batches used.

A fine observation of the NMR spectra of the employed batches confirmed the presence of some residuals of: Dihexylamine (DHA), diethyl malonate (DEM), the in-situ produced ethanol (EtOH) as well as the diethyl ether (Et_2O) residues from the washing steps since the dilution in diethyl ether is performed first for the purification process.

The extraction experiments were carried out using batches of THMA synthesized using a reflux setup (refer to Chapter 2, § I - B). Thus, when first performing the extraction experiments, we underestimated the effect of the residuals of impurities on the extraction performance of Pd(II).

In the course of the study, the kinetic limitations of the extraction of Pd(II) with THMA were revealed, and it was well understood that equilibrium is too far from being reached for one hour of extraction. In the figure below, we present the extraction progress of Pd(II) with pure THMA in toluene.

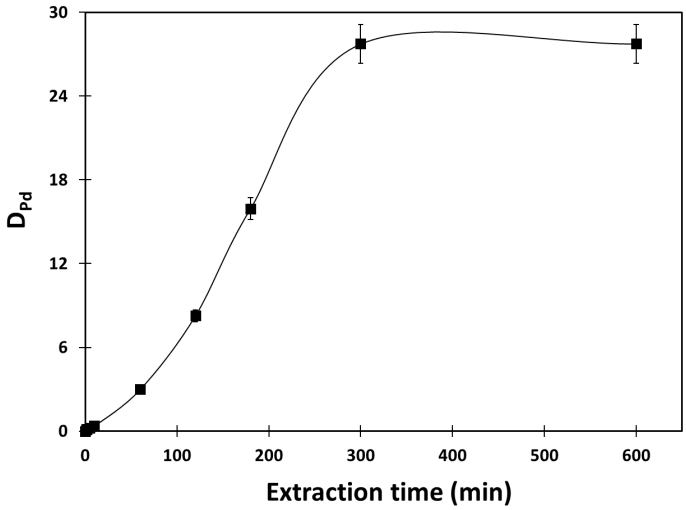

Figure 85: Extraction of Pd(II) with pure THMA as a function of time. Initial $[Pd]_{aq}$ 500 $mg.L^{-1}$, $[THMA]_{org}$ 0.2M in toluene, $[HNO_3]_{aq}$ 3M, A/O = 1, T = 21°C.

Therefore, we first did a screening on the effect of the several impurities on Pd(II) extraction with THMA, *i.e.* DHA, DEM, EtOH, Et_2O. To do so, we proceeded first to prepare a well-purified batch of THMA using a reflux distillation setup (refer to Chapter 2, § I - B - 2). The purity of this batch was verified through NMR analysis. Working with this batch confirmed the excellent performance regarding the extraction of Pd(II). (Refer to Chapter 2, § VI).

The effect of the impurities on the extraction of Pd(II) was carried out by fixing the concentration of THMA at 0.2M, and amounts of 20 mol% were added for each impurity.

The operating conditions were chosen in this chapter to reveal the kinetic differences when studying the effect of impurities on the extraction kinetics of Pd(II). In order to investigate the kinetic effects, the extraction conditions were modified to disfavour mass transfer by decreasing the interfacial area between aqueous and organic phases. Thus, we set the stirring speed at 1200 rpm, where

emulsification of both phases was ensured, and we assumed that the concentration in metal was homogeneous in each phase. Nevertheless, when stirring at 1200 rpm, the mass transfer is still limited by the reduced interfacial area, and therefore, equilibrium was reached after a longer shaking time.

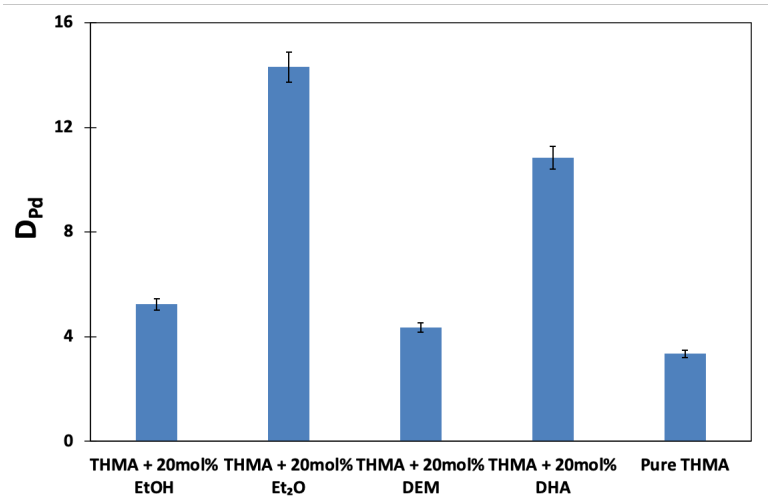

Figure 86: Effect of impurities on the extraction of Pd(II) with 0.2M THMA in toluene. Initial $[Pd]_{aq}$ 500 $mg.L^{-1}$, $[HNO_3]_{aq}$ 3M, 1 h extraction, 1200 rpm, A/O 1, T =21 °C.

First, we conclude that the degree of purity of THMA directly impacts its performance in Pd(II) extraction. Among these impurities, DHA and Et_2O increased the extraction of Pd(II) the most, where for Et_2O D_{Pd} was almost 15, and it reached 12 for DHA.

We mention that the preliminary results obtained with Et_2O could not be reproduced, and the beneficial effect vanished when repeating the same extraction procedure. This can be related to the substantial volatility of this organic solvent. Therefore, we only focused our study on DHA.

These preliminary results were considered an asset for improving the extraction kinetics performance of THMA. Therefore, a detailed kinetic study performed to highlight the beneficial effect of DHA on the extraction of Pd(II) with THMA, is detailed hereafter.

II. Extraction of Pd(II) with DHA

High molecular weight amines and quaternary ammonium salts have been used among nitrogen-containing extractants for the extraction of PGMs from chloride media.[119,246–251] In addition to their extraction properties, their role as a phase transfer catalyst in the extraction of Pd(II) from aqueous hydrochloric acid solutions has been documented.[107] However, the extraction of Pd(II) with amine-based functions from nitrate media has been rarely reported in the literature.[252–254]

In order to get insights into the extraction of Pd(II) from nitrate media with DHA, we studied the extraction of Pd(II) with DHA in toluene at different nitric concentrations, for 1 hour and 24 hours of extraction (Figure 87).

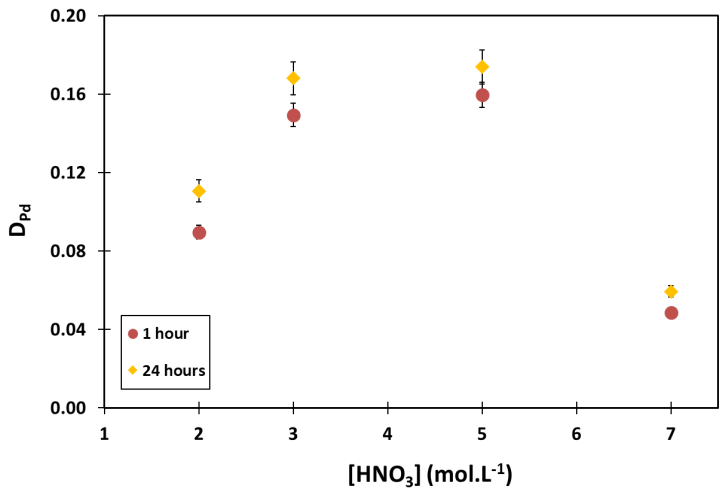

Figure 87: Palladium distribution ratio in extraction with DHA at different nitric acid concentrations, for 1 hour and 24 hours. Initial $[Pd]_{aq}$ 500 mg.L^{-1}, $[DHA]_{org}$ 0.2M in toluene, A/O 1, T=21°C.

First, the extraction of Pd(II) with DHA is low. At 3M HNO_3, the distribution ratio of Pd(II) was only 0.1 for 24 hours of extraction, which confirms that secondary amines are not efficient for the extraction of Pd(II) from nitrate media. An increase of the distribution ratio of Pd(II) was noticed when increasing the concentration of nitric acid up to 5M, then a decrease of D_{Pd} was observed. This behaviour is approximately the same at 1 h and 24 h. We add that Pd(II) extraction performance slightly increased with the extraction duration.

III. Impact of added DHA on the extraction of Pd(II) with THMA

A. Extraction of Pd(II) with mixed DHA/THMA at equilibrium

The impact of the controlled addition of DHA to pure THMA on the extraction of Pd(II) was investigated. To do so, we proceeded first to prepare a well-purified batch of THMA. The purity of the ligand was verified by NMR and it was over 99% (refer to Chapter 6 § II - A).

The concentration of THMA was set at 0.2M, and DHA was added in quantity varying from 0 to 50 mol% respective to THMA. This investigation was first carried at equilibrium (24 hours of extraction) for 3M and 5M HNO_3.

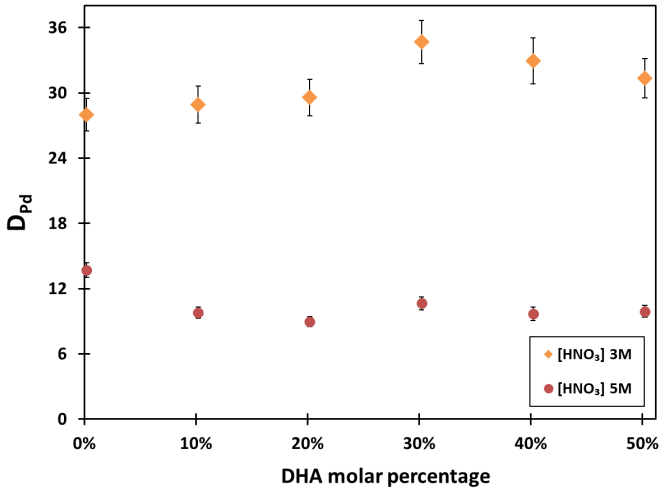

Figure 88: Palladium distribution ratio with mixed THMA/DHA systems in toluene for 24 h of extraction. THMA concentration 0.2M, DHA molar percentage 0 to 50 mol%, initial $[Pd]_{aq}$ 500 mg/L, $[HNO_3]_{aq}$ 3M and 5M, A/O = 1, T=21°C.

For both acidities, the distribution ratios obtained of Pd(II) upon extraction with THMA/DHA systems were almost the same as those obtained with pure THMA. This revealed that the thermodynamic outcomes of Pd(II) extraction with DHA/THMA mixed systems were the same.

In this regard, we characterized the kinetic effect of adding DHA on the extraction of Pd(II) with THMA.

B. Pd(II) extraction with mixed THMA/DHA for 1 hour

The first experiment was conducted by fixing the concentration of HNO_3 at 3M in the aqueous phase (Figure 89).

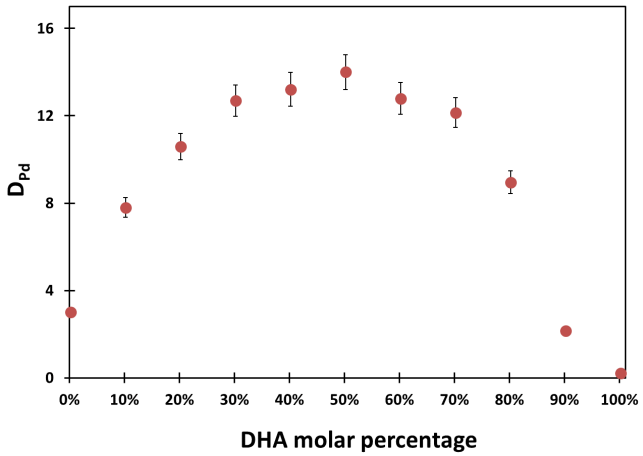

Figure 89: Pd(II) distribution ratio with 0.2M THMA in toluene with added DHA after 1 h of extraction. DHA molar percentage 0 to 100 mol% respective to THMA, initial $[Pd]_{aq}$ 500 mg/L, $[HNO_3]_{aq}$ 3M, A/O=1, stirring speed 1200 rpm.

First, we noticed by setting the stirring speed at 1200 rpm, D_{Pd} dropped to 3, (75% extraction percentage), using pure THMA 0.2M in toluene, after 1 hour extraction.

Then, the distribution ratio of Pd(II) increased with increasing molar percentage of DHA in the organic phase. The maximum extraction was attained (D_{Pd} = 14) at 50 mol% DHA. Above 50 mol% of added DHA, there is no longer any benefit from the addition of DHA. In addition, further increase of added DHA led to a decrease in the extraction efficiency of Pd(II). For instance, at 90 mol% DHA, D_{Pd} dropped to 2 (69% extraction yield).

Finally, when the added quantity of DHA exceeded 80 mol%, we could visually observe an increase in the viscosity of the organic phase. This could explain the lower extraction yield of Pd(II), as the increase of viscosity leads to a reduced diffusion of molecules and ions. The ability of high molecular weight amines to extract nitric acid is reported in the literature.[255,256] The increase in viscosity likely stems from the aggregation of DHA-nitrate species formed upon the extraction of nitric acid by DHA. However, we did not further characterize the extraction systems to confirm this increase in viscosity through viscosity measurements, nor did we perform SAXS measurements to ensure the formation of aggregation.

The second set of experiments characterized the effect of adding DHA on the extraction of Pd(II) from 5M HNO_3 with THMA for 1 hour. For this study, we limited our investigation to a range of 0-50 mol% of added DHA (Figure 90).

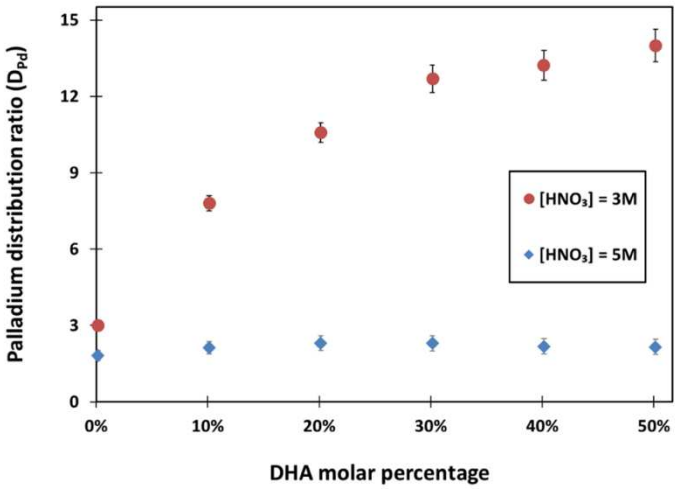

Figure 90: Palladium distribution ratio with mixed THMA/DHA systems in toluene for 1 h. THMA concentration 0.2M, DHA molar percentage 0 to 50 mol%, initial $[Pd]_{aq}$ 500 $mg.L^{-1}$, stirring speed 1200 rpm.

In contrast to the results obtained at 3M HNO_3, the beneficial effect of DHA on the extraction of Pd(II) with THMA for 1 hour disappeared at 5M HNO_3. Indeed, the distribution ratio of Pd(II) remained

invariant despite the increase in the molar ratio of DHA respective to THMA. This behaviour can be related to:

- At 5M HNO_3, instead of extracting acid in the organic phase, the protonation of DHA favours the formation of DHA salt, which transfers to the aqueous phase
- Full protonation of DHA in the organic phase and the extraction is then promoted by THMA only

Two new sets of experiments were carried out to check these assumptions, and are presented below.

IV. Total Organic Carbon concentration (TOC) analysis

We first suggested when using a higher concentration of aqueous HNO_3, DHA was protonated and formed a salt instead of extracting nitric acid in the organic phase, which passed into the aqueous phase. In this regard, analyses of the total organic carbon concentration of 3M and 5M HNO_3 aqueous phases after contact with 0.1M DHA were performed.

An organic solution of 0.1M DHA in toluene was brought into contact with aqueous phases of 3M and 5M HNO_3 for 1 hour. The total organic carbon concentrations in the aqueous phases, after prequilibration, were then analyzed. The total organic carbon concentrations originating from the transfer of toluene to 3M and 5M HNO_3 were also analyzed by bringing into contact an organic solution of toluene with aqueous phases of 3M and 5M HNO_3. Thus, the concentration of DHA in the aqueous phase was deduced from the difference of the carbon concentration measured in the aqueous phase upon its contact with 0.1M DHA and the carbon concentration from the toluene transfer (Table 43).

The final concentration of DHA in the organic phase was calculated as follows:

$$[\mathrm{DHA}]_{\mathrm{org,final}} = [\mathrm{DHA}]_{\mathrm{org,initial}} - [\mathrm{DHA}]_{\mathrm{aq}} \quad (292)$$

Table 43: Concentration of DHA in the organic phase upon 1 h contact with 3M and 5M HNO_3. Initial $[DHA]_{org}$ 0.1M in toluene. T = 21°C

	$[HNO_3]$ = 3M	**$[HNO_3]$ = 5M**
$[DHA]_{org}$	0.074 M	0.066M

First, we notice that the final concentration of DHA after bringing into contact with 3M and 5M HNO_3 decreased, revealing that a slight transfer of DHA in the aqueous phase took place. However, the

final concentration of DHA in the organic phase upon contact with 5M HNO_3 is slightly lower than that with 3M HNO_3. This low difference could not explain the loss of the beneficial effect of DHA at 5M HNO_3. Therefore our hypothesis was not valid.

V. Acid uptake of DHA

Nitric acid extraction from aqueous phase using long chain of aliphatic amines dissolved in a hydrocarbon solvent was firstly reported by Smith and Page.[255] The authors reported that the acid-binding properties of high-molecular-weight amines depend on the fact that acid salts of these bases are insoluble in water but swiftly soluble in organic solvents, such as benzene, chloroform and kerosene.

The neutralization reaction between amine and nitric acid can be represented as:

$$(R_2HN)_{org} + (HNO_3)_{aq} \rightleftharpoons (R_2HNHNO_3)_{org} \quad (293)$$

Where R_2HN stands for the amine base and R_2HNHNO_3 stands for the amine nitrate, and the subscripts (aq) and (org) indicate the aqueous and organic phases, respectively.

For higher aqueous nitric acid concentration, still more nitric acid may be extracted, and the amine nitrate complex forms a molecular addition compound with associated nitric acid and the amine nitrate-nitric acid species.

This implies the following equilibrium:

$$(R_2HNHNO_3)_{org} + (HNO_3)_{aq} \rightleftharpoons (R_2HNHNO_3.HNO_3)_{org} \quad (294)$$

The acid uptake of DHA was analyzed at different nitric acid concentrations in the aqueous phase. In Figure 91, the ratio of the concentration of HNO_3 in the organic phase, over the initial concentration of DHA in the organic phase, is plotted against the initial concentration of nitric acid in the aqueous phase.

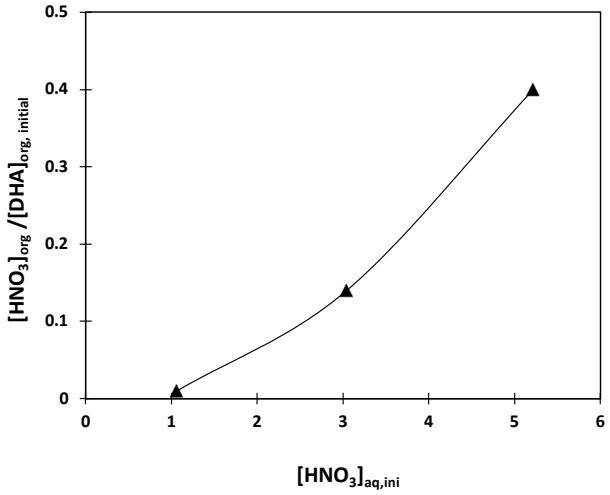

Figure 91: Plot of $[HNO_3]_{org}/[DHA]_{org}$ at different acidities in the aqueous phase. $[DHA]_{org}$ 0.2M in toluene, 1 hour of extraction, A/O = 5, T = 21°C.

The concentration of nitric acid extracted in the organic phase increases with the acidity in the aqueous phase, which confirms that the protonation of DHA is promoted at higher concentrations of nitric acid.

Therefore, this lack of kinetic effect when using a higher concentration of aqueous HNO_3 may be due to the competition between nitric acid extraction and Pd(II) complexation, which suppresses the DHA-promoted extraction, and the extraction is then mainly promoted by THMA.

VI. Interfacial tension measurements

In general, when using amines and ammonium salts as phase transfer catalysts, the authors explained the enhancement of the extraction kinetics through an interfacial mechanism, promoted by the adsorption of the protonated amine at the interface.[107] Indeed, the latter caused a decrease in the interfacial tension. According to the authors, the adsorbed amine will first complex Pd(II) at the interface, and then transfers to the organic phase, where a ligand substitution occurs with the extracting ligand. Thus, the catalytic effect is of chemical origins.

In this regard, we measured the interfacial tension of THMA at the 3M HNO_3/toluene interface upon adding DHA in the organic phase.

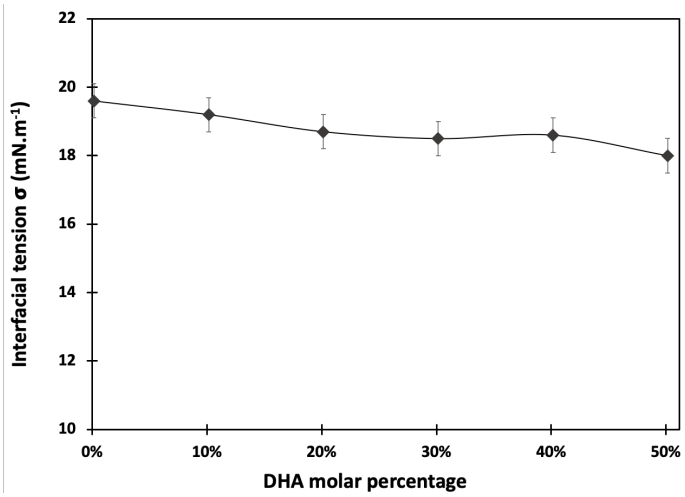

Figure 92: Variation of the interfacial tension upon addition of DHA in the organic phase. 0.2M THMA in toluene, DHA molar percentage 0 mol% to 50 mol% respective to THMA, $[HNO_3]_{aq}$ 3M, T = 23°C.

The interfacial tension was almost invariant upon increasing the DHA molar percentage with respect to THMA. Therefore, we can assume that the increase in the extraction kinetics of Pd(II) with THMA upon the addition of DHA is not related to a change in the interfacial properties of the system. However, this cannot be taken as proof of the absence of intermediate species between Pd(II) and DHA, that may exist at the interface.

In this regard, a detailed kinetic study was necessary in order to evidence more clearly the kinetic effect of DHA on the extraction of Pd(II) with THMA.

VII. Palladium extraction kinetics with mixed THMA/DHA systems

In Chapter 4, we have demonstrated the reliability of screening the extraction kinetics in small batch experiments. In the present chapter, we further expanded the application of this methodology, using the developed experimental setup, for a kinetic study of Pd(II) extraction with mixed DHA/THMA systems.

For this investigation, the concentration of THMA was set at 0.2M, and a controlled amount of DHA was added (10-50 mol%). The reported extraction time corresponds to the shaking time, which ranges 1 from 6 min. The average absolute error in extraction time for each point was determined as the delay between the agitation turn off and the time required to reach the maximum centrifugation speed. Assuming that afterwards during centrifugation, mass transport is negligible, the time absolute errors are estimated at 6 s for each point, and are positive.

The interpretation of the experimental data was made using a first-order model. As a result, the rate of palladium extraction can be expressed as follows:

$$-\frac{d[Pd]_{aq}}{dt} = k([Pd]_{aq,t} - [Pd]_{aq,eq}) \quad (295)$$

The integration of Eq. (295) gives Eq. (296):

$$\ln([Pd]_{aq,t} - [Pd]_{aq,eq} = -kt + \ln([Pd]_{aq,0} - [Pd]_{aq,eq}) \quad (296)$$

Where k is the rate constant, t is the time, $[Pd]_{aq,t}$ is the concentration of Pd in the aqueous phase at time t, $[Pd]_{aq,eq}$ is the concentration of Pd in the aqueous phase.

Four experiments with a DHA amount increasing from 0 to 50% were carried out, and the plots of $\ln([Pd]_{aq,t} - [Pd]_{aq,eq} = f(t)$ are represented in Figure 93.

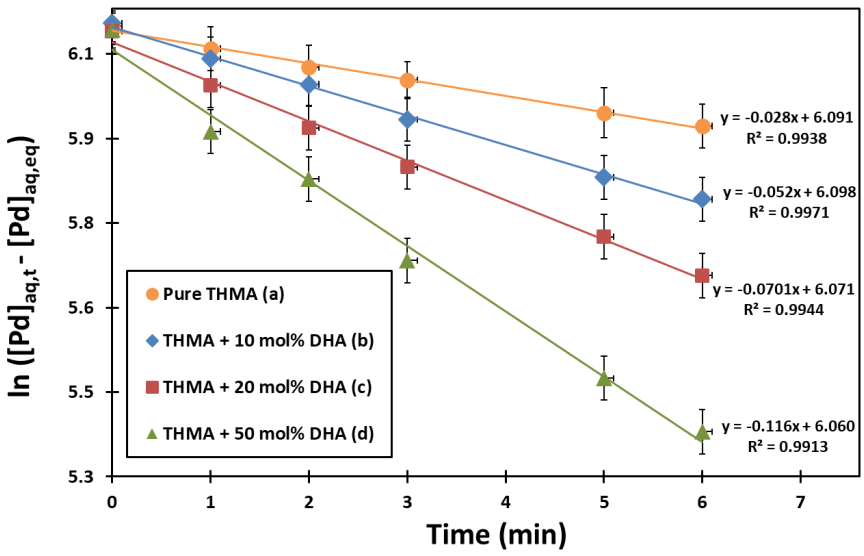

Figure 93: First-order model for the extraction of Pd(II) with pure THMA and mixed THMA/DHA system in toluene. $[THMA]_{org}$ 0.2M, and 10 mol% DHMA, 20 mol% DHA and 50 mol% DHA, initial $[Pd]_{aq}$ 500 mg/L, $[HNO_3]_{aq}$ 3M, stirring speed 1200 rpm.

The data of each experiment are in agreement with the first-order model according to the straight line obtained, with a regression coefficient higher than 0.99.

The extraction kinetics of Pd(II) is enhanced in the presence of DHA, with a regular increase in the observed rate constant. For example, the rate constants increased from 0.028 min^{-1} for the extraction with pure THMA to 0.116 min^{-1} with 50 mol% added DHA, corresponding to an extraction half-time of 25 min and 6 min, respectively. Thus, without DHA, Pd(II) extraction is slow but still takes place.

We mention that the extraction half-times were calculated as follows:

$$\tau\,(min) = \frac{\ln\,(2)}{k} \tag{297}$$

In parallel, we notice that the addition of 10 mol% DHA leads to a doubling of the rate constant, where it increases from 0.028 min^{-1} to 0.052 min^{-1}. Afterwards, further addition of DHA leads to a proportional increase of the observed rate constant (Figure 94).

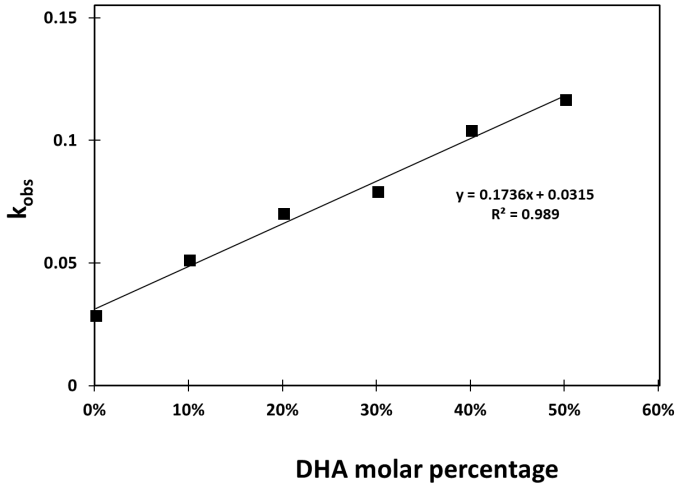

Figure 94: Evolution of observed rate constant k_{obs} of Pd(II) extraction with 0.2M THMA in toluene from aqueous 3M HNO_3 solution with respect to the added DHA quantity. Initial $[Pd]_{aq}$ 500 mg/L, $[HNO_3]_{aq}$ 3M, stirring speed 1200 rpm.

The observed rate constant can then be decomposed into two terms:

$$k_{obs} = k_{THMA} + k_{DHA} \tag{298}$$

Where k_{THMA} and k_{DHA} are the contributions of THMA and DHA in the observed rate constant, respectively.

From Figure 94, we conclude the contribution of k_{DHA} is proportional to the DHA quantity as given by Eq.(299):

$$k_{DHA} = 0.87[DHA] \tag{299}$$

In conclusion, this study emphasized that DHA has a kinetic effect on the extraction of Pd(II) principally, since the thermodynamic outcome of the extraction of Pd(II) was almost the same with the addition of DHA.

In conclusion, analysis of the observed rate constant suggests that the extraction of Pd(II) with THMA/DHA mixture, takes place through two simultaneous mechanisms:

- A direct extraction with THMA
- An indirect extraction mediated by DHA, and of first-order respective to DHA

The results obtained from the present kinetic study are sufficient to substantiate that the slow extraction kinetics are observed only at low THMA concentration and that DHA is implicated in the formation of intermediate molecular species responsible for the extraction of Pd(II).

We mention again that the interfacial tension measurements may be insufficient to prove the non-formation of adsorbed species of Pd-DHA at the interface. In Chapter 4, § VI – B, we assumed that the rate-limiting step of the complexation of Pd(II) with THMA is more likely to take place in the bulk phase, since we could not explain the experimental results of the corresponding extraction law, following an interfacial mechanism. In this regard, we strongly suggest that the enhancement of the extraction rate of Pd(II) with THMA upon adding DHA, probably originates from the formation of intermediate molecular species in the aqueous phase, responsible for the extraction of Pd(II). In this regard, we suggest the following mechanism for the extraction of Pd(II) with THMA in the presence of DHA:

1- DHA is protonated in the organic phase

$$\mathrm{DHA_{org}} + \mathrm{H^+_{aq}} \underset{k_{-1}}{\overset{k_1}{\rightleftharpoons}} \mathrm{DHA.H^+_{org}} \tag{300}$$

2- The protonated DHA can penetrate more easily than THMA the interface to reach the aqueous phase

$$\mathrm{DHA.H^+_{org}} \underset{k_{-2}}{\overset{k_2}{\rightleftharpoons}} \mathrm{DHA.H^+_{aq}} \tag{301}$$

3- DHA binds to Pd(II) in the aqueous phase

$$\mathrm{DHA.H^+_{aq}} + \mathrm{Pd(NO_3)^-_{3,aq}} \underset{k_{-3}}{\overset{k_3}{\rightleftharpoons}} \mathrm{DHA.Pd(NO_3)_{2,aq}} + \mathrm{HNO_{3,aq}} \tag{302}$$

4- The formed complex transfers rapidly to the organic phase

$$\mathrm{DHA.\,Pd(NO_3)_{2,aq}} \underset{k_{-4}}{\overset{k_4}{\rightleftharpoons}} \mathrm{DHA.\,Pd(NO_3)_{2,org}} \tag{303}$$

5- A fast transfer between DHA and THMA occurs in the organic phase, and DHA is released again in the organic phase

$$\mathrm{DHA.\,Pd(NO_3)_{2,org}} + 2\mathrm{THMA_{org}} \underset{k_{-5}}{\overset{k_5}{\rightleftharpoons}} \mathrm{(THMA)_2Pd(NO_3)_{2,org}} + \mathrm{DHA_{org}} \tag{304}$$

We, therefore, explained the enhancement of the extraction reaction through a catalytic role of DHA, where the formation of the intermediate species of Pd-DHA, lowers the activation energy of the extraction reaction (Figure 95), which eases the transfer of Pd(II) in the organic phase.

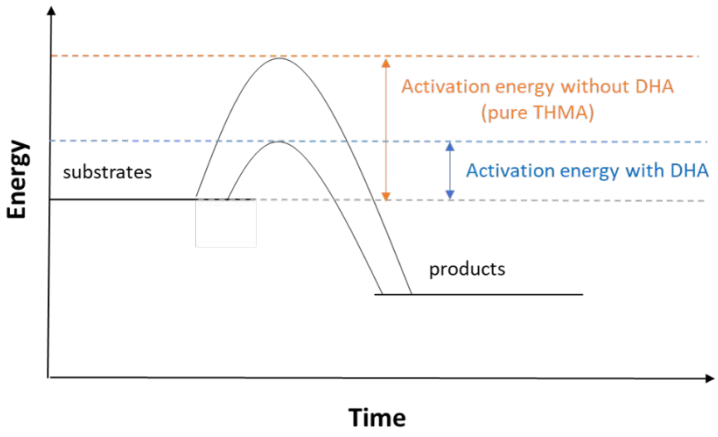

Figure 95: Sketch showing the variation of the activation energy of the extraction of Pd(II) with pure THMA and THMA/DHA mixed system.

However, deep characterization of the organic phase was not carried out, and therefore, we did not confirm whether mixed (DHA-THMA/Pd) complexes were formed.

VIII. Extraction solvent formulation: Optimization of added DHA quantity

In the previous sections, the beneficial effect of DHA on the extraction kinetics was demonstrated using a fixed amount of THMA (0.2M) and increasing the amount of DHA. These results suggest that adding 50 mol% DHA is optimal for improving extraction kinetics. Therefore, one can say that this gain

in performance is also the result of using a larger amount of extractant. We mention that the distribution ratio of Pd(II) with 0.2M DHA at 3M HNO_3 is 0.14 for 1 hour of extraction.

In this regard, we examined the impact of controlled DHA addition to THMA, when the total concentration of extractant ([THMA] + [DHA]) is fixed at 0.2M. Thus, the addition of DHA is associated with a decrease in the THMA concentration. The distribution ratios of Pd(II) were plotted against the molar ratio of DHA (x_{DHA}) in the extraction solvent (Figure 96).

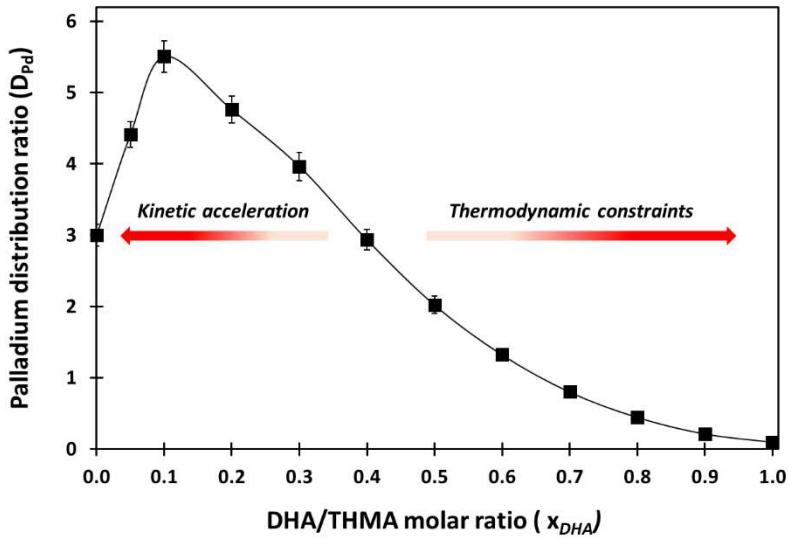

Figure 96: Pd(II) distribution ratio after extraction with THMA/DHA mixtures. [THMA] + [DHA] = 0.2M in toluene. Initial $[Pd]_{aq}$ 500 mg/L, $[HNO_3]_{aq}$ 3M, 1 h extraction, stirring speed 1200 rpm.

Palladium distribution ratios increased rapidly as the molar ratio of DHA in the organic phase increased, and a maximum of D_{Pd} = 5.5 was reached for x_{DHA} = 0.1. Inversely, exceeding this limit, palladium distribution ratios decreased continuously, reaching D_{Pd} = 0.14 for pure DHA. As expected, the extraction of Pd(II) was highly dependent on a sufficient THMA concentration in the organic phase. Provided the THMA content in the solvent is sufficient to allow the extraction of Pd(II), the contributory effect of DHA is apparent. At the maximum point (x_{DHA} = 0.1), the THMA concentration is still close to 0.2 M (0.18 precisely), and the DHA concentration is 0.02 M, very close to 10 mol% respective to THMA. Afterwards, Pd(II) extraction efficiency decreases, as the THMA content in the organic phase decreases. Thus, it can be concluded that the benefit of DHA addition is optimal at 10 mo%. Further addition of DHA increases the kinetics however, the increase is insufficient to counterbalance the loss of efficiency due to the lower amount of THMA.

How these results are presented is similar to the classic studies that synergistic phenomena. In our case, it is clear that mass transfer is limiting, at least on the left of Figure 96, and that thermodynamic

equilibrium is not reached. Therefore, the results should not be taken as evidence of synergy. The non-linear behaviour of the extraction results obtained with THMA/DHA mixtures results from an enhancement of the extraction kinetics of Pd(II), counterbalanced by thermodynamic constraints due to poor Pd(II) extraction with pure DHA. The rise in extraction yield when $x_{DHA} \leq 0.1$ ($x_{THMA} \geq 0.9$), where D_{Pd} with THMA/DHA mixtures are higher than D_{Pd} with THMA, have been proven to result from an enhancement of kinetics by DHA. Then, for the range of $0.1 \leq x_{DHA} \leq 0.4\text{-}0.6$, a decrease in D_{Pd} was observed, but they were still higher than D_{Pd} with THMA at 0.2M concentration. The thermodynamical constraints are still partially overcome by the kinetic acceleration. Finally, when $x_{DHA} > 0.6$, the system is entirely governed by thermodynamic limitations. This approach demonstrates that synergy studies under thermodynamic conditions require proof that there are no kinetic limitations. Kinetics studies are often overlooked, whereas our results demonstrate that they can be the source of an apparent synergy.

Extraction half-time is lowered from 13 min to 10 min upon doubling the DHA amount from 10 mol% to 20 mol% (Table 44). Thus, unless kinetics is the most critical parameter, we think it is not worth adding > 10 mo% DHA.

Table 44: Extraction half-times of Pd(II) with DHA/THMA mixed systems.

DHA molar percentage	Extraction half-time (min)
0%	25
10%	13
20%	10
30%	9
40%	7
50%	6

IX. Extraction of Pd(II) with crude THMA

As DHA proved to have a beneficial effect on the extraction of Pd(II) with THMA from nitric acid media, we investigated the possibility of employing unpurified THMA to prepare the extraction solvent.

As described in Chapter 2, § I - B - 2, the synthesis of THMA starting with an excess of DHA with respect to DEM, (> 2 eq.), results in the presence of residuals of DHA in the final product. In general, acid washing eliminates the residuals of amine. However, for this investigation, THMA was

synthesized following the same synthetic steps, except that no purification steps were performed. Therefore, after cooling the crude mixture, it was analyzed to determine the molar ratio of residual of DHA, then directly diluted in toluene to get the desired concentration of THMA (0.2M), as there is no organic solvent employed for the synthesis.

The determination of the molar ratio of residual DHA was performed through integration of corresponding signal area in ^{1}H NMR spectrum (Figure 97), and the amount of DHA found in the final product was approximately 10 mol%.

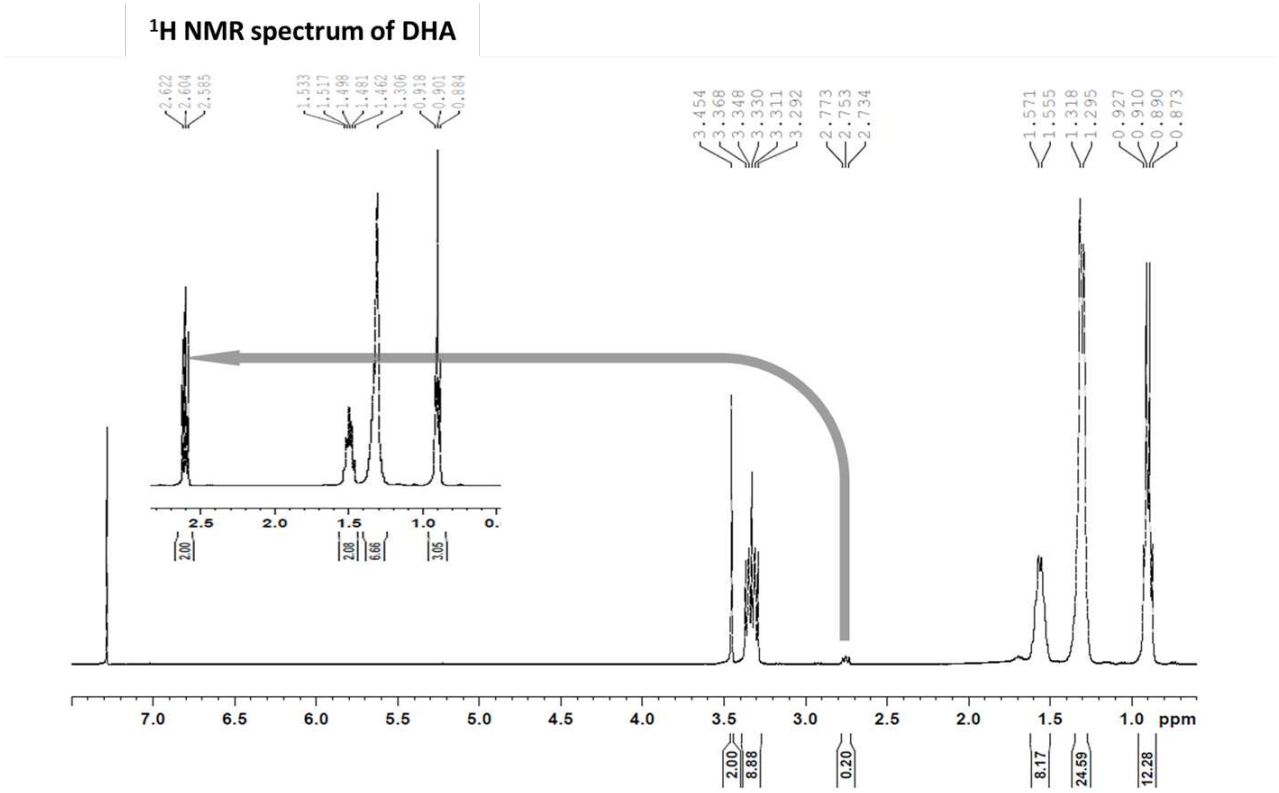

Figure 97: ^{1}H NMR spectra of THMA and DHA (embodied spectrum).

The crude solvent was afterwards employed for the extraction of Pd(II) from 3M HNO_3. For this investigation, the extraction was carried out at 2000 rpm. Comparison of the results obtained during Pd(II) extraction between purified THMA and crude THMA in toluene are presented in Table 45.

Table 45: Extraction of Pd(II) with purified THMA and crude THMA synthesized with an excess of DHA (10 mo%). THMA concentration 0.2M in toluene, initial $[Pd]_{aq}$ 500 mg/L, $[HNO_3]_{aq}$ 3M, stirring speed 2000 rpm, A/O = 1.

	Purified 0.2M THMA	**Crude 0.2M THMA**
Extraction time	24 h	1 h
D_{Pd}	28	34

The extraction of Pd(II) using purified THMA was carried out for 24 h, so the extraction equilibrium was ensured to be reached, and the corresponding D_{Pd} is 28. In parallel, for 1 hour of extraction using 0.2M of crude THMA, the extraction equilibrium was reached, and D_{Pd} reached 34. These results show that the kinetics limitations associated with the extraction of Pd(II) using THMA are successfully overcome by using crude THMA. Moreover, the extraction performance of the crude THMA was slightly better than the purified one (DHA free). Indeed, D_{Pd} increased from 28 when using purified THMA to 34 when using crude THMA.

X. Extraction of Pd(II) and Pt(IV) from chloride media

The extraction of PGMs with malonamide from chloride media is documented in the literature.[178,180,181] Several malonamide based molecules were tested for the extraction of Pd(II) and Pt(IV) (refer to Chapter 1, § VIII - C - 1). The best results for the extraction of Pd(II) from chloride media, without the need of a labilizing agent, were obtained in 1,2-dichloroethane at 8M HCl.[181]

In this regard, we further extended our investigation to assess the efficiency of THMA in the extraction of Pd(II) from chloride media. In addition, we evaluated the extraction of Pt(IV) with THMA. From an industrial application perspective, we chose to work with Solvesso^{TM} 150 as a diluent. These experiments were carried out using crude THMA, following the same procedure described in the previous section Table 46.

Table 46: Pd(II) and Pt(IV) distribution ratio (D_{Pd} and D_{Pt}) and Pt/Pd selectivity ($S_{Pt/Pd}$) with crude THMA in Solvesso^{TM} 150 from hydrochloric acid media. THMA concentration 0.2M, initial $[Pd]_{aq}$ 500 mg/L, initial $[Pt]_{aq}$ 500 mg/L, 1 h extraction, A/O = 1, stirring speed 2000 rpm.

	[HCl] = 1M	**[HCl] = 6M**
D_{Pd}	35.4	1
D_{Pt}	10.3	27.4
$S_{Pt/Pd}$	0.29	27.4

First, the possibility of an efficient extraction of Pd(II) with THMA from chloride media is completely feasible since D_{Pd} was 35.4 at 1M HCl.

Furthermore, the extraction of Pd(II) and Pt(IV) strongly depended on the acidity of the aqueous phase. The distribution ratio of Pd(II) decreased from 35.4 to 1, by increasing the concentration of HCl from 1M to 6M. Whereas the distribution ratio of Pt(IV) increased from 10.3 to 27.4. This dependence can be related to the different chlorocomplexes of Pd(II) and Pt(IV) in aqueous chloride media.[130] Indeed, Pd(II) exists as $[PdCl_4]^{2-}$, while Pt(IV) forms $[PtCl_6]^{2-}$ complexes. Although the acid uptake of

THMA in chloride media was not studied, we suggest that a further protonation of THMA at higher acidity will favour an ion exchange reaction. Therefore, increasing the concentration of HCl in the aqueous phase will favour the extraction of Pt(IV), which can explain the higher distribution ratios of Pt(IV) at 6M HCl.

Altogether, these preliminary results on platinum group metals extraction from chloride media demonstrate the potential interest of THMA for the extraction and purification of these metals. As a comparison, the extraction of PGMs with alkyl sulfides from chloride media requires the addition of a fatty amine to obtain acceptable kinetics. Therefore, it could be worth envisioning the study of the optimum DHA quantity before adapting the technology to PGMs separation from chloride media.

XI. Extraction of Pd(II) with THMA in the presence of a surfactant: Brij S10

In this study, we demonstrated the beneficial effect of added DHA on the extraction of Pd(II) with THMA. In the light of the obtained results, we could evidence that the acceleration of the extraction rate of Pd(II) in the presence of DHA is of chemical origins. Therefore, we were interested in finding another solution to improve the extraction kinetics of THMA.

In the area of liquid-liquid extraction of metal ions, there is growing experimental evidence that reversed micelles, and microemulsions significantly influence both the extraction kinetics and equilibria.[55] Therefore, we were interested in screening the extraction kinetics of Pd(II) with THMA in the presence of a surfactant, Brij S10 (polyethylene glycol octadecyl ether) (Figure 98).

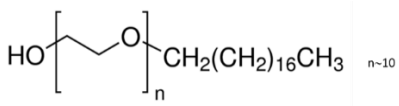

Figure 98: Chemical structure of Brij S10.

For this study, we screened the effect of adding Brij S10 to the distribution ratio of Pd(II) (Figure 99). To do so, aqueous phases of Pd(II) were prepared, and the concentration of Brij S10 was adjusted at 0.05M in the aqueous phase.

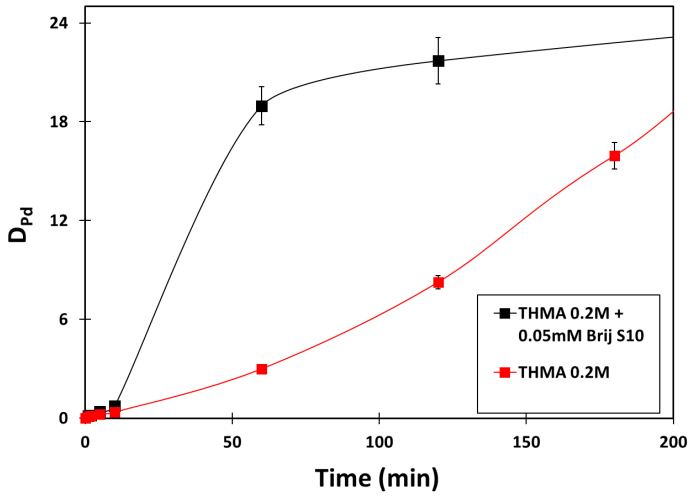

Figure 99: Palladium distribution ratio in extraction with 0.2M THMA and 0.2M THMA + 0.05M Brij S10, initial $[Pd]_{aq}$ 500 mg/L, $[HNO_3]$ 3M, 1 h extraction, stirring speed 1200 rpm, A/O 1, T = 21°C.

The distribution ratio of Pd(II) increased faster when adding Brij S10 to the aqueous phase. Indeed, it reached approximately 19 when adding Brij S10 in the aqueous phase for 1 hour of extraction, while D_{Pd} was almost 3 with 0.2M THMA.

This behaviour is related to the formation of micelles, which are well known to affect the rates of chemical reactions by selectively sequestering the reagents through electrostatic and/or hydrophobic interactions.[257] The first studies in this field described the complexation rate increase when both the ligand and the metal ion are concentrated in the micelles instead of being spread over the whole volume of the solution. Besides, an increase of the specific interfacial area is promoted by the presence of micelles, which can explain the increase of the rate of extraction.[258]

In conclusion, using a surfactant represents another solution for accelerating the extraction kinetics performance of THMA.

XII. Conclusion

In this chapter, we presented THMA as a performing extracting molecule for the extraction of Pd(II) from nitrate and chloride media.

Screening the extraction kinetics in batch experiments enabled evidence of the possibility of accelerating the slow extraction kinetics of THMA by using an excess of DHA, which is a starting reagent for the synthesis of THMA. The beneficial effect of DHA on the extraction performance of THMA depended on the acidity of the aqueous phase. This was related to the protonation of DHA at higher acidities, which was evidenced by the characterization of acid uptake.

A detailed kinetic study allowed to justify that the enhancement of the extraction reaction in the presence of DHA is of chemical origins, and that DHA is implicated in the formation of intermediate molecular species responsible for the extraction of Pd(II).

Furthermore, we proposed an extracting molecule formulation to prepare a performing extraction solvent. This formulation can be directly obtained after reaction between DHA and DEM, the two starting reagents for the synthesis of THMA. Therefore, we showed that the crude reaction product, synthesized with an excess of DHA, could be used directly for solvent extraction without further preparation or purification after a single dilution in the required diluent, as this synthesis is performed solvent-free. This proves to be particularly attractive since both reagents, DEM and DHA, are registered chemicals, easy to handle and non-flammable. Therefore, the use of THMA does not pose any regulatory problems as long as it is prepared in situ.

In addition, when studying the impact of controlled addition of DHA to THMA, while keeping the total extractant concentration constant, non-linear dependence of the distribution ratio of Pd(II) was obtained, which we demonstrated as an apparent synergy driven by the kinetic limitations of the system. In doing so, we emphasized the great importance of mastering the extraction kinetics, which, if neglected, can lead to possible pitfalls related to a misinterpretation of the solvent extraction results.

The extraction performances were extended to Pd(II) and Pt(IV) extraction from chloride media. This study was carried out using Solvesso^{TM} 150 as a diluent from an industrial application perspective. Good extraction yields were obtained for both metals, with an acceptable separation factor of both metals at 6M HCl. These preliminary results on platinum group metals extraction from chloride media demonstrate the potential interest of THMA for the extraction and purification of these metals.

Finally, using Brij S10 proved also to increase the extraction kinetics of Pd(II) with THMA.

General conclusion

This PhD thesis aimed to characterize the extraction kinetics of Pd(II), Nd(III) and Fe(III) with malonamide ligands of **different topologies**. Three molecules, THMA, DBMA and TDMA, were initially selected according to their different potential ability to **self-organize in the organic phase**. THMA, DBMA and TDMA all possess the same coordinating malonamide (1,3-diamide) moiety, and differ in the length of their central and lateral alkyl chains substituents. TDMA presents the smallest polar head with a long tail, suggesting a higher affinity for aggregation, compared to DBMA, which also has a long tail, but a bulkier head due to the presence of two butyl chains instead of two methyl substituents. THMA presents a more hindered polar head, decorated with four hexyl chains, and was anticipated to have a lower aggregation capacity.

Third phase formation revealed to be limiting for complete extraction studies, especially with TDMA. The use of aliphatic diluents was also cumbersome, and **toluene was chosen as the diluent** for the continuation of the work with DBMA and THMA. **The absence of third phase formation** was ensured in the considered experimental conditions. In **toluene, no pre-organization is observed**, and the study of the impact of this parameter on extraction kinetics was not pursued.

A systematic thermodynamic study of the extraction of Pd(II), Fe(III) and Nd(III) with THMA and DBMA was conducted. The extraction efficiency of Pd(II) with the two malonamides follows this order: THMA > DBMA. This could be related to **electronic density brought by the bulky substituents on the nitrogen atoms.** The acid uptake characterization showed that **THMA is more basic than DBMA**, and for both ligands, $L(HNO_3)_{org}$ adducts were found through graphical slope analysis. The maximum extraction of Pd(II) with THMA is reached at a lower nitric acid concentration compared to DBMA. The extraction of Pd(II) with THMA and DBMA as a function of the concentration of H^+ showed that the latter **plays a cooperative role in the case of DBMA**, while **it is competitive in the case of THMA**. The stoichiometry of the extracted complexes of Pd(II), Nd(III) and Fe(III) was proposed using the graphical slope method. In general, the metal-to-diamide stoichiometry was found to be (1:2) for Pd(II), (1:3) for Nd(III) and Fe(III). It was also established that **the extraction of Fe(III) with THMA requires on average 5 nitrate ions.** This high number of nitrate ions could be related to the extraction of **anionic species $\mathbf{Fe(NO_3)_5^{2-}}$ or the extraction of polymeric hydrolyzed species of Fe(III).**

The extraction kinetics of Pd(II), Nd(III) and Fe(III) with THMA and DBMA were characterized in batch experiments and using the single drop technique. The **extraction kinetics of Nd(III) is very**

fast with both ligands, suggesting that its transfer is diffusion controlled. The extraction kinetics of the three metals with DBMA follow this order: Nd(III) >> Pd(II) >Fe(III) and the slow extraction of Pd(II) and Fe(III) compared to Nd(III) can be related to chemical limitations of transfer. The effect of ligand topology on extraction kinetics was evidenced as **the extraction of Pd(II) is much faster with DBMA than with THMA**. Similarly, Nd(III) extraction is twice faster with DBMA than with THMA.

An experimental methodology based on the initial rate method was implemented to **study the extraction kinetics in small batch experiments**, which proved extremely useful for rapid and reliable screening of several parameters on the extraction kinetics. Based on this methodology, the extraction rate laws of Pd(II) with THMA and DBMA were determined:

- **Extraction rate law of Pd(II) with THMA**

$$-\frac{\mathrm{d}[\mathrm{Pd}^{2+}]_{\mathrm{aq}}}{\mathrm{dt}} = \mathrm{k}_1[\mathrm{Pd}^{2+}]_{\mathrm{aq}}^{1}[\mathrm{THMA}]_{\mathrm{org}}^{2}[\mathbf{H}^{+}]_{\mathbf{aq}}^{\mathbf{-1}}[\mathrm{NO}_3]_{\mathrm{aq}}^{2} \quad (305)$$

- **Extraction rate law of Pd(II) with DBMA**

$$-\frac{\mathrm{d}[\mathrm{Pd}^{2+}]_{\mathrm{aq}}}{\mathrm{dt}} = \mathrm{k}_2[\mathrm{Pd}^{2+}]_{\mathrm{aq}}^{1}[\mathrm{DBMA}]_{\mathrm{org}}^{2}[\mathbf{H}^{+}]_{\mathbf{aq}}^{\mathbf{1}}[\mathrm{NO}_3]_{\mathrm{aq}}^{2} \quad (306)$$

Since **DBMA is more surface-active than THMA**, and considering that its interfacial adsorption follows an ideal behaviour described by Langmuir isotherm, an interfacial mechanism has been proposed for the extraction of Pd(II) with DBMA. For this mechanism, it was assumed that the reaction of **a protonated DBMA adsorbed at the interface with the adsorbed adduct $\mathbf{LPd(NO_3)_{2,ads}}$ is the rate-limiting step**.

In contrast, **the same stepwise interfacial Pd(II) extraction mechanism could not be applied to THMA**. An Inverse first-order dependence of the extraction rate law on proton concentration has been previously reported with readily protonated ligands that release their proton upon complexation with a metal, which is not supposed to be the case with THMA. In this regard, we strongly suggest that the extraction of Pd(II) with THMA may follow a similar stepwise mechanism as with DBMA, but with **the rate-limiting step located in one of the bulk phases**.

Difficulties were encountered for the complete interpretation of the extraction of Fe(III) results. This cation is prone to **hydrolysis**, thus both the aquocation $\mathbf{Fe(H_2O)_6^{3+}}$ and the **hydrolyzed species** can participate in the extraction reaction. Due to the enhanced reactivity of the hydroxo species, *i.e.* $\mathrm{Fe(OH)^{2+}}$, very often the unhydrolyzed species $\mathbf{Fe(H_2O)_6^{3+}}$ **lose their kinetic importance**.

Although a detailed study of the speciation of Fe(III) in the aqueous phase was not performed in this work, the preliminary results acquired from the kinetic studies shed light on the **complexity of the involved reactions**. In this regard, we suggested that the large global transfer constants obtained with THMA, under unfavourable conditions for the extraction of Fe(III) (low nitrate ions concentration), are related to the reaction of the hydrolyzed species, which exhibit faster extraction kinetics compared to the non-hydrolyzed ones. In parallel, a decrease in the global transfer constants was observed, once the conditions were favourable for Fe(III) extraction (high nitrate ions concentrations), so it was assumed that the observed kinetics result from the extraction of the aquocations $Fe(H_2O)_6^{3+}$. Moreover, **a deviation of the partial order of nitrate ions concentration** in the extraction rate law was observed, depending on the imposed experimental conditions, which allowed us to suggest further the involvement of several species in the extraction reaction.

Despite its high Pd(II) extraction capacity, THMA suffers from **slow extraction kinetics**. The **acceleration** of the extraction is possible by **adding dihexylamine (DHA)**. A **detailed kinetic study in small batch experiments**, allowed to justify that DHA is involved in the **formation of intermediate molecular species** responsible for Pd(II) extraction. This study also enabled to propose a **formulation of extracting molecules** in order to prepare a performing extraction solvent. This formulation can be **readily obtained** after reaction between the two reagents needed to prepare THMA, diethyl malonate (DEM) and DHA, so that **crude product** can be employed directly for solvent extraction, **without work-up nor purification**, after sole dilution in the required diluent. The extraction performances of THMA were extended to the **extraction of Pd(II) and Pt(IV) from chloride media,** and promising results were obtained.

Altogether, this work has demonstrated the impact of the extractant topology on the thermodynamic and kinetic outcomes of an extraction reaction. In addition, this work has highlighted the great interest in thoroughly understanding the different molecular forces that govern the extraction, thermodynamically and kinetically. By comparing the kinetic and thermodynamic results of Pd(II) extraction with two diamides molecules, which have the same molecular formula, but different topology, we were able to emphasize the dramatic influence of the latter on the extraction properties of the ligands. Likewise, the thermodynamic characterization of the extraction of uranium U(VI) and thorium Th(IV), with THMA and DBMA, is currently being studied at the laboratory, and reverse extraction selectivity has been observed in some conditions. These results also prove the direct impact of the topology of these extractants on their extraction properties.

Perspectives

For the continuation of this work, it seems crucial to investigate the dependence of the extraction kinetics of Pd(II) with THMA on the specific interfacial area. These experiments can be performed using the single drop technique by varying the size of the organic droplets. The experimental results obtained with THMA could not be related to an interfacial mechanism, so it was suggested that the rate-limiting step is possibly located in one of the bulk phases. Therefore, studying the extraction kinetics of Pd(II) with THMA for different specific interfacial areas can help to assess the contribution of the interfacial mechanism. Besides, characterizing the solubility of THMA in the aqueous phase can also be useful in estimating the extent to which the rate-limiting step may be localized in the aqueous phase.

This PhD thesis work is included in a project, which focuses on the in-depth characterization of the interfacial behaviour of THMA and DBMA, performed in collaboration with Dr. R. MOTOKAWA's team at the Japan Atomic Energy Agency (JAEA). It involves probing the interface at the nanoscale in different diluents using X-Ray and neutron reflectivity. The structuring of both ligands at the interface is currently studied, and will help to understand their different interfacial properties. The study will also include the effect of aqueous solutes (nitric acid and aqueous metals concentrations) and diluents on the structuring of the interface.

In the light of the results obtained from the kinetic study of the extraction kinetics of Pd(II) with THMA/DHA mixture, it seems crucial to establish a detailed mechanistic study of the extraction of Pd(II) with THMA in the presence of DHA. The kinetic study conducted in small batch experiments proved that DHA is implicated in forming intermediate molecular species responsible for the extraction of Pd(II). In this respect, we assume that further investigation of the extraction kinetics of Pd(II) with THMA/DHA mixture using appropriate tools, could shed light on the rate-limiting step and thus the extraction mechanism of Pd(II) extraction with THMA alone.

Screening the extraction kinetics in small batch experiments has enabled a formulation of an extraction solvent to overcome the slow extraction kinetics of Pd(II) with THMA. This study was developed without the need for sophisticated tools. This provides new perspectives for optimizing new formulations to improve the kinetic separation of metals, for which extraction kinetics is known to be slow, *i.e.* the separation of platinum group metals (PGMs). The preliminary results performed with THMA on the selective extraction of Pt(IV) versus Pd(II) from chloride media have demonstrated the potential interest of THMA for the extraction and purification of these metals. These studies could be further investigated, with a particular focus on the potential application of the proposed extraction solvent in PGMs refining.

Likewise, the application of this methodology is considered to study the extraction kinetics of ruthenium with monoamides. Among the fission products formed by irradiation of the fuel in the nuclear reactor, ruthenium is considered as one of the most problematic. This is due to its significant contribution to the β-γ radioactivity of the spent fuel in the first years of cooling. In addition, the speciation of ruthenium is very complex in nitric acid media, mainly due to the sensitive equilibria that occur between the different species of nitrosyl ruthenium present in solution, making it difficult to separate completely from uranium and plutonium. Although the equilibrium aspects of extraction of ruthenium in the nitric acid-TBP system with hydrocarbon diluent have been widely studied and are well documented in the literature, there is a lack of comprehensive information on the kinetics aspects of ruthenium extraction. We point out that the chemistry of ruthenium in aqueous phase is supposed to govern its transfer kinetics, due to the various chemical species in the aqueous phase. Therefore, we assume that the methodology implemented to study the extraction kinetics will be an advantageous asset to perform an intensive screening on the different chemical parameters that may influence the extraction kinetics of ruthenium, and that a separation process based on a kinetic selectivity could be eventually proposed.

Résumé de la thèse en français

L’extraction liquide/liquide est un procédé largement utilisé dans le recyclage des combustibles nucléaires, la purification des métaux à partir de minerais, les industries pétrochimiques ou pharmaceutiques. Des efforts considérables ont été consacrés au développement de nouvelles molécules et à l’optimisation des conditions d’extraction. L'optimisation des procédés d'extraction nécessite une analyse approfondie des caractéristiques thermodynamiques et cinétiques du système. Cependant, les performances d'extraction ne sont souvent caractérisées que par une description du système lorsque l'équilibre est atteint. Cela conduit à un manque de compréhension de la cinétique d'extraction, qui peut limiter les performances des procédés en raison de la lenteur du transfert de masse.

Bien que la caractérisation de la cinétique d'extraction soit d'une grande importance dans le développement d'un procédé à l'échelle industrielle, sa description détaillée reste un sujet complexe. Ceci est dû aux nombreux paramètres qui doivent être pris en compte, et à la précision requise pour les évaluer, afin de décrire au mieux le mécanisme du processus d'extraction. La vitesse d'un transfert de masse dans une extraction liquide/liquide est fonction de la réaction chimique ainsi que de la diffusion des composants à travers les phases. A cet égard, la localisation de la réaction et l'identification de la nature des limitations du transfert de masse sont des éléments clés pour des investigations plus poussées.

Certains auteurs ont proposé une description du mécanisme d'extraction basée sur les ordres partiels des réactifs dans la loi de vitesse d'extraction. La détermination de ces ordres partiels est généralement réalisée à l'aide d'outils macroscopiques. Parmi ceux-ci, on peut citer la technique de la goutte unique, les cellules agitées avec une aire interfaciale constante, à savoir la cellule de Lewis, la cellule de Nitsch, la cellule ARMOLLEX, ou les cellules fortement agitées. Cependant, le criblage de la contribution de chaque réactif avec les dispositifs susmentionnés pour déterminer l'étape limitante présente plusieurs inconvénients : En plus d'être chronophages, ces dispositifs consomment une grande quantité de réactifs qui peuvent être coûteux et générer un volume important de déchets. Ainsi, le développement d'une méthodologie rapide et fiable pour l'acquisition de données cinétiques est un défi permanent.

Entre le besoin d'étudier la cinétique d'extraction et la recherche d'une méthodologie simple pour le faire, ce travail de thèse a conduit à la mise en place d'une approche expérimentale permettant d'accéder facilement à la cinétique d'extraction, et dans le meilleur des cas, de l’améliorer. Cette étude a été menée en étudiant l'extraction du palladium Pd(II), du fer Fe(III) et du néodyme Nd(III) avec des extractants de type malonamide. Ces extractants, qui ont été développés dans le cadre de la partition actinide/lanthanide, ont récemment attiré l'attention sur le recyclage des métaux du groupe du platine

(MGP). Trois molécules, *N,N,N',N'*-tétrahexylmalonamide (THMA), *N,N*-diméthyl-*N',N'*-dibutyltétradécylmalon-amide (DBMA) et *N,N,N',N'*-tétraméthyltétradécylmalonamide (TDMA), ont été sélectionnées sur la base de leurs différentes capacités potentielles d'auto-organisation dans la phase organique. Les trois ligands possèdent tous le même fragment de coordination malonamide (1,3-diamide), et diffèrent par la longueur et la position de leurs chaînes alkyles, centrale et latérales. Le TDMA a une tête polaire peu encombrée et une longue chaîne hydrophobe, qui prédispose à une meilleure agrégation, par rapport au DBMA, qui possède également une longue chaîne hydrophobe, mais une tête polaire plus encombrée, en raison de la présence deux chaînes butyle au lieu de deux substituants méthyle. Le THMA a une tête polaire encore plus encombrée, ornée de quatre chaînes hexyle, et devrait avoir une capacité d'agrégation plus faible.

Le premier chapitre est consacré à l'état de l'art de l'extraction des métaux. Les caractéristiques thermodynamiques de l'extraction liquide/liquide ont été brièvement décrites. Ensuite, un aperçu de la cinétique d'extraction des ions métalliques a été présenté, avec une focalisation sur la vitesse de la réaction chimique. Plusieurs théories ont été établies pour décrire le transfert par diffusion à proximité de l'interface. La théorie de double film est la plus courante. Dans le cas de la récupération de cations métalliques et en raison de leur faible solubilité dans les huiles qui les rend difficiles à transférer à partir d'une phase aqueuse, le processus d'extraction nécessite l'utilisation de ligands d'extraction dissous dans la phase organique et qui peuvent interagir avec des cations hydratés afin de solubiliser un complexe. Selon le type d'extractant et, par la suite, ses interactions chimiques avec le métal, les réactions d'extractions ont été classées en extraction par solvatation, par échange de cations ou par échange d'anions. En outre, l'extraction des espèces métalliques de la phase aqueuse peut s'accompagner de l'élimination de certaines des molécules d'eau d'hydratation et de la formation d'un nouveau composé dans la phase organique. Finalement, l'extractant peut subir des modifications dans la phase organique en raison de la dimérisation, de l'extraction d'acide *etc.* Dans l'ensemble, une réaction chimique d'extraction se déroule en plusieurs étapes. Chaque étape a sa propre vitesse. Il arrive qu'une seule étape soit suffisamment lente pour que sa vitesse détermine la vitesse de l'ensemble des réactions d'extraction. L'effet des paramètres hydrodynamiques, en particulier la vitesse d'agitation sur la vitesse d'extraction, est un critère souvent utilisé pour distinguer la nature du régime d'extraction : diffusionnel ou chimique.

Les outils expérimentaux disponibles pour étudier la cinétique d'extraction ont été présentés. Il a été constaté que les résultats de la cinétique d'extraction peuvent dépendre fortement de l'outil expérimental utilisé, qui est régi par la mesure dans laquelle l'hydrodynamique a été contrôlée et les processus de diffusion ont été éliminés. Ces techniques ont été divisées en deux groupes : (i) les

techniques avec contact direct entre la phase organique et la phase aqueuse par exemple la goutte unique, les cellules agitées à aire interfaciale constante et les cellules fortement agitées ; (ii) les techniques faisant intervenir un troisième support par exemple la cellule de diffusion rotative, cellule rotative stabilisée et la cellule rotative à membrane.

La réaction d'extraction peut avoir lieu à l'interface ou au sein de l'une des phases ('bulk'). La réaction d'extraction limitant la vitesse peut avoir lieu dans la phase aqueuse si l'extractant est soluble dans la phase aqueuse. En parallèle, un extractant montrant un caractère amphiphile peut induire une réaction interfaciale. Une attention particulière a été accordée aux paramètres affectant les propriétés interfaciales de l'extractant. L'hydrophobie de l'extractant et la longueur de la chaîne alkyle influencent directement la distribution de l'extractant ainsi que son adsorption à l'interface. De même, l'activité interfaciale de l'extractant dépend de la nature de l'environnement dans les deux phases, organique (la longueur et la structure de la chaîne hydrocarbonée du diluant) et aqueuse (acidité). Ainsi, divers exemples de réactions interfaciales rapportés dans la littérature ont été mentionnés. Certains mécanismes rapportés dans la littérature ont été passés en revue. Ainsi, des mécanismes dont l'étape limitante considérée dans la phase aqueuse tel le cas de l'extraction du Zn(II) avec dithizone, des mécanismes dont l'étape limitante est considérée être interfaciale tel le cas de l'extraction de U(VI) avec un monoamide, ont été présentés. L'utilisation de contacteurs classiques pour la détermination de la loi de vitesse d'extraction a été envisagée dans plusieurs études. De grands volumes étaient nécessaires pour ces études. À cet égard, certaines des lois de vitesse rapportées dans la littérature en utilisant ces techniques ont été résumées en mettant l'accent sur les volumes requis pour réaliser chaque étude.

Par la suite, certains des extractants disponibles pour l'extraction de Pd(II) et de Pt(IV) à partir de mieux chlorures et nitrates ont été présentés. Dans un premier temps, un focus a été effectué sur la cinétique d'extraction des MGP (métaux du groupe du platine), et la possibilité de séparation basée sur leurs différences de labilité chimiques. Dans un second temps, quelques mécanismes d'extraction du Pd(II) ont été présentés.

Enfin, les propriétés des malonamides ont été résumées. Leur application dans l'extraction des actinides et des lanthanides a été présentée, ainsi que leur application dans l'extraction des MGP à partir de mieux chlorures et nitrates a été détaillée. Il s'est avéré que leurs structures dictent largement leur capacités d'extraction. Aussi, ces molécules possèdent un caractère amphiphile et un caractère basique leur permettant d'extraire l'acide. Et pour finir, les études cinétiques précédemment rapportées utilisant ces ligands ont été revues.

Dans le deuxième chapitre, le choix des sytèmes extractants a été fait, y compris le choix de diluant et les conditions expérimentales. Tout d'abord, les synthèses de THMA et TDMA ont été présentées. Les conditions expérimentales de la synthèse de THMA ont été optimisées de manière à avoir le produit final avec le plus grand degré de pureté, considérant que celui-ci a un impact direct sur la performance d'extraction du Pd(II). Le TDMA a été préparé par alkylation du carbone central du tétraméthylmalonamide commercialisé, dissous dans le terahydrofurane (THF), par réaction avec de l'hydrure de sodium et avec du bromododécane. Le THMA a été préparé sous reflux, par réaction de diéthylmalonate (DEM) avec dihexylamine (DHA).

Ensuite, une étude thermodynamique systématique a été réalisée. Ainsi, la stœchiométrie des complexes formés et les coefficients de distribution des différents métaux avec les trois ligands ont été déterminés. Des diluants aliphatiques ont été sélectionnés afin de déceler l'effet de l'organisation des ligands sur l'extraction des métaux, *i.e.* heptane, cyclohexane, iso-octane. Un criblage rapide de l'extraction en utilisant ces diluants a montré que la formation de troisièmes phases peut être limitante pour la suite de l'étude, surtout avec le TDMA. Par conséquent, l'étude a été conduite en utilisant le toluène comme diluant où l'absence de troisième phase est assurée. Ainsi, l'effet de l'organisation sur l'extraction n'a pas pu être étudié, vu qu'en utilisant le toluène, les phases organiques sont exemptes d'une organisation supramoléculaire.

Les stœchiométries des complexes formés ont été déterminées grâce à la méthode des pentes. En général, il s'est avéré qu'avec le Pd(II) des complexes de stœchiométrie (1:2) (métal : ligand) sont formés. Tandis qu'avec le Nd(III) et le Fe(III) des complexes de stœchiométrie (1 : 3) sont formés. L'extraction du Fe(III) et du Nd(III) avec THMA et DBMA est faible. De plus, la méthode des pentes a montré que le Fe(III) avec THMA nécessite en moyenne 5 ions nitrates. Ce nombre élevé d'ions nitrate pourrait être lié à l'extraction d'espèces anioniques $Fe(NO_3)_5^{2-}$ ou à l'extraction d'espèces hydrolysées de Fe(III). Le THMA a montré une extraction très efficace et sélective du Pd(II) en présence du Fe(III) et Nd(III). Cela pourrait être lié à la densité électronique apportée par les substituants volumineux sur les atomes d'azote.

L'extraction d'acide avec THMA et DBMA dans le toluène a été caractérisée par dosage acido-basique, pour différentes concentrations de ligands et à différentes concentrations d'acide nitrique dans la phase aqueuse. Les stœchiométries des complexes extraits ont été déterminées par analyse graphique des pentes. Les valeurs obtenues des pentes ont montré que des complexes de type $L(HNO_3)$ sont formés avec les deux ligands. De plus, le THMA est plus basique que le DBMA, ce qui est particulièrement visible à de faibles concentrations d'acide nitrique dans la phase aqueuse ($[HNO_3] \leq 3M$). L'extraction de Pd(II) avec le THMA et le DBMA à différentes concentrations d'acide

nitrique a été étudiée. Le maximum d'extraction du Pd(II) avec THMA est obtenu à des concentrations plus basses d'acide nitrique par rapport au DBMA. De plus, l'extraction du Pd(II) en fonction de la concentration en proton a montré que ce dernier joue un rôle coopératif dans le cas de DBMA, alors qu'il est compétitif dans le cas du THMA.

Dans le troisième chapitre, la cinétique d'extraction du Pd(II), Nd(III) et Fe(III) a été caractérisée. En premier lieu, l'étude cinétique a été réalisée en expériences classiques sur petite échelle. Ensuite, des systèmes bien définis ont été étudiés en utilisant la colonne à goutte unique. Cette étude cinétique a été précédée par une caractérisation des propriétés interfaciales du THMA et DBMA à travers des mesures de tension interfaciale. Il a été constaté que le DBMA est plus tensioactif que le THMA. Une relation entre les valeurs expérimentales de la tension interfaciale et la concentration du ligand avec THMA et DBMA a été établie grâce à l'équation de Szyszkowski, et la conformité du modèle a été assurée par des coefficients de régression élevés. Ces régressions ont permis de démontrer que la constante d'adsorption du DBMA est plus grande que celle du THMA.

Les expériences sur petite échelle ont indiqué que la cinétique d'extraction des trois métaux avec DBMA suit cet ordre : Nd(III) > Pd(II) > Fe(III). Ces résultats ont démontré qu'en exploitant la lenteur de l'extraction du Fe(III) avec DBMA par rapport au Pd(II), une séparation cinétique est certainement réalisable. Un facteur de séparation ($S_{Pd/Fe}$) supérieur à 1000 peut être atteint au bout de quelques minutes d'extraction, comparativement à un facteur de séparation de 14 obtenu à l'équilibre. En outre, les expériences sur petite échelle ont montré que la cinétique d'extraction du Pd(II) avec le DBMA est beaucoup plus rapide qu'avec le THMA. Ainsi, l'équilibre d'extraction du Pd(II) avec le DBMA a été atteint en 15 minutes environ, alors qu'avec le THMA, plus de 8 h ont été nécessaires pour atteindre l'équilibre.

Les constantes globales de transfert de Pd(II), Nd(III) et Fe(III) lors de l'extraction avec THMA et DBMA ont ensuite été déterminées en utilisant la technique de la goutte unique. La cinétique d'extraction du Nd(III) s'est avérée être la plus rapide avec les deux ligands, et sa constante de transfert globale est de l'ordre de 10^{-5} $m.s^{-1}$, ce qui suggère que son transfert est contrôlé par diffusion. De plus, l'extraction de Nd(III) est deux fois plus rapide avec le DBMA qu'avec le THMA. La cinétique d'extraction des trois métaux avec la DBMA suit cet ordre: Nd(III) >> Pd(II) > Fe(III), et la lenteur de l'extraction du Pd(II) et du Fe(III) par rapport au Nd(III) peut être liée aux limitations chimiques du transfert.

La cinétique d'extraction du Pd(II) avec THMA et DBMA a été caractérisée pour différentes concentrations des ligands. Premièrement, il s'est avéré que la cinétique d'extraction du Pd(II) est plus

rapide avec DBMA qu'avec THMA, ce qui était en accord avec les résultats obtenus avec les expériences clasiques sur petite échelle. Ensuite, en doublant la concentration de DBMA, la constante de transfert globale a diminué de moitié. Alors que pour le THMA, lorsque sa concentration a été doublée, la constante de transfert globale de Pd(II) était presque constante. Ces résultats ont mis en évidence l'impact de la structure du ligand sur la cinétique d'extraction du Pd(II). La présence de chaînes alkyles latérales volumineuses avec l'absence de chaîne centrale, le cas de THMA, entraine une perte des performances cinétiques pour l'extraction du Pd(II). En revanche, pour le DBMA, la réduction de l'encombrement des chaînes latérales, en présence d'une longue chaîne centrale conduit à un gain visible de la cinétique d'extraction.

Enfin, Il a été suggéré que la cinétique d'extraction du Fe(III) dépend fortement de la nature de l'espèce extraite. L'extraction rapide des espèces hydrolysées de Fe(III) peut conduire à certaines ambiguïtés lors de l'interprétation des résultats. Les constantes de transfert global du Fe(III) en extraction avec THMA ont été déterminées pour différentes concentrations en ions nitrates. Ainsi, il a été conclu que lorsque les conditions ne sont pas favorisées thermodynamiquement pour l'extraction de l'aquocation $Fe(H_2O)_6^{3+}$ ($[NO_3^-]$ faibles), l'extraction rapide des espèces hydrolysées dicte la constante de vitesse observée. Inversement, tant que les conditions expérimentales sont thermodynamiquement favorisées pour l'extraction du $Fe(H_2O)_6^{3+}$ ($[NO_3^-]$ modérées ou élevées), la vitesse lente de transfert du $Fe(H_2O)_6^{3+}$ régit la constante de vitesse observée de l'extraction. L'explication de ces observations a été liée aux limitations chimiques de transfert, néanmoins, ces différences dans les cinétiques observées peuvent être aussi liées aux limitations de la diffusion au transfert.

Dans le quatrième chapitre, une méthodologie expérimentale basée sur la méthode de la vitesse initiale a été mise œuvre pour la détermination des lois de vitesse d'extraction. Cette méthodologie consiste à cribler l'effet des concentrations des différents réactifs dans des expériences sur petite échelle. D'après les résultats obtenus dans ces expériences, les lois de vitesse d'extraction de Pd(II) sont les suivantes :

- AvecTHMA:

$$-\frac{d[Pd^{2+}]_{aq}}{dt} = k_1[Pd^{2+}]_{aq}^{1}[THMA]_{org}^{2}[\mathbf{H^+}]_{\mathbf{aq}}^{\mathbf{-1}}[NO_3]_{aq}^{2}$$

- Avec DBMA:

$$-\frac{d[Pd^{2+}]_{aq}}{dt} = k_1[Pd^{2+}]^1_{aq}[THMA]^2_{org}[\mathbf{H^+}]^{\mathbf{1}}_{\mathbf{aq}}[NO_3]^2_{aq}$$

Les résultats obtenus à partir des expériences sur petite échelle ont été validés avec une sélection d'expériences utilisant la technique de la goute unique, où l'aire interfaciale est connue. Pour ce faire, l'ordre partiel lié à la concentration de H^+ avec les deux ligands a été choisi comme référence, et les mêmes résultats ont été obtenus en utilisant la colonne à goutte unique. Cette méthode n'a pas pu être appliquée dans le cas du Nd(III), car la cinétique d'extraction de ce dernier avec les deux ligands est très rapide, et l'équilibre est atteint en moins de 2 min. L'application de cette méthode nécessite de réduire le temps d'extraction, ce qui devrait induire une erreur importante sur les résultats expérimentaux, compte tenu du dispositif expérimental utilisé.

L'étude de la cinétique d'extraction du Fe(III) s'est avérée compliquée en raison de la participation possible des espèces hydrolysées du Fe(III) dans la réaction d'extraction, ce qui peut poser certaines ambiguïtés concernant les réactions ayant lieu. Sur la base des résultats obtenus dans les expériences sur petite échelle et en utilisant la technique de la goutte unique, un changement de l'ordre partiel de la concentration des ions nitrates a été remarqué dans l'équation de vitesse en fonction des conditions expérimentales. Ainsi deux cas ont été discutés : La cinétique d'extraction du Fe(III) dans des conditions favorables d'extraction et la cinétique d'extraction dans des conditions défavorables d'extraction. Bien que la spéciation du Fe(III) dans la phase aqueuse n'ait pas été étudiée, il a été suggéré que le changement de l'ordre partiel des ions nitrates en fonction des conditions expérimentales imposées peut être lié à la participation de différentes espèces de Fe(III). Cette interprétation découle des résultats obtenus avec les expériences réalisées sur petite échelle et avec la goutte unique.

L'étude de la cinétique d'extraction du Pd(II) avec le THMA et le DBMA a été approfondie, et des mécanismes d'extraction ont été proposés. En prenant en compte le fait que le DBMA est tensioactif, et que son adsorption à l'interface suit un comportement idéal décrit par la loi d'adsorption de Langmuir, un mécanisme interfacial a été proposé pour l'extraction de Pd(II) avec le DBMA. L'étape déterminante de la vitesse de la réaction a été considérée comme l'adsorption d'un second ligand à l'interface. Ce mécanisme proposé pouvait expliquer les résultats expérimentaux.

En parallèle, avec le THMA, il a d'abord été proposé que l'extraction du Pd(II) suit le même mécanisme par étapes qu'avec le DBMA, avec une étape limitante différente. Ainsi, il a été proposé que l'étape limitante de la vitesse d'extraction soit l'adsorption de l'espèce protonée de THMA à l'interface. Cependant, en considérant cela, la loi de vitesse d'extraction obtenue ne pouvait pas expliquer les

résultats expérimentaux. Ensuite, il a été proposé que le complexe interfacial formé doit se désorber par lui-même de l'interface, et que cette étape constitue l'étape limitante. Cependant, en considérant cette hypothèse, il n'a pas été possible d'expliquer les résultats expérimentaux, puisque la dépendance inverse du premier ordre par rapport à la concentration du proton n'apparaît pas dans la loi de vitesse d'extraction. Il convient de mentionner qu'en proposant le mécanisme d'extraction avec le THMA, les hypothèses travaillées ont été limitées au cas d'une réaction interfaciale. Néanmoins, le THMA peut suivre le même mécanisme par étapes que le DBMA, avec une étape limitante située dans une des phases. Dans l'ensemble, aucun mécanisme plausible n'a pu être identifié jusqu'à présent pour l'extraction de Pd(II) avec le THMA.

Dans le cinquième chapitre, le bénéfice d'un excès de dihexylamine (DHA) employée lors de la préparation du THMA a été démontré par un gain de performance cinétique. Le rendement d'extraction du Pd(II) dépend de la pureté du ligand, c'est pourquoi l'effet de plusieurs impuretés a été évalué, à savoir l'éther diéthylique (Et_2O) provenant des étapes de lavage, l'éthanol (EtOH) produit *in-situ*, le diéthylmalonate (DEM) et la dihexylamine (DHA). Une amélioration du rendement d'extraction a été constatée en présence de ces derniers. Cependant, seul l'effet de la DHA a été étudié en détail. Des lots synthétiques de THMA contenant une quantité contrôlée de DHA ont été préparés et ont été testés dans l'extraction de Pd(II). L'effet bénéfique du DHA s'est avéré être d'origine cinétique puisque les résultats thermodynamiques de l'extraction du Pd(II) avec le THMA pur et le mélange THMA/DHA étaient presque similaires.

Pour l'étude cinétique, les conditions expérimentales ont été définies de manière à exacerber les effets de la cinétique d'extraction. Ainsi, la vitesse d'agitation a été fixée à 1200 min^{-1} et la durée d'extraction a été fixée à 1 h. Une augmentation du rendement d'extraction a été constatée avec l'augmentation de la quantité de DHA dans la phase organique. L'augmentation maximale a été atteinte à 50 % molaire de DHA. Au-delà de cette limite, l'extraction de Pd(II) a diminué à nouveau. De plus, l'effet bénéfique de la DHA a disparu pour des concentrations élevées en acide nitrique dans la phase aqueuse, et ceci a été lié à la protonation complète de la DHA. Une étude a été réalisée pour préciser l'effet cinétique du DHA sur l'extraction de Pd(II) avec le THMA. L'extraction a été réalisée pendant de courtes durées (maximum 6 min). Un modèle de premier ordre a été utilisé pour interpréter les données expérimentales. Une augmentation de la constante de vitesse a été remarquée avec l'augmentation du pourcentage molaire de DHA dans la phase organique. D'après cette étude, il a été conclu que l'extraction de Pd(II) a lieu selon deux mécanismes simultanés : (i) une extraction directe avec le THMA (ii) une extraction indirecte médiée par la DHA. De plus, cette étude a prouvé que la DHA est impliquée dans la formation d'espèces moléculaires intermédiaires responsables de l'extraction du Pd(II).

Cette étude a également permis de proposer une formulation des molécules extractantes afin de préparer un mélange d'extraction performant. Cette formulation peut être facilement obtenue après réaction entre les deux réactifs nécessaires à la préparation du THMA, DEM et DHA, de sorte que le produit brut obtenu peut être employé directement pour l'extraction, sans traitement ni purification, après seule dilution dans le diluant requis. Les performances d'extraction du THMA ont été étendues à l'extraction de Pd(II) et Pt(IV) à partir de milieux chlorure, et des résultats prometteurs ont été obtenus, ce qui peut élargir le domaine d'application de cette molécule dans le recyclage des MGP. Enfin, une solution alternative pour l'accélération de l'extraction du Pd a été proposée en utilisant le tensioactif Brij S10.

En conclusion, l'objectif de cette thèse était de caractériser la cinétique d'extraction de Pd(II), Nd(III) et Fe(III) avec des ligands malonamides de différentes topologies. Trois molécules THMA, DBMA et TDMA ont été initialement sélectionnées pour cette étude. La formation de la troisième phase s'est révélée limitante pour les études d'extraction complètes, surtout avec le TDMA. Le toluène a été choisi comme diluant pour la suite des travaux avec le DBMA et le THMA. Dans ces conditions, aucune pré-organisation n'est observée, et l'étude de l'impact de ce paramètre sur la cinétique d'extraction n'a pas été poursuivie.

La cinétique d'extraction de Pd(II), Nd(III) et Fe(III) avec le THMA et le DBMA a été caractérisée dans des expériences classiques, puis en utilisant la technique de la goutte unique. La cinétique d'extraction de Nd(III) est très rapide avec les deux ligands, ce qui suggère que son transfert est contrôlé par diffusion. La cinétique d'extraction des trois métaux avec le DBMA suit cet ordre : Nd(III) >> Pd(II) >Fe(III) et la lenteur de l'extraction de Pd(II) et de Fe(III) par rapport à Nd(III) peut être liée aux limitations chimiques du transfert. L'effet de la topologie du ligand sur la cinétique d'extraction a été mis en évidence car l'extraction de Pd(II) est beaucoup plus rapide avec le DBMA qu'avec le THMA. De même, l'extraction de Nd(III) est deux fois plus rapide avec le DBMA qu'avec le THMA.

Une méthodologie expérimentale basée sur la méthode de la vitesse initiale a été mise en œuvre pour étudier la cinétique d'extraction dans des expériences classiques sur petite échelle, ce qui s'est avéré extrêmement utile pour un dépistage rapide et fiable de plusieurs paramètres sur la cinétique d'extraction. Sur la base de cette méthodologie, les lois de vitesse d'extraction de Pd(II) avec le THMA et le DBMA ont été déterminées. Le DBMA est plus tensioactif que le THMA, et considérant que son adsorption interfaciale suit un comportement idéal décrit par l'isotherme de Langmuir, un mécanisme interfacial a été proposé pour l'extraction de Pd(II) avec le DBMA. En revanche, le même mécanisme d'extraction

Pd(II) interfacial par étapes n'a pas pu être appliqué au THMA. Une dépendance inverse de premier ordre de la loi de vitesse d'extraction sur la concentration en proton a été précédemment rapportée avec des ligands facilement protonés qui libèrent leur proton lors de la complexation avec un métal, ce qui n'est pas supposé être le cas avec le THMA. À cet égard, il a été suggéré que l'extraction de Pd(II) avec le THMA peut suivre un mécanisme par étapes similaire à celui du DBMA, mais avec l'étape limitant la vitesse située au sein de l'une des phases.

Des difficultés ont été rencontrées pour l'interprétation complète des résultats de l'extraction du Fe(III). Ce cation est enclin à l'hydrolyse, ainsi l'aquocation $Fe(H_2O)_6^{3+}$et l'espèce hydrolysée peuvent toutes deux participer à la réaction d'extraction. En raison de la réactivité accrue des espèces hydroxo, c'est-à-dire $Fe(OH)^{2+}$très souvent les espèces non hydrolysées $Fe(H_2O)_6^{3+}$perdent leur importance cinétique. Bien qu'une étude détaillée de la spéciation du Fe(III) en phase aqueuse n'ait pas été réalisée au cours de ce travail, les résultats préliminaires acquis à partir des études cinétiques mettent en lumière la complexité des réactions impliquées. À cet égard, il a été suggéré que les grandes constantes globales de transfert obtenues avec le THMA, dans des conditions défavorables pour l'extraction du Fe(III) (faible concentration en ions nitrate), sont liées à la réaction des espèces hydrolysées, qui présentent une cinétique d'extraction plus rapide par rapport aux espèces non hydrolysées. En parallèle, une diminution des constantes de transfert global a été observée, une fois que les conditions étaient favorables à l'extraction du Fe(III) (concentrations élevées en ions nitrate), il a donc été supposé que la cinétique observée résulte de l'extraction des aquocations $Fe(H_2O)_6^{3+}$. De plus, une déviation de l'ordre partiel de la concentration en ions nitrate dans la loi de vitesse d'extraction a été observée, en fonction des conditions expérimentales imposées, ce qui a permis de suggérer davantage l'implication de plusieurs espèces dans la réaction d'extraction.

Malgré sa capacité d'extraction élevée pour Pd(II), le THMA souffre d'une cinétique d'extraction lente. L'accélération de l'extraction est possible en ajoutant de la dihexylamine (DHA). Une étude cinétique détaillée en petites expériences batch, a permis de justifier que la DHA est impliquée dans la formation d'espèces moléculaires intermédiaires responsables de l'extraction du Pd(II). Cette étude a également permis de proposer une formulation des molécules extractantes afin de préparer un solvant d'extraction performant. Cette formulation peut être facilement obtenue après réaction entre les deux réactifs nécessaires à la préparation du THMA, le diéthylmalonate (DEM) et la DHA, de sorte que le produit brut peut être employé directement pour l'extraction par solvant, sans traitement ni purification, après une seule dilution dans le diluant requis. Les performances d'extraction du THMA ont été étendues à l'extraction de Pd(II) et de Pt(IV) à partir de milieux chlorurés, et des résultats prometteurs ont été obtenus.

Dans l'ensemble, ce travail a démontré l'impact de la topologie de l'extractant sur les résultats thermodynamiques et cinétiques d'une réaction d'extraction. En outre, ce travail a mis en évidence le grand intérêt de comprendre pleinement les différentes forces moléculaires qui régissent l'extraction, thermodynamiquement et cinétiquement. En comparant les résultats cinétiques et thermodynamiques de l'extraction de Pd(II) avec deux molécules de diamides, qui ont la même formule moléculaire, mais une topologie différente, il a été possible de souligner l'influence dramatique de cette dernière sur les propriétés d'extraction des ligands.

Pour la suite de ce travail, il semble crucial d'étudier la relation entre la cinétique d'extraction du Pd(II) par le THMA et l'aire interfaciale spécifique. Ces expériences peuvent être réalisées en utilisant la technique de la goutte unique en faisant varier la taille des gouttelettes organiques. Les résultats expérimentaux obtenus avec le THMA n'ont pas pu être reliés à un mécanisme interfacial, il a donc été suggéré que l'étape limitant la vitesse se situe probablement dans l'une des phases. Par conséquent, l'étude de la cinétique d'extraction de Pd(II) avec le THMA pour différentes zones interfaciales spécifiques peut aider à évaluer la contribution du mécanisme interfacial. En outre, la caractérisation de la solubilité du THMA dans la phase aqueuse pourrait également être utile pour estimer dans quelle mesure l'étape de limitation de vitesse peut être localisée dans la phase aqueuse.

Ce travail de thèse est inclus dans un projet, qui se concentre sur la caractérisation approfondie du comportement interfacial du THMA et du DBMA, réalisé en collaboration avec l'équipe du Dr. R. MOTOKAWA à l'Agence Japonaise de l'Énergie Atomique (JAEA). Il s'agit de sonder l'interface à l'échelle nanométrique dans différents diluants en utilisant la réflectivité des rayons X et des neutrons. La structuration des deux ligands à l'interface est actuellement étudiée, et aidera à comprendre leurs différentes propriétés interfaciales. L'étude comprendra également l'effet des solutés aqueux (concentrations d'acide nitrique et de métaux aqueux) et des diluants sur la structuration de l'interface.

À la lumière des résultats obtenus par l'étude cinétique de la cinétique d'extraction de Pd(II) avec le mélange THMA/DHA, il semble crucial d'établir une étude mécanistique détaillée de l'extraction de Pd(II) avec le THMA en présence de DHA. L'étude cinétique menée dans des expériences sur petite échelle a prouvé que la DHA est impliqué dans la formation d'espèces moléculaires intermédiaires responsables de l'extraction de Pd(II). À cet égard, il s'avère qu'une étude plus approfondie de la cinétique d'extraction de Pd(II) avec le mélange THMA/DHA en utilisant des outils appropriés, pourrait mettre en lumière l'étape limitant la vitesse et donc le mécanisme d'extraction de Pd(II) avec le THMA seul.

Le criblage de la cinétique d'extraction a permis de formuler un solvant d'extraction pour surmonter la lenteur de la cinétique d'extraction du Pd(II) avec le THMA. Cette étude a été développée

sans avoir recours à des outils sophistiqués. Elle offre de nouvelles perspectives pour l'optimisation de nouvelles formulations afin d'améliorer la séparation cinétique des métaux, pour lesquels la cinétique d'extraction est connue pour être lente, comme dans le cas de la séparation des métaux du groupe du platine (MGP). Les résultats préliminaires obtenus avec le THMA sur l'extraction sélective du Pt(IV) par rapport au Pd(II) en milieu chlorure ont démontré l'intérêt potentiel du THMA pour l'extraction et la purification de ces métaux. Ces études pourraient être approfondies, avec une attention particulière sur l'application potentielle du solvant d'extraction proposé dans le raffinage des platinoïdes.

De même, l'application de cette méthodologie est envisagée pour étudier la cinétique d'extraction du ruthénium avec des monoamides. Parmi les produits de fission formés par l'irradiation du combustible dans le réacteur nucléaire, le ruthénium est considéré comme l'un des plus problématiques. Ceci est dû à sa contribution significative à la radioactivité β du combustible usé au cours des premières années de refroidissement. En outre, la spéciation du ruthénium est très complexe en milieu acide nitrique, principalement en raison des équilibres sensibles qui se produisent entre les différentes espèces de ruthénium nitrosyle présentes en solution, ce qui rend difficile sa séparation complète de l'uranium et du plutonium. Bien que les aspects d'équilibre de l'extraction du ruthénium dans le système acide nitrique-TBP avec diluant hydrocarbure aient été largement étudiés et soient bien documentés dans la littérature, il y a un manque d'informations complètes sur les aspects cinétiques de l'extraction du ruthénium. Il convient de souligner que la chimie du ruthénium en phase aqueuse est censée régir sa cinétique de transfert, en raison des diverses espèces chimiques présentes dans la phase aqueuse. Par conséquent, la méthodologie mise en œuvre pour étudier la cinétique d'extraction pourrait être un atout très utile pour effectuer un criblage poussé des différents paramètres chimiques qui peuvent influencer la cinétique d'extraction du ruthénium, et qu'un processus de séparation basé sur une sélectivité cinétique pourrait éventuellement être ensuite proposé.

Chapter 6: Experimental part

I. Chemical Reagents

Organic compounds: *N,N'*-dimethyl-*N,N'*-dibutyltetradecylmalonamide (DBMA, 98% purity) was kindly provided by the CEA France, while the production was performed by Pharmasynthèse (former Panchim), France. *N,N,N',N'*-tetramethylmalonamide (TMMA, 97% purity), diethyl malonate (99% purity) and dihexylamine (97% purity) were purchased from Sigma-Aldrich. 1-Bromotetradecane ($CH_3(CH_2)_{13}Br$, 98% purity) was purchased from Alfa Aesar. All compounds were used without further purification.

Organic diluents: Toluene, Solvesso 150^{TM} , heptane, diethyl ether, cyclohexane, tetrahydrofuran and iso-octane were purchased from Carlo Erba reagents.

Salts: Palladium(II) nitrate hydrate ($Pd(NO_3)_2.xH_2O$, ca. 40% Pd, 99.9% purity), palladium(II) chloride (99.9% purity) and platinum(IV) chloride (99.9% purity) were purchased from Strem Chemicals. Iron(III) nitrate nonahydrate ($Fe(NO_3)_3.9H_2O$, ≥98% Fe), neodymium(III) nitrate hexahydrate ($Nd(NO_3)_3.6H_2O$, 99.9% purity), magnesium sulfate anhydrous ($MgSO_4 \geq 99.5\%$) and lithium nitrate ($LiNO_3$, 98%) were purchased from Sigma-Aldrich.

Acids: Concentrated nitric (HNO_3, 69.5% conc.) and hydrochloric (HCl, 37% conc.) acids were purchased from Carlo Erba reagents.

II. Chemical synthesis

A. Synthesis of THMA

A mixture of diethyl malonate (8.09 g, 0.05 mol) and dihexylamine (20.1 g, 0.105 mol, 2.1 equiv.) was heated under reflux (ca. 100°C) for 7 h. Every 30 min, an argon flow was injected for 1 min to evacuate the produced ethanol. The reaction mixture was then cooled to room temperature. The resulting product could be used directly in solvent extraction experiments. For characterization and detailed study, purification was performed as follows: The resulting mixture was dissolved in 100 mL diethyl ether and then washed with an aqueous 1M HCl solution to remove unreacted dihexylamine (4 x 30 mL), with a saturated aqueous solution of $NaHCO_3$ (1 x 30 mL) and finally with brine (1 x 30 mL). The recovered organic layer was dried over $MgSO_4$ and concentrated *in vacuo*. *N*,*N*,*N*',*N*'-tetrahexylmalonamide. (THMA) was obtained as a viscous pale yellow liquid (21,5 g, 98% yield).

^{1}H NMR (400 MHz, $CDCl_3$) ***δ (ppm):*** *3.45 (s, 2H, $COCH_2CO$), 3.34 (dd, J_1 = 15.4Hz, J_2 = 7.8 Hz, 4H, N-CH_2), 3.32 (dd, J_1 = 15.4 Hz, J_2 = 7.7 Hz, 4H, N-CH_2), 1.57–1.55 (m, 8H, N-CH_2-$\underline{CH_2}$), 1.32–1.29 (m, 24H, CH_2,), 0.92 (t, J = 6.7 Hz, 6H, CH_3), 0.88 (t, J = 6.6 Hz, 6H, CH_3)* **^{13}C NMR** ***(100.6 MHz, $CDCl_3$) δ (ppm):*** *166.6, 48.4, 46.0, 40.8, 31.5, 31.5, 28.9, 27.5, 26.6, 26.5, 22.5, 13.9, 13.9*
IR (neat) ***ν* (*cm^{-1}*):** *2927, 2903, 2850, 1634, 1456, 1420, 1376.*

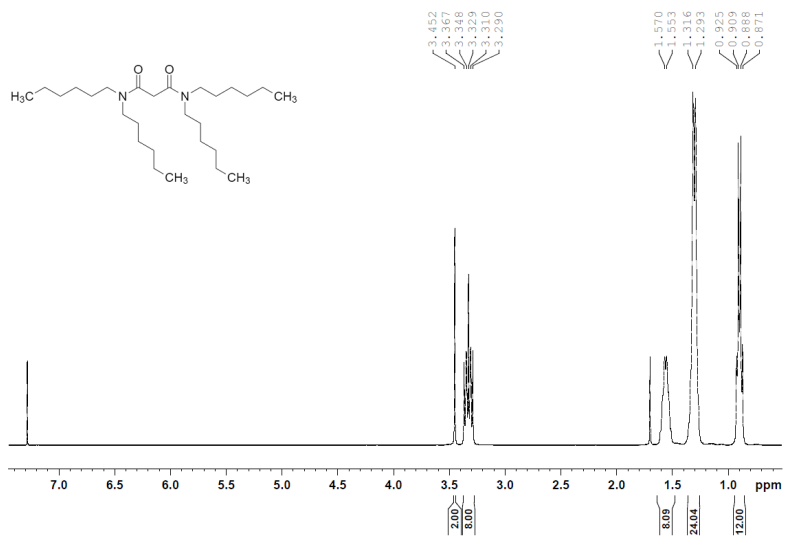

Figure 100: ^{1}H NMR spectrum of THMA (400 MHz, solvent $CDCl_3$).

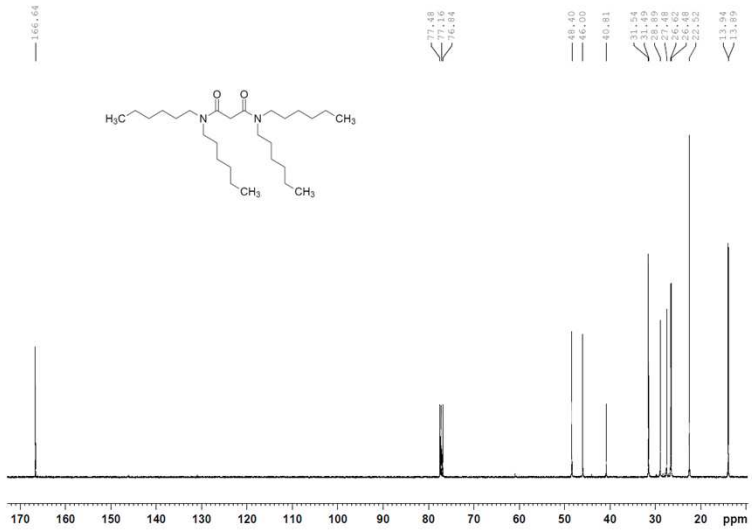

Figure 101: ^{13}C NMR spectrum of THMA (100 MHz, solvent $CDCl_3$).

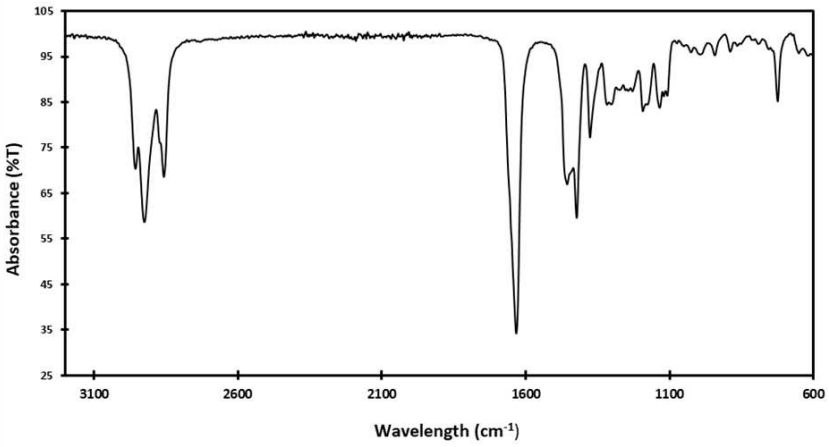

Figure 102: FT-IR spectrum of THMA.

Wavenumber / cm^{-1}	Assignment
2850 cm^{-1} – 2927 cm^{-1}	ν CH_2 (stretching)
1634 cm^{-1}	ν C=O (stretching)
1456 cm^{-1}	ν CH_2 (bending)
1420 cm^{-1}	ν C-N (stretching)
1376 cm^{-1}	ν C-H (bending)

B. Chemical synthesis of TDMA:

In a 50 mL flask under an argon atmosphere, sodium hydride NaH (60% in mineral oil, 0.12 g, 12 mmol) was introduced and washed twice with 10 mL of pentane. Excess of pentane was removed and dry THF (5 mL) was added under argon atmosphere. *N,N,N',N'*-tetramethylmalonamide (TMMA) (0.4 g, 2.5 mmol, 1.0 eq.) was added dropwise under vigorous agitation. After 30 minutes, 1-bromotetradecane (0.76 g, 2.75 mmol, 1.1 eq) was added, and the mixture was heated under reflux (ca. 75°C) for 16 h. The resulting product was then cooled and 1 mL of ethanol was added to quench the residue of NaH. The resulting mixture was dissolved in 50 mL of ethyl acetate and then washed with a saturated aqueous solution of ammonium chloride (20 mL). The organic phase obtained after decantation was washed with water (15 mL), then a brine solution (20 mL). The recovered organic layer was dried over $MgSO_4$ and concentrated *in vaccuo*. The final product obtained was recrystallized in a mixture of chloroform/pentane. *N,N,N',N'*-tetramethyltetradecylmalonamide (TDMA) was obtained as a white powder (0.57g, 64% yield).

^{1}H NMR (400 MHz, $CDCl_3$) *δ (ppm):* *3.61 (t, J=6.7 Hz, 1H, COCHCO), 3.03 (s, 6H, N-CH_3), 2.99 (s, 6H, N-CH_3), 1.91 (q, J_1 = 14.9 Hz, J_2 = 6.9 Hz 2H, $\underline{CH_2}$–CH_2), 1.27 (m, 23H, CH_2), 0.90 (t, J = 6.7 Hz, 3H, CH_2- $\underline{CH_3}$)*

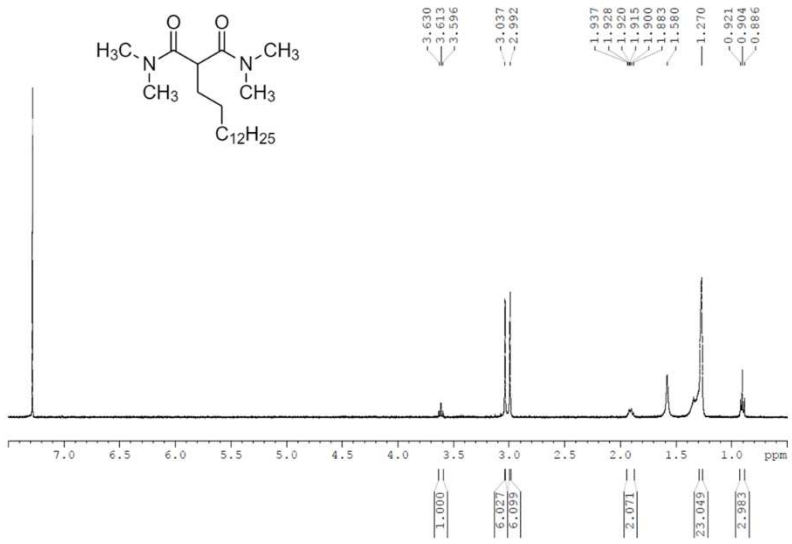

Figure 103: ^{1}H NMR spectrum of TDMA (400 MHz, solvent $CDCl_3$).

III. Sample preparation procedure

A. Metallic aqueous phases

Aqueous phases containing the desired metallic cations were prepared from the corresponding metallic salts ($Pd(NO_3)_2.xH_2O$), $Nd(NO_3)_3.6H_2O$, $Fe(NO_3)_3.9H_2O$, $PdCl_2.2H_2O$, $PtCl_4$) dissolved in an aqueous HNO_3 or HCl solution of the desired concentration. Stock solutions were prepared prior to any investigation, and the desired concentrations of the aqueous phases were obtained by dilution.

B. Preparation of aqueous phases with constant $[H^+]$ or $[NO_3^-]$

Aqueous phases with constant concentrations of H^+or NO_3^- were prepared by mixing aqueous solutions of nitric acid and solutions of lithium nitrate. Aqueous solutions of lithium nitrate were prepared by dissolving the lithium nitrate salt in water. Stocks of 5M were prepared, and dilutions were made to reach the desired concentration.

Table 47: Preparation of aqueous solutions (V = 1 L) of different nitrate ions concentrations and fixed $[H^+]$ 1.5M.

$[H^+]$ 1.5M **$[NO_3^-]$ 1.5M**	**$[H^+]$ 1.5M** **$[NO_3^-]$ 2M**	**$[H^+]$ 1.5M** **$[NO_3^-]$ 3M**	**$[H^+]$ 1.5M** **$[NO_3^-]$ 4M**
	$[HNO_3]$ 3M	$[HNO_3]$ 3M	$[HNO_3]$ 3M
$[HNO_3]$ 3M	V = 500 mL	V = 500 mL	V = 500 mL
V = 1000 mL	$[LiNO_3]$ 1M	$[LiNO_3]$ 3M	$[LiNO_3]$ 5M
	V = 500 mL	V = 500 mL	V = 500 mL

Table 48: Preparation of aqueous solutions (V = 1 L) of different nitrate ions concentrations and fixed $[H^+]$ 1.5M.

$[H^+]$ 1.5M **$[NO_3^-]$ 5M**		**$[H^+]$ 3M** **$[NO_3^-]$ 5M**		**$[H^+]$ 5M** **$[NO_3^-]$ 5M**	
$[HNO_3]$ 5M	V = 300 mL	$[HNO_3]$ 6M	V = 500 mL	$[HNO_3]$ 5M	V = 1000 mL
$[LiNO_3]$ 5M	V = 700 mL	$[LiNO_3]$ 4M	V = 500 mL		

C. Preparation of organic phases

The organic phase was prepared by first weighing a mass of the ligand (THMA, DBMA, TDMA), and then dissolving it with the desired solvent. Then, a dilution was applied to reach the desired concentration.

1. Preparation of THMA/DHA mixture

The preparation of the mixture of DHA/THMA for a fixed concentration of THMA (0.2M), was carried out by adding to a known mass of THMA, the corresponding mass of DHA leading to the desired molar percentage. Then, the preparation of the 0.2M THMA solution, was carried out by weighing from the prepared solution, a mass taking into account the new mass percentage of THMA. The same was done for the experiments performed with diethyl malonate, diethyl ether and ethanol. In the table below, we summarize the experimental conditions employed to investigate the effect of DHA.

Table 49: Preparation of THMA/DHA mixture, [THMA] 0.2M.

Desired %mol DHA	Weighed mass of THMA	Weighed mass of DHA	Real %mol DHA	THMA mass percentage	Mass of THMA to weigh 0.2M [THMA]
10%	1.0067 g	0.0486	10.24%	95%	0.092 g
20%	1.0652 g	0.1106	19.7%	91%	0.097 g
30%	1.0274 g	0.1831	29.63%	85%	0.103 g
40%	1.1401 g	0.336	40.88%	77%	0.113 g
50%	1.0082 g	0.423	49.79%	70%	0.124 g
60%	1.0285 g	0.65	58.89%	61%	0.143 g
70%	1.016 g	1.0135	70.22%	50%	0.175 g
80%	1.0069 g	1.7288	80.23%	37%	0.238 g
90%	1.0061	3.9002	90.03%	21%	0.427 g

The THMA/DHA mixtures with a fixed total concentration of the extractant were prepared by mixing a volume of 0.2M THMA with 0.2M DHA, such as the total volume is 1 mL.

Table 50: Preparation of THMA/DHA mixtures, [THMA] + [DHA] = 0.2M.

X_{DHA}	Volume of 0.2M DHA	Volume of 0.2M THMA	Total volume
0.1	0.1 mL	0.9 mL	1mL
0.2	0.2 mL	0.8 mL	
0.3	0.3 mL	0.7 mL	
0.4	0.4 mL	0.6 mL	
0.5	0.5 mL	0.5 mL	
0.6	0.6 mL	0.4 mL	
0.7	0.7 mL	0.3 mL	
0.8	0.8 mL	0.2 mL	
0.9	0.9 mL	0.1 mL	

IV. Pre-equilibration of the organic phase

The organic phases were pre-equilibrated by bringing them into contact for 1 h with a five-fold volume of an aqueous solution of HNO_3 or HCl of molarity identical to that of the aqueous metal solution employed for the extraction step.

V. Solvent extraction experiments

Extraction experiments were carried out in 2 mL Eppendorf tubes with equal volumes of the aqueous and organic phases (A/O =1). The two phases were shaken with a thermostated orbital mixer (Eppendorf Thermomixer® C) for 1 min to 24 h. at 21°C ± 2°C. The stirring speed was set at 2000 rpm unless otherwise stated in the text. Tubes were then centrifuged to ensure good phase separation.

Centrifugation duration was fixed at 30 s for the kinetic experiments. For each extraction performed, aliquots of the aqueous phases (100 µL), before and after extraction, were directly diluted with a 2% HNO_3/HCl aqueous solution (90/10). After extraction, aliquots of the loaded organic phases (500µL) were back-extracted during 1 h with 1 mL of a 0.1M aqueous thiourea solution. The resulting phases were separated and 250µL of the final aqueous phase were taken and diluted with a 2% HNO_3/HCl aqueous solution (90/10). We add that if the organic phase contains only Fe(III), back-extraction was performed with water

Evidence from preliminary investigations showed that all the metals were totally stripped during the process and that no metal precipitation occurred prior to analysis. Dilution factors have been chosen so that a minimum 10-fold dilution is operated to avoid matrix effects during analysis. Except for the analysis of Fe(III) for the kinetic order determination, dilution factors were 5 since low concentration of Fe(III) was extracted in the organic phase.

VI. Analytical determination of metal content

Metals concentration in each solution was determined using inductively coupled plasma atomic emission spectroscopy (ICP/AES, SPECTRO ARCOS ICP Spectrometer, AMETEK Materials Analysis). The selected spectral lines to assay metals were free from interference. The given concentrations were calculated as the average of three replicates at different wavelengths for each metal. Relative standard deviations have been determined and lie between 1 and 3%. Quantification limits (LoQ) in each analyzed phase were determined for each metal from the dilution factor applied and the background equivalent concentration calculated by the spectrometer for each optical line. Confidence intervals were selected taking into account the error of the spectrometer and the precision of the equipment used for dilution. Altogether, the relative errors between 5% and 10%. All results showed a total mass balance in each metal in the range of ± 5% of the initial load in the aqueous phase.

The measurements were carried out after dilution of the samples and calibration of the apparatus for the detection of the elements concerned using standard solutions (prepared by dilution of standards and distributed over a range of concentrations from 0 to 15 $mg.L^{-1}$). The wavelengths retained for the analysis are the following:

Table 51: Wavelengths retained for the determination of Pd, Nd, Fe and Pt concentration.

	Pd	Fe	Nd	Pt
Wavelength (nm)	340.247	238.562	401.225	172.313
	324.270	239.562	430.358	191.170
	360.955	259.941	106.109	203.711
	229.651	261.187	417.731	306.471

VII.Single drop technique

1. Description of the technique

It consists of two column sections, each measuring 1 meter long, which gives a total length of 2 meters. The column is thermostatically controlled by a double jacket. The experimental setup was in CAP configuration. The injection is done with a fixed needle connected to a peristaltic pump. The needle is stainless steel and has an internal diameter of 0.18 mm. The recovery of the drops is made through a movable glass funnel, which is also connected to a peristaltic pump. REGLO pumps were used.

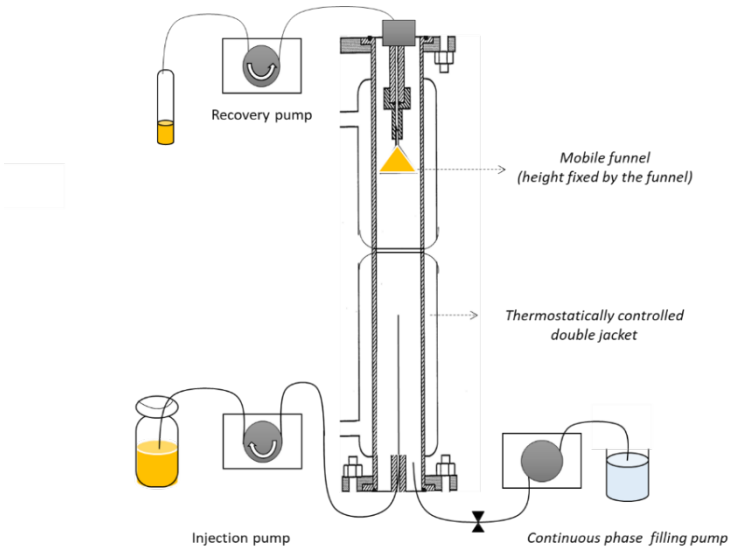

Figure 104: Sketch of the single drop technique (CAP operation).[34]

2. Operating mode

When the column was installed, the idle injection time was determined, for an injection rate of 0.143 ml.min^{-1}, and it was estimated to be 20 minutes. This corresponds to the time required to recover the drops from the funnel. It is used to establish the minimum time needed to recover all the drops of a given height contained in the recovery system.

Before any investigation, pumps were calibrated. Calibration was performed by setting a volume of fluid (pre-equilibrated organic phase) to dispense for the specified time. Then, the dispensed amount was weighed, and the volume was calculated based on the density of the organic phase, which was determined for each experiment. The actual measured value of the volume was entered on the screen of the pump, which automatically completes the calibration.

The column was first filled with the aqueous phase using a pump, and the organic phase was injected at the bottom of the column. Once injected into the column, the drops were collected at the top into a funnel using a dedicated peristaltic pump. The funnel is movable and allows working at several heights on the same column without disturbing the injection of the drops. For our investigations, the studied heights were, 40 cm, 60 cm, 80 cm, 90 cm, 100 cm, 110 cm, 120 cm and 130 cm. Sampling started 30 min after the first droplet generation. Three samples of 1 mL each were collected for each height. The height was changed every 25 min.

For each studied height, the drop flight time, is the time for a drop to detach from the needle and enter the funnel. This constitutes the transfer time. An average of three values was taken.

Likewise, for each studied height, the droplet was calculated from the injection rate (calibrated pump) and the number of drops (manual counting).

The droplet diameter is calculated from the injection rate (calibrated pump) and the number of drops (manual counting).

$$d_{droplet} = 2\sqrt[3]{\frac{3}{4\pi}\frac{Q}{f}}$$

As,

$$V_{droplet} = \frac{Q}{f}$$

Where V denotes the volume of the droplet (mL), Q is the injection flow rate ($mL.min^{-1}$) and f is the frequency of droplet formation (number of drops per minute).

The time required to form 10, 15 and 20 drops was determined for each studied height, from which the average diameter value was calculated.

The concentration of the continuous aqueous phase was analyzed before and at the end of the experiment. The recovered organic phase for each height, was back-extracted following the procedure described above.

VIII. NMR

The NMR spectra were recorded on a Brucker Ultrashield 400 plus engine. The irradiation frequencies are 400 MHz for the ^{1}H nucleus, 100 MHz for the ^{13}C, respectively. Chemical shifts δ are expressed in ppm with the residual solvent signals ($CDCl_3$) as reference.

IX. IR

The infrared absorption spectra were recorded using a Perkin-Elmer Spectrum IR-FT 100 instrument, equipped with ATR (Attenuated Total Reflection) technology allowing direct and fast analysis of a sample in liquid form without any preparation. The spectra were recorded in the range 380-4000 cm^{-1} with a resolution of 1 cm^{-1}.

X. SAXS

Small angle X-Ray scattering (SAXS) spectra were recorded in transmission geometry on a XENOCS setup equipped with a Mo anode (λ 0.71 Å) over a Q range from 0.2 nm^{-1} to 10 nm^{-1} using a MAR345 2D imaging plate detector. Samples were analyzed in Quartz capillaries of 2 mm diameter. Spectra were corrected for the background and detector noise by subtraction of an empty capillary. To check the calibration of the scattering vector, *i.e.* to determine the sample to detector distance, silver behenate was used in a sealed capillary as a standard. The intensity was normalized by using Lupolen as a standard.

XI. Interfacial tension

All interfacial tension measurements were carried out using a Krüss spinning drop tensiometer (SDT) equipped with a high resolution USB3 camera. The tensiometer is combined with the ADVANCE software. This software performs image analysis applying either the approximation functions of Vonnegut, or making use of an evaluation algorithm based on a Young-Laplace fit. For the current measurements, Young-Laplace-fit equation was used for interfacial tension determination. The densities of all samples were determined using DSA 5000 densimeter at 23 °C. All the organic phases were pre-equilibrated by contacting them for 30 min with a five-fold volume of 3 M aqueous nitric acid concentration. The capillary was filled with the aqueous phase (3M HNO_3). A drop of the sample (organic phase) was injected with a syringe. The capillary was sealed. Interfacial tension measurements were performed at a controlled temperature of 23°C at a high rotation rate (>5000 rpm). The reported values were recorded after the drops reached equilibrium, and no further decrease in interfacial tension

values was observed. Calibration of the tensiometer was performed before each measurement to obtain the image scale.

XII.Acid titration

Acid titration of the organic and aqueous phases before and after acid extraction was carried out using 686 Metrohm titroprocessor. Aliquots of the aqueous phase (50 μL) before and after acid extraction were withdrawn, poured into water, and then titrated with 0.1M NaOH. For the organic phase, aliquots of 250 μL were withdrawn after extraction and poured into water, and the mixture was shaken for 1 hour at 1000 rpm, and then titrated with 0.1M NaOH.

References

1. Bird R.B. Bird, W.E Stewart, E.N. Lightfoot, Transport phenomena. New York, John Wiley and Sons Inc., 1960, doi:10.1002/aic.690070245.

2. EL. Cussler, Diffusion: mass transfer in fluid systems. Cambridge University Press,1984.

3. A. Giovanni, Mass transfer with chemical reaction. Amsterdam, Elsevier, 1967.

4. F. Kamenetskii, F.D. Albertovich, Diffusion and heat transfer in chemical kinetics. Princeton: Princeton University Press, 2015, doi.org/10.1515/9781400877195.

5. W.G. Whitman, The two-film theory of gas absorption. *Chem. Metall. Eng.* (29) (1923) 146-148.

6. W.G. Whitman, D.S. Davis, Comparative absorption rates for various gases. *Ind. Eng. Chem*. 16 (12) (1924) 1233-1237, doi:10.1021/ie50180a008.

7. G. Cote, Extraction liquide-liquide - Présentation générale. Technique de l'ingénieur J2760 v2. Published online 2017.

8. H. Irving, R.J.P. Williams, Order of stability of metal complexes. *Nature.* 162 (4123) (1948) 746-747.

9. L. Helm, A.E. Merbach, Inorganic and bioinorganic solvent exchange mechanisms. *Chem. Rev.* 105 (6) (2005) 1923-1960, doi:10.1021/cr030726o.

10. J. Rydberg, Solvent Extraction Principles and Practice. 2nd ed. New York: M. Dekker; 2004. rev. expanded.

11. C.B. Honaker, H. Freiser, Kinetics of extraction of zinc dithizonate. *The Journal of Physical Chemistry.* 66 (1) (1962) 127-130, doi:10.1021/j100807a027.

12. B.E. McClellan, H. Freiser, Kinetics and mechanism of extraction of zinc, nickel, cobalt, and cadmium with diphenylthiocarbazone, di-o-tolylthiocarbazone, and di-α-naphthylthiocarbazone. *Anal. Chem.* 36 (12) (1964) 2262-2265, doi:10.1021/ac60218a013.

13. H. Uslu, D. Datta, D. Santos, H.S. Bamufleh, C. Bayat, Separation of 2,4,6-trinitrophenol from aqueous solution by liquid–liquid extraction method: Equilibrium, kinetics, thermodynamics and molecular dynamic simulation. *Chemical Engineering Journal.* 299 (2016) 342-352, doi:10.1016/j.cej.2016.04.080.

14. Y. Li, G. Gokel, J. Hernandez, L. Echegoyen, Cation-exchange kinetics of sodium complexes with amide- and ester-substituted crown ethers in homogeneous solution. *J. Am. Chem. Soc.* 116 (7) (1994) 3087-3096, doi:10.1021/ja00086a043.

15. S. Swaminathan, T.R. Das, A.K. Mukherjee, Kinetics of extraction of iron(III) by bis(2-ethylhexyl)phosphoric acid in a laminar liquid-liquid jet reactor. *Ind. Eng. Chem. Res.* 26 (5) (1987) 1033-1037, doi:10.1021/ie00065a030

16. J.W. Roddy, Mechanism of the slow extraction of iron(III) from acid perchlorate solutions by di(2-ethylhexyl)phoshoric acid in n-octane. *J. Inorg. Nucl. Chem.* 33 (1971) 1099-1118.

17. J.D. Miller, R.L. Atwood, Discussion of the kinetics of copper solvent extraction with hydroxy oximes. *J. Inorg. Nucl. Chem.* 37 (12) (1975) 2539-2542, doi:10.1016/0022-1902(75)80888-8.

18. D.S. Flett, D.N. Okuhara, D.R. Spink, Solvent extraction of copper by hydroxy oximes. *J. Inorg. Nucl. Chem.* 35 (7) (1973) 2471-2487, doi:10.1016/0022-1902(73)80315-X.

19. W.J. Albery, R.A. Choudhery, P.R. Fisk, Kinetics and mechanism of interfacial reactions in the solvent extraction of copper. *Faraday Discussions of the Chemical Society*. 77 (1984) 53-65, doi:10.1039/dc9847700053.

20. W.J. Albery, R.A. Choudhery, The kinetics and mechanism of the solvent extraction of copper. *The Journal of Physical Chemistry.* 92 (5) (1988) 1142-1151, doi:10.1021/j100316a029.

21. T. Sekine, H. Inagaki, Kinetic studies of solvent extraction of metal complexes—VII. *J. Inorg. Nucl. Chem.* 42 (1) (1980) 115-117, doi:10.1016/0022-1902(80)80055-8.

22. V. Toulemonde, Liquid-liquid extraction kinetics of uranyle nitrate, actinides (III) and lanthanides (III) nitrates by amide extractants. Paris VI University, 1995.

23. M. Dal Don, Solvent extraction kinetics of lanthanides (III) and actinides (III) nitrates from aqueous nitrate solutions by malonamide molecule. PhD thesis, Paris XI University, 1997.

24. T. Sekine, H. Honda, Y. Zeniya, Kinetic studies of solvent extraction of metal complexes—VI. *J. Inorg. Nucl. Chem.* 38 (7) (1976) 1347-1350, doi:10.1016/0022-1902(76)80148-0.

25. J.A. Connor JA, N. Tindale, R.F. Dalton, Mechanistic studies of extraction of copper (II) from aqueous acid by 5-nonyl-2-hydroxybenzaldoximes in organic solvents. The effects of mixed solvents and modifiers. *Hydrometallurgy*. 26, (3) (1991) 265-280, doi:10.1016/0304-386X(91)90004-6.

26. P.R. Danesi, C. Cianetti, E.P. Horwitz, H. Diamond, Armollex: an apparatus for solvent extraction kinetic measurements. *Sep. Sci. Technol*. 17 (7) (1982) 961-968, doi:10.1080/01496398208082106.

27. J.A. Daoud, N. Abdel Rahman, H.F. Aly, Kinetic studies on the extraction of U(IV) by TBP in kerosene from nitrate medium. *J. Radioanal. Nucl. Chem*. 221 (1-2) (1997) 41-44, doi:10.1007/BF02035240.

28. I. Komasawa, T. Otake, Kinetic studies of the extraction of divalent metals from nitrate media with bis(2-ethylhexyl)phosphoric acid. *Ind. Eng. Chem.* 22 (4) (1983) 367-371, doi:10.1021/i100012a003.

29. M. Weigl, A. Geist, U. Müllich, K. Gompper, Kinetics of americium(III) extraction and back extraction with BTP. *Solvent Ext. Ion Exch*. 24 (6) (2006) 845-860, doi:10.1080/07366290600948582.

30. H. Watarai, H. Freiser, Role of the interface in the extraction kinetics of zinc and nickel ions with alkyl-substituted dithizones. *J. Am. Chem. Soc.* 105 (2) (1983) 189-190, doi:10.1021/ja00340a007.

31. P. R. Danesi, R. Chiarizia, C.F. Coleman, The kinetics of metal solvent extraction. *Crit. Rev. Anal. Chem*. 10 (1) (1980) 1-126, doi:10.1080/10408348008542724.

32. W. Nitsch, Die Behandlung der Stoffübertragung zwischen flüssigen Phasen als Problem der Grenzflächenreaktionen. *Berichte der Bunsengesellschaft für physikalische Chemie*. 69 (9-10) (1965) 884-893, doi:10.1002/bbpc.19650690922.

33. B. Dinh, Investigation of the extraction kinetics of uranyl nitrate by tributyl phosphate: application of the single drop method in pulsed medium. PhD thesis, Ecole centrale de Paris, 1986.

34. L. Bosland, Thermodynamic and kinetics study of the extraction of lanthanides nitrates by a malonamide: dimethyl dioctyl hexylethoxy malonamide. PhD thesis, Ecole centrale de Paris, 2006.

35. R. Berlemont, Kinetics extraction of uranium (VI) and plutonium(IV) using *N,N*-dialkylamides. PhD thesis, University Paris VI, 2018.

36. M. Wegener, N. Paul, M. Kraume, Fluid dynamics and mass transfer at single droplets in liquid/liquid systems. *Int. J. Heat Mass Transf.* 71 (2014) 475-495. doi:10.1016/j.ijheatmasstransfer.2013.12.024.

37. R. Clift, J.R. Grace, M.E. Weber, Bubbles, drops, and particles. New York, Academic Press, 1978.

38. J. Zhang, Y. Wang, G.W. Stevens, W. Fei, A state-of-the-art review on single drop study in liquid–liquid extraction: Experiments and simulations. *Chin. J. Chem. Eng*. 27 (12) (2019) 2857-2875. doi:10.1016/j.cjche.2019.03.025.

39. M. Adekojo Waheed, M. Henschje, A. Pfennig, Simulating sedimentation of liquid drops. *Int. J. Numer. Methods Eng*. 59 (14) (2004) 1821-1837.

40. M. Wegener, A.R.Paschedag, Mass transfer enhancement at deformable droplets due to Marangoni convection. *Int. J. Multiph. Flow,* 37 (1) (2011) 76-83, doi:10.1016/j.ijmultiphaseflow.2010.08.005.

41. B. Arendt, R. Eggers, Interaction of Marangoni convection with mass transfer effects at droplets. *Int. J. Heat Mass Transf.* 50 (13-14) (2007) 2805-2815, doi:10.1016/j.ijheatmasstransfer.2006.10.055.

42. F.H. Garner, A.H.P. Skelland. Effects of surface active agents on extraction from droplets. *Ind. Eng. Chem*. 48 (1) (1956) 51-58.

43. A. Beitel, W.J. Heideger. Surfactant effects on mass transfer from drops subject to interfacial instability. *Chem. Eng. Sci*. 26 (5) (1971) 711-717.

44. J.B. Lewis, The mechanism of mass transfer of solutes across liquid-liquid interfaces, *Chem. Eng. Sci*. 3 (1954) 248-259.

45. G.J. Hanna, R.D. Noble, Measurement of liquid-liquid interfacial kinetics. *Chem. Rev.* 85 (6) (1985) 583-598. doi:10.1021/cr00070a004.

46. W. Nitsch, K. Hillekamp, Zur kinetic der zinkionnextraktion aus wasser in dithizonbeladene solventien. *Chem-Ztg*. 96 (5) (1972) 254-261.

47. S.P. Carter, H. Freiser, Apparatus for following extraction kinetics. *Anal. Chem*. 51 (7) (1979) 1100-1101, doi:10.1021/ac50043a080.

48. P.R.Subbaraman, S. Cordes, H. Freiser, Effect of auxiliary complexing agents on the rate of extraction of zinc(II) and nickel(II) with diphenylthiocarbazone. *Anal. Chem*. 41 (13) (1969) 1878-1880, doi:10.1021/ac60282a041.

49. H. Watarai, L. Cunningham, H. Freiser, Automated system for solvent extraction kinetic studies. *Anal. Chem*. 54 (13) (1982) 2390-2392, doi:10.1021/ac00250a062.

50. W.J. Albery, J.F. Burke, E.B. Leffler, K. Hadgraft, Interfacial transfer studied with a rotating diffusion cell. *J. Chem. Soc., Faraday Trans. 1,* 72 (1976) 1618-1626, doi:10.1039/f19767201618.

51. M.A. Bromley, C. Boxall, A study of cerium extraction by TBP and TODGA using a rotating diffusion cell, *Nukleonika*. 60 (4) (2015) 589-864, doi:10.1515/nuka-2015-0121.

52. M.A. Bromley, C. Boxall, A study of cerium extraction kinetics by TODGA in acidified and non-acidified organic solvent phases in the context of fission product management, *Progress in Nuclear Science and Technology,* 5 (0) (2018) 70-73 doi:10.15669/pnst.5.70

53. J.P. Simonin, P. Turq, C. Musikas, Rotating stabilised cell: a new tool for the investigation of interfacial extraction kinetics between liquid phases, *Faraday Trans*. 17 (87) (1991) 2715-2721. doi:10.1039/ft9918702715

54. J.P. Simonin, J. Weill, Rotating membrane cell technique for the study of liquid/liquid extraction kinetics. a new tool for the investigation of interfacial extraction kinetics between liquid phases, *Solvent Ext. Ion Exch*. 16 (6) (1998) 1493-1514, doi:10.1080/07366299808934591

55. K. Osseo-Asare, Aggregation, reversed micelles, and microemulsions in liquid-liquid extraction: the tri-n-butyl phosphatediluent-water-electrolyte system, *Adv. Colloid Interface Sci*. 37 (1-2)(1991) 123-173, doi:10.1016/0001-8686(91)80041-H.

56. J. Szymanowski, Kinetics and interfacial phenomena, *Solvent Ext. Ion Exch*. 18 (4) (2000) 729-751, doi:10.1080/07366290008934705.

57. C. Erlinger, L. Belloni, T. Zemb, C. Madic, Attractive interactions between reverse aggregates and phase separation in concentrated malonamide extractant solutions, *Langmuir,* 15 (7) (1999) 2290-2300, doi:10.1021/la980313w.

58. L. Berthon, L. Martinet, F. Testard, C. Madic, T. Zemb, Solvent penetration and sterical stabilization of reverse aggregates based on the DIAMEX process extracting molecules: Consequences for the third phase formation, *Solvent Ext. Ion Exch*. 25 (5) (2007) 545-576, doi:10.1080/07366290701512576.

59. G.F. Vandegrift, E.P. Horwitz, Interfacial activity of liquid-liquid extraction reagents—I. *J. Inorg. Nucl. Chem*. 42 (1) (1980) 119-125, doi:10.1016/0022-1902(80)80056-X.

60. L. Berthon, F. Testard, L. Martinet, T. Zemb, C. Madic, Influence of the extracted solute on the aggregation of malonamide extractant in organic phases: Consequences for phase stability. *C. R. Chim.* 13 (10) (2010) 1326-1334, doi:10.1016/j.crci.2010.03.024.

61. F. Testard, L. Berthon, T. Zemb, Liquid–liquid extraction: An adsorption isotherm at divided interface? *C. R. Chim*. 10 (10-11) (2007) 1034-1041, doi:10.1016/j.crci.2007.04.014.

62. G. Martin-Gassin, P.M Gassin, L. Couston, O. Diat, E. Benichou, P.F. Brevet, Nitric acid extraction with monoamide and diamide monitored by second harmonic generation at the water/dodecane

interface. *Colloids Surf. A Physicochem. Eng. Asp*. 413 (2012) 130-135, doi:10.1016/j.colsurfa.2012.02.049.

63. P.M. Gassin, Active liquid/liquid interfaces: contributions of non linear optics and tensiometry. PhD thesis, Lyon I Univesity, 2013.

64. R. Diss, G. Wipff, Lanthanide cation extraction by malonamide ligands: From liquid–liquid interfaces to microemulsions. A molecular dynamics study. *Phys. Chem. Chem. Phys.* 7 (2) (2005) 264-272, doi:10.1039/B410137E.

65. K. Prochaska, Interfacial activity of metal ion extractant. *Adv. Colloid Interface Sci*. 95 (1) (2002) 51-72, doi:10.1016/S0001-8686(00)00084-1.

66. V. Vidyalakshmi, M.S. Subramanian, S. Rajeswari, T.G. Srinivasan, P.R. Vasudeva Rao, Interfacial tension studies of *N* , *N* -dialkyl amides, *Solvent Ext. Ion Exch*. 21 (3) (2003) 399-412, doi:10.1081/SEI-120020218.

67. J. Szymanowski, C. Tondre, Kinetics and interfacial phenomena in classical and micellar extraction systems, *Solvent Ext. Ion Exch*. 12 (4) (1994) 873-905, doi:10.1080/07366299408918243.

68. J. Zhao, X. Sun, W. Li, S. Meng, D. Li, Interfacial behavior of DEHEHP and the kinetics of cerium(IV) extraction in nitrate media, *J. Colloid Interface Sci*. (294) (2006) 429-435.

69. G. Martin-Gassin, P.M. Gassin, L. Couston, O. Diat, E. Benichou, P.F. Brevet, Second harmonic generation monitoring of nitric acid extraction by a monoamide at the water–dodecane interface, *Phys. Chem. Chem. Phys.* 13 (43) (2011) 19580-19586, doi:10.1039/c1cp22179e.

70. S. Nave, C. Mandin, L. Martinet et al. Supramolecular organisation of tri-n-butyl phosphate in organic diluent on approaching third phase transition. *Phys. Chem. Chem. Phys. 6 (4) (*2004) 799-808, doi:10.1039/b311702b.

71. D.S. Flett, Chemical kinetics and mechanisms in solvent extraction of copper chelates. *Acc. Chem. Res.* 10 (3) (1977) 99-104, doi:10.1021/ar50111a005.

72. P.R. Danesi, R. Chiarizia, Mass transfer rate with liquid ion exchangers. The role of interfacial chemical reactions in the extraction kinetics by dinonylnaphthalenesulphonic acid and trilaurylammonium salts, *J. Chem. Technol. Biotechnol.* 28 (9) (2010) 581-598. doi:10.1002/jctb.5700280901.

73. P.R. Danesi, G.F. Vandegrift, Kinetics and mechanism of the interfacial mass transfer of europium(III) and americium(III) in the system bis(2-ethylhexyl) phosphate-n-dodecane-sodium chloride-hydrochloric acid-water, *J. Phys. Chem.* 85 (24) (1981) 3646-3651, doi:10.1021/j150624a024.

74. R.G. Wilkins, Kinetics and mechanism of reactions of transition metal complexes. New York, VCH Publishers, Inc. 1991.

75. M. Eigen, K. Tamm, Schallabsorption in elektrolytlösungen als folge chemischer relaxation I. relaxationstheorie der mehrstufigen dissoziation. *Elektrochem*. 66 (93) (1962) 93-107.

76. T. Sekine, Y. Komatsu, Kinetic studies of the solvent extraction of metal complexes-IV. *J. Inorg. Nucl. Chem*. 37 (1975) 185-189.

77. S.J. Al-Bazi, H. Freiser, Mechanistic studies on the extraction of palladium(II) with dioctyl sulfide, *Solvent Ext. Ion Exch. 5* (2) (1987) 265-275, doi:10.1080/07366298708918566.

78. T. Sekine, Y. Koike, Y. Komatsu, Kinetic studies of the solvent extraction of metal complexes. I. The extraction of the beryllium(II)-TTA chelate from aqueous perchlorate media into carbon tetrachloride and methyl isobutyl ketone, *Bull. Chem. Soc. Jpn*. 44 (11) (1971) 2903-2911.

79. Z.N. Lou, Y. Xiong, J.J. Song et al. Kinetics and mechanism of Re(VII) extraction and separation from Mo(VI) with trialkyl amine, *Trans. Nonferrous Met. Soc. China, 2*0 (2010*)* 10-14. doi:10.1016/S1003-6326(10)60003-9.

80. M.C. Fuerstenau, M.R. Elmore, B.R.Palmer, KN Han, Kinetics of extraction in the cupric-chloro-quaternary amine system, *Metallurgical Transacations B, 1*8 (3) (1987) 483-488, doi:10.1007/BF02654259.

81. J. Zhao, W. Li, Y. Xiong, Kinetics of cerium(IV) extraction with DEHEHP from HNO_3 -HF medium using a constant interfacial cell with laminar flow, *Solvent Ext. Ion Exch.* 24 (2) (2006) 165-176, doi:10.1080/07366290500464078.

82. Y. Baba, K. Inoue, The kinetics of solvent extraction of palladium(II) from acidic chloride media with sulfur-containing extractants, *Ind. Eng. Chem. Res*. 27 (9) (1988) 1613-1620, doi:10.1021/ie00081a010.

83. K. Inoue, T. Maruuchi, Solvent extraction of palladium with SME 529: Equilibria and kinetics. *Hydrometallurgy, 16 (1) (*1986) 93-104, doi:10.1016/0304-386X(86)90054-X.

84. N.E. El-Hefny, S.I. El-Dessouky, Equilibrium and kinetic studies on the extraction of gadolinium(III) from nitrate medium by di-2-ethylhexylphosphoric acid in kerosene using a single drop technique. *J. Chem. Technol. Biotechnol.* 81 (3) (2006) 394-400, doi:10.1002/jctb.1408.

85. N.S. Awwad, H.A. Ibrahium, Kinetic extraction of titanium (IV) from chloride solution containing Fe(III), Cr(III) and V(V) using the single drop technique, *J. Environ. Chem. Eng*. 1 (1-2) (2013) 65-72, doi:10.1016/j.jece.2013.03.009.

86. N.S. Awwad, Equilibrium and kinetic studies on the extraction and stripping of uranium(VI) from nitric acid medium into tri-phenylphosphine oxide using a single drop column technique, *Chem. Eng. Process. 43* (12) (2004) 1503-1509, doi:10.1016/j.cep.2004.02.005.

87. J.S. Preston, Z.B. Luklinska, Solvent extraction of copper(II) with ortho-hydroxyoximes-I Kinetics and mechanism of extraction, *J. Inorg. Nucl. Chem.* 42 (1980) 431-439.

88. R.K. Biswas, M.A. Hanif, M.F. Bari, Kinetics of forward extraction of manganese(II) from acidic chloride medium by D2EHPA in kerosene using the single drop technique, *Hydrometallurgy,* 42 (3) (1996) 399-409, doi:10.1016/0304-386X(95)00102-M.

89. H.L. Finston, T. Inoue Y, The effect of SCN^- on the extraction of Fe(III)-TTA, *J. Inorg. Nucl. Chem.* 29 (1) 1967, 199-208, doi:10.1016/0022-1902(67)80159-3.

90. H.L. Finston, Y. Inoue, A rate promoted synergistic effect on the solvent extraction system Fe(III)-TTA-SCN, *J. Inorg. Nucl. Chem.* 29 (9) (1967) 2431-2440, doi:10.1016/0022-1902(67)80299-9.

91. C. Foulon, D. Pareau, G. Durand, Thermodynamic and kinetics studies of palladium (II) extraction by extractant mixtures conataining LIX 63, *Hydrometallurgy,* 51 (1999) 139-153.

92. C. Foulon, D. Pareau, M Stambouli, G. Durand, Thermodynamic and kinetic studies of palladium (II) extraction by extractant mixtures containing LIX 63. Part II. Kinetic study, *Hydrometallurgy*, 54 (1999) 49-63.

93. G. Cote, K.M. Ganguly, D. Bauer, Influence of thiocyanate ions on the kinetics and thermodynamics of palladium(II) extraction with dialkyl sulphides, *Hydrometallurgy,* 23 (1) (1989) 37-45, doi:10.1016/0304-386X(89)90016-9.

94. A. Geist, C. Hill, G. Modolo, 6,6′- *Bis* (5,5,8,8-tetramethyl-5,6,7,8-tetrahydro-benzo[1,2,4]triazin-3-yl) [2,2′]bipyridine, an effective extracting agent for the separation of americium(III) and curium(III) from the lanthanides, *Solvent Ext. Ion Exch.* 24 (4) (2006) 463-483, doi:10.1080/07366290600761936.

95. J.S. Oh, H. Freiser, Kinetics and mechanism of extraction of zinc and nickel with substituted diphenylthiocarbazones, *Anal. Chem.* 39 (3) (1967) 295-298, doi:10.1021/ac60247a007.

96. F.W. Lewis, L.M. Harwood, M.J. Hudson, Highly efficient separation of actinides from lanthanides by a phenanthroline-derived bis-triazine ligand, *J. Am. Chem. Soc.* 133 (33) (2011) 13093-13102, doi:10.1021/ja203378m.

97. F.W. Lewis, L.M. Harwood, M.J. Hudson, BTBPs versus BTPhens: some reasons for their differences in properties concerning the partitioning of minor actinides and the advantages of BTPhens. *Inorg. Chem.* 52, (9) (2013) 4993-5005, doi:10.1021/ic3026842.

98. M.C. Costa, M. Martins, A.P. Paiva, Solvent extraction of iron(III) from acidic chloride media using *N* , *N* ′-dimethyl- *N* , *N* ′-dibutylmalonamide, *Sep. Sci. Technol.* 39 (15) *(*2005) 3573-3599, doi:10.1081/SS-200036785.

99. M. Regel, A.M. Sastre, J. Szymanowski, Recovery of zinc(II) from HCl spent pickling solutions by solvent extraction, *Environ. Sci. Technol.* 35 (3) (2001) 630-635, doi:10.1021/es001470w.

100. T. Sato, T. Nakamura, M. Ikeno, The extraction of iron(III) from aqueous acid solutions by di(2-ethylhexyl)phosphoric acid, *Hydrometallurgy,* 15 (1985) (2) 209-217, doi:10.1016/0304-386X(85)90055-6.

101. J. Jayachandran, P.M Dhadke, Liquid-liquid extraction separation of iron (III) with 2-ethyl hexyl phosphonic acid mono 2-ethyl hexyl ester, *Talanta,* 44 (7) (1997) 1285-1290, doi:https://doi.org/10.1016/S0039-9140(97)02190-5.

102. S.A. Ansari, M.S. Murali, P.N. Pathak, V.K Manchanda, Separation of iron from cobalt in nitrate medium using Cyanex-923 as extractant, *J. Radioanal. Nucl. Chem.* 262 (2) (2004) 469-472, doi:10.1023/B:JRNC.0000046779.46066.fd.

103. B.R. Reddy, P.V.R. Bhaskara Sarma, Extraction of iron(III) at macro-level concentrations using TBP, MIBK and their mixtures, *Hydrometallurgy,* 43 (1-3) (1996) 299-306, doi:10.1016/0304-386X(95)00117-Y.

104. R.G. Pearson, Hard and soft acids and bases, *J. Am. Chem. Soc.* 85 (1963) 3533-3539.

105. R.G. Parr, R.G. Pearson, Absolute hardness: companion parameter to absolute electronegativity. *J. Am. Chem. Soc*. 105 (26) (1983) 7512-7516, doi:10.1021/ja00364a005.

106. J. Wang, W. Xu, H. Liu, F. Yu, H. Wang, Extractant structures and their performance for palladium extraction and separation from chloride media: A review, *Miner. Eng.* 163 (2021) 106798, doi:10.1016/j.mineng.2021.106798.

107. J. Szymanowski, D. Bauer, G. Cote, K. Prochaska, The surface activity of triisooctylamine and the mechanism of palladium (II) extraction by dihexyl sulphide in the presence of triisooctylamine, *J. Chem. Technol. Biotechnol.* 48 (1) (2007) 1-15, doi:10.1002/jctb.280480102.

108. M.J. Cleare, P. Charlesworth, D.J. Bryson, Solvent extraction in platinum group metal processing. *J. Chem. Technol. Biotechnol*. 29 (4) (2007) 210-224, doi:10.1002/jctb.503290403.

109. S.J. Al-Bazi, H. Freiser, Phase transfer catalysis in palladium extraction by 1-(2-pyridylazo)-2-naphtol (PAN), *Solvent Ext. Ion Exch.* 5 (6) (1987) 997-1016, doi:10.1080/07366298708918606.

110. G. Cote, D. Bauer, S. Daamach, Strategies for enhacement of phase-transfer rate in liquid-liquid systems: extraction of palladium (II) by dialkyl sulphides in the presence of other platinum-group metals, *J. Chem. Res.* (1989) 158-159.

111. M. Wisniewski, J. Szymanowski, G. Cote, E. Meissner, Interfacial activity and rate of palladium(II) extraction with fluorinated sulphides, *J. Chem. Techn. Biotech.* 60 (1) (1994) 31-37, doi:10.1002/jctb.280600106.

112. L. Pan, Z. Zhang, Solvent extraction and separation of palladium(II) and platinum(IV) from hydrochloric acid medium with dibutyl sulfoxide, *Miner. Eng.* 22 (15) (2009) 1271-1276, doi:10.1016/j.mineng.2009.07.006.

113. V.V. Potapov, R.A. Khisamutdinov, Y.I. Murinov, L.A. Baeva, A.D. Ulendeeva, N.K. Lyapina, Extraction of palladium(II) and platinum(IV) from hydrogen chloride solutions with 3,7-dimethyl-5-thianonane-2,8-dione and complexation of this reagent with the platinum metals, *Russ. J. of Appl. Chem.* 74 (7) (2001) 1098-1102.

114. J. Narita, K. Morisaku, K. Tamura et al. Extraction properties of palladium(II) in HCl solution with sulfide-containing monoamide compounds, *Ind. Eng. Chem. Res*. 53 (9) (2014) 3636-3640. doi:10.1021/ie404363b.

115. A. Uheida, Y. Zhang, M. Muhammed, Selective extraction of palladium (II) from chloride solutions with nonylthiourea dissolved in chloroform, *Solvent Ext. Ion Exch.* 20 (6) (2002) 717-733, doi:10.1081/SEI-120016075.

116. A. Paiva, M. Martins, O. Ortet, Palladium(II) recovery from hydrochloric acid solutions by *N,N′*-dimethyl-*N,N′*-dibutylthiodiglycolamide, *Metals,* 5 (4) (2015) 2303-2315, doi:10.3390/met5042303.

117. H. Narita, M. Tanaka, K. Morisaku, Palladium extraction with *N,N,N′,N′*-tetra-n-octyl-thiodiglycolamide, *Miner. Eng. 21 (6) (*2008) 483-488, doi:10.1016/j.mineng.2008.01.011.

118. M. Rovira, J.L. Cortina, A.M. Sastre; Selective liquid-liquid extraction of palladium (II) from hydrochloric acid media by di-(2-ethylhexyl) thiophosphoric acid (DEHTPA), *Solvent Ext. Ion Exch.* 17 (2) (1999) 333-349, doi:10.1080/07366299908934616.

119. B. Swain, J. Jeon, S.Kyoung, J. Lee, Separation of platinum and palladium from chloride solution by solvent extraction using Alamine 300, *Hydrometallurgy, 104 (*2010) 1-7, doi:10.1016/j.hydromet.2010.03.013.

120. P. Tarapcik, Extraction of palladium from nitrate solutions with TBP in tetrachloromethane, *Radiochem. Radioanal. Lett.* 49 (6) (1981) 353-359.

121. G.H. Rizvi, J.N. Mathur, M.S. Murali, R.H. Iyer, Recovery of fission product palladium from acidic high level waste solutions, *Sep. Sci. Technol. 31 (13) (1*996) 1805-1816, doi:10.1080/01496399608001011.

122. S.A. El-Reefy, J.A. Daoud, H.F. Aly, Extraction of palladium from nitrate solution by triphenylphosphine or triphenylphospine oxide in chloroform, *J. Radioanal. Nucl. Chem.* 158 (2) (1992) 303-312, doi:10.1007/BF02047117.

123. J.A. Daoud, S.A. El-Reefy, H.F. Aly, Palladium extraction by triphenylphosphine sulfide in benzene, *J. Radioanal. Nucl. Chem.* 166 (5) (1992) 441-449, doi:10.1007/BF02167789.

124. T. Fujii, H. Yamana, M. Watanabe, H. Moriyama, Extraction of palladium from nitric acid solutions by octyl(phenyl)-N,N-diisobutylcarbamoyl- methylphosphine oxide, *J. Radioanal. Nucl. Chem*. 247 (2) (2001) 435-437.

125. K. Kirishma, International conference on nuclear waste management and environmental remediation, Prague, Czech Rep., ASME. (1) (1993) 667.

126. R. Ruhela, J.N. Sharma, B.S. Tomar *et al*. *N, N, N′, N′*-tetra(2-ethylhexyl) thiodiglycolamide T(2EH)TDGA: A novel ligand for the extraction of palladium from high level liquid waste (HLLW), *Radiochim. Acta*. 98 (4) (2010), doi:10.1524/ract.2010.1712.

127. M. Elizalde, B. Menoyo, A. Ocio, M. Rúa, Palladium(II) extraction from nitric acid solutions by LIX 34, *J. Chem. Technol. Biotechnol*. 89 (6) (2014) 884-889, doi:10.1002/jctb.4327.

128. S.J. Al-bazi, Platinum metals-solution chemistry and separation methods (ion-exchange and solvent extraction), *Talanta,* 31 (10) (1984) 815-836, doi:10.1016/0039-9140(84)80204-0.

129. M.J. Hudson, An introduction to some aspects of solvent extraction chemistry in hydrometallurgy, *Hydrometallurgy,* 9 (2) (1982) 149-168, doi:10.1016/0304-386X(82)90014-7.

130. F.L. Bernardis, R.A. Grant RA, D.C. Sherrington, A review of methods of separation of the platinum-group metals through their chloro-complexes, *React. Funct. Polym.* 65 (3) (2005) 205-217.

131. Y. Baba, T. Eguchi, K. Inoue, Solvent extraction of palladium with dihexyl sulfide, *J. Chem. Eng. Japan,* 19 (5) (1986) 361-366, doi:10.1252/jcej.19.361.

132. Y. Baba, E. Toshiya, I. Katsutoshi, Solvent extraction of palladium(II) from aqueous chloride media with 1,2-bis(tert-hexylthio)ethane, *Bull. Chem. Soc. Jpn*. 59 (5) (1986) 1321-1325.

133. H. Wang, J. Pan, J. Gu, Extraction kinetics of palladium(II) with bis(2-ethylhexyl) sulfoxide from hydrochloric acid media, *Ind. Eng. Chem. Res*. 30 (6) (1991), 1257-1261.

134. J. Szymanowski, Interfacial activity of hydroxyoximes and mechanism and kinetics of palladium(ll) extraction, Journal f. prakt. Chemie. Band 333 (1) (1991).

135. E. Ma, H. Freiser, Mechanistic studies on the extraction of palladium(II) with 2-hydroxy-5-nonylbenzophenone oxime (LIX 65N), *Solvent Ext. Ion Exch.* 1, (3), (1983), 485-496, doi:10.1080/07366298308918410.

136. E. Ma, H. Freiser, Solvent extraction equilibria and kinetics in the palladium(II)-hydrochloric acid-7-(1-vinyl-3,3,5,5-tetramethylhexyl)-8-quinolinol system, *Inorg. Chem*. 23 (21) (1984), 3344-3347, doi:10.1021/ic00189a015.

137. Y. Baba, M. Iwasaki, K. Yoshizuka, K. Inoue, Kinetics of palladium (II) extraction with *N,N*-dioctylglycine, *Hydrometallurgy,* 33 (1-2) (1993) 83-93, doi:10.1016/0304-386X(93)90007-Z.

138. K. Kondo, J. Oishi, F. Nakashio, Extraction kinetics of palladium with dioctylmonothiophosphoric acid, *J. Chem. Eng. Japan*, 23 (3) (1990) 365-367.

139. K. Kondo, H. Nishio, F. Nakashio, Kinetics of solvent extraction of palladium with didocylmonothiophosphoric acid, *J. Chem. Eng. Japan,* 22 (3) (1989), 269-273.

140. A. Ohashi; S. Tsukahara, H. Watarai, Acid-catalyzed interfacial complexation in the extraction kinetics of palladium(II) with 2-(5-bromo-2-pyridylazo)-5-diethylaminophenol, *Anal. Chim. Acta*. 364 (1998) (1-3) 53-62, doi:10.1016/S0003-2670(98)00167-6.

141. K. Ohashi, K. Otsuka, Y. Meguro, S. Kamata, Kinetics of extraction of palladium(II) with o-xylylene bis-(diethyldithiocarbamate) or 3-mercapto-1,5-diphenylformazan from aqueous chloride medium, *Anal. Sci*. 4 (5) (1988) 517-521, doi:10.2116/analsci.4.517.

142. R. Poirot, D. Bourgeois, D. Meyer, Palladium extraction by a malonamide derivative (DMDOHEMA) from nitrate media: extraction behavior and third phase characterization, *Solvent Ext. Ion Exch.* 32 (5) (2014) 529-542, doi:10.1080/07366299.2014.908587.

143. R. Mastretta, R. Poirot, D. Bourgeois, D. Meyer, Palladium isolation and purification from nitrate media: Efficient process based on malonamides, *Solvent Ext. Ion Exch.* 37 (2) (2019) 140-156, doi:10.1080/07366299.2019.1630073.

144. K. Nash, A Review of the basic chemistry and recent developments in trivalent f-elements separations, *Solvent Ext. Ion Exch.* 11 (4) (1993) 729-768, doi:10.1080/07366299308918184.

145. L. Nigond, C. Musikas, Cuillerdier C. Extraction by N,N,N',N'-tetraalkyl-2-alkylpropane-1,3-diamide II. U(VI) and Pu(IV), *Solvent Ext. Ion Exch.* 12 (2)(1994) 297-323, doi:10.1080/07366299408918212.

146. C. Cuillerdier, C. Musikas, P. Hoel, L. Nigond, X. Vitart, Malonamides as new extractants for nuclear waste solutions, *Sep. Sci. Technol.* 26 (9) (1991) 1229-1244, doi:10.1080/01496399108050526.

147. G.M. Nair, D.R. Prabhu, G.R. Mahajan, Methylbutylmalonamide as an extractant for U(VI), Pu(IV) and Am(III), *J. Radioanal. Nucl. Chem.* 186 (1) (1994) 47-55, doi:10.1007/BF02163241.

148. G.R. Mahajan, D.R. Prabhu, V.K. Manchand, L.P. Badheka, Substituted malonamides as extractants for partitioning of actinides from nuclear waste solutions, *Waste Management,* 18 (2) (1998) *125-133,* doi:10.1016/S0956-053X(98)00015-4.

149. T.H. Siddall, M.L. Good, Proton magnetic resonance studies and extraction properties of some simple diamides, *J. Inorg. Nucl. Chem.* 29 (1) (1967) 149-158, doi:10.1016/0022-1902(67)80155-6.

150. L. Spjuth, J.O. Liljenzin, M. Skålberg et al. Extraction of actinides and lanthanides from nitric acid solution by malonamides, *Radiochim. Acta*. 78 (1997) 39-46, doi:10.1524/ract.1997.78.special-issue.39.

151. Y. Sasaki, S. Tachimori, Extraction of actinides (III), (IV) (V), (VI) and lanthanides (III) by structurally tailord diamides, *Solvent Ext. Ion Exch.* 20 (1) (2002), 21-34, doi:10.1081/SEI-100108822.

152. S.A. Ansari, P.K. Mohapatra, V.K. Manchanda , A novel malonamide grafted polystyrene-divinyl benzene resin for extraction, pre-concentration and separation of actinides, *J. Hazard. Mater.* 161 (2-3) (2009) 1323-1329, doi:10.1016/j.jhazmat.2008.04.093.

153. L. Rao L, P. Zanonato, P. Di Bernardo, A. Bismondo; Complexation of Eu(III) with alkyl-substituted malonamides in acetonitrile, *J. Chem. Soc., Dalton Trans.* (13) (2001) 1939-1944, doi:10.1039/b009795k.

154. B. Gannaz, R. Chiarizia, M.R. Antonio, C. Hill, G. Cote, Extraction of lanthanides(III) and Am(III) by mixtures of malonamide and dialkylphosphoric acid, *Solvent Ext. Ion Exch.* 25 (3) (2007) 313-337*,* doi:10.1080/07366290701285512.

155. P.B. Ruikar, M.S. Nagar, Synthesis and characterization of some new mono- and diamide complexes of plutonium(IV) and dioxouranium(VI) nitrates, *Polyhedron*. 14 (20-21) (1995) 3125-3132, doi:10.1016/0277-5387(95)00078-7.

156. C. Musikas, H. Hubert, Extraction by *N,N′*-tetraalkylmalonamides II, *Solvent Ext. Ion Exch.* 5 (5) (1987) 877-893, doi:10.1080/07366298708918598.

157. G. Modolo, H. Vijgen, D. Serrano-Purroy *et al.* DIAMEX counter-current extraction process for recovery of trivalent actinides from simulated high active concentrate. *Sep. Sci. Technol.* 42 (3) (2007), 439-452, doi:10.1080/01496390601120763.

158. L. Lefrançois, F. Belnet, D. Noel, C. Tondre, An Attempt to theoretically predict third-phase formation in the dimethyldibutyltetradecylmalonamide (DMDBTDMA)/dodecane/water/nitric acid extraction system. *Sep. Sci. Technol.* 34 (5) (1999) 755-770, doi:10.1080/01496399908951143.

159. L. Lefrançois, M. Hébrant, C. Tondre, J.J. Delpuech, C. Berthon, C. Madic, *Z,E* Isomerism and hindered rotations in malonamides: an NMR study of *N,N*'-dimethyl-*N,N′*-dibutyl-2-tetradecylpropane-1,3- diamide, J. Chem. Soc., Perkin Trans. 2, (1999), 1149-1158.

160. M.Soledade, C.S. Santos, A.P Paiva, Iron(III) extraction from chloride media by *N,N′*-tetrasubstituted malonamides: An interfacial study, *J. Colloid Interface Sci.* 413 (2014) 78-85, doi:10.1016/j.jcis.2013.09.017.

161. C. Erlinger, D. Gazeau, T. Zemb *et al*. Effect of nitric acid extraction on phase behavior microstructure and interactions between primary aggregates in the system dimethyldibutyltetradecylmalonamide (DMDBTDMA)/ n- dodecane/ water: A phase analysis and small angle X-Ray scattering (SAXS) characterization study, *Solvent Ext. Ion Exch.* 16 (3) (1998) 707-738, doi:10.1080/07366299808934549.

162. C. Musikas, H. Hubert, The extraction by N,N'-tetraalkylmalonamides I. The HClO4 and HNO3 extraction, *Solvent Ext. Ion Exch.* 5 (1) (1987) 151-174, doi:10.1080/07366298708918559.

163. L. Lefrançois, J.J. Delpuech, M. Hébrant, J. Chrisment, C. Tondre, Aggregation and protonation phenomena in third phase formation: an NMR study of the quaternary malonamide/dodecane/nitric acid/water system. *J. Phys. Chem. B*. 105 (13) (2001) 2551-2564, doi:10.1021/jp002465h.

164. B. Gannaz, M.R. Antonio, R. Chiarizia, C. Hill, G. Cote, Structural study of trivalent lanthanide and actinide complexes formed upon solvent extraction. *Dalton Transactions,* (38) (2006) 4553. doi:10.1039/b609492a.

165. Q. Tian Q, M.A. Hughes, The mechanism of extraction of HNO3 and neodymium with diamides, *Hydrometallurgy,* 36 (3) (1994) 315-330, doi:10.1016/0304-386X(94)90029-9.

166. L. Martinet, Supramolecular organization of organic phases for DIAMEX solvent extraction process. PhD thesis, Paris University XI, 2006.

167. B. Gannaz, R. Chiarizia, M.R. Antonion, C. Hill, G. Cote, Extraction of lanthanides(III) and Am(III) by mixtures of malonamide and dialkylphosphoric acid, *Solvent Ext. Ion Exch.* 25 (3) (2007) 313-337, doi:10.1080/07366290701285512.

168. M. Bao, G.X. Sun, Extraction of uranium (VI) with *N,N,N',N*'-tetrabutylmalonamide and *N,N,N',N'*-tetrahexylmalonamide. *J. Radioanal. Nucl. Chem.* 231 (1-2) (1998) 203-205.

169. Y.S.H. Wang, G.X. Sun, B.R. Bao, *N,N,N',N'*-tetrabutylmalonamide as a new extractant for extraction of nitric acid and uranium(VI) in toluene, *J. Radioanal. Nucl. Chem*. 224, (1-2) (1997) 151-153, doi:10.1007/BF02034629.

170. S.A. Ansari, P. Pathak, P.K. Mohapatra, V.K. Manchanda, Aqueous partitioning of minor actinides by different processes, *Sep. Purif. Rev.* 40 (1) (2011) 43-76, doi:10.1080/15422119.2010.545466.

171. J. Veliscek-Carolan J. Separation of actinides from spent nuclear fuel: A review. *J. Hazard. Mater*. 318 (2016) 266-281, doi:10.1016/j.jhazmat.2016.07.027.

172. E.A. Mowafy, H.F. Aly, Extraction behaviours of Nd(III), Eu(III), La(III), Am(III) and U(VI) with some substituted malonamides from nitrate medium, *Solvent Ext. Ion Exch.* 20 (2) (2002) 177-194, doi:10.1081/SEI-120003020.

173. E.A. Mowafy, HF Aly, Extraction behaviors of trivalent lanthanides from nitrate medium by selected substituted malonamides, *Solvent Ext. Ion Exch.* 24 (5) (2006), 677-692, doi:10.1080/07366290600762322.

174. R. Poirot, X. Le Goff, O. Diat, D. Bourgeois D. Meyer, Metal recognition driven by weak interactions: a case study in solvent extraction, *ChemPhysChem*. 17 (14) (2016) 2112-2117, doi:10.1002/cphc.201600305.

175. B.K. McNamara, G.J. Lumetta, B.M. Rapko, Extraction of Eu(III) with tetrahexylmalonamide, *Solvent Ext. Ion Exch.* 17 (6), (1999), 1403-1421 doi:10.1080/07366299908934655.

176. L. Spjuth, J.O. Liljenzin, M.J. Hudson, M.G.B. Drew, P.B. Iveson, C. Madic, Comparison of extraction behaviour and basicity of some substituted malonamides, *Solvent Ext. Ion Exch.* 18 (1) (2000), doi:10.1080/07366290008934669.

177. P. Malik, A.P. Paiva, Solvent extraction of rhodium from chloride media by *N* , *N* ′-dimethyl- *N* , *N* ′-diphenyltetradecylmalonamide, *Solvent Ext. Ion Exch.* 26 (1) (2008) 25-40, doi:10.1080/07366290701784126.

178. P. Malik, A.P. Paiva, A novel solvent extraction route for the mutual separation of platinum, palladium, and rhodium in hydrochloric acid media. *Solvent Ext. Ion Exch.* 28 (1) (2010) 49-72, doi:10.1080/07366290903408599.

179. P. Malik, A.P. Paiva, Liquid-liquid extraction of ruthenium from chloride media by *N,N'* -dimethyl- *N,N'* -dicyclohexylmalonamide, *Solvent Ext. Ion Exch.* 29 (2) (2011) 176-189, doi:10.1080/07366299.2011.539463.

180. M.C. Costa, A. Assunção, C. Nogueira, A.P. Paiva, Liquid-liquid extraction of platinum from chloride media by *N,N* ′-dimethyl- *N,N*′-dicyclohexyltetradecylmalonamide, *Solvent Ext. Ion Exch.* 31 (1) (2013) 12-23, doi:10.1080/07366299.2012.700588.

181. A.P. Paiva, G.I. Carvalho, M.C. Costa, C. Nogueira, The solvent extraction performance of *N,N'* -dimethyl- *N,N'* -dibutylmalonamide towards platinum and palladium in chloride media, *Sep. Sci. Technol.* 49 (7) (2014) 966-973, doi:10.1080/01496395.2013.878721.

182. E.A. Mowafy, D. Mohamed, Recovery of palladium from concentrated nitrate solutions with N,N' -2-dimethyl-N,N'-dioctyltetradecylmalonamide as new extractant. *Orient J. Chem*. 33 (5) (2017) 2377-2385, doi:10.13005/ojc/330530.

183. M. Charbonnel, M. Dal Don, C.Berthon, M. Presson, C. Madic, C. Moulin, Extraction of lanthanides (III) and actinides (III) by N,N'-substituted malonamides: Thermodynamic and kinetics data. *Proceedings of ISEC*. (1999) 1333-1338.

184. M. Weigl, A. Geist, K. Gompper, J.I. Kim, Kinetics of lanthanide/actinide co-extraction with N,N'-diemthyl-N,N'-dibutyltetradecylmalonic diamide (DMDBTDMA), *Solvent Ext. Ion Exch.* 19 (2) (2001) 215-229. doi:10.1081/SEI-100102692.

185. J.P. Simonin, L. Perigaud, K. Perrgaud, T.H. Vu, Kinetics of liquid/liquid extraction of europium(III) cation by two malonic diamides, *Solvent Ext. Ion Exch.* 32 (4) (2014) 365-377.

186. G. Hellé, C. Mariet, G. Cote, Liquid–liquid microflow patterns and mass transfer of radionuclides in the systems Eu(III)/HNO3/DMDBTDMA and U(VI)/HCl/Aliquat® 336, *Microfluidics and Nanofluidics,* 17 (6) (2014) 1113-1128, doi:10.1007/s10404-014-1403-1.

187. Vansteene A, Jasmin JP, Cote G, Mariet C. Segmented Microflows as a Tool for Optimization of Mass Transfer in Liquid−Liquid Extraction: Application at the Extraction of Europium(III) by a Malonamide. *Industrial & Engineering Chemistry Research*. 2018;57(34):11572-11582. doi:10.1021/acs.iecr.8b02079.

188. S. Sriram, P.K. Mohapatra, A.K. Pandey, V.K. Manchanda, L.P. Badheka, Facilitated transport of americium(III) from nitric acid media using dimethyldibutyltetradecyl-1,3-malonamide. *J. Membr. Sci.* 177 (1-2) (2000) 163-175, doi:10.1016/S0376-7388(00)00474-9.

189. F. Testard, P. Bauduin, L. Martinet *et al.* Self-assembling properties of malonamide extractants used in separation processes, *Radiochim. Acta*. 96 (4-5) (2008) 265-272 doi:10.1524/ract.2008.1487.

190. B. Abécassis, F. Testard, T. Zemb, L. Berthon, C. Madic, Effect of *n* -octanol on the structure at the supramolecular scale of concentrated dimethyldioctylhexylethoxymalonamide extractant solutions, *Langmuir,* 19 (17) (2003) 6638-6644, doi:10.1021/la034088g.

191. P. Bauduin, F. Testard, L. Berthon, T. Zemb, Relation between the hydrophile/hydrophobe ratio of malonamide extractants and the stability of the organic phase: investigation at high extractant concentrations, *Phys. Chem. Chem. Phys.* 9, (28) (2007) 3776, doi:10.1039/b701479a.

192. B. Braibant, Preparation and study of fluorinated systems for the liquid/liquid extraction of strategic metals. PhD thesis. University of Montpellier, 2018.

193. P.B. Ruikar, M.S. Nagar, Synthesis and characterization of some new mono- and diamide complexes of plutonium(IV) and dioxouranium(VI) nitrates, *Polyhedron*. 14 (20-21) (1995) 3125-3132, doi:10.1016/0277-5387(95)00078-7.

194. P.B. Ruikar, D.R. Prabhu, G.R. Mahajan, M.S. Nagar, G.M. Nair, M.S. Subramanian, The Synthesis and Characterisation of Some Aliphatic Monoamides and Diamide*s,* Radiochemistry Division, BARC, Bombay; 1992.

195. S. Wahu, J.C. Berthet, P. Thuéry *et al.* Structural versatility of uranyl(VI) nitrate complexes that involve the diamide ligand Et2N(C=O)(CH2)n(C=O)NEt2 ($0 \leq n \leq 6$), *Eur. J. of Inorg. Chem.* (23) (2012) 3747-3763, doi:10.1002/ejic.20200243.

196. P.R.V. Rao, R. Dhamodaran, T.G. Srinivasan, C.K. Mathews, The effect of diluent on third phase formation in thorium nitrate- TBP system: some novel empirical correlations, *Solvent Ext. Ion Exch.* 11 (4) (1993) 645-662 doi:10.1080/07366299308918179.

197. S.J. Chen, D.F. Evans, B.W Ninham, D.J. Mitchell, F.D. Blum, S. Pickup, Curvature as a determinant of microstructure and microemulsions. *J Phys. Chem*. 90 (5) 842-847 doi:10.1021/j100277a027.

198. B.F. Smith, K.V. Wilson, P.R. Gibson, M.M. Jones, G.D. Jarvinen, Amides as phase modifiers for *N,N'*-tetraalkylmalonamide extraction of actinides and lanthanides from nitric acid solutions, *Sep. Sci. Technol.* 32 (1-4) (1997) 149-173, doi:10.1080/01496399708003192.

199. C. Déjugnat, L. Berthon, V. Dubois *et al.* Liquid-liquid extraction of acids and water by a malonamide: I-anion specific effects on the polar core microstructure of the aggregated malonamide, *Solvent Ext. Ion Exch.* 32 (6) (2014) 601-619, doi:10.1080/07366299.2014.940229.

200. L. Nigond, Prpopriétés extractantes des *N,N,N',N*'-tetraalkyl-alkyl-2 propane diamides-1,3. PhD thesis. University of Clermont-Ferrand II. 1992.

201. J.N. Mathur, Synergism of trivalent actinides and lanthanides, *Solvent Ext. Ion Exch.* 1 (2) (1983) 349-412, doi:10.1080/07366298308918406.

202. G.J. Lumetta, B.K. McNamara, B.M.Rapko, J.E. Hutchison, Complexation of uranyl ion by tetrahexylmalonamides: an equilibrium modeling and infrared spectroscopic study, *Inorg. Chim. Acta*. 293 (2) (1999) 195-205, doi:10.1016/S0020-1693(99)00238-8.

203. R. Poirot, Palladium extraction by a malonamide; Behavior and specificities compared to lanthanides. PhD thesis. University of Montpellier, 2014.

204. R.J. Knight, R.N. Sylva, Spectrophotometric investigation of iron (III) hydrolysis in light and heavy water at 25°C. *J. Inorg. Nucl. Chem.* 37 (1975) 779-783.

205. R. Milburn, W.C. Vosburgh, A spectrophotometric study of the hydrolysis of iron(III) ion. II. Polynuclear species, *J. Am. Chem. Soc*. 77 (1954) 1352-1354.

206. W. Schneider, Hydrolysis of Iron(III)…Chaotic Olation Versus Nucleation, *Comments Inorg. Chem*. 3 (4) (1984) 205-223.

207. A.L. Rose, T. David Waite, Reconciling kinetic and equilibrium observations of iron(III) solubility in aqueous solutions with a polymer-based model, *Geochim. Cosmochim. Acta*. 71 (23) (2007) 5605-5619, doi:10.1016/j.gca.2007.02.024.

208. M.A. Blesa, E. Matijević, Phase transformations of iron oxides, oxohydroxides, and hydrous oxides in aqueous media. *Adv. Colloid Interface Sci.* 29 (3-4) (1989) 173-221. doi:10.1016/0001-8686(89)80009-0.

209. P.L. Brown, R.N. Sylva, The hydrolysis of metal ions. Part 9. Iron(iii) in perchlorate, nitrate, and chloride media, *J. Chem. Soc. Dalton Trans.*(1986) 1901-1906.

210. C.H. Chang, E.I. Franses, Adsorption dynamics of surfactants at the air/water interface: a critical review of mathematical models, data, and mechanisms. *Colloids Surf. A Physicochem. Eng. Asp*.100 (1995) 100:1-45. doi:10.1016/0927-7757(94)03061-4.

211. L. Lefrançois L. Analyse et nouvelle approche prédictive du phénomène de formation d'une troisième phase dans les systèmes (alkymalonamide-hydrocarbure-acide-eau). PhD thesis, University of Nancy 1, 1999.

212. C. Erlinger, Towards a physical interpretation of third phase formation in liquid-liquid extraction. Application to the diamex process for the treatment of high radioactive nuclear wastes. PhD thesis, University of Paris XI, 1998.

213. W. Harkins, E. Graffon, Monomolecular films on water: The oriented adsorption of derivatives of benzene. *J. Am. Chem. Soc*. 47 (1925) 1329-1335.

214. H. Bruchertseifer, R. Cripps, S. Guentay, B. Jaeckel, Analysis of iodine species in aqueous solutions. *Anal. Bioanal. Chem*. 375 (8) (2003) 1107-1110, doi:10.1007/s00216-003-1779-3.

215. A.D. Awtrey, R.E. Connick, The absorption spectra of I_2 , I_3^- , I^- , IO_3^- , $S_4O_6^-$ and $S_2O_3^-$. Heat of the Reaction $I_3^- = I_2 + I^-$, *J. Am. Chem. Soc*. 73 (4) (1951) 1842-1843, doi:10.1021/ja01148a504.

216. R. Nagl, P. Zimmermann, T. Zeiner, Interfacial mass transfer in water–toluene systems. *J. Chem. Eng. Data*. 265 (2) (2020) 328-336, doi:10.1021/acs.jced.9b00672.

217. A.K. Das, Studies on the kinetics and mechanism of complex formation in the reactions of ferron with iron(III) and uranium(VI), *Ind. J. Chem.* 33A (1994) 740-745.

218. R. Chiarizia, P.R. Danesi, S. Fornarini, Extraction kinetics of iron(III) from aqueous nitrate solutions to toluene solutions of tri-n-butylacetohydroxamic acid, *J. Inorg. Nucl. Chem.* 41 (10) (1979) 1465-1474, doi:10.1016/0022-1902(79)80213-4.

219. DAS P, Bhattacharya S, Banerjee R. Thermodynamic and kinetic studies on the iron(III)-hydroxamate interaction in acid media. *J Coord Chem*. 1989;19:311-320.

220. K.J. Hall, T.I. Quickenden, D.W. Watts, Rate constants from initial concentration data, *J .Chem. Educ*. 53 (8) (1976), doi:10.1021/ed053p493

221. P.D. Wentzell, S.R. Crouch, Comparison of reaction-rate methods of analysis for systems following first-order kinetics, *Anal. Chem*. 58 (13) (1986) 2855-2858, doi:10.1021/ac00126a059

222. J. Casado, M.A. Lopez-Quintela, F.M. Lorenzo-Barral, The initial rate method in chemical kinetics: Evaluation and experimental illustration, *J. Chem. Educ*. 63 (5) (1986) 450, doi:10.1021/ed063p450.

223. R.K. Biswas, D.A. Begum, Kinetics of extraction and stripping of Ti(IV) in HCl–D2EHPA–kerosene system using the single drop technique, *Hydrometallurgy*, 55 (2000) 57-77.

224. M.I. Saleh, M.F. Bari, M.S. Jab, B. Saad, Kinetics of lanthanum(III) extraction from nitrate-acetato medium by Cyanex 272 in toluene using the single drop technique*, Hydrometallurgy,* 67 (1-3) (2002) 45-52, doi:10.1016/S0304-386X(02)00140-8

225. D.E. Davey, R.W. Cattrall, T.J. Cardwell, R.J. Magee, The rate of mass transfer of metal chlorides between hydrochloric acid and alkylammonium chloride solutions—I. *J. Inorg. Nucl. Chem. 40 (6) (*1978) 1135-1140, doi:10.1016/0022-1902(78)80524-7.

226. X. Zeng, J.A. Mathews, J. Li, Urban mining of E-waste is becoming more cost-effective than virgin mining, *Environ. Sci. Technol*. 52 (8) (2018) 4835-4841, doi:10.1021/acs.est.7b04909.

227. M. Simoni, E.P. Kuhn, L.S. Morf, R. Kuendig, F. Adam, Urban mining as a contribution to the resource strategy of the Canton of Zurich, *Waste Management, 45 (*2015) 10-21, doi:10.1016/j.wasman.2015.06.045.

228. F. Tesfaye, D. Lindberg, J. Hamuyuni, P. Taskinen , L. Hupa, Improving urban mining practices for optimal recovery of resources from e-waste. *Miner. Eng*. 111 (2017) 209-221, doi:10.1016/j.mineng.2017.06.018

229. Y. Geng, J. Fu, J. Sarkis, B. Xue, Towards a national circular economy indicator system in China: an evaluation and critical analysis. *J. Clean. Prod. 23 (1) (*2012) 216-224, doi:10.1016/j.jclepro.2011.07.005.

230. J. Park, J. Sarkis, Z. Wu, Creating integrated business and environmental value within the context of China's circular economy and ecological modernization, *J. Clean Prod*. 18 (15) 2010 1494-1501, doi:10.1016/j.jclepro.2010.06.001.

231. W. McDowall, Y. Geng, B. Huang, Circular economy policies in China and Europe, *J. Ind. Ecol*. 21 (3) (2017) 651-661, doi:10.1111/jiec.12597.

232. European Commission (EC). Communication from the commission; Europe 2020, A Strategy for Smart, Sustainable and Inclusive Growth, COM (2010) 2020 Final; European Commission (EC): Brussels, Belgium. eur-lex.europa.eu.

233. K. Nose, T.H. Okabe, Chapter 2.10 - Platinum group metals production. In: Seetharaman S, ed. *Treatise on Process Metallurgy*. Elsevier; 2014:1071-1097. doi:10.1016/B978-0-08-096988-6.00018-3

234. S.K. Padamata, A.S. Yasinskiy, P.V. Polyakov, E.A. Pavlov, DYu. Varyukhin, Recovery of noble metals fromsSpent catalysts: A review, *Metall. Mater Trans. B,* 51 (5) (2020) 2413-2435, doi:10.1007/s11663-020-01913-w

235. Cowley A. Johnson Matthey PGM Market Report February 2021. 2021. Published 2021. https://matthey.com/-/media/files/pgm-market/pgm-market-report-may-21-english.pdf

236. A.K. Awasthi, F. Cucchiella, I. D'Adamo, Modelling the correlations of e-waste quantity with economic increase, *Sci. Total Environ*. 613-614 (2018) 46-53, doi:10.1016/j.scitotenv.2017.08.288.

237. J. Tollefson, Worth its weight in platinum, *Nature,* 450 (7168) (2007) 334-335, doi:10.1038/450334a.

238. D. Bourgeois, V. Lacanau, R. Mastretta, C. Contino-Pépin, D. Meyer, A simple process for the recovery of palladium from wastes of printed circuit boards, *Hydrometallurgy,* 191 (2020) 105241, doi:10.1016/j.hydromet.2019.105241.

239. V. Lacanau, F. Bonneté, P. Wagner *et al.* From electronic waste to Suzuki−Miyaura cross-coupling reaction in water: direct valuation of recycled palladium in catalysis, *ChemSusChem.* 13 (19) (2020) 5224-5230, doi:10.1002/cssc.202001155.

240. D. Fontana, M. Pietrantonio, S. Pucciarmati, G.N. Torelli, C. Bonomi, F. Masi, Palladium recovery from monolithic ceramic capacitors by leaching, solvent extraction and reduction*, J. Mater. Cycles Waste Manag*. 20 (2) (2018) 1199-1206, doi:10.1007/s10163-017-0684-3.

241. E.Y. Yazici, H. Deveci, Extraction of metals from waste printed circuit boards (WPCBs) in H2SO4–CuSO4–NaCl solutions, *Hydrometallurgy,* 139 (2013) 30-38, doi:10.1016/j.hydromet.2013.06.018.

242. S. Ilyas, R.R. Srivastava, H. Kim, H.A. Cheema, Hydrometallurgical recycling of palladium and platinum from exhausted diesel oxidation catalysts, *Sep. Purif. Technol.* 248 (2020) 117029, doi:10.1016/j.seppur.2020.117029.

243. A. Ashiq, J. Kulkarni, M. Vithanage, Chapter 10 - Hydrometallurgical recovery of metals from E-waste, *Electronic Waste Management and Treatment Technology,* (2019) 225-246, doi:https://doi.org/10.1016/B978-0-12-816190-6.00010-8.

244. M. Kaya, Recovery of metals and nonmetals from electronic waste by physical and chemical recycling processes, *Waste Manag. 57 (2016)* 64-90, doi:10.1016/j.wasman.2016.08.004.

245. V. Manchanda, Amides and diamides as promising extractants in the back end of the nuclear fuel cycle: an overview, *Sep. Purif. Technol.* 35 (2) (2004) 85-103, doi:10.1016/j.seppur.2003.09.005.

246. J.Y. Lee, J. Kumar Rajesh, J.S. Kim, H.K. Park, H.S. Yoon, Liquid–liquid extraction/separation of platinum(IV) and rhodium(III) from acidic chloride solutions using tri-iso-octylamine, *J. Hazard. Mater.* 168 (1) (2009) 424-429, doi:10.1016/j.jhazmat.2009.02.056.

247. J.Y. Lee, J.R. Kumar, J.S Kim, D.J. Kim, H.S. Yoon, Extraction and separation of Pt(IV)/Rh(III) from acidic chloride solutions using Aliquat 336, *J. Ind. Eng. Chem*. 15 (3) (2009) 359-364, doi:10.1016/j.jiec.2008.12.006

248. A. Cieszynska, D. Wieczorek, Extraction and separation of palladium(II), platinum(IV), gold(III) and rhodium(III) using piperidine-based extractants, *Hydrometallurgy,* 175 (2018) 359-366, doi:https://doi.org/10.1016/j.hydromet.2017.12.019.

249. V.V. Belova, A.I. Khol'kin, T.I. Zhidkova, Extraction of platinum-group metals from chloride solutions by salts of quaternary ammonium bases and binary extractants, *Theor. Found. Chem. Eng.* 41 (5) (2007) 743-751, doi:10.1134/S004057950705051X.

250. K. Inoue, T. Furusawa, I. Nagamatsu, Y. Baba, K. Yoshizuka, Solvent extraction of palladium (II) with trioctylmethylammonium chloride. *Solvent Ext. Ion Exch.* 6 (5) (1988) 755-769, doi:10.1080/07366298808917964.

251. A. Jaree, N. Khunphakdee, Separation of concentrated platinum(IV) and rhodium(III) in acidic chloride solution via liquid–liquid extraction using tri-octylamine, *J. Ind. Eng. Chem.* 17 (2) (2011) 243-247, doi:10.1016/j.jiec.2011.02.013

252. E.A. Mezhov, V.V. Druzhenkov, A.N. Sirotinin, Study of extraction of palladium from nitric acid solutions with nitrogen-containing compounds, as applied to recovery of fission palladium from spent nuclear fuel of nuclear power plants: 3. Optimization of extraction process for palladium recovery and refining, *Radiochemistry,* 44 (2) (2002) 141-145.

253. V. Mikulaj, F. Macášek, P. Rajec, Simultaneous extraction of palladium and technetium from nitrate solutions with tri-n-octylamine. *J. Radioanal. Chem*. 51 (1) (1979), 55-62, doi:10.1007/BF02519923.

254. A. Zhang, G. Wanyan, M Kumagai, Extraction chemistry of palladium(II). Mechanism of antagonistic synergistic extraction of palladium by a 4-aroyl derivative of 1-phenyl-3-methyl-pyrazolone-5- one and trialkylamine of high molecular weight, *Transition Metal Chemistry,* 29 (5) (2004) 571-576, doi:10.1023/B:TMCH.0000037532.41519.61.

255. E.L. Smith, J.E. Page, The acid-binding properties of long-chain aliphatic amines, *J. Chem. Technol. Biotechnol*. 67, (2) (1948) 48-51, doi:10.1002/jctb.5000670203.

256. V. Vdovenko, M. Koval's Kaya, Y. Shirvinskii, Extraction of sulphuric acid solutions of thorium by octylamine, *Radiokhimiya,* 3 (1961) 1-6.

257. M. Hébrant, Metal ion extraction in microheterogeneous systems, *Coord. Chem. Rev. 253 (17-18) (*2009) 2186-2192, doi:10.1016/j.ccr.2009.03.006.

258. C. Tondre, M. Hébrant, H. Watarai, Rate of interfacial reactions compared to bulk reactions in liquid–liquid and micellar processes: An attempt to clarify a confusing situation, *J. Colloid Interface Sci.* 243 (1) (2001) 1-10, doi:10.1006/jcis.2001.7889.

Appendix I

I. Mass transfer kinetics

A. Extraction with DBMA

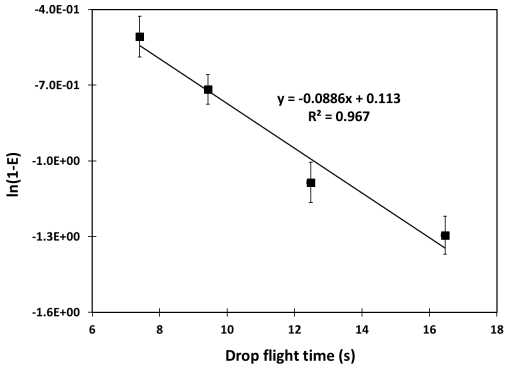

Figure 105: Dependence of ln(1-E) as a function of time for the extraction of Nd(III) with 0.6M DBMA in toluene. Initial $[Nd]_{aq}$ 1 $g.L^{-1}$, $[HNO_3]_{aq}$ 3M, T = 21°C.

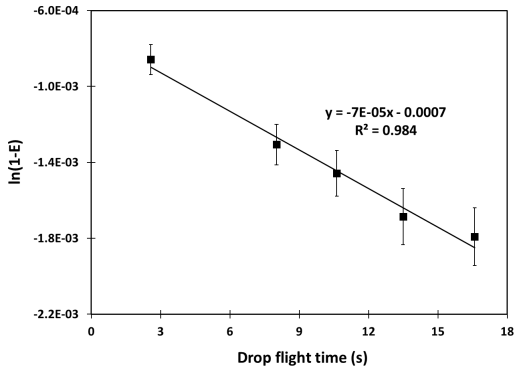

Figure 106: Dependence of ln(1-E) as a function of time for the extraction of Fe(III) with 0.6M DBMA in toluene. Initial $[Fe]_{aq}$ 10 $g.L^{-1}$, $[HNO_3]_{aq}$ 3M, T = 21°C.

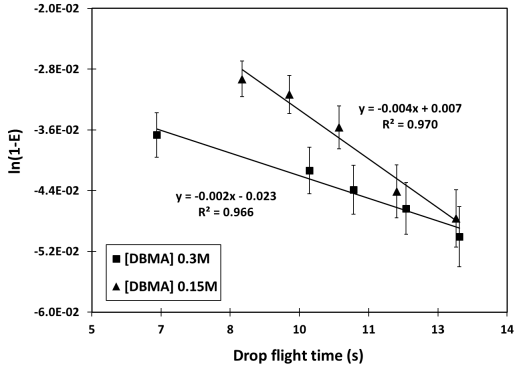

Figure 107: Dependence of ln(1-E) as a function of time for the extraction of Pd(II) with DBMA in toluene. Initial $[Pd]_{aq}$ 1 $g.L^{-1}$, $[HNO_3]_{aq}$ 3M, T = 21°C.

B. Extraction of Fe(III) and Nd(III) with THMA

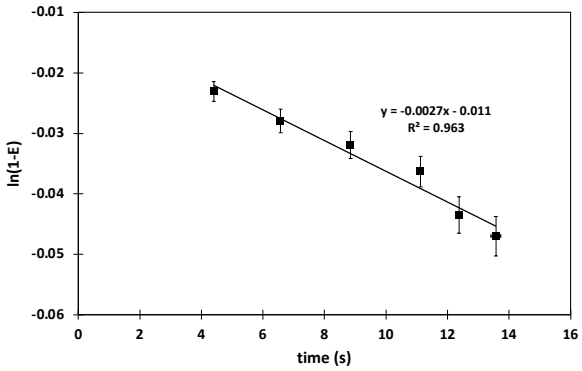

Figure 108: Dependence of ln(1-E) as a function of time for the extraction of Fe(III) with 0.6M THMA in toluene. Initial $[Fe]_{aq}$ 10 $g.L^{-1}$, $[HNO_3]_{aq}$ 3M, T = 21°C.

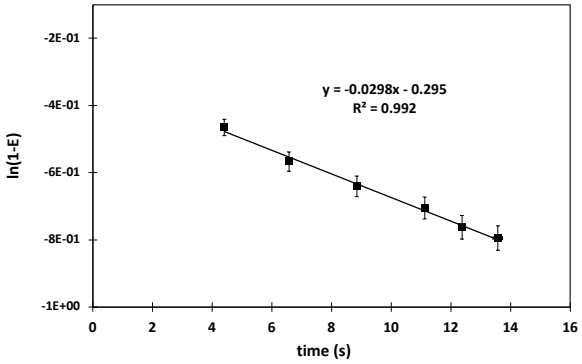

Figure 109: Dependence of ln(1-E) as a function of time for the extraction of Nd(III) with 0.6M THMA in toluene. Initial $[Nd]_{aq}$ 1 $g.L^{-1}$, $[HNO_3]_{aq}$ 3M, T = 21°C.

C. Extraction of Fe(III) with THMA

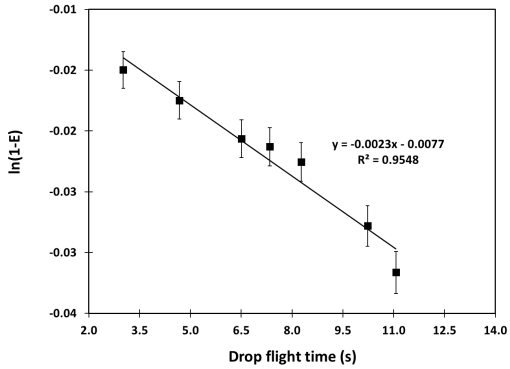

Figure 110: Dependence of ln(1-E) as a function of time for the extraction of Fe(III) with 0.8M THMA in toluene. Initial $[Fe]_{aq}$ 7 $g.L^{-1}$, $[H^+]_{aq}$ 1.5M, $[NO_3^-]_{aq}$ 2M, T = 21°C.

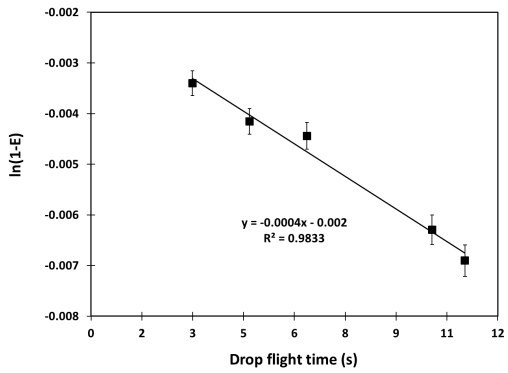

Figure 111: Dependence of ln(1-E) as a function of time for the extraction of Fe(III) with 0.8M THMA in toluene. Initial $[Fe]_{aq}$ 7 $g.L^{-1}$, $[H^+]_{aq}$ 1.5M, $[NO_3^-]_{aq}$ 3M, T = 21°C.

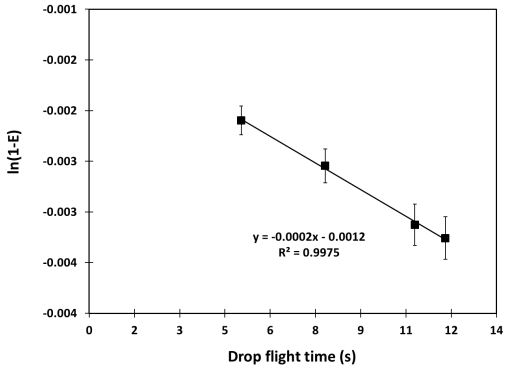

Figure 112: Dependence of ln(1-E) as a function of time for the extraction of Fe(III) with 0.8M THMA in toluene. Initial $[Fe]_{aq}$ 7 $g.L^{-1}$, $[H^+]_{aq}$ 1.5M, $[NO_3^-]_{aq}$ 4M, T = 21°C.

D. Global transfer constants of Pd(II) with THMA and DBMA

The experiments carried out with the single drop technique to validate the partial order of H^+ with DBMA and THMA allowed to establish global transfer constants of Pd(II).

Table 52: Global transfer constants and distribution ratios of Pd(II) in extraction with 0.2M THMA and 0.2M DBMA in toluene for different concentrations of H^+ $[NO_3^-]_{aq}$ 5M, T=21°C.

	DBMA	**THMA**
$[H^+]$ = 1.5M	D_{Pd} = 5.5	D_{Pd} = 173
	K_{org}^{g} ($m.s^{-1}$) = (1.36 ± 0.15)*10^{-6}	K_{org}^{g} ($m.s^{-1}$) = (1.28 ± 0.18)*10^{-8}
$[H^+]$ = 3M	D_{Pd} = 7.1	D_{Pd} = 64
	K_{org}^{g} ($m.s^{-1}$) = (1.78 ± 0.11)*10^{-6}	K_{org}^{g} ($m.s^{-1}$) = (2.69 ± 0.27)*10^{-8}
$[H^+]$ = 5M	D_{Pd} = 8.5	D_{Pd} = 14.5
	K_{org}^{g} ($m.s^{-1}$) = (2.01 ± 0.23)*10^{-6}	K_{org}^{g} ($m.s^{-1}$) = (9.19 ± 0.47)*10^{-8}

Appendix II

I. Validation of the methodology with the single drop technique

A. Extraction of Pd(II) with DBMA

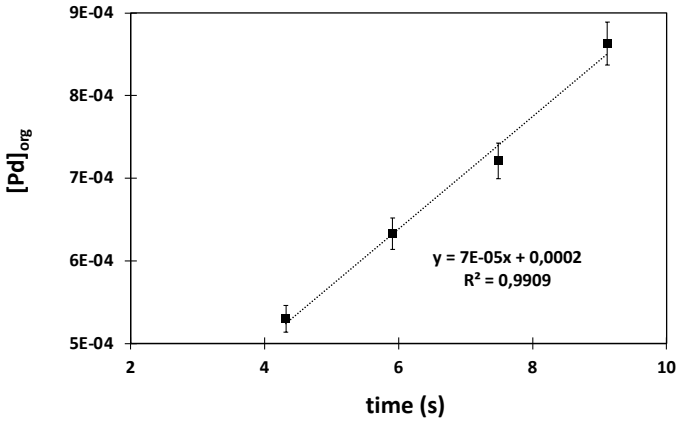

Figure 113: Dependence of $[Pd]_{org}$ as a function of time for the extraction of Pd(II) with 0.2M DBMA in toluene. Initial $[Pd]_{aq}$ 200 mg.L^{-1}, $[H^+]_{aq}$ 3M, $[NO_3^-]_{aq}$ 5M, T=21°C.

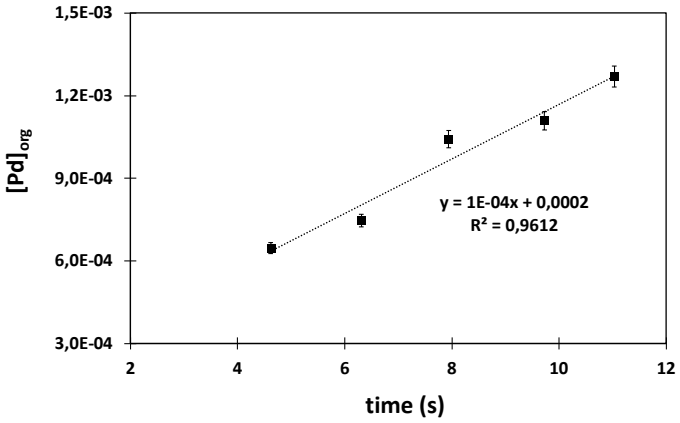

Figure 114: Dependence of $[Pd]_{org}$ as a function of time for the extraction of Pd(II) with 0.2M DBMA in toluene. Initial $[Pd]_{aq}$ 200 mg.L^{-1}, $[H^+]_{aq}$ 5M, $[NO_3^-]_{aq}$ 5M, T=21°C.

Table 53: Determination of R_f for the extraction of Pd(II) with 0.2M DBMA in toluene. Initial $[Pd]_{aq}$ 200 mg.L^{-1}, $[NO_3^-]_{aq}$ 5M.

	Slope	d (m)	R_f (mol.m^{-2}.s^{-1})
$[H^+]_{aq}$ 3M	$(6.81 \pm 0.46)*10^{-5}$	$2.12*10^{-3}$	$(2.4 \pm 0.16)*10^{-8}$
$[H^+]_{aq}$ 5M	$(9.89 \pm 1.14)*10^{-5}$	$2.10*10^{-3}$	$(3.46 \pm 0.41)*10^{-8}$

B. Extraction of Pd(II) with THMA

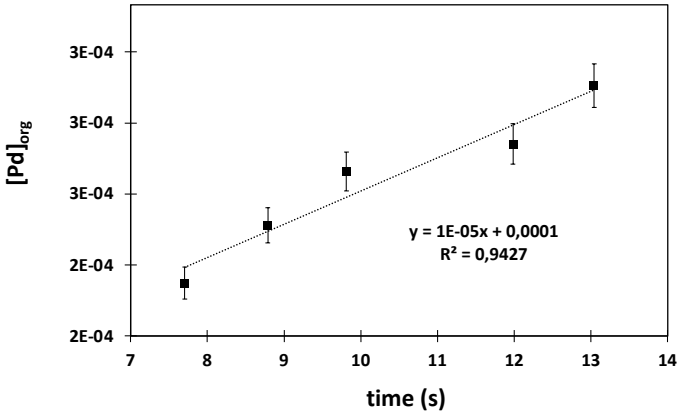

Figure 115: Dependence of $[Pd]_{org}$ as a function of time for the extraction of Pd(II) with 0.2M THMA in toluene. Initial $[Pd]_{aq}$ 200 mg.L^{-1}, $[H^+]_{aq}$ 1.5M, $[NO_3^-]_{aq}$ 5M, T=21°C.

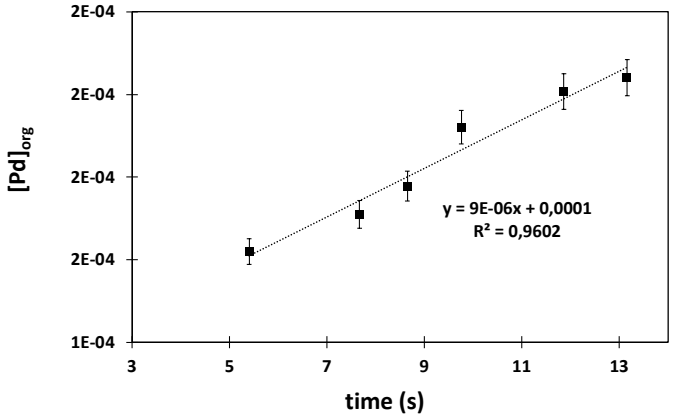

Figure 116: Dependence of $[Pd]_{org}$ as a function of time for the extraction of Pd(II) with 0.2M THMA in toluene. Initial $[Pd]_{aq}$ 200 mg.L^{-1}, $[H^+]_{aq}$ 3M, $[NO_3^-]_{aq}$ 5M, T=21°C.

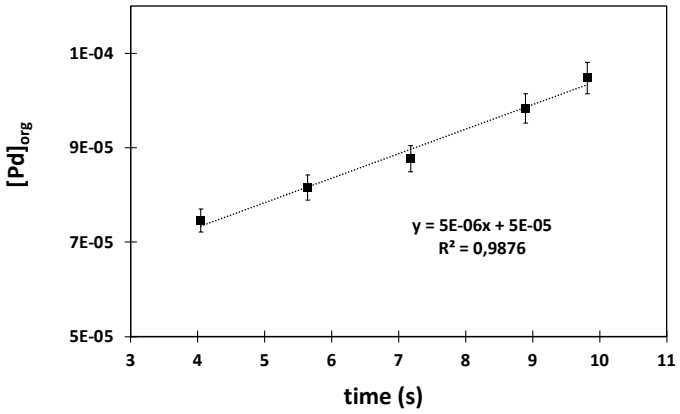

Figure 117: Dependence of $[Pd]_{org}$ as a function of time for the extraction of Pd(II) with 0.2M THMA in toluene. Initial $[Pd]_{aq}$ 200 mg.L^{-1}, $[H^+]_{aq}$ 5M, $[NO_3^-]_{aq}$ 5M, T=21°C.

Table 54: Determination of R_f for the extraction of Pd(II) with 0.2M THMA in toluene. Initial $[Pd]_{aq}$ 200 mg.L^{-1}, $[NO_3^-]_{aq}$ 5M.

	Slope	**d (m)**	**R_f (mol.m^{-2}.s^{-1})**
$[H^+]_{aq}$ 1.5M	$(1.40 \pm 0.19)*10^{-5}$	$1.99*10^{-3}$	$(4.7 \pm 0.66)*10^{-9}$
$[H^+]_{aq}$ 3M	$(8.83 \pm 0.89)*10^{-6}$	$1.99*10^{-3}$	$(2.93 \pm 0.29)*10^{-9}$
$[H^+]_{aq}$ 3M	$(5.18 \pm 0.33)*10^{-6}$	$1.93*10^{-3}$	$(1.67 \pm 0.10)*10^{-9}$

C. Extraction of Fe(III) with THMA

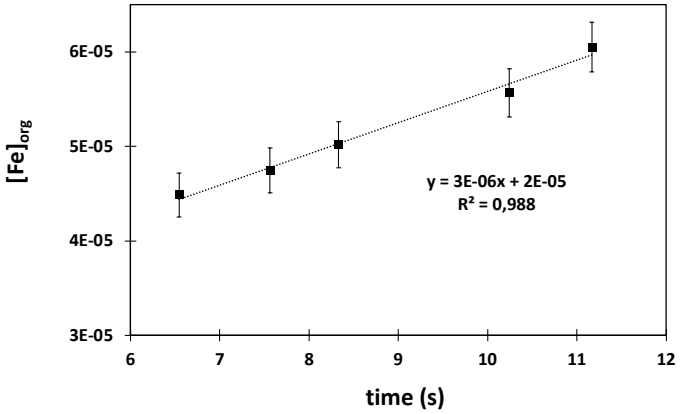

Figure 118: Dependence of $[Fe]_{org}$ as a function of time for the extraction of Fe(III) with 0.8M THMA in toluene. Initial $[Fe]_{aq}$ 7 g.L^{-1}, $[H^+]_{aq}$ 1.5M, $[NO_3^-]_{aq}$ 1.5M, T=21°C.

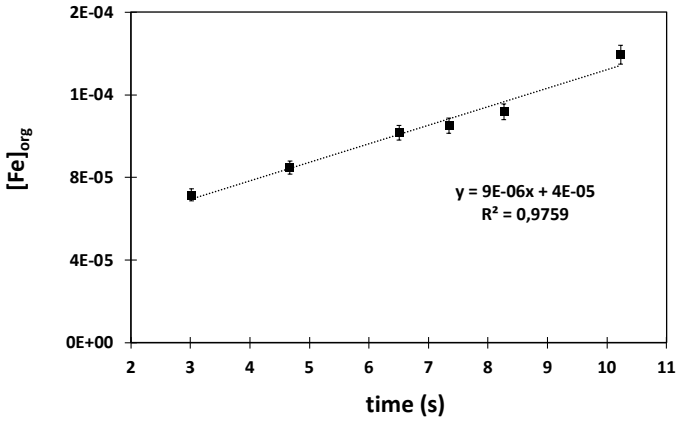

Figure 119: Dependence of $[Fe]_{org}$ as a function of time for the extraction of Fe(III) with 0.8M THMA in toluene. Initial $[Fe]_{aq}$ 7 $g.L^{-1}$, $[H^+]_{aq}$ 1.5M, $[NO_3^-]_{aq}$ 2M, T=21°C.

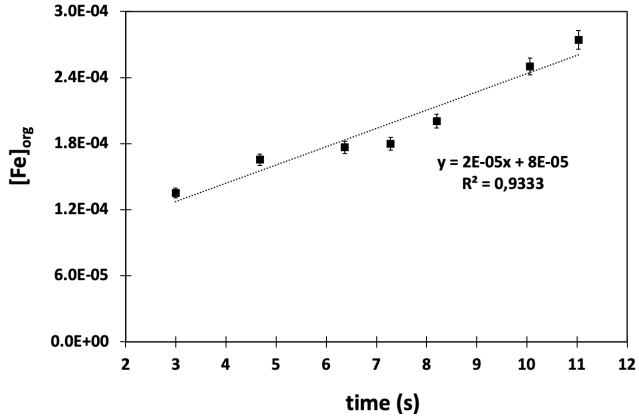

Figure 120: Dependence of $[Fe]_{org}$ as a function of time for the extraction of Fe(III) with 0.8M THMA in toluene. Initial $[Fe]_{aq}$ 7 $g.L^{-1}$, $[H^+]_{aq}$ 1.5M, $[NO_3^-]_{aq}$ 3M, T=21°C.

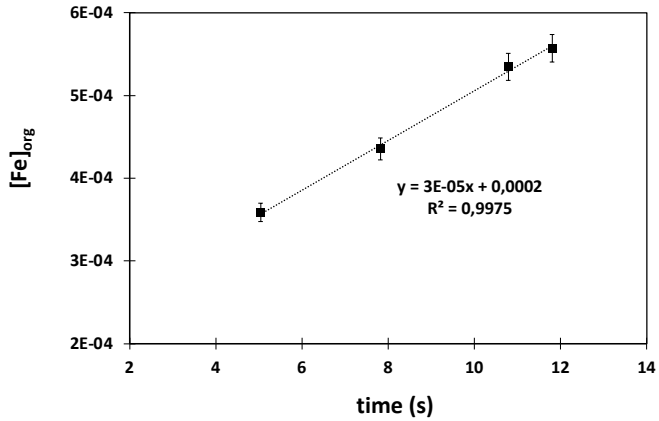

Figure 121: Dependence of $[Fe]_{org}$ as a function of time for the extraction of Fe(III) with 0.8M THMA in toluene. Initial $[Fe]_{aq}$ 7 $g.L^{-1}$, $[H^+]_{aq}$ 1.5M, $[NO_3^-]_{aq}$ 4M, T=21°C.

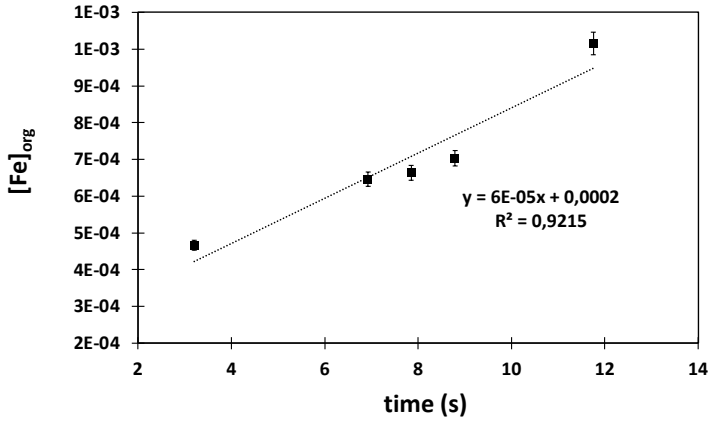

Figure 122: Dependence of $[Fe]_{org}$ as a function of time for the extraction of Fe(III) with 0.8M THMA in toluene. Initial $[Fe]_{aq}$ 7 $g.L^{-1}$, $[H^+]_{aq}$ 1.5M, $[NO_3^-]_{aq}$ 5M, T=21°C.

Table 55: Determination of R_f for the extraction of Fe(III) with 0.8M THMA in toluene. Initial $[Fe]_{aq}$ 7 $g.L^{-1}$, $[H^+]_{aq}$ 1.5M.

	Slope	**d (m)**	**R_f ($mol.m^{-2}.s^{-1}$)**
$[NO_3^-]_{aq}$ 1.5M	$(3.46 \pm 0.29)*10^{-6}$	$2.75*10^{-3}$	$(1.59 \pm 0.13)*10^{-9}$
$[NO_3^-]_{aq}$ 2M	$(8.97 \pm 0.42)*10^{-6}$	$2.64*10^{-3}$	$(3.94 \pm 0.31)*10^{-9}$
$[NO_3^-]_{aq}$ 3M	$(1.65 \pm 0.19)*10^{-5}$	$2.52*10^{-3}$	$(6.96 \pm 0.83)*10^{-9}$
$[NO_3^-]_{aq}$ 4M	$(2.99 \pm 0.10)*10^{-5}$	$2.42*10^{-3}$	$(1.20 \pm 0.04)*10^{-8}$
$[NO_3^-]_{aq}$ 5M	$(6.15 \pm 0.40)*10^{-5}$	$2.40*10^{-3}$	$(2.46 \pm 0.41)*10^{-8}$

Appendix III

I. Uncertainties of measurements

Errors and uncertainties occur naturally due to selection of instruments, condition of the device and laboratory, calibration of equipment, environmental condition, manual observation, and measurement of readings.

For the determination of the uncertainties, the principle of the root mean square method was used.

Let 'R' be the computed function of the independent measured variables x_1, x_2,….x_n

$$R = f(x_1, x_2, x_3 \dots x_n)$$

The principle of root mean square root method is

$$R = [(\frac{\partial R}{\partial x_1}\Delta x_1)^2 + (\frac{\partial R}{\partial x_2}\Delta x_2)^2 + \cdots + \frac{\partial R}{\partial x_n}\Delta x_n)^2]^{1/2} \quad (307)$$

- **The concentration of metal in the organic phase**

The metal concentration in the organic phase was obtained by ICP-AES analysis after back extraction of a volume of the organic sample. The organic phase was prepared by first weighing a mass of the ligand, and then dissolving it with the desired solvent. Then, a dilution was applied to obtain the desired concentration. The preparation was carried out in volumetric flasks. The withdrawing of the volumes for extraction, back-extraction, and preparation of the samples for ICP-AES analysis was performed using Eppendorf pipettes.

$$u_{C_{org}} = (u^2_{balance} + 2u^2_{volumetric\ flask} + 4u^2_{pipette} + u^2_{ICP})^{1/2} \quad (308)$$

- **The concentration of metal in the aqueous phase**

The aqueous phase is prepared by weighing a mass of the salt, then dissolving in the appropriate aqueous phase. Dilution was then applied to obtain the desired final concentration. The preparation was carried out in volumetric flasks. The withdrawal of the volumes was carried out using Eppendorf pipettes. And the analysis of the metal concentration was carried out using ICP-AES.

$$u_{C_{aq}} = (u^2_{balance} + 2u^2_{volumetric\ flask} + 3u^2_{pipette} + u^2_{ICP})^{1/2} \quad (309)$$

The relative error of the distribution ratio was calculated as follows:

$$\frac{\Delta D}{D} = \frac{\Delta C_{org}}{C_{org}} + \frac{\Delta C_{aq}}{C_{aq}} \tag{310}$$

We mention that the relative error of the ICP-AES analysis is generally observed to be 3%. This error can be higher when the determined concentrations are close to LoQ. The uncertainty for the employed analytical balance is ± 0.0001 g. We present the errors on the measurements with the volumetric flasks and the Eppendorf pipettes:

Table 56: Accuracy limits of the employed DURAN volumetric flasks.

Volumetric flask	**Accuracy limit ± ml**
2 mL	0.025
5 mL	0.025
10 mL	0.025
50 mL	0.06
100 mL	0.1
1000 mL	0.4

Table 57: Systematic errors for the used Eppendorf pipettes (provided by the manufacturer).

	Testing volume	**Systematic error (μL)**
10 μL- 100 μL	10 μL	0.3
	50 μL	0.5
	100 μL	0.8
100 μL- 1000 μL	100 μL	3
	500 μL	5
	1000 μL	6
0.5 mL – 5 mL	2500 μL	75
	5000 μL	100

*Calibration of the pipettes is performed in the laboratory, and the obtained errors are in agreement with the ones determined in the table above

II. Uncertainties on the global transfer constant

The global transfer constant is determined from the slope of the curve ln(1-E) = f(t)

$$\ln(1-\mathrm{E}) = -6\frac{\mathrm{K}_{\mathrm{org}}^{\mathrm{g}}}{\mathrm{d}}\mathrm{t} + \mathrm{b} \tag{311}$$

The slope p is:

$$\mathrm{p} = -6\frac{\mathrm{K}_{\mathrm{org}}^{\mathrm{g}}}{\mathrm{d}} \tag{312}$$

The relative error on the slope is expressed as follows:

$$\frac{\Delta\mathrm{p}}{\mathrm{p}} = \frac{\Delta\mathrm{d}}{\mathrm{d}} + \frac{\Delta\mathrm{K}_{\mathrm{org}}^{\mathrm{g}}}{\mathrm{K}_{\mathrm{org}}^{\mathrm{g}}} \tag{313}$$

- **Determination of Δp**

The error on the slope was determined with Linest function in Excel.

Let $\mathrm{y} = \mathrm{ax} + \mathrm{b}$

$$\mathrm{a} = \mathrm{slope} = \frac{(\mathrm{n}\sum \mathrm{x_i y_i}) - (\sum \mathrm{x_i})(\sum \mathrm{y_i})}{(\mathrm{n}\sum \mathrm{x_i^2}) - (\sum \mathrm{x_i})^2} \tag{314}$$

$$\mathrm{error\ slope} = \mathrm{S} * \sqrt{\frac{\mathrm{n}}{(\mathrm{n}\sum \mathrm{x_i^2}) - (\sum \mathrm{x_i})^2}} \tag{315}$$

Where,

$$\mathrm{S} = \sqrt{\frac{\sum(\mathrm{y_i} - \mathrm{ax_i} - \mathrm{b})^2}{\mathrm{n} - 2}} \tag{316}$$

In all equations, the summation sign is assumed to be from i = 1 to i = n.

- **Determination of Δd**

The diameter of the droplets was determined based on the following formula,

$$d_{droplet} = 2\sqrt[3]{\frac{3.V_{droplet}}{4\pi}} = 2\sqrt[3]{\frac{3}{4\pi}\frac{Q}{f}} \quad (317)$$

Where V denotes the volume of the droplet (mL), Q is the injection flow rate ($mL.min^{-1}$), and f is the frequency of droplet formation (number of drops per minute).

For the determination of the error on the diameter for each experience, we proceeded to determine the diameter for each height, and the standard error was determined as follows,

$$u_d = SE_d = \frac{\sigma_d}{\sqrt{n}} \quad (318)$$

Where, σ_d is the standard deviation and n is the number of measurements.

- **Determination of ΔE**

The expression of the transfer efficiency is:

$$E = \frac{C_{org}}{DC_{aq}^0} \quad (319)$$

The relative error on E is exressed as follows:

$$\frac{\Delta E}{E} = \frac{\Delta C_{org}}{C_{org}} + \frac{\Delta D}{D} + \frac{\Delta C_{aq}^0}{C_{aq}^0} \quad (320)$$

Since for the all measurements, $\Delta E \ll E$, then the error on ln (1-E) was estimated as follows:

$$\Delta \ln(1-E) \approx \frac{\Delta E}{E} \quad (321)$$